

MODELLING OF A VIBRATING-PLATE EXTRACTION COLUMN

Sudesh Rathilal

In fulfilment of the PhD (Engineering) degree, Faculty of Engineering,
University of KwaZulu-Natal

Date of submission: 19 May 2010
Supervisor: Prof. M. Carsky

As the candidate's Supervisor I agree/do not agree to the submission of this thesis.

.....
Supervisor

I, Sudesh Rathilal declare that

- (i) The research reported in this thesis, except where otherwise indicated, is my original work.
- (ii) This thesis has not been submitted for any degree or examination at any other university.
- (iii) This thesis does not contain other persons' data, pictures, graphs or other information, unless specifically acknowledged as being sourced from other persons.
- (iv) This thesis does not contain other persons' writing, unless specifically acknowledged as being sourced from other researchers. Where other written sources have been quoted, then:
 - a) their words have been re-written but the general information attributed to them has been referenced;
 - b) where their exact words have been used, their writing has been placed inside quotation marks, and referenced.
- (v) Where I have reproduced a publication of which I am an author, co-author or editor, I have indicated in detail which part of the publication was actually written by myself alone and have fully referenced such publications.
- (vi) This thesis does not contain text, graphics or tables copied and pasted from the Internet, unless specifically acknowledged, and the source being detailed in the thesis and in the References sections.

Signed:

ACKNOWLEDGEMENTS

The author would like to thank Prof. Carsky for his guidance and assistance throughout the research work.

Special thanks also goes to Dr. Heyberger for his invaluable assistance and direction provided when it was desperately required.

Appreciation is awarded to the technicians in the chemical engineering laboratory especially to Mr. Singh (Danny) who assisted on a daily basis with problems that came up during the experiments and the construction of the surge tanks.

The author also thanks his wife for proof reading the thesis and the rest of his family for their support and encouragement.

This thesis is dedicated to all the ladies in my life (young and old)

ABSTRACT

Liquid extraction, sometimes called solvent extraction, is the separation of the constituents of a liquid solution by contact with another insoluble liquid. It belongs to the class of countercurrent diffusional separation processes, where it ranks second in importance to distillation. There are many different types of columns that are available for liquid-liquid extraction and the reciprocating column (RPC) and vibrating plate column (VPE) are two types of mechanically aided columns. This research aims at developing a mathematical model for the prediction of $NTU/HETS$ and the mass transfer coefficient, k_{ox} for the VPE based on the agitation level of the plates (af – the product of frequency and amplitude of the plate motion), the plate spacing and the flow rates which will allow for the simplification in the design of this type of column. There is a lot of research that has gone into the development of mechanically aided extraction columns but it is limited when it comes to the RPC and VPE and most of this research is devoted to the RPC. The system chosen is the acetone-toluene-water system with the acetone in toluene forming the feed that is dispersed in the column as it moves upward while the water moves as a continuous phase down the column. Experiments were conducted to evaluate the hydrodynamics of the droplets moving up the column (in terms of drop sizes, size distribution and dispersed phase holdup) and to evaluate the mass transfer that occurs (in order to evaluate NTU , HTU and k_{ox}) as well as the effect of mass transfer on the hydrodynamics of the system while varying the agitation levels and spacing of the plates in the column. Successful models were developed using some of the experimental data and these correlations were verified with additional data.

CONTENTS

1	Introduction	1
2	Literature review	3
2.1	Introduction	3
2.2	Advantages of Liquid-Liquid Extraction	5
2.3	Disadvantages of Liquid-Liquid Extraction	5
2.4	Thermodynamic Relationships	6
2.5	Mass Transfer Fundamentals	8
2.6	Solvent Selection	12
2.7	Classification of Commercial Extractors	14
2.7.1	Non-mechanically Agitated Columns	16
2.7.1.1	Spray Columns	16
2.7.1.2	Packed Columns	16
2.7.1.3	Perforated-plate Columns	17
2.7.2	Mixer Settlers	17
2.7.3	Pulsed Columns	17
2.7.4	Mechanically Agitated Columns	18
2.7.4.1	Scheibel Extractor	19
2.7.4.2	Rotating-Disc Contactor (RDC)	19
2.7.4.3	Asymmetric Rotating Disk (ARD)	19
2.7.4.4	Oldshue-Rushton Extractor	19
2.7.4.5	Kühni Extractor	20
2.7.4.6	Centrifugal Extractor	20
2.7.4.7	Reciprocating-plate Extractor (RPC) and Vibrating-plate Extractor (VPE)	20

2.7.5	Comparisons of Extractor Performance	27
2.8	Hydrodynamic Regimes	28
2.9	Hydrodynamics in RPCs and VPEs	30
2.9.1	Droplet Size Distribution	30
2.9.2	Dispersed Phase Holdup	32
2.9.3	Droplet Size	48
2.9.4	Flooding	52
2.10	Entrainment	57
2.11	Power Requirement	57
2.12	Experimental Procedures	58
2.12.1	Holdup	58
2.12.2	Droplet Size Distribution:	59
2.12.3	Entrainment	60
2.12.4	Power Consumption	60
2.12.5	Axial Mixing	60
2.12.6	Concentration Analysis	61
2.12.7	Use of Radiotracers for Evaluation of Axial Dispersion, Holdup and Slip Velocity	61
2.13	Drop Dispersion and Coalescence	62
2.14	Interfacial Resistance	64
2.15	Marangoni Effect	64
2.16	Direction of Mass Transfer	66
2.17	Extractor Performance in Terms of Number and Height of Transfer Units	69
2.18	Longitudinal Mixing and Backflow	75
2.19	Mass Transfer Models	84
2.19.1	Diffusion Model	85

2.19.2	Backflow Model	88
2.19.3	Model Incorporating Backmixing and Forward Mixing	94
2.20	Efficiencies	97
3	Experimental	100
3.1	Choice of system	100
3.2	Toluene-Acetone-Water Physical Properties	101
3.3	Experimental Objectives	104
3.4	Experimental Equipment	105
3.5	Equipment Description	106
3.5.1	Column	106
3.5.2	Trays	106
3.5.3	Settling Tanks	108
3.5.4	Level Controller	108
3.5.5	Pumps	109
3.5.6	Rotameters	109
3.5.7	Surge Tanks	110
3.5.8	Water Storage Tank	111
3.5.9	Feed, Raffinate and Extract Tanks	111
3.5.10	Digital camera	111
3.5.11	Gas Chromatograph	112
3.5.12	Perspex Box	113
3.5.13	Vibration motor	114
3.5.14	Samplers	114
3.6	Hydrodynamics Experimental Procedure	116
3.7	Mass Transfer Experimental Procedure	117
3.8	Chemicals Used	117

3.9	Additional Equipment Used	118
3.10	Experimental Plan	118
3.11	Experimental Procedure:	121
3.11.1	Holdup	121
3.11.2	Size and Distribution of Droplets	122
3.11.3	Phase Samplers	123
3.11.4	GC analysis	123
3.12	Repeatability Analysis	123
4	Results and Discussion	124
4.1	Time to reach stability	124
4.2	Hydrodynamics Results	125
4.2.1	Holdup	125
4.2.2	Droplet size distribution	128
4.2.3	Sauter Mean Diameter	131
4.3	Mass Transfer Results	133
4.3.1	Holdup	133
4.3.2	Droplet size distribution	135
4.3.3	Sauter mean diameter	138
4.3.4	Extent of Mass Transfer	140
4.4	Calculation of NTU	141
4.5	Development of a Model for the Prediction of NTU	145
4.6	Calculation of HTU	147
4.7	Mass Transfer Coefficient	148
4.8	Efficiency Calculations	150
4.9	Repeatability	153
5	Conclusions and Recommendations	154

Nomenclature	158
References	163
Appendix A: Raw Data	170
Appendix B: Equipment Calibration	176
Appendix C: Effect of Flow Rates on Holdup	181
Appendix D: Drop Size Distribution	183
Appendix E: Profile Charts	192
Appendix F: Safety Data Sheets	205

List of Tables

2.1	Summary of axial mixing equations	82
2.2	Relationships between N_{ox} , exit concentrations and efficiencies	94
3.1	Physical properties	102
3.2	Alternate physical properties	102
3.3	Surface tension of pure components at 25 °C	103
3.4	Location of samplers	114
4.1	Comparison of N_{oxm} and N_{oxp}	144
A1	Data for calculation of time to reach stability	170
A2	Results for the first set of hydrodynamics experiments	171
A3	Results for the second set of hydrodynamics experiments	172
A4	Results for the first set of mass transfer experiments	173
A5	Results for the second set of mass transfer experiments	174
B1	Data for extract phase calibration chart	176
B2	Data for raffinate phase calibration chart	177
D1	Data for drop size distribution	183

List of Figures

2.1	Typical solvent extraction column	4
2.2	Type I ternary system	7
2.3	Phase splitting of a typical extraction system	7
2.4	Type II ternary system	8
2.5	Mass transfer between two liquid phases (2-film theory)	9
2.6	Classification of commercial extractors	14
2.7	Selection guide for choosing extractors	15
2.8	Unagitated extraction columns	16
2.9	Mechanically aided extractors	18
2.10	Types of reciprocating plates	22
2.11	Efficiency versus capacity for different extractors – toluene/acetone/water	27
2.12	Efficiency of mechanical extraction columns expressed as max. stages per meter	28
2.13	Flow regimes	29
2.14	Calculation sequence for flooding	55
2.15	Effect of solute transfer on coalescence	67
2.16	Equilibrium number of stages (plug flow)	70
2.17	Effects of Backmixing	76
2.18	Stage-wise extractor showing diffusion and backflow zones	80
2.19	Diffusion model material balance	85
2.20	Backflow model material balance	88
2.21	Range of driving force	92
2.22	Backmixing and forward mixing model	95
3.1	Feed and solvent flow directions	100

3.2	Toluene-acetone-water phase diagram	101
3.3	Alternate phase diagram	101
3.4	Process flow diagram of experimental equipment	105
3.5	Sieve plates	107
3.6	Top settling tank (showing the interface level and conductivity probe)	109
3.7	Feed surge tank	110
3.8	Perspex box (used during photography of droplets)	113
3.9	Dispersed and continuous phase samplers	115
3.10	Samplers attached to the Column	115
4.1	Time to reach stability	124
4.2	Hydrodynamics holdup	126
4.3	Photos of droplets for S/F ratio = 1:1	128
4.4	Droplet size distribution for S/F = 1:1; $h = 100$ mm (without mass transfer)	129
4.5	Sauter mean diameter (hydrodynamics)	132
4.6	Mass Transfer Holdup	133
4.7	Comparison of holdup during mass transfer and in the absence of mass transfer	135
4.8	Droplet size distribution for S/F = 1:1; $h = 100$ mm (with mass transfer)	136
4.9	Sauter Mean Diameter (mass transfer)	138
4.10	Effect of mass transfer on Sauter mean diameter	139
4.11	Effect of agitation level and plate spacing on the extent of extraction	140
4.12	Operating line construction (minimum agitation rate)	142
4.13	Operating line construction (maximum agitation rate)	143
4.14	<i>NTU</i> correlation	145
4.15	<i>NTU</i> model verification	146
4.16	Effect of agitation level on <i>HETS</i>	147

4.17	Mass transfer coefficient correlation	149
4.18	Mass transfer coefficient model verification	150
4.19	Effect of agitation level on volumetric efficiency	151
4.20	Effect of agitation level on overall efficiency	152
4.21	Effect of agitation level on Murphree efficiency	153
B1	Acetone in water calibration chart	177
B2	Acetone in toluene calibration chart	178
B3	Vibration motor calibration charts	179
B4	Drain pump controller calibration	180
C1	Effect of individual flow rates of holdup	181
D1	dsd – hydrodynamics (S/F = 1:1; h = 100mm)	185
D2	dsd – hydrodynamics (S/F = 1:2; h = 100mm)	186
D3	dsd – hydrodynamics (S/F = 2:1; h = 100mm)	187
D4	dsd – mass transfer (S/F = 1:1; h = 100mm)	188
D5	dsd – mass transfer (S/F = 1:2; h = 100mm)	189
D6	dsd – mass transfer (S/F = 2:1; h = 100mm)	190
D7	dsd – mass transfer (S/F = 1:1; h = 200mm)	191
E1	Profile charts for $h = 100$ mm; S/F = 1:1	193
E2	Profile charts for $h = 100$ mm; S/F = 1:2	194
E3	Profile charts for $h = 100$ mm; S/F = 2:1	195
E4	Profile charts for $h = 200$ mm; S/F = 1:1	196
E5	Calculations of NTU_m (S/F =1:1; $h = 100$ mm)	197
E6	Calculations of NTU_m (S/F =1:2; $h = 100$ mm)	199
E7	Calculations of NTU_m (S/F =2:1; $h = 100$ mm)	201
E8	Calculations of NTU_m (S/F = 1:1; $h = 200$ mm)	203

CHAPTER 1

INTRODUCTION

There are many different types of separation processes available in industry to separate mixtures into two or more distinct compounds including distillation, absorption, drying, extraction, etc. Liquid extraction (also called liquid-liquid extraction or solvent extraction) is the separation of a liquid solution by contact with another insoluble or partially insoluble liquid. It has many advantages over distillation especially for heat sensitive and azeotropic compounds.

Many devices are available for liquid extraction that may use the gravitational force or centrifugal force for the separation and may be unagitated or mechanically agitated in order to create finer dispersions and improve the mass transfer. The reciprocating column (RPC) and vibrating plate column (VPE) are 2 types of mechanically aided columns. A lot of research has gone into the development of mechanically aided extraction columns but is limited when it comes to RPC and VPE and most of this research is devoted to the RPC.

Besides the dimensions of the column (diameter and height), the VPE has many variables that may be appropriately adjusted to achieve the desired results viz. amplitude and frequency of vibrations, tray spacing, individual flow rates and the final throughput.

The purpose of this research was to investigate the effects of the various variables and develop correlations in order to optimise the performance of the VPE. It was proposed to formulate correlations for the prediction of the number of transfer units (taking into account axial dispersion) as well as the mass transfer coefficient as functions of the variables stated above.

As a result, this thesis shows investigations of the effects of agitation level (product of amplitude and frequency of the plate vibrations) and S/F (solvent to feed) ratio on drop size/distribution and holdup with and without mass transfer; effects of agitation level, S/F ratio and tray spacing on the extent of mass transfer, *NTU* and the efficiency as well as the

effects of mass transfer on drop size/distribution and holdup. Finally appropriate correlations for the prediction of NTU and mass transfer coefficient are developed empirically and the correlations are tested with additional data.

CHAPTER 2

LITERATURE REVIEW

2.1 Introduction

Liquid extraction, sometimes called solvent extraction, is the separation of the constituents of a liquid solution by contact with another insoluble liquid. It belongs to the class of countercurrent, diffusional separation processes, where it ranks second in importance to distillation (Pratt, 1983a).

The simplest extraction system involves the following components:

- Solute: the material that is to be extracted.
- Solvent: the fluid that is added to effect the extraction.
- Carrier: the non-solute portion of the feed mixture (portion that remains after extraction takes place).

Other terminology:

- Light phase: the phase with the lower density. It flows up the column and accumulates at the top.
- Heavy phase: the phase with the higher density. It flows down the column and accumulates at the bottom.
- Dispersed phase: the phase that forms drops in the column usually as it flows through a sparger.
- Continuous phase: the phase that flows in bulk without drops being formed.
- Feed: material that contains the solute that needs to be extracted (solute plus the carrier).
- Extract phase: the exit phase that is rich in solute.
- Raffinate phase: the exit phase that is lean in solute.

The location of the principal interface depends on which phase is dispersed. When the dispersed phase is the light phase (moving up the column) the interface is located at the top. On the other hand, if the dispersed phase is the heavy phase, the interface is located at the bottom of the column. Usually the phase which is fed at the lowest rate (normally solvent) is the dispersed phase (Humphrey and Keller, 1997). However, consideration of the wettability of a liquid with the internals of an extraction column must be taken into account.

There are a number of multistage schemes that may be used for the extraction process; the main ones being crosscurrent, countercurrent, and fractional extraction with the countercurrent (fig. 2.1) being the most common (Robbins, 1996).

A successful countercurrent contactor must permit high throughputs while maintaining high interfacial mass transfer rates and minimizing axial mixing (Hafez et al., 1979).

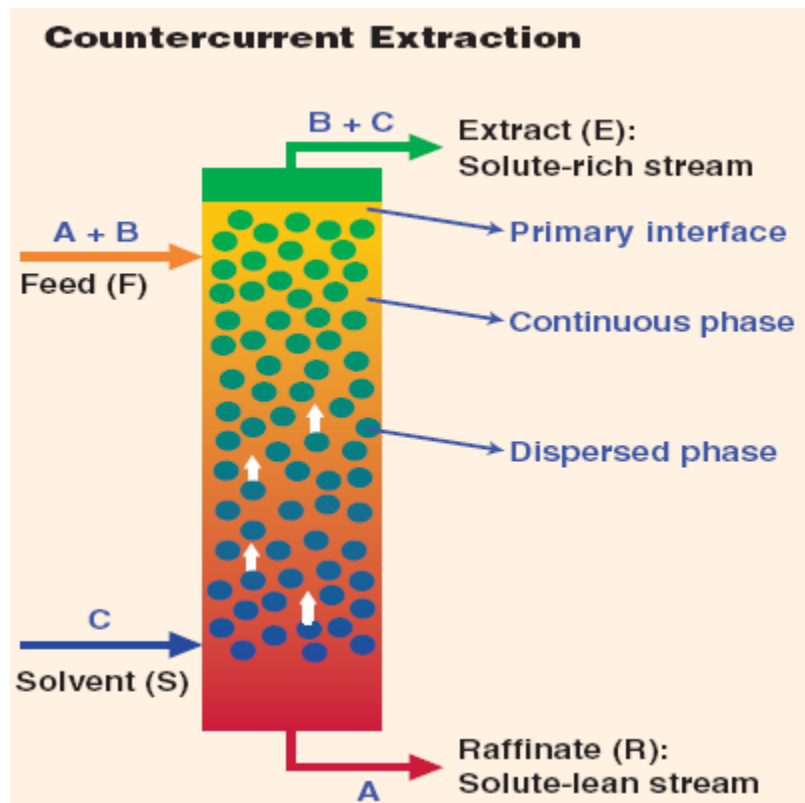


Fig. 2.1 Typical solvent extraction column (Glatz and Parker, 2004)

2.2 Advantages of Liquid-Liquid Extraction

As opposed to distillation liquid-liquid extraction is used to separate azeotropes and components with overlapping boiling points. It can offer energy savings and can be operated at low to moderate temperatures for recovery of thermally sensitive products in the food and pharmaceutical industries (Humphrey and Keller, 1997; Robbins, 1996).

In choosing a separation process the relative costs are important. Although the extraction process may involve the extractor together with other separation units, the relative costs may be lower. For the more dilute solutions particularly, where water must be vaporised in distillation for separation, extraction is more economical, especially since the heat of vaporisation of most organic solvents is substantially lesser than that of water. Extraction may also be attractive as an alternative to distillation under high vacuum and very low temperatures to avoid thermal decomposition (Treybal, 1981).

In distillation, the vapour and liquid phases produced are essentially composed of the same substances and are therefore very similar chemically. Thus the separations produced depend upon the vapour pressures of the substances. In contrast, in liquid extraction, the major constituents of the two phases are chemically very different which makes separations according to chemical type possible (Treybal, 1981).

Liquid extraction may also be less costly as a substitute for chemical methods since, unlike extraction, chemical methods consume reagents and frequently lead to expensive disposal problems for chemical by-products. Many metal separations are more economically conducted by extraction (Treybal, 1981).

2.3 Disadvantages of Liquid-Liquid Extraction

A solvent is needed for the process and this increases the complexity of the process. In industrial processes, the extraction system would consist of the extractor and at least one distillation column (or other separation process) for recovery of the solvent. If the solvent

has some degree of miscibility in the carrier, a second distillation column would be required for recovery of the solvent from the raffinate. Solvent storage tanks and a distribution system are also required (Humphrey and Keller, 1997).

2.4 Thermodynamic Relationships

For a simple ternary system, the distribution of solute and carrier between the phases at equilibrium is critical to the process. A distribution coefficient or equilibrium ratio (analogous to the equilibrium ratio or K value in distillation) is defined as follows:

$$K_C = \frac{y_C}{x_C} \quad \text{and} \quad K_A = \frac{y_A}{x_A} \quad (2.1)$$

where K_C is the distribution of component C at equilibrium

and K_A is the distribution of component A at equilibrium

The separation factor or selectivity (equivalent to relative volatility in distillation) is defined as the ratio of the K values (Humphrey and Keller, 1997):

$$\beta_{CA} = \frac{K_C}{K_A} \quad (2.2)$$

Ternary equilibrium systems may be represented on triangular diagrams. The simplest system is a Type I system shown in fig. 2.2 where there is only one immiscible pair (carrier-solvent). The carrier-solute and solvent-solute pairs are miscible. The plait point is the intersection of the raffinate phase with the extract phase boundary curves. At this point the two liquid phases have identical compositions. Tie lines connect points of equilibrium concentrations in the different phases. The tie lines converge to a point (plait point) and the two phases become one phase. A two-phase region exists below the solubility lines while a single-phase region exists above. The tie lines shown in the two-phase region connect the extract and raffinate equilibrium compositions and thus can be used to determine K values

and separation factors. Fig. 2.3 shows the phase splitting of the ternary mixtures (Humphrey and Keller, 1997; Hubbard, 1980).

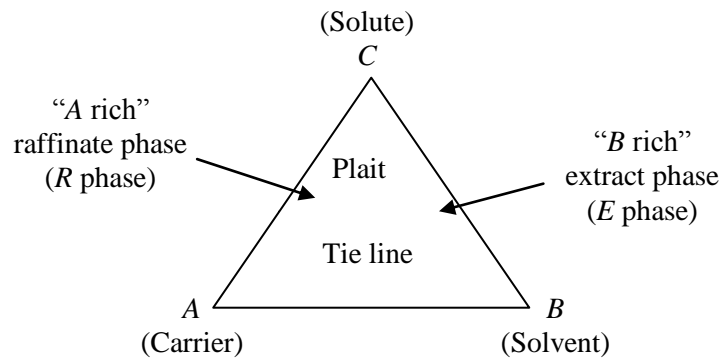


Fig. 2.2 Type I ternary system (adapted from Humphrey and Keller, 1997)

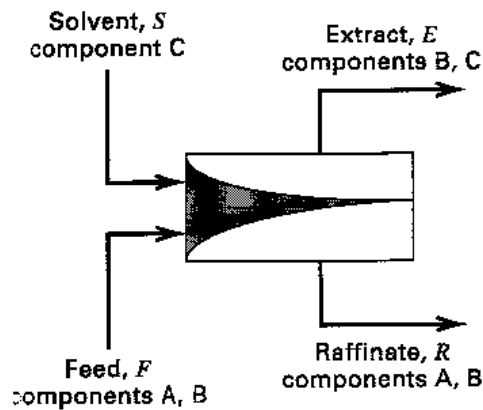


Fig. 2.3 Phase splitting of a typical extraction system (Seader and Henley, 2006)

The toluene-acetone-water system is the standard system recommended by the European Federation of Chemical Engineering as a test system for liquid extraction systems (EFCE, 1985). This system is a Type I system.

The Type II system shown below has two immiscibilities: solvent-solute and solvent-carrier (fig. 2.4). There is no plait point in this type of system.

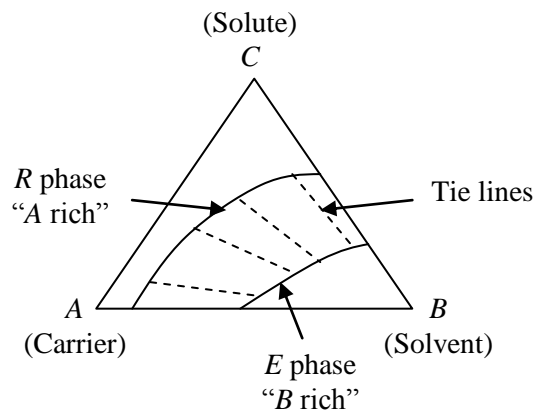


Fig. 2.4 Type II ternary system (adapted from Humphrey and Keller, 1997)

A Type III system is characterised by immiscibility in all three pairs (Humphrey and Keller, 1997; Hubbard, 1980).

2.5 Mass Transfer Fundamentals

In extraction, the solute is transferred from the raffinate to the extract phase. Fig. 2.5 shows the mass transfer process with resistances in the raffinate and extract phases (assuming no interfacial resistance).

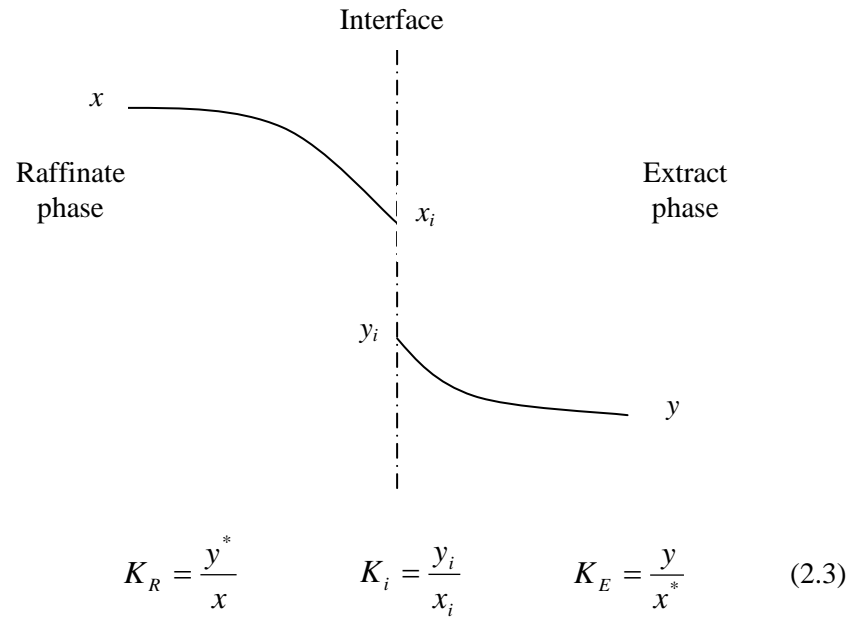


Fig. 2.5 Mass transfer between two liquid phases (2-film theory)
(adapted from Humphrey and Keller, 1997)

The two-resistance theory assumes that the resistance at the interface is negligible. The solute flux is given by the following equations:

$$N_R = k_R(x - x_i) = k_E(y_i - y) \quad (2.4)$$

$$N_R = K_R(x - x^*) = K_E(y^* - y) \quad (2.5)$$

where k_R and k_E are individual-phase mass transfer coefficients and K_R and K_E are the overall mass transfer coefficients that take into account the resistances of both phases. On the basis of the extract phase, Equations 2.4 and 2.5 may be combined as follows:

$$\frac{1}{K_E} = \frac{1}{k_E} + \frac{m}{k_R} \quad (2.6)$$

where m is the slope of the equilibrium curve plotted with the extract mole/mass fraction on the ordinate scale (Humphrey and Keller, 1997).

As stated before the two resistance theory assumes that there is no resistance to mass transfer at the interface, however, Lisa et al. (2003) investigated the phase mixing and extraction of the acetone-toluene-water system and observed the existence of an interfacial resistance. This interfacial resistance depends on the direction of mass transfer and is greater in the phase in which the equilibrium solute concentration has a small value (toluene phase). The interfacial resistance is smaller when the transfer occurs from the phase with the lower equilibrium concentration to that with a larger equilibrium concentration (toluene to water).

Mass (or mole) ratios, X (raffinate phase) or Y (extract phase) are defined as the ratio of mass (or moles) of the solute to the mass (or moles) of the other components in a particular stream or phase. They are related to mass (mole) fractions as follows (Seader and Henley, 2006; Wankat, 1980):

$$X_j = \frac{x_j}{1 - x_j}, \quad Y_j = \frac{y_j}{1 - y_j} \quad (2.7)$$

Therefore a solute material balance for the system shown in fig. 3 where there are essentially two insoluble phases such as water and toluene is (Seader and Henley, 2006):

$$X_F F_A = YS + XF_A \quad (2.8)$$

where F_A = feed rate of the carrier, A

S = flow rate of the solvent, C

The distribution of component B in terms of mass (mole) ratios is defined as (Seader and Henley, 2006):

$$K'_B = \frac{Y}{X} \quad (2.9)$$

The distribution coefficient can also be expressed as the ratio of the activity coefficients.

The extraction factor is defined as (Seader and Henley, 2006):

$$E_B = \frac{K'_B S}{F_A} \quad (2.10)$$

The larger the extraction factor, the greater the extent to which the solute is extracted. For a given system, this factor is directly proportional to the solvent to feed flow ratio.

Combining equations 2.8, 2.9 and 2.10 gives:

$$\frac{X}{X_F} = \frac{1}{1 + E_B} \quad (2.11)$$

The distribution coefficient is related to the equilibrium ratio K_{equ} as follows (Seader and Henley, 2006; Wankat, 1980):

$$K'_B = \frac{y/(1-y)}{x/(1-x)} = K_{equ} \left(\frac{1-x}{1-y} \right) \quad (2.12)$$

When values of x and y are small, K'_B approaches K_{equ} .

2.6 Solvent Selection

The selection of the solvent in the extraction process is a key decision. The following criteria should be considered when selecting a solvent (Humphrey and Keller, 1997; Mogensen, 1980).

- *Distribution coefficient* – a high value indicates high solvent affinity for the solute, which permits lower solvent/feed ratios.
- *Separation factor* – a high value reduces the number of equilibrium stages required. The separation factor may be expressed as a ratio of the activity coefficients for the solute/solvent and carrier/solvent pairs at infinite dilution:

$$\beta_{CA}^o = \frac{\gamma_{AB}^o}{\gamma_{CB}^o} \quad (2.13)$$

- *Density and viscosity* – a large difference in density between the extract and raffinate phases permits high capacities in extraction devices using gravity for phase separation. High viscosities lead to difficulties in pumping and dispersion, and reduces the rate of mass transfer.
- *Recoverability of solvent* – an efficient separation of solute and solvent is desirable for solvent recovery. A lower boiling solvent compared to the solute leads to better results.
- *Solubility of solvent* – mutual solubility of carrier and solvent should be low to prevent an additional separation system being required to recover the solvent from the raffinate. Toluene and water are virtually insoluble.
- *Interfacial tension* – a low value aids dispersion of the phases and improves contacting efficiency. They are, on the other hand, slow to coalesce and may require longer contact times for phase separation.
- *Availability and cost* – the required solvent should be commercially available. One would also have to consider that the solvent cost may represent a large initial expense for charging the system and a heavy continuing expense for replacing solvent losses.

- *Toxicity and flammability* – these are important occupational health and safety considerations.
- *Stability* – the stability of the solvent is an important consideration especially if the solvent is prone to decomposition or polymerization or if it tends to react with any of the components in the feed.
- *Corrosivity* – can lead to problems with the materials of construction.
- *Compatibility* – some solvents may not be suitable in applications where they may contaminate food or pharmaceutical products.

The minimum solvent/feed ratio may be obtained from the distribution curve. If, in a system where the miscibility of the solvent and feed are negligible, the feed concentration is M % and the equilibrium concentration of the solvent (from the distribution curve) is N %, then the minimum S/F ratio that would require an infinite number of equilibrium stages is N/M (Othmer et al., 1941).

2.7 Classification of Commercial Extractors

Extractors are classified according to the methods applied for inter-dispersing phases and producing the countercurrent flow pattern. Most of the extractors are indicated in the following diagram (fig. 2.6):

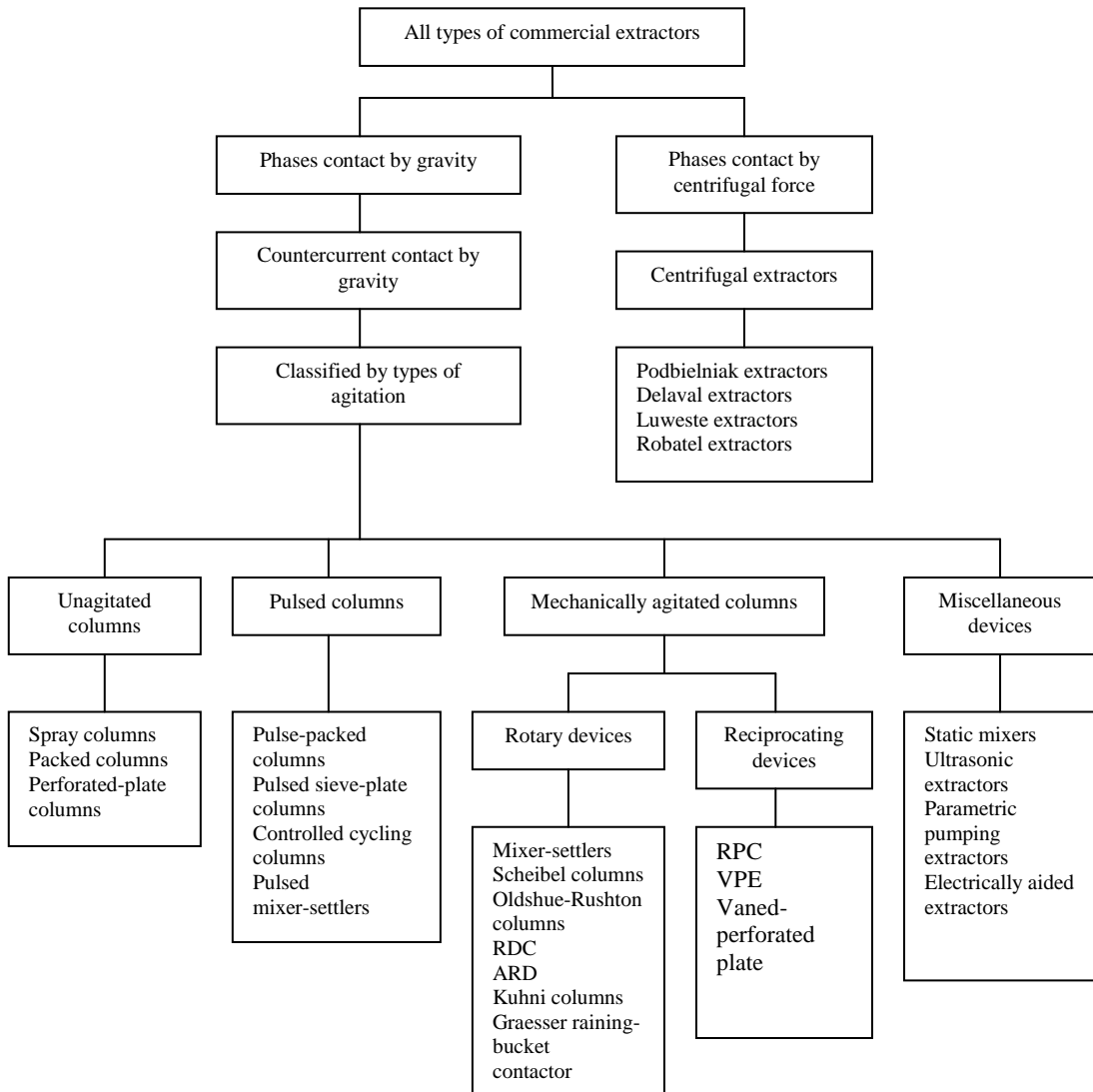


Fig. 2.6 Classification of commercial extractors (adapted from Lo, 1996)

Fig. 2.7 provides a selection guide for choosing the most appropriate contactor (Lo, 1996).

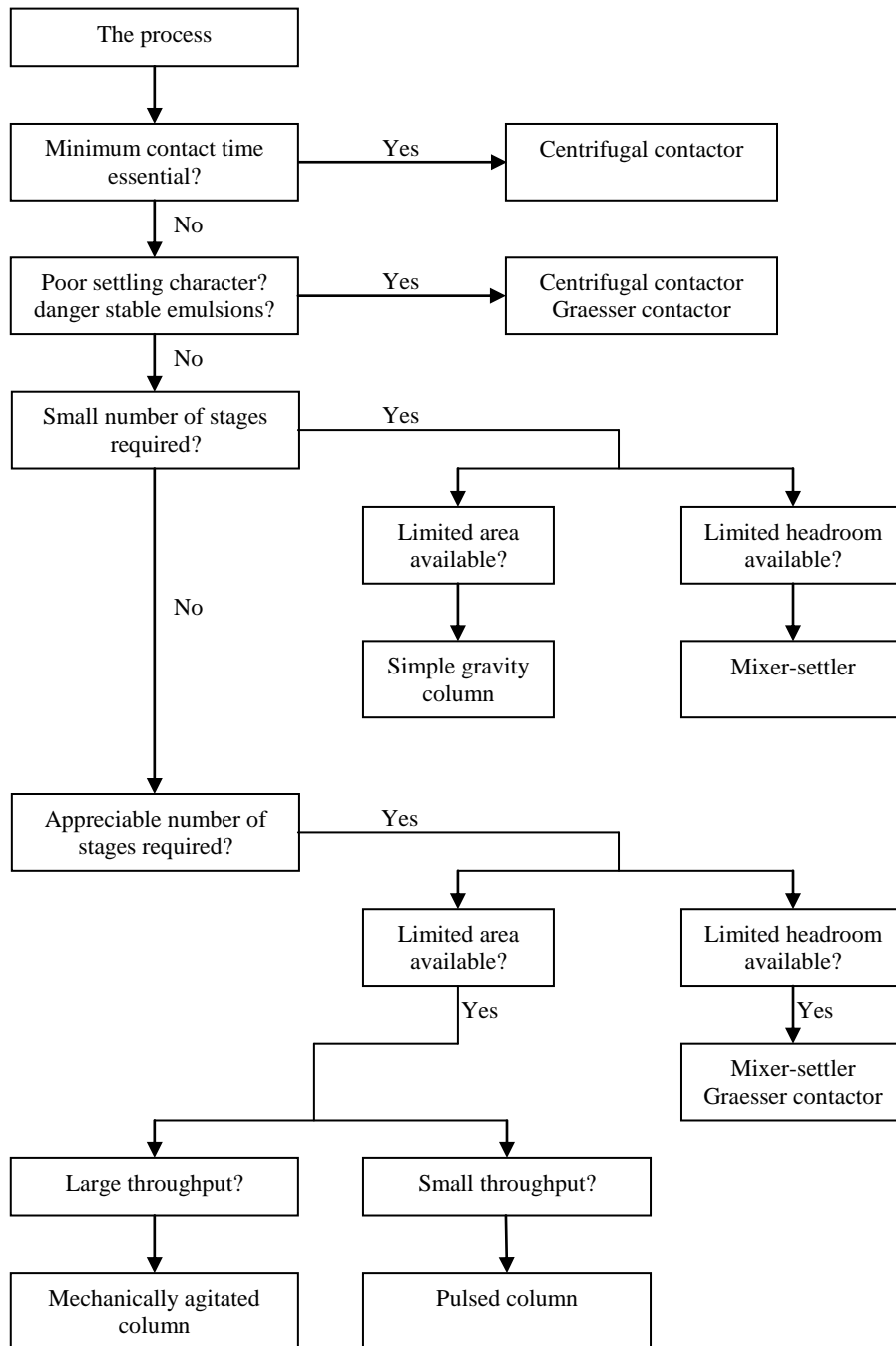


Fig. 2.7 Selection guide for choosing extractors (adapted from Lo, 1996)

2.7.1 Non-mechanically Agitated Columns

Fig 2.8 illustrates some unagitated extraction columns that are discussed below.

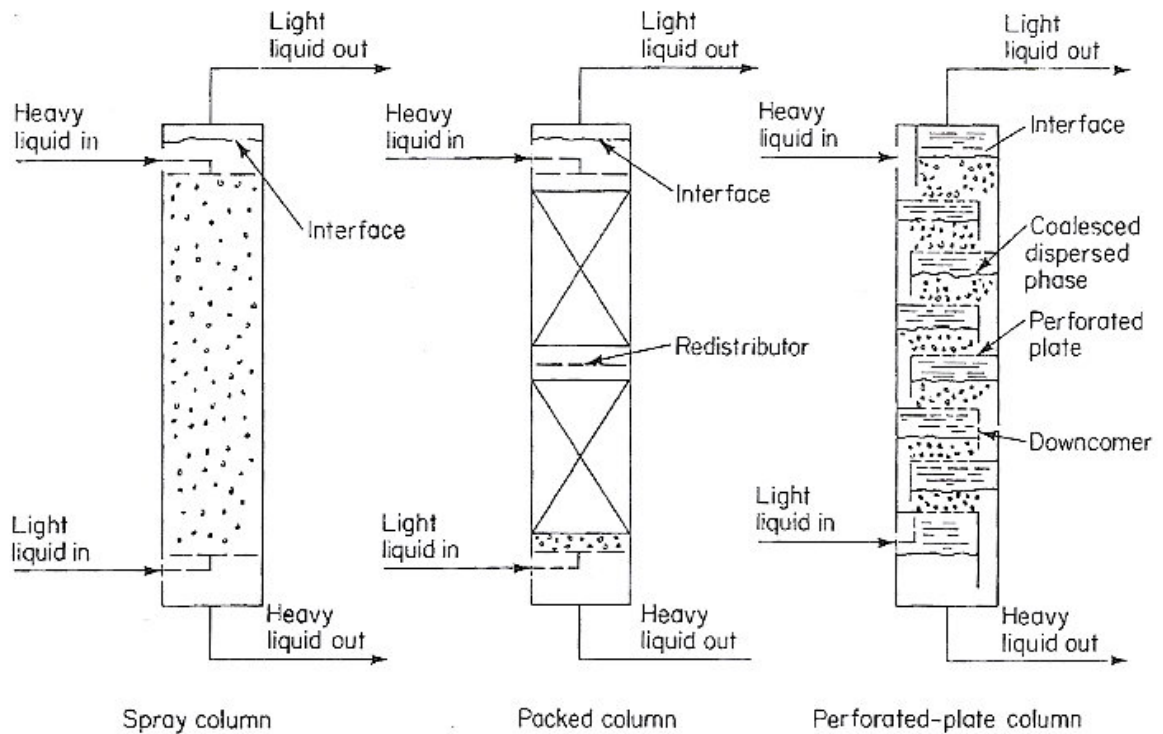


Fig. 2.8 Unagitated extraction columns (Lo, 1996)

2.7.1.1 Spray Columns

These are the simplest of construction but have very low efficiencies due to poor phase contacting and excessive backmixing in the continuous phase; however they are still used in industry for simple operations like washing, treating and neutralisation, often requiring only one or two theoretical stages (Lo, 1996).

2.7.1.2 Packed Columns

These have a better efficiency due to the improved contacting and reduced backmixing. The packing material is chosen so that it is preferentially wetted by the continuous phase in order to avoid coalescence of the dispersed phase. Usually a packed column is preferred over the

spray tower as the reduced flow capacity is less significant than the improved mass transfer (Lo, 1996).

2.7.1.3 Perforated-plate Columns

These columns have a semi-stagewise operation. If the light liquid is dispersed, the fluid flows through the perforations of each plate and is dispersed through the continuous phase. The continuous phase flows across each plate through a downcomer to the plate beneath. On the other hand, if the continuous phase is dispersed, the column is reversed and upcomers are used for the continuous phase (Lo, 1996).

2.7.2 Mixer Settlers

Simplest form of agitated vessels and may be used as a batch or continuous operation. The baffled agitated tank uses a rotating impeller to accomplish mixing and dispersion. Multiple stage extraction may be carried out by crossflow batch extraction. For continuous operation a settler is incorporated with the mixing vessel. There are many configurations of the mixing and settling parts that are incorporated into continuous extractors that may be vertical or horizontal. Stage efficiencies are at least 80% (Lo, 1996).

2.7.3 Pulsed Columns

The efficiency of sieve-plate or packed columns may be increased substantially by the application of an oscillating pulse to the contents of the column which increases both turbulence and interfacial areas. The increased mass transfer efficiency is accompanied by lower HETS or HTU values. In the top and bottom of the column, the dispersed phase coalesces at an interface layer while the fluids are moved up and down by means of a pulsating device connected to the bottom of the column. In the perforated plate column, no downcomers are used. A uniform distribution of drops is achieved producing high efficiencies with low axial mixing (Lo, 1996).

Pulsed sieve plate columns are used primarily in nuclear fuel processing plants as the application of agitation energy via compressed air pulsing may be accomplished such that the moving mechanical parts may be remote from the radioactive column environment (Logsdail and Slater, 1983; Hussain et al., 1988)

There are a lot of mechanical problems with this extractor as well as difficulties in propagating pulses throughout larger columns. On a pulse frequency/amplitude equivalence, the RPC has been found to have similar operating characteristics with less maintenance costs (Humphrey and Keller, 1997).

2.7.4 Mechanically Agitated Columns

These columns are classified into rotary-agitated columns and reciprocating or vibrating plate columns.

Some examples of the mechanically aided extractors are shown below in fig. 2.9:

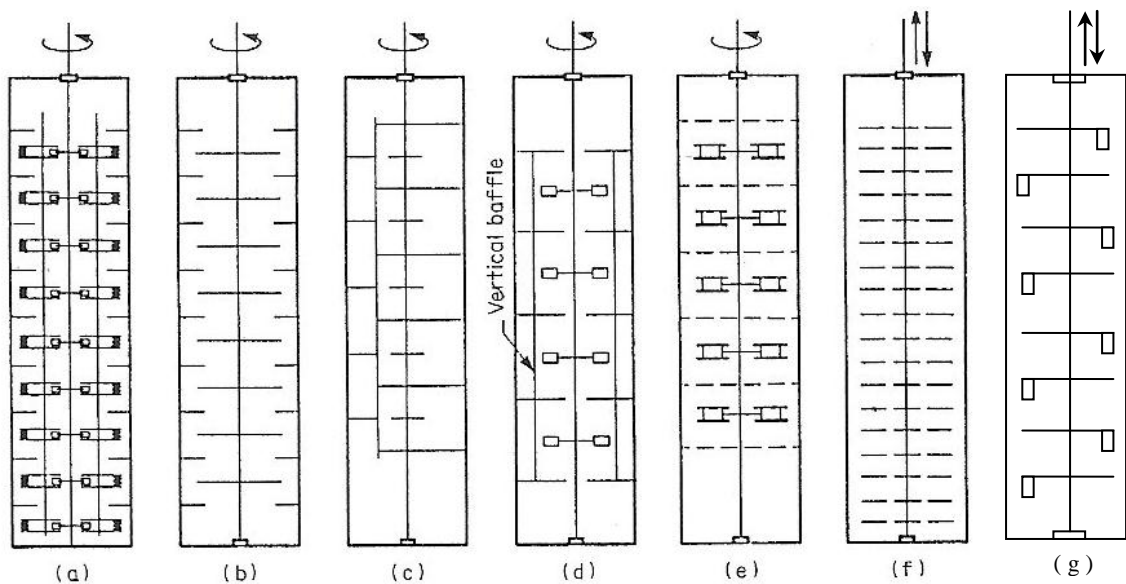


Fig. 2.9 Mechanically aided extractors (Adapted from Lo, 1996)

(a) Scheibel, (b) RDC, (c) ARD, (d) Oldshue-Rushton, (e) Kuhni, (f) RPC, (g) VPE

2.7.4.1 Scheibel Extractor

This extractor is designed to simulate a series of mixer-settler extraction units, with self-contained mesh-type coalescers between each contacting stage. Although moderately expensive the column offers a very high efficiency (Humphrey and Keller, 1997).

2.7.4.2 Rotating-Disc Contactor (RDC)

The RDC has been used in the petroleum industry for extractions involving hydrocarbon systems. Rotors on a central shaft create a dispersion and movement of the phases, while stators provide the countercurrent staging. The effectiveness can be controlled by varying the speed of rotation of the disc dispersers. The RDC has been used successfully for cases where the continuous phase is a liquid-solid slurry (Humphrey and Keller, 1997).

2.7.4.3 Asymmetric Rotating Disk (ARD)

Two zones are identified in the ARD extractor that are partially separated by a vertical baffle; an asymmetrically located mixing zone and a transfer-settling zone. The mixing zone has a number of compartments equipped with a disk-type mixing impeller mounted on a common rotor shaft. The transfer-settling zone has a series of compartments separated by annular horizontal baffles (Lo, 1996).

2.7.4.4 Oldshue-Rushton Extractor

Designed in the 1950s, the extractor comprises several compartments separated by horizontal baffles. Each compartment contains vertical baffles and an impeller mounted on a central shaft (Humphrey and Keller, 1997).

2.7.4.5 Kühni Extractor

This extractor is similar to the Scheibel column but without the coalescing sections. A baffled turbine impeller promotes radial discharge within a compartment, while horizontal baffles of variable hole arrangements separate the compartments (Humphrey and Keller, 1997).

2.7.4.6 Centrifugal Extractor

This extractor applies a centrifugal force to increase rates of countercurrent flow and separation of phases instead of relying on the force of gravity. As a result a more compact unit is produced providing very short contact times. A shorter contact time is an important feature when unstable materials are being processed. This is why the centrifugal extractor is used in the food and pharmaceutical industries. It can also handle systems that tend to emulsify along with those with low density differences and has a low space requirement. The disadvantages are its complexity and high capital and operating costs.

The first centrifugal extractor to gain widespread use in industry was the Podbielniak extractor. It consists of a drum rotating around a shaft equipped with annular passages at each end for feed and raffinate. The light phase is introduced under pressure through the shaft and then routed to the periphery of the drum. The heavy phase is also fed through the shaft but is channelled to the centre of the drum. Centrifugal force acting on the phase-density difference causes dispersion as the phases are forced through the perforations (Humphrey and Keller, 1997).

2.7.4.7 Reciprocating-plate Extractor (RPC) and Vibrating-plate Extractor (VPE)

These extractors are a descendant of the pulsed-plate column however, instead of having fixed plates with a pulsed liquid, the RPC and VPE involves moving an assembly of plates (mainly sieve plates) giving it a reciprocating movement (Humphrey and Keller, 1997). They

were first proposed in 1935 but most of the development took place from the 1960s (Lo et al., 1992).

Originally, continuous countercurrent liquid extraction was performed in columns in which the countercurrent motion was effected only by the buoyancy force due to the difference in density of the two phases. However, the rate of mass transfer in these columns is limited because the buoyancy force is usually inadequate to create a sufficiently fine dispersion as the dispersed phase flows through the inbuilt components of the column. This has led to the adoption of moving inbuilt components in order to supply additional energy for creating a large interfacial area and generating turbulence, which breaks up the dispersed phase drops and increases the interfacial area further. In practice this can be achieved either by the use of rotating impellers or disks, or by some form of vibration or pulsation (Prochazka et al., 1971; Rama Rao, Vijayan and Baird, 1991).

One disadvantage of most agitated contactors is the reduced capacity and increased longitudinal mixing. The additional energy is distributed non-uniformly over the cross-section of the column (especially in large diameter columns) resulting in the dispersion being non-uniform in size. In order to reduce longitudinal mixing such columns are frequently provided with baffles which add to the reduction of capacity. These circumstances have led to the development of RPCs (Prochazka et al., 1971).

These types of columns are generally called reciprocating-plate extraction columns, however many researchers reserve this name for the column developed by Karr in 1959 which is characterised by an open plate structure having plates with large diameter holes with a free area fraction of about 50 – 60%. The Karr column is essentially operated in the emulsion regime. The Karr column has a specific loadability of 80 – 100 m³/m²h (highest value among the columnar extractors) and theoretical number of stages between 3 – 6/m (Takacs et al., 1993).

There is still substantial backmixing in the Karr column. The other type of column has plates with smaller diameter holes with a lower fraction of free area and has downcomers for the flow of the continuous phase. These columns are termed vibrating-plate extraction columns and were developed by Prochazka in 1971. The plates of the VPE column are capable of

operating in the mixer-settler regime as well as the emulsion regime (Shen et al., 1985; Lo and Prochazka, 1983). Since the drops are dispersed across the width of the column, the axial dispersion is reduced (but still exists). The segmental downcomers also permit a larger throughput than the RPC (Lo et al., 1992).

Fig. 2.10 shows some of the commonly used plate designs currently used in industry.

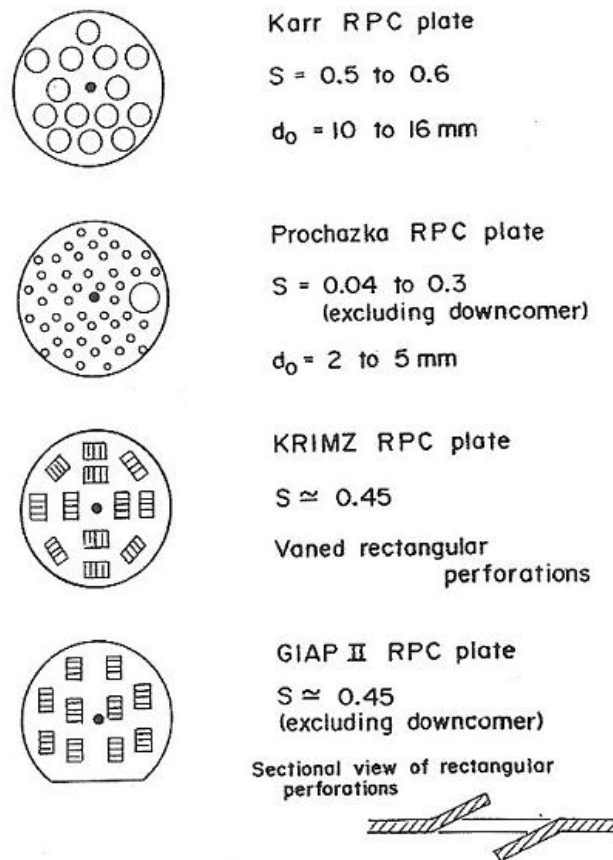


Fig. 2.10 Types of reciprocating plates (Lo et al., 1992)

A substantially uniform dispersion is achieved because the drops are formed from jets emerging from small openings at the bottom of the column. The drop size can be controlled by a suitable choice of the size of the openings in the plate and by the amplitude and frequency of the reciprocating motion. Longitudinal mixing is reduced as the perforated plates ensure that the dispersion is uniformly distributed over the cross-sectional area of the

column. In columns where downcomers are used (VPE) for the continuous phase, the capacity is much higher than that of pulsed or other types of RPCs (Prochazka et al., 1971).

The amplitude and frequency of the reciprocating motion can easily be varied and are therefore suitable variables for adjusting the action of the column to meet the requirements of particular systems and processing conditions. Prochazka et al. (1971) showed that there is a decrease in capacity and HETS (height equivalent to a theoretical stage) as the product of amplitude and frequency ($a \times f$) is increased. The capacity and HETS can be significantly varied by rather small changes in the amplitude and frequency of the reciprocating motion.

Reciprocating plate extractors have been successfully used in the pharmaceutical, chemical, food, petrochemical and hydrometallurgical industries (Karr, 1980). A suitable Karr column for appropriate laboratory work was also designed and presented by Lo and Karr (1972).

Advantages: The extractor is of simple design with low manufacturing costs and simple maintenance. Since quite a number of its constructional and operational features can be varied, the extractor can be designed for process systems of widely different properties. By changing the amplitude and frequency of the reciprocating motion, the capacity and efficiency can be varied over a very wide range, which means that it is easy to adjust an existing unit so as to obtain the best performance (Prochazka et al., 1971). The extractor offers low HETS and high throughput which provides a high volumetric efficiency. It is able to handle emulsifiable materials and solids. A wide range of materials of construction may be used including glass and Teflon and a reliable scale-up procedure is available. Compared to the pulsed column, the RPC has better uniformity in the dispersion of the phase and the large, renewal interfacial area offers greater volumetric efficiency with higher throughputs (Parthasarathy et al., 1984).

Disadvantages: Agitation could lead to fine droplets at the lower range of the size distribution which could lead to entrainment problems. At large energy inputs, axial mixing is increased which may reduce the overall effectiveness of the column (Rama Rao, Vijayan and Baird, 1991). The mechanism used to vibrate the sieve plates is more complicated and more expensive than the one used for pulsation of liquids with the complexity increasing with the diameter of the column. A slow settling emulsion may be developed that will hinder the

extraction process for liquids containing solids due to the considerable dispersion. The column is sensitive to impurities and is not suitable for liquids with solids (Takacs et al., 1993).

The advantage of VPE columns as compared to RPC columns is that the separation of phases ensures high flow rates of the dispersed phase (even in the case of high flow rates of the continuous phase). A stable mixer-settler regime is permitted over a wide range of agitation levels (product of frequency and amplitude). During this regime, it can be ensured that only one phase is dispersed because the passages available for the continuous phase suppress the dispersion of the continuous phase which is important with respect to the fact that coalescence rates depend strongly on the choice of the dispersed phase. The drops are formed or reshaped from the small holes on the plate by a mechanism similar to that of periodic outflow from a nozzle. Under these conditions, the splitting of the drops does not require high velocity. Therefore, the VPE column operates at relatively low amplitudes and frequencies which implies low mechanical stress and energy consumption (Lo and Prochazka, 1983). The RPC uses more energy to achieve the same mass transfer performance than the VPE (Ioannou et al., 1976).

No models currently exist that can be used ideally and realistically to design these types of contactors. Lo and Prochazka (1983) state that pilot scale testing is the only way of ensuring that all unknown variables are taken into account before large scale columns are designed due to factors relating to mass transfer and hydrodynamics being extremely complex and usually some of the basic information is lacking (e.g. axial mixing coefficient and mass transfer coefficient).

In order to find the optimum frequency and amplitude, experiments are conducted at different agitation levels and the HETS is plotted against agitation level (af). The agitation level at which flooding occurs is determined and the optimum level is taken as 5 – 20% of this flooding level. In order to find the maximum throughput, the maximum volumetric efficiency is plotted against throughput. If sufficient data is available the volumetric efficiency will pass through a maximum corresponding to the optimal design throughput for scale-up. During scale-up the plate spacing, stroke length and throughput are kept constant.

The following empirical equations may be used for scale-up of Karr columns (Lo and Prochazka, 1983; Karr, 1980).

The expected minimum HETS in the large column is given by:

$$\frac{(HETS)_2}{(HETS)_1} = \left(\frac{D_{c2}}{D_{c1}}\right)^{0.38} \quad (2.14)$$

The corresponding reciprocating speed will be given by:

$$\frac{(SPM)_2}{(SPM)_1} = \left(\frac{D_{c1}}{D_{c2}}\right)^{0.14} \quad (2.15)$$

Karr (1980) describes SPM as the speed of the motor (probably in terms of revolutions per minute or per second which is the same as frequency); it is assumed that the amplitude remains the same.

Axial dispersion effects must be taken into account during scale-up as it poses a problem if not considered properly and will result in a poorer performance of the large column due to the fact that axial dispersion increases with diameter due to circulation effects (Kim and Baird, 1976a; Hafez et al., 1979).

Smith et al. (2008) recently tested the performance of Karr columns with varying diameters in terms of hydrodynamics and mass transfer and found that the above scale-up equations were too conservative since, from their experiments, there was no significant change in holdup or mass transfer coefficient for varying diameter of columns. However they do specify that factors such as droplet and plate coalescence, contamination of fluids, aging of internals, and variation in physical properties drastically influences performance and must be taken into account in the design stage.

The plate displacement is nearly always a sinusoidal function of time and the velocity of the plate is given by (Lo et al., 1992):

$$u_p = \pi A f \cos(2\pi f t) \quad (2.16)$$

where A is the stoke length = $2a$ (two times the amplitude).

The velocity of the dispersed phase through a hole in the plate is given by (Lo et al., 1992):

$$U_o = \frac{u_p(1 - S_1)}{S_1} \quad (2.17)$$

The time-averaged specific energy dissipation is expressed as (Lo et al., 1992):

$$\epsilon_d = \frac{2\pi^2}{3} \left[\frac{(1 - S_1^2)}{C_o^2 S_1^2 (h/1000)} \right] (A f)^3 \quad (2.18)$$

where the orifice coefficient, C_o has a typical value of 0.6 under turbulent conditions.

Besides liquid-liquid extraction the concept of using vibrating plates in a bubble column for the gas-liquid system has been shown to enhance mass transfer while the effect of axial mixing is negligible (Yang et al., 1986; Baird and Rama Rao, 1988; Al-Sugair et al., 2006).

2.7.5 Comparisons of Extractor Performance

Fig. 2.11 shows efficiency versus capacity (sum of the flow rates of both the phases, divided by the column cross-sectional area) for various liquid-liquid extractors. Spray towers may be used when only one or two stages are needed. Where more stages are required, packings or trays are needed. When six to eight stages or more are required, mechanically aided extractors should be considered (Humphrey and Keller, 1997).

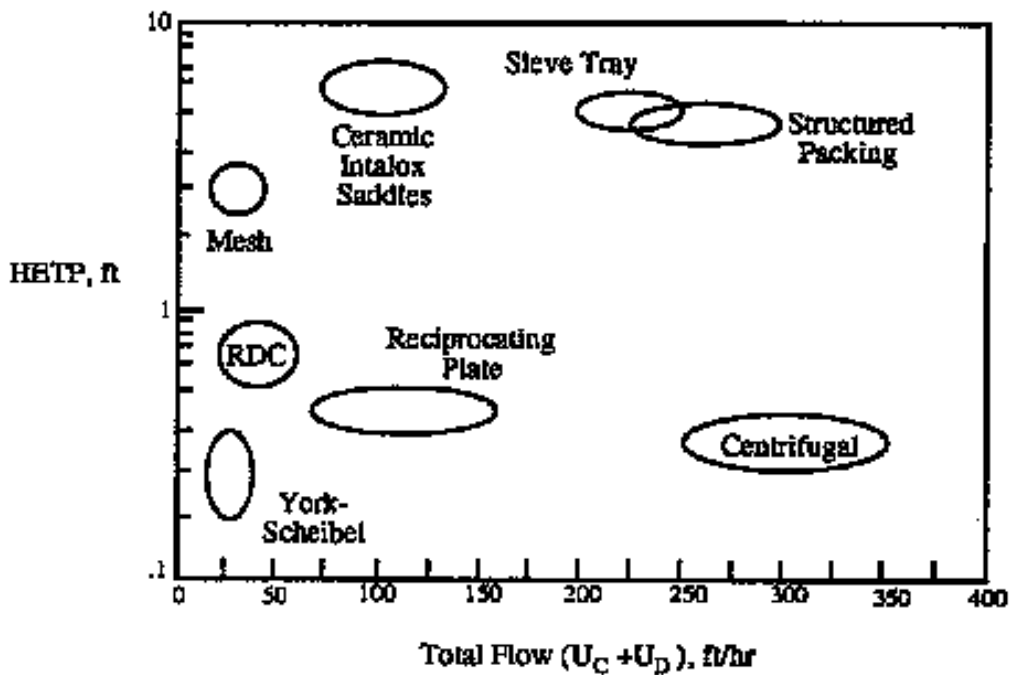


Fig. 2.11 Efficiency versus capacity for different extractors – toluene/acetone/water (Humphrey and Keller, 1997)

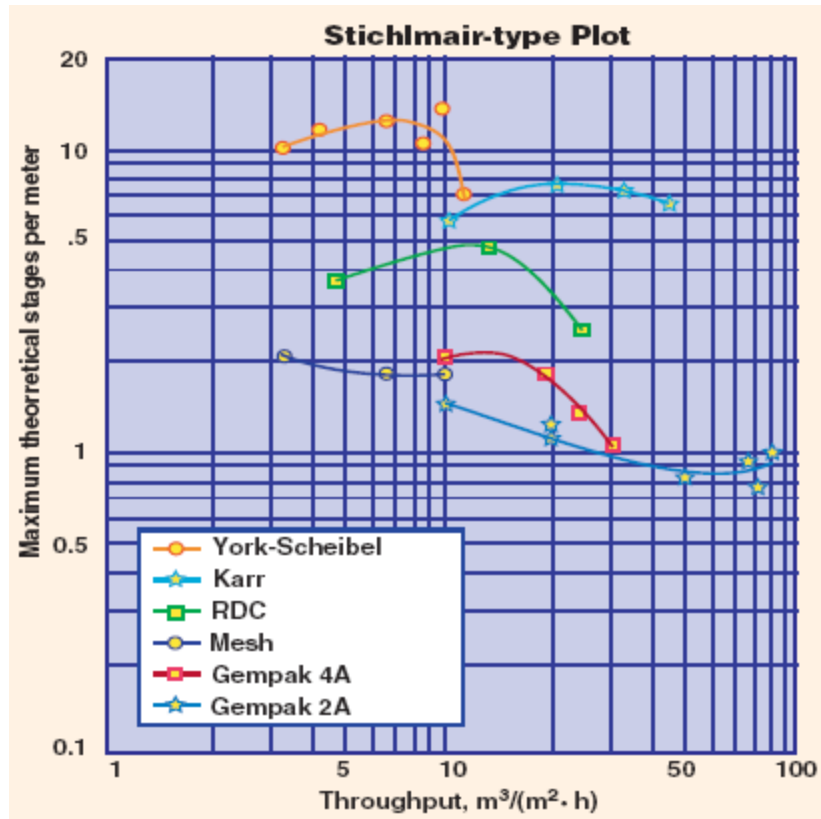


Fig. 2.12 Efficiency of mechanical extraction columns expressed as max. stages per meter
(Glatz and Parker, 2004)

Fig. 2.12 above shows how the column efficiency changes with throughput. The curve for the Karr column is fairly flat over a broad range of capacities indicating that it can operate with peak efficiency over a wide range of capacities (Glatz and Parker, 2004).

2.8 Hydrodynamic Regimes

During the operation of a VPE, one of the following regimes may exist:

1. *The mixer-settler regime:* A layer of concentrated dispersion forms under the plate whose thickness changes periodically. There is negligible holdup of the dispersed phase in the remaining volume. The latter part of the stage is passed by individual clusters of relatively large drops. The vertical component of the velocity of the drops prevails. There is no backflow of the dispersed phase through the plates.

2. *The dispersion regime:* The dense layer of the dispersed phase visible on the plates in the mixer-settler regime now expands over the height of the stage. However, there is a visible region of low local holdup near the dispersed phase inlet and outlet end. The drops are relatively large and uniform and move predominantly in the vertical direction. There is no backflow of the dispersed phase through the plates. The dispersion regime starts at the point of minimum holdup.
3. *The emulsion regime:* The dispersed stage is uniformly distributed over the height of the stage. The drops are relatively small and move erratically (difficult to identify drops moving in a vertical direction only) giving rise to their backflow through the plate. At high intensities of vibrations, the dispersed phase holdup increases enormously causing the droplets to coalesce rapidly and flooding to occur. The dispersion thus grows strongly nonhomogeneous with the motion of the large drops resembling the mixer-settler regime while the small droplets retain the character of the emulsion regime (Nemecek and Prochazka, 1974; Yadav and Patwardhan, 2008).

The mixer-settler regime is predominant at low agitation levels. As the agitation is increased, the system moves to the dispersion regime and finally to the emulsion regime at high agitation levels. Fig. 2.13 illustrates the mixer-settler and emulsion regimes.

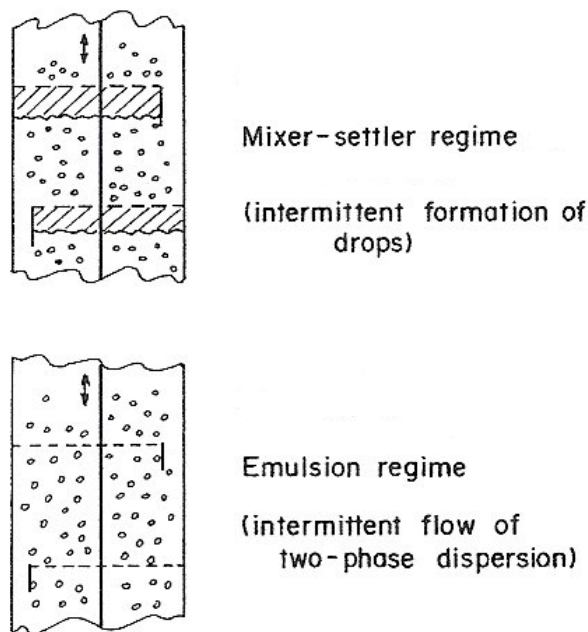


Fig. 2.13 Flow regimes (adapted from Lo et al., 1992)

2.9 Hydrodynamics in RPCs and VPEs

The hydrodynamics of RPCs are very complex, depending upon changes in droplet sizes and size distributions at different points in the column.

In deciding which phase should be dispersed, the phase that preferentially wets the column internals is selected as the continuous phase. In this way the dispersion consists of discrete droplets that move freely within the continuous phase. If the wetting phase is dispersed, it will flow as streams of uneven chunks of liquid and yield a very poor dispersion with unpredictable hydrodynamics. The volume of the droplets in the contactor during steady state operation is called the operational holdup and is usually expressed as a fraction of the effective volume of the extractor (Laddha and Degaleesan, 1983).

2.9.1 Droplet Size Distribution

Data on mean drop sizes and holdup of the dispersed phase are important in determining the interfacial area for mass transfer which in turn is important for the efficient operation, design and scale-up of extraction columns (Bensalem et al., 1986).

From evaluating droplet sizes photographically in a RPC with the system toluene-acetone-water, Bensalem et al. (1986) observed that most of the breakup of the dispersed phase drops was achieved by the first few plates and that the distribution was fairly uniform for the rest of the column. They were among the first to evaluate droplet sizes and size distribution in RPCs during mass transfer and found that both these factors were affected by the direction of mass transfer.

At low agitation, the distribution is found to be scattered indicating that there is a wide variation of droplet sizes. Very small drops are visible that are usually secondary droplets formed during the early break-up of the large drops. As agitation is increased, the size distribution together with the mean Sauter drop diameter is reduced.

Rama Rao et al. (1991) measured the droplet size distribution from photography and plotted the results on a frequency distribution curve. The Sauter mean diameter was calculated from the average on the distribution curve.

Aravamudan and Baird (1999) defined the number frequency of the frequency distribution graphs as the percentage of drops found in each class interval of 0.2 mm. It was noted that the distribution was much broader under mass transfer conditions than in the absence of mass transfer. They also found that there was a significant number of small drops that were defined as daughter drops from the breakage of the larger drops. As the agitation is increased, the distribution is shifted towards the smaller sizes and become more similar in shape and size.

Joseph and Varma (1998) found that the drop distribution in reciprocating columns was multimodal at low agitation levels due to the dual mechanism of drop breakup (i.e. the flow through the perforations and the collision with the plates). The collision of the drops with the plates predominates with an increase in the agitation level leading to a uni-modal distribution. Jiricny and Prochazka (1980) also observed bimodal distributions in a Karr column mostly near the dispersed phase inlet which disappeared towards the other end of the column. They attributed this bimodal occurrence to three factors viz. that the distributor may form small secondary drops besides the main size of drops, that the large drops entering the column split highly asymmetrically and that the small droplets created along the column are entrained by the continuous phase and accumulated towards the dispersed phase entrance end of the column. The continuous splitting and coalescence of drops along the length of the column as the dispersed phase moves through the column as well as the entrainment of the smallest of the droplets transforms the particle size distribution into a uni-modal or monomodal one. There is a drastic change in the form of the particle size distribution as the intensity of plate vibration is increased. As a result of the breakage intensity being very high, any bimodality disappears and only a monomodal distribution is observed. (Jiricny and Prochazka, 1980).

2.9.2 Dispersed Phase Holdup

In a countercurrent column, if the rate of arrival of droplets exceeds the coalescence rate at the interface, a buildup of droplets will occur at the interface which will extend over the entire column and lead to flooding. The height of droplet buildup in a sieve plate compartment is related to the mean size of droplets at the interface zone. The coalesced layer under the plates is called the static holdup and is a function of the continuous phase flow rate, orifice resistance, and interfacial tension effects. The height of the static holdup is thus given by (Laddha and Degaleesan, 1983):

$$h_t = \frac{4.5U_c^2\rho_c}{2g\Delta\rho} + \frac{6\gamma g_c}{(d_e^0)\Delta\rho g} + \frac{u_N^2[1 - (S_N/S_t)^2\rho_d]}{2gC_N^2\Delta\rho} \quad (2.19)$$

The static holdup increases strongly with continuous phase flow and will lead to flooding. At high continuous phase flow, the height of the coalesced layer increases with an increase in the dispersed phase flow depending also on the free hole area in the plates (Laddha and Degaleesan, 1983).

It was found that under realistic operating conditions an average drop size is appropriate in describing the performance of a column instead of evaluating a range of drop sizes and as a result the summation of mass transfer coefficients evaluated over a range or all the drop sizes in a distribution is not necessarily a correct design procedure (Brodkorb et al., 2003).

The Sauter mean diameter is used as an estimation of the average drop diameter of the dispersed phase in the column or section of the column. The following equation is used to calculate the Sauter mean diameter from experimental values (Baird and Lane, 1973):

$$d_{32} = \frac{6 \sum V_i}{\sum S_i} = \frac{\sum n_i d_i^3}{\sum n_i d_i^2} \quad (2.20)$$

Baird and Lane (1973) found that the Sauter mean diameter was dependent on the agitation rate (af – product of amplitude and frequency of the plate vibration) and on system properties but was not generally affected by throughput. The exception was in the absence of vibrations, where the drop size was slightly higher for higher dispersed phase flow rates (reason was attributed to a greater opportunity of coalescence) and at an agitation rate near the flooding point where larger drop sizes are observed due to coalescence effects. They also found that d_{32} decreased linearly along the length of the column from the dispersed phase inlet. However, the extent of the decrease was small and most of the droplet breakup was observed to occur in the first few plates.

The relationship between holdup and agitation rate is highly nonlinear. Camurdan et al. (1989) found that, during the emulsion regime as the agitation rate is increased, the turbulence level increases and the droplets become smaller. As this happens the drag force acting on them increases relative to buoyancy and the velocity of the droplets decreases. The result of this is an increase in residence time of the droplets which causes the holdup to increase.

Rama Rao et al. (1991) found that, at zero continuous flow and a fixed dispersed flow in a Karr column, the holdup increased continuously with an increase in af , whereas, with a constant continuous flow, the holdup decreased to a minimum and then increased. It is believed that this is due to a transition between ‘mixer-settler’ regime at low agitation levels and ‘emulsion’ regime at high agitation levels. In the mixer-settler regime, the dispersed phase forms a discrete layer beneath the plates and its upward flow through the downcomers is hindered by the downward flow of the continuous phase. In the emulsion regime, the holdup is mainly due to dispersed droplets and at very high agitation it is probable that some of the continuous phase is drawn downwards through the perforations as the plates are in their upstroke. Similar results have been observed for pulsed columns (Rama Rao et al. 1991).

Baird and Lane (1973) stated that under steady state conditions, the net weight of the dispersed phase droplets would be balanced by the drag force acting on them and derived equation 2.21. Hafez et al. (1979) and Kumar and Hartland (1988) also used this equation

stating the same justification i.e. that there is a balance of forces between fluid friction and buoyancy.

$$\frac{g\Delta\rho d(1-\phi)^3}{\rho_c u_s^2} = \frac{150\phi}{\text{Re}} + 1.75 \quad (2.21)$$

where $\text{Re} = \frac{u_s d \rho_c}{\mu_c}$ (2.22)

At intermediate *Re* numbers it was postulated that the left hand side of the equation was proportional to $\text{Re}^{-0.5}$ (Baird and Shen, 1984). Using the Sauter mean drop diameter:

$$\frac{g\Delta\rho d_{32}(1-\phi)^3}{\rho_c u_s^2} = K \left(\frac{\text{Re}}{\phi} \right)^{-0.5} \quad (2.23)$$

For the emulsion flow regime, holdup data and superficial velocities can be related using the slip velocity (Baird and Lane, 1973; Rama Rao, Vijayan and Baird, 1991; Kumar and Harland, 1988; Kumar and Hartland, 1995, Laddha and Degaleesan, 1983):

$$u_s = \frac{U_c}{(1-\phi)} + \frac{U_d}{\phi} \quad (2.24)$$

$$u_s = u_k(1-\phi) \quad (2.25)$$

The slip velocity of a droplet is considered to be the velocity one would observe while travelling with the speed of the droplet in relation to the counterflowing continuous phase and may be regarded as the vectorial difference between the dispersed and continuous phase velocities. Heyberger et al. (1983b) describes slip velocity as a result of action of external and internal forces on both the phases (continuous and dispersed) in the gravity field. It is

dependent on particle size, density and viscosity of the phases, holdup and particle-to-diameter ratio and this dependence is usually expressed as the product of the characteristic velocity and a holdup correction factor.

From equation 2.25, the characteristic velocity, u_k is the slip velocity at zero holdup.

Heyberger et al. (1983b) evaluated the use of 3 correlations for the prediction of the slip velocity proposed by other researchers as follows:

$$u_s = u_k(1 - \phi)^a \quad (2.26)$$

$$u_s = u_k(1 - \phi)\exp(b\phi) \quad (2.27)$$

$$u_s = u_k \frac{(1 - \phi)^{\varphi_1}}{1 + c[(1 - \phi)^{\varphi_2} - 1]} \quad (2.28)$$

where $\varphi_1 = 1 + 2.5 \frac{\mu_d + 0.4\mu_c}{\mu_d + \mu_c}$, and $\varphi_2 = \frac{6}{7} \left(\frac{1}{2} + 2.5 \frac{\mu_d + 0.4\mu_c}{\mu_d + \mu_c} \right)$

The above equations were evaluated for different size columns and plate geometry (while keeping the main hydrodynamic properties the same) and found them all to predict the slip velocity fairly accurately provided the constants a , b and c remain as adjustable empirical constants. a was found to be within the range 1.3 to 3.5 and the value of 1 in equation 2.25 seemed to be too low.

For small droplets, rigid sphere behavior can be assumed, resulting in u_k being estimated as the terminal velocity, u_T of a solid sphere having the same density as the dispersed phase with the sphere diameter being taken as d_{32} (Rama Rao et al., 1991)

At intermediate Reynolds number (in the order of 10), terminal velocities can be estimated from the drag coefficient curve for rigid spheres. A relationship between Re_T and Archimedes number, Ar is given below (Rama Rao et al., 1991):

$$Ar = d^3 g \rho_c (\rho_c - \rho_d) / \mu_c^2 \quad (2.29)$$

$$A = \log Ar \quad (2.30)$$

$$P = [(0.0017795A - 0.0573)A + 1.0315]A - 1.26222$$

$$R = 0.99947 + 0.01853 \sin(1.848A - 3.14)$$

$$\log Re_T = P + \log R \quad (2.31)$$

where $Re_T = \frac{u_T d \rho_c}{\mu_c} \quad (2.32)$

A model to estimate the holdup from system properties and operating conditions has been given by Rama Rao et al. (1991), with the following calculation sequence:

1. Estimate d_{32} from the equation 2.20.
2. Estimate u_T using equations 2.29 to 2.32 assuming rigid behaviour with $d = d_{32}$.
3. Set $u_k = u_T$ and solve the equations 2.24 and 2.25 for slip velocity and holdup, by iteration.

The model was tested with experimental data from a 5 cm diameter Karr column using kerosene as the dispersed phase and distilled water as the continuous phase and showed good

agreement in the emulsion regime at a frequency of 60 Hz. However, at other frequencies, the model seems to underestimate the holdup. One possible reason is that the use of d_{32} to estimate slip velocity is not accurate when there is a broad distribution of droplet sizes; at high frequencies, many fine drops were formed which could not be measured photographically.

Rama Rao et al. (1991) found that at high agitation, holdup is slightly increased by U_c , but at low agitation in the mixer-settler regime, holdup is strongly affected. U_d has a strong effect of holdup in both regimes in the Karr column.

It was found that the Sauter mean drop size was given by (Baird and Shen, 1984; Hafez et al., 1979):

$$d_{32} = 0.36 \frac{\gamma^{0.6}}{\psi^{0.4} \bar{\rho}^{0.2}} \quad (2.33)$$

where ψ , the specific mechanical power dissipation rate is given by (Baird and Shen, 1984; Hafez et al., 1979; Camurdan et al., 1989):

$$\psi = \frac{2\pi^2}{3} \left(\frac{1 - \sigma^2}{(h/1000)C_0^2 \sigma^2} \right) \bar{\rho} (Af)^3 \quad (2.34)$$

The Sauter mean drop diameter and power dissipation is defined above for high agitation levels in the absence of mass transfer. Baird and Lane (1973) and Kumar and Hartland (1988) suggested that the equation above may be extended to low levels of agitation if the power dissipation due to gravitational flows, ψ_1 is included:

$$\psi_1 = u_s g \phi \Delta \rho = g \Delta \rho \left(U_d + \frac{\phi}{1 - \phi} U_c \right) \quad (2.35)$$

Therefore at low agitation levels, the following semi-empirical equation is derived (Lo et al., 1992):

$$d_{32} = 0.23 \frac{\gamma^{0.6}}{\bar{\rho}^{0.2} (\psi + \psi_1)^{0.4}} \quad (2.36)$$

It was found that this could be correlated with the slip velocity based on the Ergun-type equation as follows:

$$u_s = \frac{1-\phi}{K^{2/3} \phi^{1/3}} d_{32} \left[\frac{g^2 \Delta \rho^2}{\rho_c \mu_c} \right]^{1/3} = \frac{u^* (1-\phi)}{\phi^{1/3}} \quad (2.37)$$

where $K = 30$ for rigid non-circulating droplets

or $K = 15$ for circulating droplets

NB. Smaller drops will be less likely to circulate than larger ones.

Drops that do not circulate internally show much lower mass transfer coefficients than circulating drops (Lo et al., 1992).

u^* is analogous but not the same as the characteristic velocity and this equation shows the difference between the model proposed by Baird and Shen (1984) and the concept of characteristic velocity.

From equation 2.37 and the slip velocity equation (equation 2.24), dividing by U_c and expressing U_c in terms of u^* shows that linearised plots may be produced of

$$\frac{(1-\phi)^2}{\phi^{1/3} \left[1 + L \left(\frac{1-\phi}{\phi} \right) \right]} \text{ vs } U_c \text{ with the inverse of the slopes being the velocity } u^* \text{ given as:}$$

$$u^* = d_{32} \left[\frac{g^2 \Delta \rho^2}{\rho_c \mu_c} \right]^{1/3} K^{-2/3} \quad (2.38)$$

from equation 2.37.

K was assumed to be 30 for rigid spheres and the results provided a reasonable correlation between model prediction and experimental data. However, the model predicts that the hydrodynamic conditions are uniform throughout the plate stack which is an approximation.

Combination of equations 2.24 and 2.37 gives:

$$\frac{U_c}{u^*} = \frac{(1 - \phi)^2}{\phi^{1/3}(1 - L) + L\phi^{-2/3}} \quad (2.39)$$

Slater (1985) suggested that

$$u_s = u_k (1 - \phi)^m + p\phi^n \quad (2.40)$$

has wide applicability. The term $p\phi^n$ reflects the effects of coalescence giving larger drops and is only used for large values of holdup ($\phi > 0.5$).

Using the definition above for u_s (equation 2.40) in order to eliminate the slip velocity for cases where the $\phi < 0.5$ gives the following relationship (Kumar and Hartland, 1995):

$$\phi(1 - \phi)^{m+1} + \left(\frac{U_d}{u_k} - \frac{U_c}{u_k} \right) \phi - \frac{U_d}{u_k} = 0 \quad (2.41)$$

In the case of RPCs, Slater (1985) found that m is related to d_{32} by the following equation:

$$m = 2.4 \times 10^3 d_{32} \quad (2.42)$$

Slater (1985) and Kumar and Hartland (1988) also suggested that $u_k = u_T$ and can be estimated assuming either rigid or mobile conditions. For the latter case:

$$\text{Re}_T = M^{-0.149} (0.94H^{0.757} - 0.857) \quad \text{for } 2 < H < 59.3 \quad (2.43)$$

or
$$\text{Re}_T = M^{-0.149} (3.42H^{0.441} - 0.857) \quad \text{for } H > 59.3$$

where
$$H = \frac{4}{3} \left(\frac{d^2 \Delta \rho g}{\gamma} \right) M^{-0.149} \left(\frac{\mu_c}{0.0009} \right)^{-0.14}$$

and
$$M = \text{modified Morton number} = \frac{g \mu_c^4 \Delta \rho}{\rho_c^2 \gamma^3} \quad (2.44)$$

Joseph and Varma (1998) investigated the effects of operating parameters and physical properties of the solute on slip velocities in a reciprocating plate column and found that the slip velocity increased with agitation level in the mixer-settler region and decreased with agitation level in the emulsion region; it increases with an increase in U_d and is not affected by U_c ; it increases with an increase in plate spacing and plate free area and depends on the nature of the solute and the direction of mass transfer.

Kumar and Hartland (1988) report that for the toluene (d - dispersed) / water (c - continuous) system in a Karr column of 76 mm diameter, the holdup did not change appreciably for $Af = 0$ to about $Af = 0.018$ m/s. However, for larger agitation levels the holdup increased rapidly with Af especially near the flooding limit. The holdup also increased with increasing U_d while the effect of U_c was less pronounced. For mass transfer of acetone, the holdup was

higher for $c \rightarrow d$ transfer and lower for $d \rightarrow c$ transfer than the holdup obtained in the absence of mass transfer. The following empirical equations were proposed:

$$\phi = 9.99(Af + V_c)^{0.30} V_d^{0.606} \quad \text{in the absence of mass transfer} \quad (2.45)$$

$$\phi = 330.40(Af + V_c)^{0.91} V_d^{0.87} \quad \text{for } c \rightarrow d \text{ direction of transfer} \quad (2.46)$$

$$\phi = 27.38(Af + V_c)^{0.437} + V_d^{0.807} \quad \text{for } d \rightarrow c \text{ direction of transfer} \quad (2.47)$$

The following equation is presented for the prediction of holdup and slip velocity in droplet dispersions:

$$\frac{4d_{32}g\Delta\rho(1-\phi)}{3\rho_c u_s^2 (1 + 4.56\phi^{0.73})} = 0.53 + \frac{24\mu_c}{d_{32}u_s\rho_c} \quad (2.48)$$

Solving for u_s and hence U_c :

$$U_c = \frac{\left[-\beta + (\beta^2 + 4\alpha(1-\phi)/(1 + 4.56\phi^{0.73}))^{0.5} \right] \phi(1-\phi)}{2[\phi + L(1-\phi)]} \quad (2.49)$$

where $\beta = \frac{24\mu_c}{0.53d_{32}\rho_c}$

and $\alpha = \frac{4d_{32}g\Delta\rho}{1.59\rho_c}$

Lo and Prochazka (1983) showed the following correlation for the prediction of holdup that was proposed by Misek:

$$\frac{U_d}{\phi} + \frac{U_c}{1 - \phi} = u_k(1 - \phi)\exp(b\phi) \quad (2.50)$$

For the toluene-water system in the absence of mass transfer, it was found that u_k and b decreases with increasing frequency of vibrations. In practical design, the holdup is kept within 15 – 25%, corresponding to 70 – 80% of the flooding throughput.

Lo and Prochazka (1983) also present the following relationships for the prediction of the maximum pressure difference across the plate and the maximum power consumption for columns with a total free plate area of 20% (VPE) using water as the continuous phase:

$$\Delta P_{max} = 9.7 \times 10^3 af + 1.8 \times 10^6 (af)^2 \quad (2.51)$$

$$P_{in} = \frac{2\pi af N \Delta P_{max} \pi D_c^2}{4\eta_m} \quad (2.52)$$

After considering various other experimental work done by different researchers Kumar and Hartland (1988) derived the following equation for holdup in the absence of mass transfer:

$$\phi = [k_1 + k_2 (Af)^3] U_d^{0.81} (U_c + U_d)^{0.32} \Delta\rho^{-0.98} \quad (2.53)$$

where $k_1 = 3.87 \times 10^3$ and $k_2 = 3.71 \times 10^7$ for no mass transfer

$k_1 = 3.25 \times 10^3$ and $k_2 = 7.54 \times 10^7$ for $c \rightarrow d$ transfer

$k_1 = 2.14 \times 10^3$ and $k_2 = 1.65 \times 10^7$ for $d \rightarrow c$ transfer

$k_1 = 7.91 \times 10^3$ and $k_2 = 3.23 \times 10^6$ for plates wetted by dispersed phase

The average absolute relative deviation in the predicted values of ϕ from experimental points was reported as 19% for the above equation.

Kumar and Hartland (1995) considered various experimental data obtained by other researchers (for holdup in various columns viz. rotating disk, asymmetric rotating disc, Kuhni, Wirx-II, pulsed perforated-plate, Karr reciprocating-plate, packed, and spray columns) in order to develop a unified correlation for the prediction of holdup in any of these columns. They developed the following equation in terms of dimensionless variables:

$$\phi = \Pi \Phi \Psi \Gamma \quad (2.54)$$

The dimensionless variables are defined as follows:

$$\Pi = C_{\Pi} + \left[\frac{\psi_m}{g} \left(\frac{\rho_c}{g\gamma} \right)^{1/4} \right]^{n_1} \quad (2.55)$$

$$\Phi = \left[U_d \left(\frac{\rho_c}{g\gamma} \right)^{1/4} \right]^{n_2} \exp \left[n_3 U_c \left(\frac{\rho_c}{g\gamma} \right)^{1/4} \right] \quad (2.56)$$

$$\Psi = C_{\Psi} \left(\frac{\Delta\rho}{\rho_c} \right)^{n_4} \left(\frac{\mu_d}{\mu_w} \right)^{n_5} \quad (2.57)$$

$$\Gamma = C_{\Gamma} \sigma^{n_6} \left[\left(\frac{h}{1000} \right) \left(\frac{\rho_c g}{\gamma} \right)^{1/2} \right]^{n_7} \quad (2.58)$$

The parameters C_{Ψ} and C_{Γ} allow respectively for the effects of mass transfer and geometrical characteristics of the columns. Kumar and Hartland (1995) formulated the above

equations and specified the corresponding values of the constants for the various columns. For the Karr reciprocating column, the following constants are specified:

C_{Π}	C_{Ψ} $c \rightarrow d$	C_{Ψ} $d \rightarrow c$	C_{Ψ} <i>no mass transfer</i>	C_{Γ}	n_1	n_2	n_3	n_4	n_5	N_6	n_7
0.13	1	0.52	1	6.87	1	0.84	3.74	-0.92	0	0	-0.48

Using these constants the correlation for the holdup for a system with either no mass transfer or $c \rightarrow d$ mass transfer becomes (Kumar and Hartland, 1995):

$$\phi = \left\{ 0.13 + \left[\frac{\psi_m \left(\frac{\rho_c}{g\gamma} \right)^{1/4}}{g} \right] \right\} \left\{ \left[U_d \left(\frac{\rho_c}{g\gamma} \right)^{1/4} \right]^{0.84} \exp \left[3.74 U_c \left(\frac{\rho_c}{g\gamma} \right)^{1/4} \right] \right\} \left\{ \left(\frac{\Delta\rho}{\rho_c} \right)^{-0.92} \right\} \left\{ 6.87 \left[\left(\frac{h}{1000} \right) \left(\frac{\rho_c g}{\gamma} \right)^{1/2} \right]^{-0.48} \right\} \quad (2.59)$$

The average absolute value of the relative error (AARE) was found to be 17.9%.

$$\text{where AARE} = \frac{1}{\text{NDP}} \sum_{i=1}^{\text{NDP}} \left(\frac{|\text{predicted value} - \text{experimental value}|}{\text{experimental value}} \right) \quad (2.60)$$

where NDP = number of data points

Kumar and Hartland (1995) showed that the above equation for the prediction of ϕ and the subsequent calculation of u_s is better than the correlation given by Slater (1985) (equation 2.50) in terms of the percentage error found for the two cases. The correlation was also tested and found satisfactory in a Karr column by Stella et al. (2008).

Camurdan et al. (1989) used equation 2.39 together with some mathematical manipulation (multiplying the numerator and denominator on the right hand side by $\phi^{2/3}$ and then taking the third power of the resulting equation) to develop a correlation for the prediction of holdup:

$$\left(\frac{U_c}{u^*}\right) = \frac{(1 - \phi)^6 \phi^2}{(1 - L)^3 \phi^3 + 3(1 - L)^2 \phi^2 + 3(1 - L)L^2 \phi + L^3} \quad (2.61)$$

The root ϕ could be sought from the above equation using the Newton-Raphson method by finding the initial estimate value of the holdup by the bisection method since the convergence is found to be sensitive to this value (Camurdan et al., 1989).

There was a good correlation between the theoretical model and experimental results of holdup, however, the data with mass transfer gave more scattered results. This is due to the fact that for mass transfer from the dispersed to continuous phase, the surface tension gradients formed around two approaching droplets (reduction in interfacial tension) causes a rapid drainage of the continuous phase which enhances coalescence. The holdup value at flooding is a function of only the ratio of the flow rates and not any physical properties and therefore this value would be the same with or without mass transfer. d_{32} was found to be much higher for mass transfer conditions than in the absence of mass transfer (Camurdan et al., 1989; Aravamudan and Baird, 1999). This was also observed by Shen et al. (1985).

Aravamudan and Baird (1999) state that the most successful correlation of holdup data is given by the slip velocity equation (equation 2.24) modified for reciprocating plate columns:

$$\frac{U_d}{\phi} + \frac{U_c + Af}{1 - \phi} = \frac{W_1 \phi}{1 - \phi} + W_2 \quad (2.62)$$

where W_1 and W_2 are adjustable velocity parameters.

The parameters were found to be greater in the presence of mass transfer than in the absence which is expected due to larger drop sizes.

Camurdan et al. (1989) came to the same conclusion as Baird and Lane (1973) showing that the equations tended to over predict the drop size at low agitation in the absence of mass transfer and as a result it under predicts the holdup. Baird and Lane (1973) suggested a value of $Af = 3$ cm/s as a lower limit for reasonable accuracy in the Karr column.

For reciprocating plate columns, the mass transfer effects under $d \rightarrow c$ conditions significantly increases the drop size and reduces the holdup compared to the behaviour in the absence of mass transfer.

The specific interfacial area in the emulsion regime is given by (Lo et al., 1992):

$$a = \frac{6\phi}{d_{32}} \quad (2.63)$$

From the above equation, it can be seen that the interfacial area will decrease resulting in a decreased mass transfer rate.

Jiricny et al. (1979a) stated that the specific holdup of the dispersed phase may vary by more than 100% along the length of the column accompanied by the variations in particle size distribution (for systems investigated with a stagnant continuous phase) (Sovova, 1983). They proposed a discrete stationary model for the flow of the continuous phase and the poly-dispersed phase taking into account the effects of forward flow, backflow, entrainment, splitting and coalescence, where the model was based on the idea of a plug flow continuous phase with a circulation superimposed. The model parameters were distributed with respect to position and particle size distribution. From the distributed model a lumped parameter model was derived that described the distribution of particle sizes. This model was limited to dispersions with a narrow distribution and either the backflow or entrainment must be zero or all fractions of sizes must be subject to the backflow.

Solution of the model showed that distinctly non-uniform holdup profiles may exist depending on flow rates, intensity of backflow and the rate of splitting and coalescence. Two distinct types of profiles may occur. The first one has a maximum holdup in the middle of the column with a monotonously decreasing profile while in longer columns, the maximum in the middle tended to level off and the decreasing profiles became more pronounced (Jiricny et al., 1979b). The shape of the profiles is highly influenced by the formation of fine droplets and their transport by the continuous phase. Because of these non-uniform profiles, high mean values cannot be obtained (Jiricny and Prochazka, 1980).

It is possible to increase the upper limit of the throughput by allowing for entrainment to take place where the fine fraction of the dispersed phase is entrained by the continuous phase. This backflow equalises the holdup profile and as a result increases limiting flow rates. Bimodal particle size distribution may prevail in the monotonous profile at the dispersed phase inlet due to accumulation of the fine fraction at this point. The distribution then gradually transforms to monomodal ones (Jiricny et al., 1979b).

Karr (1980) states that if the physical properties, especially density difference and interfacial tension, vary in different parts of the column (similar to that in a pulsed sieve-plate column (Bell and Babb, 1969)), then it is obvious that the agitation should vary as well to prevent these sections from severely limiting the throughput. The only way to change agitation intensity per unit volume is to change the tray spacing since the frequency and amplitude are fixed throughout the column. The optimum relative plate spacing in different parts of the column is given by the following relationship:

$$h \propto \frac{1}{(\Delta\rho)^{5/3}(\gamma)^{3/2}} \quad (2.64)$$

The plate thickness also has an effect on the holdup increasing with an increase in thickness. This is due to the fact that the contact time of the drops with the plate increases with thickness, decreasing the average velocity of the drops through the plates (Kostanyan et al., 1980).

2.9.3 Droplet Size

The following empirical equation was developed by Boyadzhiev and Spassov (1982) for the prediction of Sauter mean diameter for both pulsed columns and RPCs at high turbulent regimes:

$$d_{32} = (0.57 \pm 0.11) \left(\frac{\gamma}{\rho_c} \right)^{3/5} \frac{S_1^{4/5} d_0^{2/5}}{(2af)^{6/5}} \quad (2.65)$$

For the system acetone/toluene(dispersed)/water(continuous) in a RPC, Bensalem et al. (1986) found the following correlations for the effect of agitation rate ($Af = 2af$) on d_{32} (in c.g.s. units):

$$d_{32} = 0.56(Af)^{-0.59} U_c^{-0.164} \quad (\text{no mass transfer}) \quad (2.66)$$

The effect of dispersed phase superficial velocity was found to be negligible in the absence of mass transfer.

$$d_{32} = 0.757(Af)^{0.4} U_c^{-0.232} U_d^{0.414} \quad (d \rightarrow c \text{ transfer}) \quad (2.67)$$

$$d_{32} = 0.41(Af)^{-0.59} \quad (c \rightarrow d \text{ transfer}) \quad (2.68)$$

This correlation is similar to the one developed in the absence of mass transfer.

Rama Rao et al. (1991) found that the frequency of agitation had a significantly stronger effect on droplet size than the amplitude (due to the stronger effect of frequency than amplitude on hole velocity), and the data for a given flow rate and system could be correlated quite well with the product af^2 . The effects of the other variables could be included in the following empirical formula:

$$d_{32} = 0.001 \exp(-X) \quad (2.69)$$

where $X = 8.98 \times 10^{-5} af^2 d_0^{0.5} U_c^{-1.2} U_d^{-1.5} \Delta\rho^{-1} \gamma^{-0.4}$

From this relationship, it can be seen that a reduction in interfacial tension and/or a reduction in density difference results in smaller droplets. A reduction in buoyancy inhibits the formation of a discreet layer of droplets beneath the plates, which reduces coalescence opportunities and increases the residence time of droplets in the continuous phase Rama Rao et al., 1991).

Kumar and Hartland (1996) developed a unified correlation for the prediction of drop size in eight different types of columns (viz. Rotating disk, asymmetric rotating disk, Kuhni, Wirz-II, pulsed perforated plate, Karr reciprocating plate, packed, and spray columns). The correlation is made up of a two-term additive model that takes into account the ratio of interfacial tension to buoyancy forces at low agitation and isotropic turbulence at high agitation which is then extended to include the gravitational constant and tray spacing.

The unified correlation is given by (Kumar and Hartland, 1996):

$$d_{32} = C_\psi e^n \left[\frac{1}{\left[C_\Omega \left(\frac{\gamma}{\Delta\rho g} \right)^{0.5} \right]^2} + \frac{1}{\left[C_\pi \epsilon^{-0.4} \left(\frac{\gamma}{\rho_c} \right)^{0.6} \right]^2} \right]^{1/2} \quad (2.70)$$

The constants for the pulsed perforated plate column and the Karr column are given as follows:

$$\begin{aligned}
 C_{\Psi} &= 0.95 \quad \text{for } c \rightarrow d \text{ solute transfer} \\
 &= 1.48 \quad \text{for } d \rightarrow c \text{ solute transfer} \\
 C_{\Omega} &= 1.30 \\
 C_{\pi} &= 0.67 \\
 n &= 0.50
 \end{aligned}$$

The data fitted the correlation with an error, AARE = 19.7%

The error was reduced to 16.1% when the correlation was extended to include tray spacing and for the pulsed column and Karr column the equation becomes (Kumar and Hartland, 1996):

$$\frac{d_{32}}{h} = \frac{C_{\Psi} e^{0.32}}{\frac{1}{1.55 \left(\frac{\gamma}{\Delta \rho g h^2} \right)^{1/2}} + \frac{1}{0.42 \left[\left(\frac{\epsilon}{g} \right) \left(\frac{\Delta \rho}{g \gamma} \right)^{1/4} \right]^{-0.35} \left[h \left(\frac{\Delta \rho g}{\gamma} \right)^{1/2} \right]^{-1.15}}} \quad (2.71)$$

$$\begin{aligned}
 C_{\Psi} &= 1 \quad \text{for no mass transfer} \\
 &= 0.92 \quad \text{for } c \rightarrow d \text{ solute transfer} \\
 &= 1.67 \quad \text{for } d \rightarrow c \text{ solute transfer}
 \end{aligned}$$

NB. h is expressed in meters.

This correlation was also tested and found satisfactory in a Karr column by Stella et al. (2008).

Joseph and Varma (1998) calculated the geometric mean, d_{50} of droplets in a VPE by plotting the experimental values against the cumulative number of droplets (based on a percentage) and finding the corresponding diameter at 50% as well as the geometric standard deviation, δ . They found that there was a good correlation between d_{32} and d_{50} according to the following relationship:

$$\ln d_{32} = \ln d_{50} + 2.5 \ln^2 \delta \quad (2.72)$$

Usman et al., 2008 found a slightly different relationship:

$$\ln d_{32} = \ln d_{50} + 2.5 \delta^2 \quad (2.73)$$

where the standard deviation is given by:

$$\ln \delta = \exp \left(\sqrt{\frac{1}{n} \sum_i^n (\ln d_i - \ln d_{50})^2} \right) \quad (2.74)$$

After carrying out investigations in a reciprocating plate column, Joseph and Varma (1998) found that d_{32} decreases with an increase in the agitation level; it increases with an increase in U_d but is not influenced by U_c ; d_{32} also increases with the plate perforation diameter, plate free area and the plate spacing. Also, d_{32} decreases from the bottom to the top of the column in the mixer-settler region and is uniform for the entire column in the emulsion region. d_{32} was also influenced by the nature of solute and the direction of mass transfer.

NB. Equation 2.36 does not consider the effects of the variation of drop size with the vertical position in the column and the effect of the dispersed phase holdup on drop size. Aravamudan and Baird (1999) demonstrate an alternative approach for the prediction of drop diameter that considers the effect of holdup on the coalescence frequency.

$$d_{32} = \frac{1 + C_\phi \phi}{\left[\frac{1}{C_b \left(\frac{\gamma}{g \Delta \rho} \right)^{0.5}} + \frac{1}{C_t \left(\frac{\gamma}{\rho_c} \right)^{0.6} (\epsilon_d - \epsilon_m)^{0.4}} \right]} \quad (2.75)$$

According to this model, drop size varies inversely with the sum of two groups which represent buoyancy and agitation effects. The other difference between this equation and equation 2.36 is that it has 3 adjustable parameters whereas equation 2.36 only has one. Analysis showed that C_ϕ was statistically insignificant under non-mass-transfer conditions, but had a large value under mass transfer conditions, indicating a strong relationship between holdup and drop diameter (Aravamudan and Baird, 1999).

Kim and Baird (1976b) investigated the effect of hole size on the hydrodynamics of a Karr column and found that a reduction in hole diameter increases the mass transfer rate at the expense of throughput and the axial dispersion is not very high in either direction.

2.9.4 Flooding

There are two types of flooding in the reciprocating plate column; at low and zero agitation levels it can occur by the buildup of discrete layers of the phase preventing countercurrent flow, while at high agitation there is an entrainment type of flooding due to formation of excessive fine drops (Rama Rao et al., 1991).

Lo and Prochazka (1983) report the following semitheoretical equation for the prediction of flooding rates developed by Baird and colleagues:

$$1.5U_{dF} + U_{cF} = 0.0224 \left(\frac{\gamma^3}{\psi^2 \bar{\rho}} \right)^{0.2} \left(\frac{g^2 \Delta \rho^2}{\rho_c \mu_c} \right)^{1/3} \quad (2.76)$$

where ψ is given by:

$$\psi = \frac{2\pi^2}{3} \left(\frac{1-\sigma^2}{(h/1000)C_0^2\sigma^2} \right) \bar{\rho}(Af)^3 \quad (2.77)$$

Baird and Shen (1984) combined the two equations for slip velocity (equations 2.24 and 2.25) as follows:

$$u_k(1-\phi) = U_c \left(\frac{1}{1-\phi} + \frac{L}{\phi} \right) \quad (2.78)$$

where L = ratio of flow rates (U_d/U_c)

At flooding the holdup increased unstably. The flooding condition corresponds to:

$$\left(\frac{dU_c}{d\phi} \right)_F = 0 \quad \left(\frac{dU_d}{d\phi} \right)_F = 0 \quad (2.79)$$

These equations state that flooding will occur when U_d or U_c reaches a maximum with respect to holdup.

Solution of the above equations result in the following (shown also by Hafez et al., 1979, Kumar and Hartland, 1988 and Laddha and Degaleesan, 1983):

$$\phi_F = \frac{(L^2 + 8L)^{1/2} - 3L}{4(1-L)} \quad (2.80)$$

$$U_{cF} = u_k(1-\phi_F)^2(1-2\phi_F) \quad (2.81)$$

$$U_{dF} = 2u_k \phi_F^2 (1 - \phi_F) \quad (2.82)$$

These equations have been successfully applied to many columns including the rotating disc contactor, however, Baird and Shen (1984) showed that the concept of characteristic velocity requires some modification before it can be applied to RPCs. A model for the Karr column is proposed below.

Rearrangement and expansion of the slip velocity equations (equations 2.37 and 2.78) given by Baird and Shen (1984) in the holdup model is given below:

$$U_c = \frac{(1 - \phi)^2 u^*}{\phi^{1/3}(1 - L) + L\phi^{-2/3}} \quad (2.83)$$

The holdup will have to be obtained by trial and error for given values of the flow rates.

In the special case of flooding:

$$\left(\frac{dU_c}{d\phi} \right)_F = 0 \quad (2.84)$$

$$\text{Hence, } \phi_F = \frac{(9L^2 + 54L + 1)^{1/2} - 7L - 1}{10(1 - L)} \quad (2.85)$$

The holdup at flooding reaches a limit of 0.4 as $L \rightarrow \infty$.

Experimental measurements of holdup at flooding had to be obtained carefully because of the potential instability of the flow regime. Adaptation of equation 2.83 for the flooding

condition provides a relationship between the flow rate, the operating conditions and the system properties as follows:

$$U_{cF} = u^* \frac{(1 - \phi_F)^2}{\phi_F^{1/3} (1 - L) + L \phi_F^{-2/3}} \quad (2.86)$$

ϕ_F was plotted against L and dimensionless U_{cF}/u^* was plotted against L and good correlations were obtained with the experimental data. The model calculation sequence is given below (fig. 2.14):

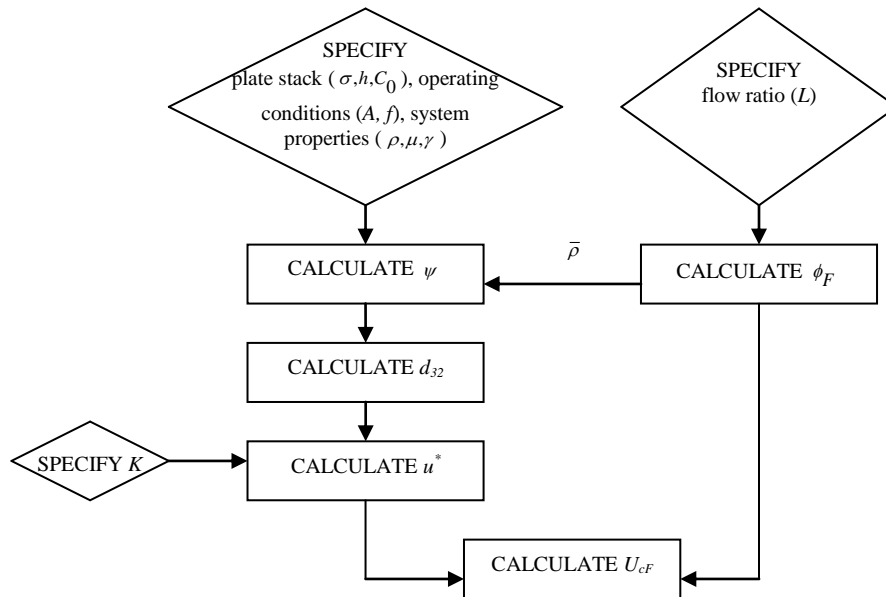


Fig. 2.14 Calculation sequence for flooding (Baird and Shen, 1984)

Baird and Shen (1984) found good correlation between the model prediction of U_{cF} and the observed value for cases where no mass transfer occurred and where mass transfer occurred in the $c \rightarrow d$ direction. However, in the $d \rightarrow c$ direction, the model seemed to under-predict the velocity and this was assumed to be due to the enhanced coalescence effects in the $d \rightarrow c$ direction of mass transfer. The holdups were found to be reduced for this direction of mass transfer as well. There was, however, an indication that the effect of $d \rightarrow c$ mass transfer decreases at higher agitation levels.

Rearrangement of the equations used by Hafez et al. (1979) at flooding (equation 2.37):

$$u_{sF} = \left[\frac{(1-\phi)^3}{K\phi_F^{0.5}} \right]^{2/3} d_{32} \left[\frac{g^2 \Delta\rho^2}{\rho_c \mu_c} \right]^{1/3} \quad (2.87)$$

which shows that u_{sF} is proportional to $(1-\phi)^2$ instead of $(1-\phi)$ as suggested by Baird and Shen (1984).

Using the definition for d_{32} (equations 2.33 and 2.34), equation 2.87 becomes:

$$u_{sF} = 01126 \frac{(1-\phi_F)^2}{K^{2/3} \phi_F^{1/3}} \left[\frac{\gamma^3 \sigma^4 (h/1000)^2}{\bar{\rho}^3 (Af)^6 (1-\sigma^2)^2} \right]^{0.2} \left[\frac{g^2 \Delta\rho^2}{\mu_c \rho_c} \right]^{1/3} \quad (2.88)$$

This equation is restricted to well-agitated systems in which the drop size is predominantly determined by turbulence conditions ($Af > 3$ cm/s).

A test of this correlation was shown by Hafez et al. (1979) by plotting the observed u_{sF} from the values of U_{cF} and U_{dF} against the right hand side of the above equation. A 45° line would indicate proper correlation and a good correlation was obtained.

Slater (1985) derived the flooding conditions as follows:

$$U_{dF} = (m+1)u_k (1-\phi_F)^m \phi_F^2 \quad (2.89)$$

$$U_{cF} = u_k (1-\phi_F)^{m+1} [1 - (m+1)\phi_F] \quad (2.90)$$

$$L = \frac{(m+1)\phi_F^2}{(1-\phi_F)(1-\phi_F-m\phi_F)} \quad (2.91)$$

Rearranging the above to give a quadratic in ϕ_F will provide ϕ_F with a unique solution:

$$\phi_F = \frac{-L(m+2) + [L^2(m+2)^2 + 4(m+1)(1-L)L]^{1/2}}{2(m+1)(1-L)} \quad (2.92)$$

2.10 Entrainment

Rama Rao et al. (1991) found that entrainment is zero at low agitation levels until a threshold is reached and then increases with agitation. The entrainment problem could be reduced by the addition of coalescence plates at the base of the plate stack (possibly below the dispersed phase distributor).

2.11 Power Requirement

The power requirement of the RPC is clearly less than that of a pulsed plate column of equal size. In a pulsed extractor the entire volume of fluid in the column must, during one half of every pulsation cycle, be raised to a height equal to twice the pulse amplitude, whereas in the reciprocating plate extractor only the set of plates is raised and their weight is only a small fraction (say about 10%) of the weight of the liquids. Also, in pulsed columns the entire charge of liquid must be accelerated, whereas in the reciprocating-plate column only the liquid in the immediate vicinity of the plates is accelerated. Finally, the passages for the continuous phase, which are an essential feature of the VPE, significantly reduce the frictional losses in flow through the plates (Prochazka et al., 1971).

Rama Rao et al. (1991) tried to use the following equation to estimate the time-average power dissipation assuming quasi-steady (fully developed) flow for sinusoidal oscillations:

$$\bar{P} = \frac{16\pi^2}{3} \rho N A_c \left(\frac{1 - \sigma^2}{C_o \sigma^2} \right) (af)^3 \quad (2.93)$$

According to this equation, a logarithmic plot of \bar{P} versus af should produce a straight line with a slope of 3. However, the experimental data did not match the prediction. The data better suited a logarithmic plot of \bar{P} versus af^2 with a slope of 2.2.

2.12 Experimental Procedures

2.12.1 Holdup

Baird and Shen (1984) used the method of displacement to evaluate the holdup of the column. The column operation was allowed to reach steady state. The interface level was marked and feed pumps and the drain pump as well as the feed valves and the drain valves were shut off simultaneously. Enough time was allowed for the dispersed phase to coalesce under the marked interface level. The continuous phase was pumped into the column in order to displace the coalesced dispersed phase into a measuring cylinder until the interface returned to the marked level. The effective volume of the column was measured from the dispersed phase distributor to the interface. Volume fraction holdup ϕ was calculated as the volume in the cylinder over the effective volume of the column.

Local holdup was obtained by rapidly removing about 200 ml of the dispersion from 2 sampling points along the length of the column after steady state operation was achieved. The dispersed phase content was then found volumetrically; however, Baird and Lane (1973) found that the measurements of local holdup were highly sensitive to the sampling rate.

Another way of measuring the holdup is to allow the column to first reach steady state, and then to measure the amount of toluene in the upper tank between the interface and the surface of the toluene layer. Both the water feed line and the toluene feed line must be closed simultaneously. The contents of the column should be drained from the bottom of the tank. The amount of toluene present could then be measured and the amount that was present in

the top layer could be subtracted from this value. The holdup is then reported as the fraction of toluene in the continuous phase (ppm) (Rama Rao et al., 1991).

Baird and Lane (1973) performed experiments on a system where the dispersed phase moved down the column and the interface was located at the bottom of the extractor. The overall holdup was evaluated by shutting off the flows and allowing the dispersed phase droplets to fall to the interface. The resulting increase in interface level in relation to the volume of the column between the initial interface and the top of the agitated section was used to determine the overall holdup.

In order to investigate the effects of the operating variables on the holdup, the following tests could be done. Perform experiments at zero continuous flow and a constant dispersed flow for different agitations (products of af). Plot holdup, ϕ against af for different values of frequency. Perform experiments at a fixed value of continuous flow and dispersed flow. Again plot holdup, ϕ against af for different values of frequency. Perform experiments for a fixed value of continuous flow and varying values of dispersed flow. Then perform experiments for a fixed value of dispersed flow and varying values of continuous flow (Rama Rao et al., 1991).

Jiricny and Prochazka (1980) measured local holdups in a Karr column in order to evaluate the holdup profiles of the column. Their measurement was based on the determination of differences in static pressure across short sections of the column. After every 2 stages, a differential pressure induction transducer connected to pressure taps along the column measured pressure differences and related this to holdup in that section of the column.

2.12.2 Droplet Size Distribution

A section of the column was photographed towards the middle of the column during steady state operation. The photographed section must be surrounded by a rectangular water-filled (continuous phase) box made of clear (Perspex) plastic to eliminate refractive distortion. A particle size counter was used to measure the drop size distribution. The distribution could then be used to calculate the Sauter mean drop diameter. (Baird and Lane, 1973; Rama Rao

et al., 1991). Jiricny and Prochazka (1980) photographed sections of the column and evaluated the particle size distribution by analysing between 300 and 500 drops per photograph whereas Bensalem et al. (1986) felt that analysing 200 droplets was sufficient.

2.12.3 Entrainment

Since toluene is completely immiscible in water, a sample is taken from the bottom of the column during normal operation. The sample is allowed to settle. The amount of toluene could be measured with a measuring cylinder and reported as ppm of toluene in sample.

2.12.4 Power Consumption

An approximate indication of the power consumption could be obtained by connecting an A.C. voltmeter in parallel with an A.C. ammeter in series with the line to the vibration motor. The data should be corrected by subtracting the measured power when the column was run dry at the same amplitude and frequency (Rama Rao et al., 1991).

2.12.5 Axial Mixing

Hafez et al. (1979) used two methods for measuring the axial mixing in the continuous phase. The first method was used by Kim and Baird (1976a) in which a single pulse of sodium hydroxide solution was injected into the column at four points around the wall about 50 cm below the top of the plate stack. It then reacted with dilute hydrochloric acid in the aqueous phase in the presence of a phenolphthalein indicator. The rate of color migration can then be related to the axial dispersion coefficient. This method is suitable only when no circulation currents exist.

The second technique uses a conventional pulse injection of a salt tracer solution (NaCl or NH₄Cl) with the response being measured by a conductivity cell fed through a thin capillary line from a point near the base of the plate stack, a fixed distance below the injection point.

Karr et al. (1987) used a tracer of 9 mass % ammonium chloride in water. Methanol was added to bring the density of the tracer close to that of water (within 1%). The tracer was injected pulse-wise at the desired aqueous and organic flow rates. Responses in the aqueous phase were measured by electrical conductivity probes.

2.12.6 Concentration Analysis

Bensalem et al. (1986) evaluated the outlet concentration of the aqueous phase for the acetone-toluene-water system by a density meter and found that steady state was reached for the Karr column after the contents of the column had been replaced at least five times.

Lisa et al. (2003) and Vatanatham et al. (1999) investigated the mass transfer resistance for the toluene-acetone-water system and used the refractometric method to determine the acetone concentration at the entrance and exit of both phases.

Most other researchers used chromatographic analysis.

2.12.7 Use of Radiotracers for Evaluation of Axial Dispersion, Holdup and Slip Velocity

Din et al. (2008) states that the use of a non-radioactive tracer for the evaluation of axial dispersion or shutting off flows in order to measure holdup has many disadvantages including low sensitivity, poor statistics, the requirement of phase separation before measurements are made and that the plant must be shut down in order to measure the holdup of the dispersed phase. They used a radioisotope in a pulsed sieve plate extractor to overcome these shortcomings. ^{99m}Tc in the form of sodium pertechnetate was used as a radioactive tracer injected into the column. Axial dispersion, holdup and slip velocity was measured online by monitoring the movement of the tracer in the column and analysing the residence time distribution.

2.13 Drop Dispersion and Coalescence

Coalescence has been shown to have a considerable effect on the fundamental mass transfer process as compared to its effects on drop size, holdup of dispersed phase and interfacial area for mass transfer. The mechanism for mass transfer shows its dependence on drop size varying from molecular diffusion for small drops (which behave as rigid spheres) to the development of internal droplet circulation, oscillation and turbulent eddy transfer mechanisms as the drop size is increased (Komasawa, 1978).

Komasawa (1978) showed that for single drops (where no coalescence takes place) the overall mass transfer coefficients for the toluene-acetone-water system, with solute transfer from the continuous to dispersed phase, agree well with rigid drop behaviour in the case of small drops. For larger drops, the overall mass transfer coefficients for both directions of mass transfer lie between the predicted values for circulating drop behaviour. The coefficients for the transfer from continuous to dispersed phase appear to be higher but the differences are small. Thus, the large difference in the mass transfer coefficient is brought about by differences in drop size.

Komasawa (1978) also showed that there is a large difference in mass transfer coefficients for swarms of drops (in a Oldshue-Rushton column) determined mainly by the differences in drop size rather than any enhancement of mass transfer rate due to surface instability. A critical drop size in the range 0.1 to 0.2 cm corresponds to the occurrence of liquid motion within the drops. For drops as small as 0.15 cm, turbulent flow conditions inside the drops are unlikely to occur and only some limited circulation is to be expected.

When extraction occurs in columns where there is drop-drop interaction, the effect of instability of the interface occurs and affects the mass transfer. Depending on the direction of solute transfer, the hydrodynamics of the dispersed phase and especially the drop size varies in a manner which either increases or suppresses the system coalescing properties. The drop size is the main factor and the size usually encountered is close to the critical size over which internal flow inside the drops will develop. Therefore mass transfer characteristics are determined more by the effects of interfacial instability of the dispersed phase hydrodynamics rather than the direct enhancement in the rate of mass transfer resulting from

interfacial instability or micro motion of the liquid at the vicinity of the interface (Komasawa, 1978).

For dispersion in a sieve tray column, the drop size of the dispersion is proportional to the hole diameter. The drop diameter decreases linearly until the critical hole diameter of 0.25 cm and then decreases steeply beyond this point. The characteristic velocity shows a similar profile at the same hole diameter (Laddha and Degaleesan, 1983).

The breakup of drops occurs by the mechanism of drop detachment at a perforation during the mixer-settler regime. The impact of turbulent eddies on drops cause the breakup in the emulsion regime (Lo et al., 1992).

Ban et al. (2000) investigated the time it takes for coalescence to take place in the toluene-acetone-water system. They found that the average coalescence time decreases with increasing acetone concentration when mass transfer takes place from the dispersed to the continuous phase. The droplets start oscillating when the concentration is high and this restrains coalescence. When the transfer is from continuous to dispersed phase, the coalescence is retarded. At low concentration, the coalescence behaviour can be explained from the difference in local interfacial tension by estimating the concentration profile within the droplets.

Mass transfer in extraction columns occur during drop formation and drop coalescence as well as during drop ascent/descent which all follow different mechanisms of mass transfer. All of the mechanisms are affected by the influences of undetectable or uncontrollable variables such as contamination or wettability which may be considerable. As a result the mass transfer coefficients having an error of about 10 – 20% have to be accepted (Brodkorb et al., 2003).

2.14 Interfacial Resistance

Lisa et al. (2003) investigated the mass transfer resistances for the toluene-acetone-water system across a flat interface and found that there was an existence of interfacial resistance in the order of 10^3 s/m. The resistance was greater in the phase in which the equilibrium solute concentrations have a smaller value (organic phase for toluene-acetone-water system) regardless of the transfer direction and mixing intensity and generally had a lower value for the transfer of solute from the phase with the lower equilibrium concentration to that with a larger equilibrium concentration (aqueous to the organic phase). As a result Lisa et al. (2003) recommends that the phase with the lowest equilibrium concentration (that is with higher resistance) should be selected as the continuous phase because the mixing would be more intensive.

2.15 Marangoni Effect

In terms of thermodynamics, it generally means that when two liquids come into contact with each other, every interface will tend towards a state of lower surface tension and will attain this state by increasing the area which exhibits the lower interfacial tension. In other words, a liquid with low surface tension spreads on liquids with high surface tension (Pertler, et al., 1995).

Marangoni convection plays an important role in small systems, like thin liquid films and droplets, and is the dominant transfer mechanism under zero-gravity conditions (Arendt and Eggers, 2007). If Marangoni convection exists, the mass transfer coefficient is considerably increased; the coefficient depends on the concentration difference, the properties of the phase interface, like interfacial tension, and the direction of the transfer; the equation for pure diffusion cannot be used to calculate the mass transfer coefficient if the concentration difference goes above a critical value.

Arendt and Eggers (2007) derived an equation to calculate the mass transfer coefficient due to Marangoni convection as follows:

$$k_m = \sqrt{\frac{D}{\pi t} \frac{\gamma_{ref} - \gamma_{eq}}{\gamma_{ref}}} \frac{d}{(h/1000)} \quad (2.94)$$

where t is the contact time.

Arendt and Eggers (2007) carried out tests to investigate the Marangoni effect for the toluene-acetone-water system. In their experiments, the aqueous phase was dispersed.

The following simplified equations were used to calculate the mass transfer coefficient in the dispersed phase. For an internally stagnant droplet where the mass transfer resistance in the continuous phase may be neglected and for long contact times:

$$k_d \approx \frac{2\pi^2}{3} \frac{D_d}{d} \text{ or } Sh_d \approx 6.58 \quad (2.95)$$

For circulating droplets with negligible outside resistance and long contact times:

$$k_d \approx 17.9 \frac{D_d}{d} \text{ or } Sh_d \approx 17.9 \quad (2.96)$$

The critical drop diameter, above which interfacial convection and oscillating convection is expected was calculated using the following equations:

$$d_{crit} = 0.33 \rho_c^{-0.14} \Delta \rho^{-0.43} \mu_c^{0.3} \gamma^{0.24} \quad (2.97)$$

where d_{crit} was found to be 4.1 mm

$$\text{and } d_{crit} = 0.162 \left(\frac{\rho_d}{\Delta\rho} \right)^{0.5} \quad (2.98)$$

where d_{crit} was found to be 4.4 mm

In their experiments the drop diameters were below this value for the $c \rightarrow d$ (toluene to water) direction of mass transfer and as a result oscillating droplets and the Marangoni effect were unlikely to occur probably due to the flat interface. However, they do state that studies show that these effects do take place for this system since it is affected by the shape of the interface and the relative movement of the phases (Arendt and Eggers, 2007).

For the $d \rightarrow c$ (water to toluene) transfer, there is evidence of the Marangoni effect and the mass transfer should be calculated by the model of an internally circulating droplet at long contact times superimposed by the model for Marangoni convection. The mechanisms can be calculated separately. The Marangoni effect increases with an increase in the amount of solute in the feed.

Drop sizes are usually much larger when mass transfer occurs from the dispersed to the continuous phase due to Marangoni effects (Bensalem et al., 1986).

2.16 Direction of Mass Transfer

The direction of solute transfer affects the droplet coalescence characteristics as well as the mean drop size, holdup and characteristic velocity due to Marangoni effects and other interfacial instabilities. During the $d \rightarrow c$ transfer, the mean drop size is increased resulting in a decrease in holdup and increase in settling velocity or characteristic velocity (Laddha and Degaleesan, 1983).

The interfacial tension between continuous and dispersed phase is lowered by solute (Laddha and Degaleesan, 1983). When acetone is transferred from toluene (dispersed) to water

(continuous) the interfacial tension is lowered in the film leading to greater drainage in the film and enhanced coalescence which leads to smaller droplets as shown in fig. 2.15(a). When acetone moves from the water to toluene, the interfacial tension is higher drawing in the continuous phase and counteracting the tendency of drainage of the film and coalescence is retarded which results in larger drops (fig. 2.15(b)). In the absence of mass transfer, intermediate coalescence occurs resulting in medium sized drops (Bensalem et al., 1986; Laddha and Degaleesan, 1983; Kumar and Hartland, 1996).

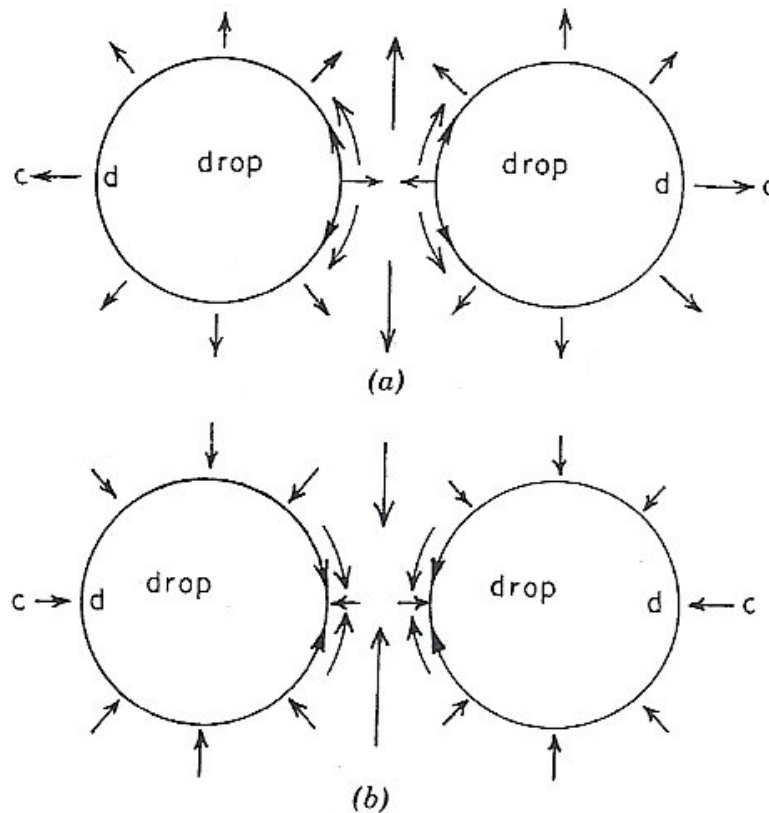


Fig. 2.15 Effect of solute transfer on coalescence (Laddha and Degaleesan, 1983)

(a) $d \rightarrow c$ transfer; (b) $c \rightarrow d$ transfer

During transfer of acetone from the toluene phase into the aqueous phase, a stable density profile (interfacial stability) is obtained. For transfer in the opposite direction, an unstable density profile (interfacial instability) is obtained (Pertler et al., 1995; Komasaawa, 1978).

Traditional diffusive transport theories are based on the assumption that equilibrium conditions exist at the two-dimensional phase boundary and no resistance to mass transfer occurs at the boundary. However, the phase boundary should be regarded as a three-dimensional area with independent physical characteristics. Therefore, transport mechanisms within the phase boundaries must be taken into consideration. In connection with instabilities, when two liquid phases are brought into contact during extraction, the two bulk phases are directly mixed which causes an increase in mass exchange (Pertler et al., 1995).

Within a stable density profile (transfer of acetone from toluene to water), the intensity and occurrence of macroscopic visible eddies depend on the concentration difference and flow conditions of the bulk phases. When these eddies fade away, further mass transfer occurs across the boundary causing a rapid equalisation in the area of the phase boundary (compared with diffusive transport in the bulk phases) which suggests that another transport mechanism exists during this phase. This small scale eruptional movement was detected intermittently only during the early stages of contact. Mass transfer across the phase boundary is then limited by transport in the bulk phases where a simple model such as the two-film model (presupposes equilibrium and negligible mass transfer resistance at the boundary) could be used to model the mass transfer (Pertler et al., 1995; Komasaawa, 1978).

During mass transfer of acetone from water to toluene phase, an unstable density profile exists. Intensive turbulence appears within the phase boundary as well as intensive convective mixing of the bulk phases resulting in fast equilibration (Pertler et al., 1995).

For the toluene-acetone-water system, Saien et al. (2006) found that the rate of mass transfer was greater in the dispersed to continuous phase direction.

Shen et al. (1985) investigated the system *n*-butyric acid/kerosene (dispersed)/water (continuous) in a Karr column and found that H_{ox} was much greater for $d \rightarrow c$ transfer than for $c \rightarrow d$ transfer. This is due to the mass transfer-induced coalescence effects in the $d \rightarrow c$ case which is responsible for larger drop size, lower holdup and greatly reduced mass transfer performance. This disadvantage is partly offset by larger throughputs at a fixed agitation level or by higher agitation levels being allowed (before flooding takes place) for

the $d \rightarrow c$ case. This reduces H_{ox} , however the axial mixing effects are quite severe at this higher frequency level.

Aravamudan and Baird (1999) investigated the system i-propanol/Isopar M (dispersed)/water (continuous) in a Karr column and came up with similar conclusions i.e. that d_{32} is much higher during mass transfer than in the absence of mass transfer and that d_{32} is larger for mass transfer in the $d \rightarrow c$ case.

2.17 Extractor Performance in Terms of Number and Height of Transfer Units

Contactor performance may be expressed either in terms of theoretical (ideal) stages or in terms of transfer units. The theoretical stage concept usually applies to mixer-settler type contactors only while the transfer unit concept usually applies to differential columns. However, agitated compartmental columns (e.g. VPE and RPC) form an intermediate class and can be treated in terms of either concept (Pratt, 1983a).

The size of an extractor is related to the compromise between solvent/feed ratio and the number of stages. The minimum solvent/feed ratio is that which would create a pinch point in the calculations resulting in an infinite number of stages being required to perform the extraction. The extraction factor (based on solute-free flows) given below is the driving force for the mass transfer (Robbins, 1996).

$$E = m \frac{S'}{F'} \quad (2.99)$$

The minimum solvent/feed ratio will be given by $1/m$ corresponding to $E = 1$ (Robbins, 1996).

By plotting the equilibrium relationship on a solute-free basis the equilibrium line will be straight and calculations similar to the McCabe-Thiele method are possible. By stepping off between the operating line and equilibrium line, the theoretical number of stages may be

evaluated (Robbins, 1996). The plug flow case is shown in fig. 2.16 while the effect of axial mixing is discussed later.

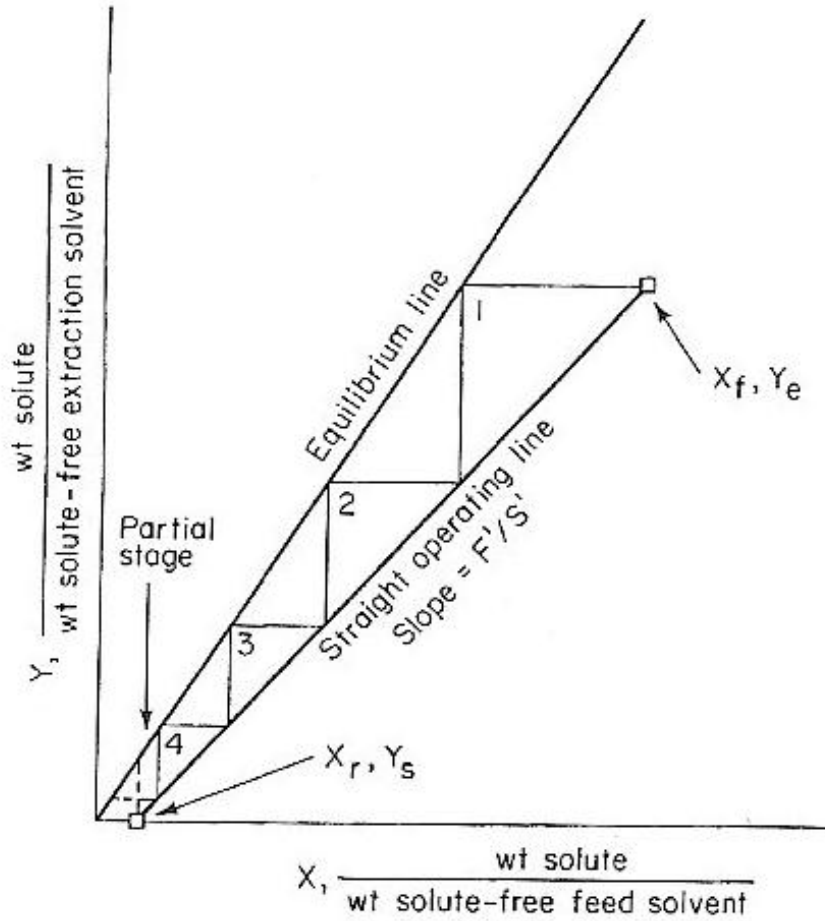


Fig. 2.16 Equilibrium number of stages (plug flow) (Robbins, 1996)

For immiscible solvents, $F' = R'$ and $S' = E'$. A material balance around the feed end of the column down to any stage n will be given by (Robbins, 1996):

$$Y_{n+1} = \frac{F'}{S'} X_n + \frac{S' Y_E - F' X_F}{S'} \quad (2.100)$$

and a material balance around the raffinate end of the column up to any stage n will be given by:

$$Y_n = \frac{F'}{S'} X_{n-1} + \frac{S'Y_S - R'X_R}{S'} \quad (2.101)$$

The overall material balance will be given by (Robbins, 1996):

$$Y_E = \frac{F'X_F + S'Y_E - R'X_R}{E'} \quad (2.102)$$

When the equilibrium and operating lines are both straight, the number of stages may be given by the Kremser equation (Robbins, 1996):

$$NTU_{theoretical} = \frac{\ln \left[\left(\frac{X_F - Y_S/K_S}{X_R - Y_S/K_S} \right) \left(1 - \frac{1}{E} \right) + \frac{1}{E} \right]}{\ln E} \quad \text{for } E \neq 1 \quad (2.103)$$

$$N_{ox} = \frac{\ln \left[\left(\frac{X_F - Y_S/K_S}{X_R - Y_S/K_S} \right) \left(1 - \frac{1}{E} \right) + \frac{1}{E} \right]}{1 - 1/E} \quad (2.104)$$

based on overall driving force in the dispersed phase for $E \neq 1$

$$NTU_{theoretical} = N_{ox} = \frac{X_F - Y_S/K_S}{X_R - Y_S/K_S} - 1 \quad \text{for } E = 1 \quad (2.105)$$

Usman et al. (2006) showed that there are basically 3 types of number of transfer units, depending on the nature of the concentration profile along the column. The first is the true number of transfer units, N_{ox} , which is the true overall number of transfer units based on the x phase:

$$N_{ox} = \frac{k_{ox} a H}{U_c} \quad (2.106)$$

The measured number of transfer units is defined as follows:

$$N_{oxm} = \int_{x_i}^{x_o} \frac{dx}{x_e - x} \quad (2.107)$$

Where x_o is the outlet concentration of solute in the x phase, x_i is the inlet concentration and x_e the equilibrium concentration.

The third type of number of transfer units can be calculated graphically or by numerical integration of equation (2.107). This apparent number of transfer units assumes that both the phases move in plug flow (piston flow) and that the equilibrium line and operating line are straight (Usman et al., 2006):

$$N_{oxp} = \frac{1}{[(y_i - y_o)/m(x_o - x_i)] - 1} \ln \frac{(y_i - mx_o)}{(y_o - mx_i)} \quad (2.108)$$

where the subscripts i and o refer to the inlet and outlet concentrations, respectively of the x and y phases.

Pratt (1983a) defines another type of number of transfer units i.e. the number of transfer units per stage which is given by:

$$N_{ox,P}^1 = \int_{c_{x2}}^{c_{x1}} \frac{dc_x}{c_x - c_x^*} = \frac{c_{x1} - c_{x2}}{(c_x - c_x^*)_{lm}} = \frac{k_{ox}ah}{U_x} \quad (2.109)$$

Where the subscript P refers to plug flow and the subscripts $x1$ and $x2$ refer to the inlet and outlet concentrations of a particular stage; $(c_x - c_x^*)_{lm}$ is the logarithmic mean of $(c_{x1} - c_{x1}^*)$ and $(c_{x2} - c_{x2}^*)$.

Shen et al. (1985) calculated NTU values for a Karr column and corrected them for axial mixing to calculate the true number of transfer units (N_{ox}). The true height of transfer units (H_{ox}) was calculated from the following equation:

$$H_{ox} = H/N_{ox} \quad (2.110)$$

H_{ox} is a direct measure of the mass transfer product and is different from H_{oxp} , which is obtained from the observed exit concentrations assuming plug flow for each phase. Due to axial mixing in the columns, H_{ox} is always less than H_{oxp} with the difference increasing as agitation levels are increased due to the fact that as agitation increases so does the axial mixing effects.

Shen et al. (1985) investigated the system *n*-butyric acid/kerosene (dispersed)/water (continuous) in a Karr column and tested the effects of using a full stainless steel plate stack (not wet by the dispersed phase) compared to replacing some of the steel plates with Teflon plates. This increased the dispersed phase wetting effect of the plates which had the effect of increasing H_{ox} , increasing the agitation level at which flooding occurred and increasing the throughput at which flooding occurred. This is due to the effect of drop-plate coalescence rather than drop-drop coalescence.

The number of stages for the plug flow case may be calculated from experimental values as follows:

Aravamudan and Baird (1999) investigated the system *i*-propanol/Isopar M (dispersed)/water (continuous) in a Karr column and showed that in the absence of axial dispersion in the dispersed phase, the steady state differential material balance is given by:

$$U_d dc_d = -k_{od} a (c_d - c_d^*) dz \quad (2.111)$$

For a straight line equilibrium relationship passing through the origin ($c_d^* = mc_d$):

$$U_d dc_d = -k_{od} a c_d (1 - m) dz$$

Integrating the above equation between the following limits:

$$\text{At } z = 0, c_d = c_{do} \text{ and at } z = H, c_d = c_{dH}$$

$$\text{Then } c_{dH} = c_{do} \exp(-N_{od}(1 - m))$$

$$N_{od} = \frac{k_{od} a H}{U_d} = \frac{\ln\left(\frac{c_{do}}{c_{dH}}\right)}{1 - m} \quad (2.112)$$

This equation may then be used to calculate the number of transfer units from experimental values of c_{do} and c_{dH} . Two methods were used to calculate the N_{od} as it was assumed that there may have been an entrainment of microdrops of water (which could hold a significant amount of solute) in the raffinate stream because of the low values of raffinate concentration being obtained. In the first method the directly measured value of c_{dH} was used in equation 2.112 whereas in the second method c_{dH} was calculated from a solute material balance (Aravamudan and Baird, 1999).

A well known concept to estimate the interfacial area of a droplet dispersion is:

$$a = \frac{6\phi}{d_{32}} \quad (2.113)$$

Combining equations 2.113 and 2.114, the overall mass transfer coefficient may be calculated from experimental values of the holdup and Sauter mean diameter (Aravamudan and Baird, 1999):

$$k_{od} = \frac{N_{od} U_d}{a H} = \frac{N_{od} U_d d_{32}}{6\phi H} \quad (2.114)$$

Aravamudan and Baird (1999) compared the calculated values of mass transfer coefficients with 4 different models and found that the experimental values followed the same trend as the oscillation drop model by Handlos and Baron (Pratt, 1983b) given below, although the model over predicts the values slightly:

$$Sh = \frac{0.00375Pe^*}{1 + \mu_d/\mu_c} \quad (2.115)$$

2.18 Longitudinal Mixing and Backflow

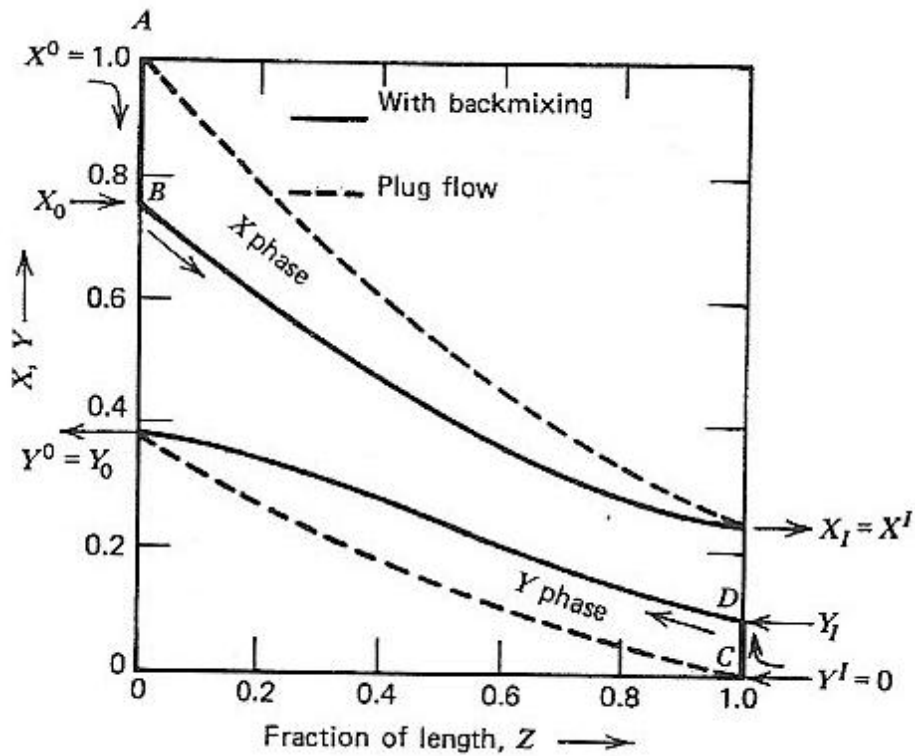
Mechanical agitation or pulsation in extraction equipment generates a larger interfacial area, however it increases the axial mixing in the phases and lowers the driving force available for mass transfer. Under piston flow conditions the driving force is estimated as the logarithmic mean concentration difference, however, if axial mixing is not taken into account, this leads to an overestimation of the driving force resulting in the mass transfer coefficient being lower than when axial mixing is considered (Kannan et al., 1990; Baird, 1974).

In the early years (until about 50 years ago), counter current extraction columns were designed on the basis of ideal “plug flow” in each of the phases. Then it was realised that the effects of axial mixing, mainly in the continuous phase, leads to significantly non-ideal flow, which reduces the driving force for countercurrent mass transfer. The Karr column is an example of a column without well-defined compartments or stages and for these types of columns axial mixing is characterized by the axial dispersion coefficient, e_t . The axial dispersion coefficient in the continuous phase, e_c is usually quite large for unagitated columns because of the channelling effect of the dispersed phase. As agitation is increased, e_c goes through a minimum value, and then at higher values of agitation e_c increases (Aravamudan and Baird, 1999).

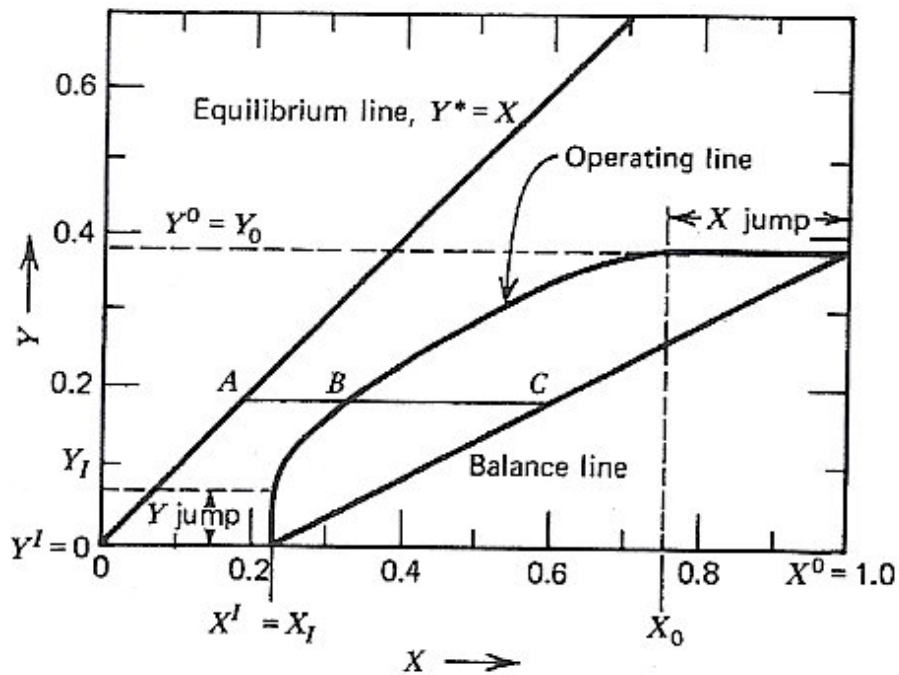
Kim and Baird (1976a) states that the maximum effectiveness of mass transfer in agitated columns is often found well below the flooding point due to the fact that as agitation is increased, the beneficial effect of increased interfacial area is offset and eventually reversed by axial dispersion. The effect of axial dispersion is the reduction of the axial concentration

gradients in each phase. In the limiting case of high axial dispersion, perfect mixing exists in each phase resulting in only one equilibrium stage being obtained.

The following figures show the effects of backmixing on the concentration profiles (fig. 2.17(a)) and the operating line (fig. 2.17(b)) (Pratt and Baird, 1983).



(a)



(b)

Fig. 2.17 Effects of Backmixing (Pratt and Baird, 1983)

(a) – Effect of Backmixing on Concentration Profile

(b) – Effect of backmixing on the operating line

The effect of backmixing is indicated in fig. 2.19 (a) by the concentration jumps AB and CD at the X and Y phase inlets and the zero slopes at the exits which have the effect of reducing the concentration difference between the phases resulting in more transfer units being required as compared to the plug-flow case.

The inlet concentration jumps are also indicated in fig. 2.19 (b) showing the effect on the operating line. The true operating line has a displacement from the plug flow operating line (also called the balance line – represents overall material balance of the extractor). The effect of backmixing is also indicated in the reduction of the driving force based on the X phase from AC to AB in fig. 2.19 (b).

Prochazka et al. (1971) have developed a procedure for determining the effect of back-mixing on the stage efficiency, η . They have developed an equation that gives the relative increase in the number of actual stages, i.e. the relative increase in the length of the column required, due to the effect of back-mixing. A simplified form of the equation is given below when the extraction factor does not differ much from unity and when there is no back-mixing in the raffinate phase:

$$\frac{n_s}{n_{si}} = 1 + (0.95\eta^{1.5} + 0.07)e \quad (2.116)$$

Where, n_s = number of actual stages

n_{si} = number of actual stages required at zero back-mixing

η = stage efficiency

e = coefficient of back-mixing in the continuous phase

Usually η does not exceed 0.5. Therefore, for values of the back-mixing coefficient less than 0.5, the relative increase of the column will not exceed 20%.

Back-mixing in the dispersed phase is negligible. Prochazka et al. (1971) showed that e increased linearly with an increase in the product of amplitude and frequency; e decreased exponentially with an increase in flow rates; e decreased linearly with an increase in plate spacing (Prochazka, et al., 1971).

Nemecek and Prochazka (1974) studied the effects of longitudinal mixing and backflow of the dispersed phase through the plates using tracer tests and found that the intensity of longitudinal mixing was characterised as the result of the action of a driving force (concentration gradient of a given phase in the direction of the column axis) and a resistance (divided into the resistance to transport through the plate and that within the stage). The backflow model (discussed later) takes into account the first resistance only while the differential model (discussed later) takes into account only the second resistance. Both resistances must be taken into account to properly account for longitudinal mixing. The

resistance within a stage is strongly affected by the distance from the plates and is therefore a function of the intensity of vibrations, plate geometry, plate spacing and the character of the flow of the dispersed phase which affects the longitudinal mixing of the continuous phase. Nemecek and Prochazka (1974) also specify that the intensity of longitudinal mixing of the continuous phase in the presence of the dispersed phase is very different from that of single phase flow and therefore caution should be exercised when using single phase flow correlations to predict longitudinal mixing.

Heyberger et al. (1983a) showed that the backmixing in the dispersed phase is negligible and that for the prediction of the concentration profiles in a VPE, variable backmixing coefficients must be considered as a constant value does not predict the profiles accurately.

Density gradients have a significant effect on axial mixing especially during mass transfer. Baird and Rama Rao (1991) performed experiments on a Karr column and evaluated the effect of temperature profiles (for hot and cold water mixing) and concentration profiles (for mixing of water and salt solutions) on axial dispersion coefficients. Axial dispersion was shown to increase strongly for the unstable density case (Baird and Rama Rao, 1991; Holmes et al., 1991). For a concentrated system, mass transfer will result in a vertical density gradient in the continuous phase. For a low density solute transferring from a low density dispersed phase to a higher density continuous phase in a countercurrent manner, the density of the continuous phase will decrease as it moves down the column. This unstable density gradient can enhance axial mixing and as a result decrease the mass transfer rates. On the other hand, if the density gradient is stable (density decreases with height), it has no significant effect on axial mixing (Aravamudan and Baird, 1996; Aravamudan and Baird, 1999). Rama Rao and Baird (1998) confirm that the stable density gradient has similar axial mixing as in the absence of a density gradient, however unstable density gradients must be avoided.

Ju et al. (1990) found, from their investigation of a Karr column, that the axial dispersion coefficient decreases in the inhomogeneous dispersed phase flow regime (mixer-settler and diffusion regimes) and increased in the emulsion regime and increased with phase velocities of both phases. The axial dispersion coefficient is better correlated with a^2f than with af .

Previous models that investigated longitudinal mixing were mainly for single phase flow. Novotny et al. (1970) and Nemecek and Prochazka (1974) based their models on the backflow model and assumed that axial dispersion resulted from both backflow of the continuous phase through the plate holes and axial mixing between neighbouring plates. Therefore, the assumption was that the column consisted of well mixed regions around the plates (where the backflow model will apply) and diffusion regions between the plates (where the axial-diffusion model will apply) as shown in the fig. 2.18:

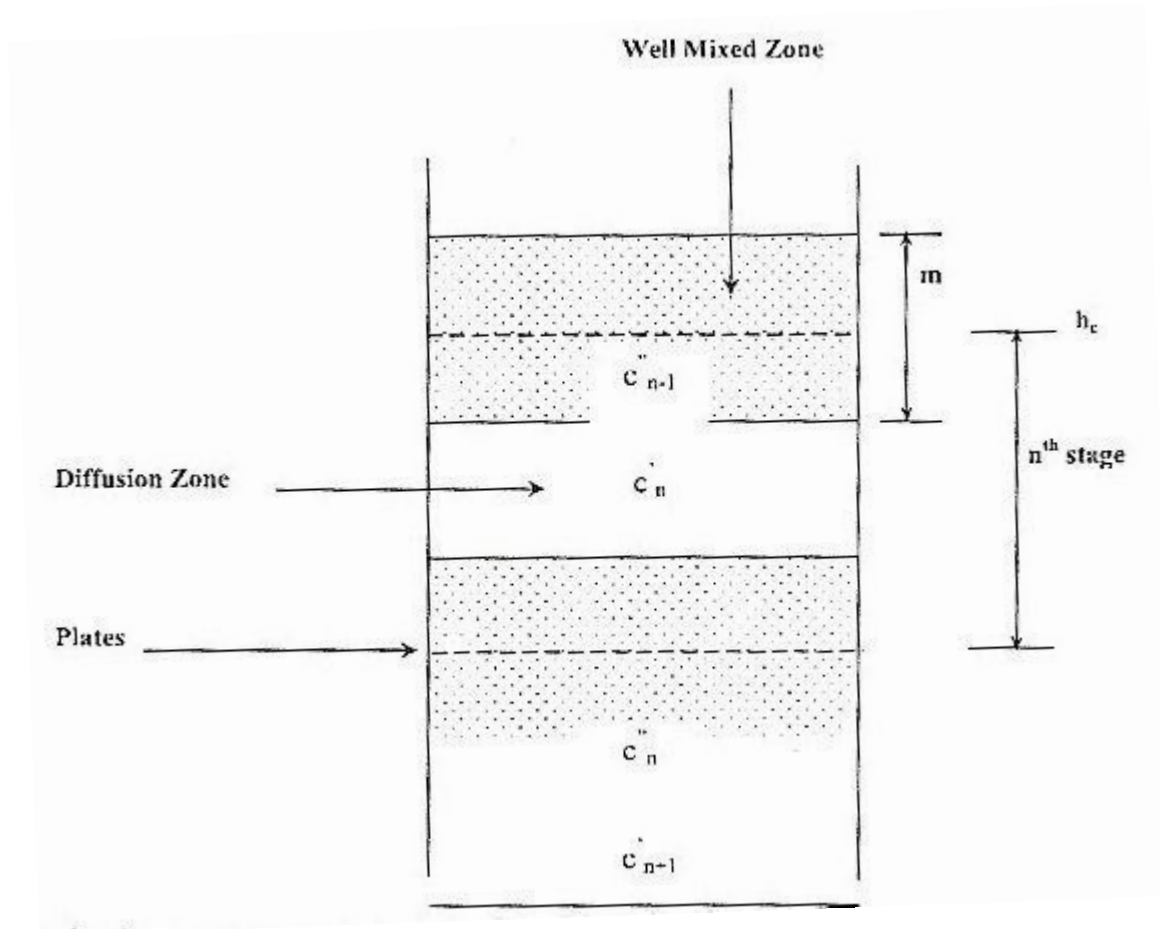


Fig. 2.18 Stage-wise extractor showing diffusion and backflow zones

(Stella and Pratt, 2006)

Nemecek and Prochazka (1974) also presented the role of axial dispersion for two-phase flow and highlighted the need to include the influence of the dispersed phase on the axial mixing in the continuous phase. The axial mixing coefficient was considered as the sum of the single phase dispersion and an increment due to the presence of the dispersed phase. The effective backmixing coefficient is given by:

$$q_e = \frac{U_c + U_d}{U_c} \left(\frac{\phi_1}{\pi} - \frac{1}{2} + \frac{2Af \cos \phi_1}{U_c + U_d} \right) + \frac{U_d(1 + q_d)}{U_c} \quad (2.117)$$

where $\phi_1 = \arcsin \left(\frac{U_c + U_d}{2\pi Af} \right)$

Stella and Pratt (2006) present another correlation developed by Prvcic et al. (1989) for the effective backmixing coefficient in the continuous phase:

$$q_c = \left[\frac{L_1 - 1}{L_1 \pi} \right] \left[\phi_1 + \cot \phi_1 - \left(\frac{\pi}{2} \right) \right] - \left[\frac{1 + q_d}{L_1} \right] \quad (2.118)$$

where $\phi_1 = \sin^{-1} \left[\frac{V_d(L_1 - 1)}{\pi Af} \right]$

The backmixing coefficient is given by:

$$\alpha_c = \left[\left(1 + \frac{1}{q_c} \right) \exp(Pe_c) - 1 \right]^{-1} \quad (2.119)$$

where $Pe_c = U_c \frac{(h/1000) - m_1}{E_c}$ (2.120)

and $m_1 = K_4 \left(\frac{2a}{\pi} \right)$

The final correlation for the diffusion coefficient is:

$$E_c = \frac{K_2(2Af)d_0}{S_1^{1.5}} + K_3d_{32} \left[\frac{4g\Delta\rho(u_T - U_c)\phi((h/1000) - m_1)}{\rho_c(1 - \phi)} \right]^{1/3} \quad (2.121)$$

Stella and Pratt (2006) found that the backmixing coefficient decreases with increasing continuous phase flow rate, while the dispersed phase flow rate had little effect due to the small density differences, also shown by Nemecek and Prochazka (1974). The backmixing increased with increasing agitation rates which results in an increase in the size of the well-mixed regions around the plates shown also by Stevens and Baird (1990).

For the two-phase flow in a Karr column, Stella and Pratt (2006) used equation 2.121 to evaluate the axial dispersion coefficient. This value was used to calculate the Peclet number and as a result it was possible to evaluate the backmixing coefficient. By fitting experimental data to equation 2.121 the dimensionless numbers were evaluated and it was shown that this adjusted two-phase model which was derived for pulsed columns could be used for RPCs with appropriate values for the constants.

Some other results on axial mixing that have been developed over the years are included in the following table 2.1 (Novotny et al., 1970; Nemecek and Prochazka, 1974; Kim and Baird, 1976a; Hafez et al., 1979; Kostanyan et al., 1980; Parthasarathy et al., 1984; Stevens and Baird, 1990; Ju et al., 1990):

Ref.	System	Result
Novotny et al. (1970)	RPC Single phase	$q_c = \left\{ (1 + 1/q) \exp \left[6.6 \left(\frac{h}{1000} - 4.5 \right) \frac{S_1^{3/2} U_c}{d_0 Af} \right] - 1 \right\}^{-1}$ $q = \frac{\phi_1}{\pi} - \frac{1}{2} + \frac{2Af}{U_c} \cos(\phi_1)$ $\phi_1 = \arcsin \left(\frac{U_c}{2\pi Af} \right)$
Nemecek and Prochazka (1974)	VPE Two-phase	$q_e = \frac{U_c + U_d}{U_c} \left(\frac{\phi_1}{\pi} - \frac{1}{2} + \frac{2Af \cos \phi_1}{U_c + U_d} \right) + \frac{U_d(1 + q_d)}{U_c}$ $\phi_1 = \arcsin \left(\frac{U_c + U_d}{2\pi Af} \right)$

Kim and Baird (1976a)	RPC Two-phase	$E = 5.62A^{1.41}f^{0.73}(h/1000)^{-0.88}$
Hafez et al. (1979)	RPC Two-phase	$E = 5.56A^{1.77}f^{1.0}(h/1000)^{1.32}$
Kostanyan et al. (1980)	VPE Two-phase	$E_c = \frac{h}{1000} \left[\frac{1}{0.5U_c + af} + 8 \left(\frac{\delta}{d_0} \right)^{1/3} \left(\frac{(h/1000) + D_c}{D_c} \right)^{4/3} \frac{S_1^{2/3}}{af} \right]^{-1}$
Parthasarathy et al. (1984)	RPC Two-phase	$\frac{E_c}{V_c H} = Pe^{-1}$ $= (4.22 \times 10^{-2})A^{0.457}f^{0.344}U_c^{-0.37}d_0^{0.274}S_1^{-0.68}(h/1000)^{-0.687}$
Stevens and Baird (1990)	RPC Single phase	$E = \left\{ \frac{\ln\left(\frac{1+q}{q}\right)}{(h/1000)U_c} + \frac{2S_1\left(1 - \frac{K_2A}{(h/1000)}\right)}{K_1d_0\left[(U_c + 2\pi Af)\left(\left(\frac{\pi}{2\sqrt{3}S_1}\right)^{0.5} - 1\right)\right]} \right\}^{-1}$ $q = \frac{\phi_1}{\pi} - \frac{1}{2} + \frac{2Af}{U_c} \cos(\phi_1)$ $\phi_1 = \arcsin\left(\frac{U_c}{2\pi Af}\right)$
Ju et al. (1990)	RPC Two-phase	$E = (15 - 1.82a^2f)U_c^{0.01}U_d^{0.16}S_1^{0.73}$ for $af < 2.54$ cm/s $E = (10.38 - 1.29a^2f)U_c^{0.46}U_d^{0.2}S_1^{0.39}$ for $af \geq 2.54$ cm/s

Table 2.1 Summary of axial mixing equations

Stevens and Baird (1990) also identified the existence of two separate hydrodynamic regions in their single phase investigations of a RPC where it was assumed that two different mechanisms of axial dispersion occurred as shown in fig. 2.20. The first region is the volume swept out by the reciprocating plate where the axial mixing is high. Here the mixing is a function of the energy supplied to the fluid by the movement of the plate relative to the fluid. The second region is between the plates where the axial mixing is sufficiently lower. This mixing is caused by the motion of vortices shed from the plates on either side of the plates.

The m shown in fig. 2.18 is not necessarily equal to the oscillation stroke ($2a$) and Stevens and Baird (1990) showed that it is actually below $2a$ due to the fact that the plate velocity at the outermost part of the swept region is very low and as a result little energy is dissipated. The equations shown in the above table are limited to conditions when the two regions do not overlap.

2.19 Mass Transfer Models

Most extractor designs assume that both phases (continuous and dispersed) move in a plug-flow manner. This assumption cannot be made for VPE columns due to axial dispersion of the phases mainly in the continuous phase which results in a reduction in the effective driving force for mass transfer. The factors that contribute to this non-uniform axial dispersion in the continuous phase are (Stella and Pratt, 2006):

- Entrainment of the continuous phase in the wake of the dispersed phase droplets.
- Energy dissipation of droplets causes a circulatory flow of the continuous phase.
- Molecular and turbulent eddy diffusion together with channelling and stagnant flow effects.

Pratt and Baird (1983) provided two types of models to describe axial dispersion that occurs in liquid-liquid contactors. The first model is the *diffusion model*, which assumes a turbulent backdiffusion of solute superimposed on plug flow of the phases. This model is approached in practice by differential extractors such as packed and baffle-plate columns. The second model is the *backflow model*, with well-mixed non-ideal stages between which backflow occurs. This model assumes a series of stages interconnected with each stage containing a mixing device and may or may not include a settler in which partial or complete coalescence occurs.

It is felt that the diffusion model is more appropriate for the Karr column because the relatively large open area of the plates allows for considerable interchange of liquid between inter-plate regions. However, the backflow model is more appropriate for columns with plates that have a smaller fractional open area (like the VPE) (Kim and Baird, 1976a).

2.19.1 Diffusion Model

Fig. 2.19 shows a differential slice of the column that is considered in the development of the diffusion model equations. The model makes the following assumptions:

- The backmixing of each phase may be characterised by a constant turbulent diffusion coefficient E_j .
- A constant mean velocity and concentration of each phase exists through every cross section.
- The volume mass transfer coefficient is constant or can be averaged over the column.
- The solute concentration gradients in each phase are continuous (except at the phase inlets).
- The two phases (dispersed and continuous or raffinate and solvent phases) are immiscible or have a constant miscibility irrespective of solute concentration.
- The volumetric flow rates of the feed and solvent are constant throughout.
- The equilibrium relation is linear or can be approximated by a straight line.

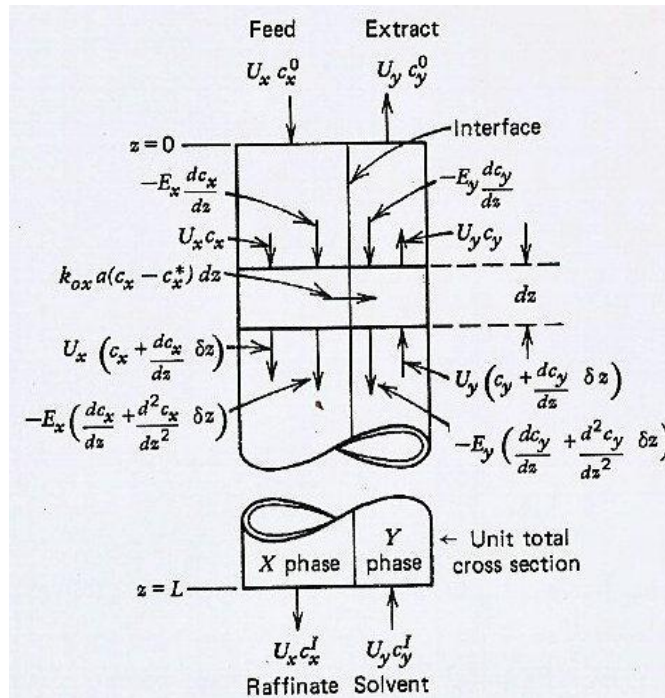


Fig. 2.19 Diffusion model material balance (Pratt and Baird, 1983)

The equations that describe the model are as follows:

$$e_x \frac{d^2 c_x}{dz^2} - U_x \frac{dc_x}{dz} - k_{ox} a(c_x - c_x^*) = 0 \quad (2.122)$$

$$e_y \frac{d^2 c_y}{dz^2} - U_y \frac{dc_y}{dz} + k_{ox} a(c_x - c_x^*) = 0 \quad (2.123)$$

For systems that have a linear equilibrium relation given by

$$c_x^* = mc_y + q \quad (2.124)$$

the above equations may be expressed in the dimensionless form:

$$\frac{d^2 X}{dz^2} - P_x B \frac{dX}{dz} - N_{ox} P_x B(X - Y) = 0 \quad (2.125)$$

$$\frac{d^2 Y}{dz^2} + P_y B \frac{dY}{dz} + E N_{ox} P_y B(X - Y) = 0 \quad (2.126)$$

where $E = mU_x/U_y$

$$X = \frac{c_x - (mc_y^I + q)}{c_x^o - (mc_y^I + q)} = \text{dimensionless concentration of X phase} \quad (2.127)$$

$$Y = \frac{m(c_y - c_y^I)}{c_x^o - (mc_y^I + q)} = \text{dimensionless concentration of Y phase} \quad (2.128)$$

The superscripts *o* and *I* refer to the feed and solvent inlets, respectively.

Integration of equation 2.122 gives the true number of backmix transfer units based on the x phase:

$$N_{ox} = \int_{c_{xI}}^{c_{xo}} \frac{d \left[c_x - \left(\frac{e_x}{U_x} \right) \left(\frac{dc_x}{dz} \right) \right]}{(c_x - c_x^*)_B} = \frac{k_{ox} a H}{U_x} \quad (2.129)$$

The height of a transfer unit (HTU) is calculated from the following equation:

$$H_{ox} = H / N_{ox} \quad (2.130)$$

2.19.2 Backflow Model

The model better describes a column that has a series of interconnected stages as illustrated in fig. 2.10 (Pratt and Baird, 1983):

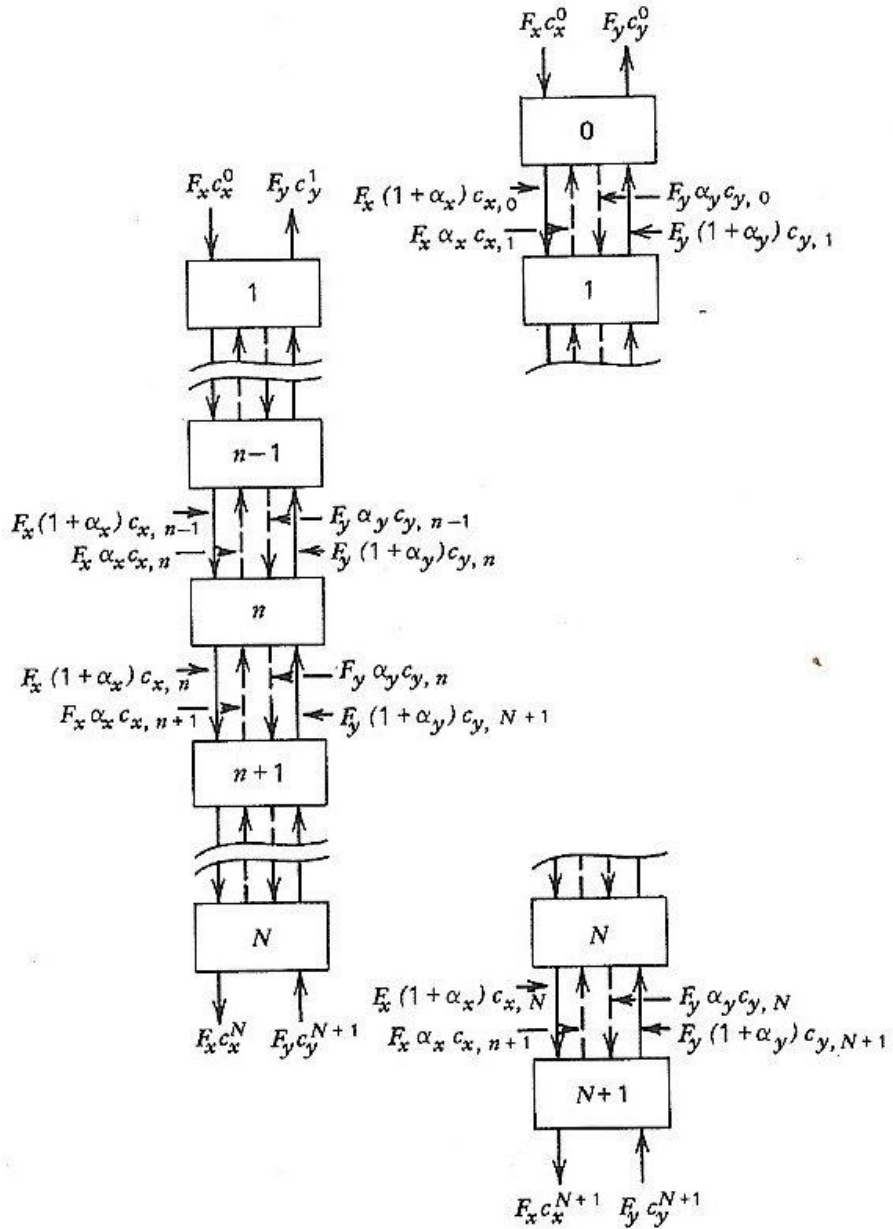


Fig. 2.20 Backflow model material balance (Pratt and Baird, 1983)

The following assumptions are made in the development of the model:

- Each stage is well mixed, and backmixing occurs by mutual entrainment of the phases between stages, after coalescence if appropriate.
- The backmixing is expressed as α_j which is the ratio of the backmixed to net forward interstage flow and is constant for all stages.
- All mass transfer occurs in the mixer.
- The value of $k_{ox}aV$ is constant for each stage.
- The two phases (dispersed and continuous or raffinate and solvent phases) are immiscible or have a constant miscibility irrespective of solute concentration.
- The volumetric flow rates of the feed and solvent are constant throughout.
- The equilibrium relation is linear or can be approximated by a straight line.

Here the feed inlet is represented by the superscript o while the solvent inlet is represented by the superscript $N+1$. In total the extractor will have N compartments in the active part of the column.

The material balances of the 2 phases around stage n will be given as follows:

$$(1 + \alpha_x)c_{x,n-1} - (1 + 2\alpha_x)c_{x,n} + \alpha_x c_{x,n+1} = \frac{k_{ox}as \left(\frac{h}{1000} \right)}{F_x} (c_{x,n} - c_{x,n}^*) \quad (2.131)$$

$$\alpha_y c_{y,n-1} - (1 + 2\alpha_y)c_{y,n} + (1 + \alpha_y)c_{y,n+1} = \frac{-k_{ox}as \left(\frac{h}{1000} \right)}{F_y} (c_{x,n} - c_{x,n}^*) \quad (2.132)$$

If a linear equilibrium relationship may be assumed, the above balances may be put into the dimensionless form: NB. For acetone-toluene-water, $c_d^* = 0.832c_c$ (Saien et al., 2006).

$$(1 + \alpha_x)X_{n-1} - (1 + 2\alpha_x)X_n + \alpha_x X_{n+1} = N_{ox}^1 (X_n - Y_n) \quad (2.133)$$

$$\alpha_y Y_{n-1} - (1 + 2\alpha_y)Y_n + (1 + \alpha_y)Y_{n+1} = -N_{ox}^1 \mathbf{E}(X_n - Y_n) \quad (2.134)$$

$$\text{where } N_{ox}^1 = \frac{k_{ox} aV}{F_x} = \frac{k_{ox} a(h/1000)}{U_x} \quad (2.135)$$

= number of perfectly mixed transfer units per stage

X and Y are given by equations 2.127 and 2.128, respectively with the superscript I replaced by $N+I$

If we express equations 2.133 and 2.134 in E operator form (i.e. $EX_n = X_{n+1}$), Y may be eliminated to give:

$$[(E - 1)^4 - \alpha(E - 1)^3 - \beta(E - 1)^2 - \gamma(E - 1)]X_n = 0 \quad (2.136)$$

$$\text{where } \alpha = \frac{1 + N_{ox}^1}{\alpha_x} - \frac{1 - \mathbf{E}N_{ox}^1}{(1 + \alpha_y)} \quad (2.137)$$

$$\beta = N_{ox}^1 \left[\frac{1}{\alpha_x} + \frac{\mathbf{E}}{(1 + \alpha_y)} \right] + \frac{1 + N_{ox}^1(1 - \mathbf{E})}{\alpha_x(1 + \alpha_y)} \quad (2.138)$$

$$\gamma = \frac{N_{ox}^1(1 - \mathbf{E})}{\alpha_x(1 + \alpha_y)} \quad (2.139)$$

Pratt and Baird (1983) also provide solutions to these models for different cases depending on whether there is backmixing in one or both or none of the phases, the value of the extraction factor, \mathbf{E} , whether or not the equilibrium line is linear, etc.

Axial mixing in the dispersed phase is assumed not to occur or is negligible (Aravamudan and Baird, 1999; Prochazka et al., 1971). In this case, axial mixing only occurs in the

continuous phase and the dispersed phase moves in plug flow. The assumption is supported by the relatively low residence time of the dispersed phase and the fact that there is no evidence to show the backflow of entrained drops in the continuous phase. Aravamudan and Baird (1999) also state that in general, axial mixing in the dispersed phase is very difficult to measure and although forward mixing does occur, it is difficult to predict.

Heyberger et al. (1983a) measured axial mixing coefficients of the dispersed phase for the acetone/water (continuous)/toluene (dispersed) system for $d \rightarrow c$ transfer in a VPE and found that the backmixing coefficients were low.

Pratt and Baird (1983) offers the following simplified solution for the prediction of the actual number of stages (compartments) for axial mixing in the continuous phase only and with a straight line for the equilibrium curve:

$$N \cong \frac{\log \left\{ \frac{\alpha_4(\mu_3 - \mu_4)(E - Y^o)}{E^2(\mu_3 - 1)(1 - Y^o)} \right\}}{\log \mu_4} \quad (2.140)$$

where $Y^o = Y$ at the X-phase inlet end, external to the contactor

$$\mu_3 - 1 = -\frac{\beta}{2} - \left[\left(\frac{\beta}{2} \right)^2 - \gamma \right]^{1/2} \quad (2.141)$$

$$\mu_4 - 1 = -\frac{\beta}{2} + \left[\left(\frac{\beta}{2} \right)^2 - \gamma \right]^{1/2} \quad (2.142)$$

$$\beta = \frac{1 + N_{ox}^1(2 - E + \alpha_y)}{(1 + \alpha_y)(1 + N_{ox}^1)} \quad (2.143)$$

$$\gamma = \frac{N_{ox}^1(1 - E)}{(1 + \alpha_y)(1 + N_{ox}^1)} \quad (2.144)$$

$$a_4 = \frac{E}{\mu_4 + \alpha_y(\mu_4 - 1)} \quad (2.145)$$

The above solution offers 6 equations with 7 unknowns which allows for 1 degree of freedom. When evaluating the performance of an extractor, the value of N will be known and N_{ox}^1 and α_y could be estimated from the above equations.

Pratt (1983a) also gives equations to calculate the number of transfer units per stage for cases where there is complete mixing in the continuous phase or complete mixing in both the phases (fig. 2.21).

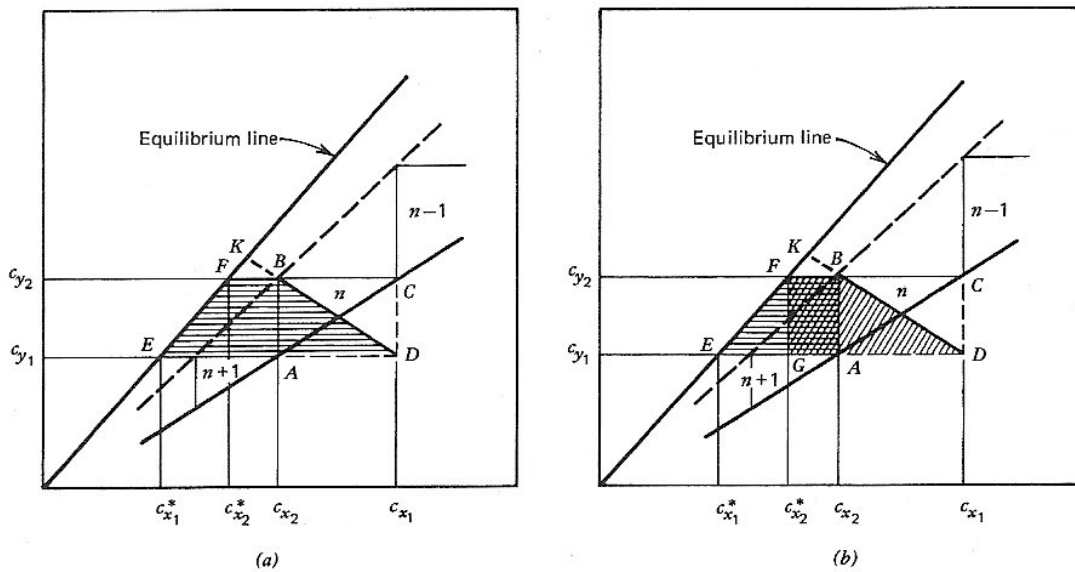


Fig. 2.21 Range of driving force for (Pratt, 1983a)

(a) Plug flow stage;

(b) complete backmixing of X phase (area AEFB) and Y phase (area DGFB)

If the x phase is dispersed, then the backmixing is likely to be more severe in the y phase. If the y phase is completely mixed so that its composition remains constant at c_{y2} , c_x^* will have a constant value of c_{x2}^* throughout the stage and the expression to calculate the number of transfer units per stage will be given by:

$$N_{ox,X}^1 = \frac{(c_{x1} - c_{x2})}{(c_x - c_{x2}^*)_{lm}} = \frac{k_{ox}a(h/1000)}{U_x} \quad (2.146)$$

Where $(c_x - c_{x2}^*)_{lm}$ is the logarithmic mean of $(c_{x1} - c_{x2}^*)$ and $(c_{x2} - c_{x2}^*)$. This equation can also be expressed in terms of c_y for a linear equilibrium relationship and noting that $dc_x = U_y/U_x dc_y$ (Pratt, 1983a):

$$\begin{aligned} N_{ox,X}^1 &= -S \ln \left(\frac{c_{y2}^* - c_{y2}}{c_{y2}^* - c_{y1}} \right) \\ &= -S \ln \left(1 - \frac{c_{y2} - c_{y1}}{c_{y2}^* - c_{y1}} \right) = -S \ln (1 - E_{My}) \end{aligned} \quad (2.147)$$

If both phases are completely backmixed then (Pratt, 1983a):

$$N_{ox,B}^1 = \frac{c_{x1} - c_{x2}}{c_{x2} - c_{x2}^*} = \frac{k_{ox}a(h/1000)}{U_x} = \frac{E_{Mx}}{1 - E_{Mx}} \quad (2.148)$$

It is easier to express these relationships in terms of dimensionless concentration X and Y and these are summarised in table 2.2 (Pratt, 1983a):

Case Number and Description	X Phase	Y Phase
Case 1—Piston flow	$N_{oxP}^1 = \frac{-\ln [X_2(E + 1) - E]}{E + 1}$ $X_2 = \frac{E + \exp [-N_{oxP}^1(E + 1)]}{E + 1}$	$N_{oyP}^1 = \frac{-\ln [1 - Y_2(S + 1)]}{S + 1}$ $Y_2 = \frac{1 - \exp [-N_{oyP}^1(S + 1)]}{S + 1}$
Case 2—X phase completely backmixed	$N_{oxX}^1 = \frac{1}{E} \ln \left[\frac{X_2}{X_2(E + 1) - E} \right]$ $= -S \ln (1 - E_{My})$ $X_2 = \frac{E \exp (EN_{oxX}^1)}{(1 + E) \exp (EN_{oxX}^1) - 1}$	$N_{oyX}^1 = \ln \left[\frac{1 - SY_2}{1 - Y_2(S + 1)} \right]$ $= -\ln (1 - E_{My})$ $Y_2 = \frac{\exp (N_{oyX}^1) - 1}{(S + 1) \exp (N_{oyX}^1) - S}$
Case 3—Y phase completely backmixed	$N_{oxY}^1 = \ln \left[\frac{1 - E(1 - X_2)}{X_2(E + 1) - E} \right]$ $= -\ln (1 - E_{Mx})$ $X_2 = \frac{1 + E[\exp (N_{oxY}^1) - 1]}{(1 + E) \exp (N_{oxY}^1) - E}$	$N_{oyY}^1 = \frac{1}{S} \ln \left[\frac{1 - Y_2}{1 - Y_2(S + 1)} \right]$ $= -E \ln (1 - E_{Mx})$ $Y_2 = \frac{\exp (SN_{oyY}^1) - 1}{(S + 1) \exp (SN_{oyY}^1) - 1}$
Case 4—Both phases completely backmixed	$N_{oxB}^1 = \frac{1 - X_2}{X_2(E + 1) - E}$ $= \frac{E_{Mx}}{1 - E_{Mx}}$ $X_2 = \frac{EN_{oxB}^1 + 1}{N_{oxB}^1(E + 1) + 1}$	$N_{oyB}^1 = \frac{Y_2}{1 - Y_2(S + 1)}$ $= \frac{E_{My}}{1 - E_{My}}$ $Y_2 = \frac{N_{oyB}^1}{N_{oyB}^1(S + 1) + 1}$

Table 2.2 Relationships between N_{ox} , exit concentrations and efficiencies

(Pratt and Baird, 1983)

2.19.3 Model Incorporating Backmixing and Forward Mixing

Wichterlova et al. (1991) states that although the backflow model describes the flow of the continuous phase in agitated columns, it is a poor representation of the flow of the dispersed phase. The estimates of the backflow in the dispersed phase using different methods provide different results. They claim that the residence time of the dispersed phase is affected more by the forward mixing of the dispersed phase due to the drop size distribution rather than the back-mixing due to plate agitation.

A stage-wise model for a VPE with back-flow in the continuous phase and short-cut flow in the dispersed phase, developed by Wichterlova et al. (1991) is shown in fig. 2.22.

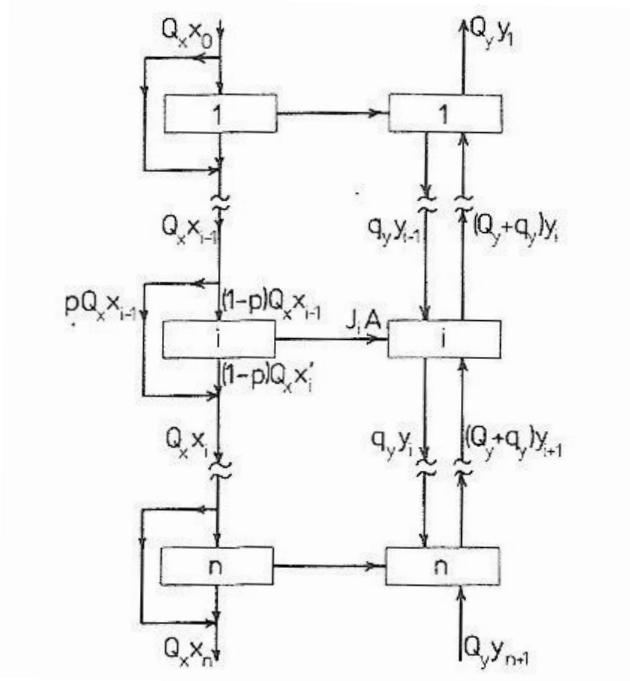


Fig. 2.22 Backmixing and forward mixing model (Wichterlova et al., 1991)

q represents the back-flow in the y (continuous) phase and p represents the short-cut (forward) flow in the x (dispersed) phase. p is the portion of the dispersed phase that passes through the stage with zero residence time.

Drop coalescence and re-dispersion results in cross-mixing of the dispersed phase which is taken into account by assuming that complete mixing of the phase occurs between stages. Further assumptions are that the flows, longitudinal mixing, and volumes of the phases in the stage are not dependent on time and are constant along the length of the extractor.

The differential equations representing the solute balances describe the dynamic behaviour of the extractor.

For the dispersed phase:

$$v_x \left(\frac{dx'_i}{dt} \right) = Q_x(x_{i-1} - x_i) - J_i A_{in} \quad (2.149)$$

$$\text{where } x'_i = \frac{(x_i - px_{i-1})}{(1-p)} \quad i = 1, \dots, n \quad (2.150)$$

For the continuous phase:

$$v_y \left(\frac{dy_i}{dt} \right) = Q_y(y_{i+1} - y_i) + q_y(y_{i-1} - 2y_i + y_{i+1}) + J_i A_{in} \quad i = 1, \dots, n-1 \quad (2.151)$$

$$v_y \left(\frac{dy_n}{dt} \right) = Q_y(y_{n+1} - y_n) + q_y(y_{n-1} - y_n) + J_n A_{in} \quad (2.152)$$

The boundary conditions that are valid at any time are as follows:

$$x_0 = x_{in}, \quad y_0 = y_l, \quad y_{n+1} = y_{in} \quad (2.153)$$

x may be regarded as the mean value weighted by the flow while x' is the mean value weighted by the volume of the dispersed phase.

The volume of the stage is given by the sum of the individual phase volumes of the stage:

$$V = v_x + v_y \quad (2.154)$$

From their experiments of a stationary continuous phase, Wichterlova et al. (1991) found that the short-cut flow coefficient did not increase with agitation unlike the back-flow

coefficient of the continuous phase. The steady state solution of the above model may be transformed into a solution without short-cut flow by replacing NTU by a combined number NTU' that takes into account the longitudinal mixing of the dispersed phase:

$$NTU' = \frac{1}{\frac{1}{NTU} + \frac{p}{1-p}} \quad (2.155)$$

Wichterlova et al. (1991) also verified the assumption that the slip velocity, at a given holdup, does not depend on the flow ratio. In the emulsion regime, the longitudinal mixing, interfacial area, and mass transfer coefficient are affected mainly by the turbulence generated by the motion of the plates and the effect of flow ratios has little effect on these parameters and their dependence may be neglected.

2.20 Efficiencies

On the basis of the raffinate phase, the tray efficiency of the extraction column may be expressed as follows (Humphrey and Keller, 1997):

$$E_R = \frac{x_n - x_{n-1}}{x_n^* - x_{n-1}} \quad (2.156)$$

The sieve tray efficiency is a strong function of the Weber number We . A minimum of about 4 is required for maximum tray efficiency (Humphrey and Keller, 1997).

$$We = \frac{\rho_d U_o^2 d_o}{\gamma} \quad (2.157)$$

The overall tray efficiency of extraction sieve trays can be approximated by the following equation – corrected for units (Humphrey and Keller, 1997):

$$E_o = \frac{1722.5(h/1000)^{0.5} \left(\frac{U_d}{U_c} \right)^{0.42}}{\gamma} \quad (2.158)$$

The Murphree efficiency may be calculated from:

$$E_{Mx} = \frac{N_{ox}^1}{1 + N_{ox}^1} \quad (2.159)$$

The Murphree efficiency is defined as the ratio of the actual concentration change of a phase within a stage to that that would have occurred if equilibrium was achieved (Pratt, 1983a):

$$E_{Mx} = \frac{x_{n-1} - x_n}{x_{n-1} - x_n^*} \quad (2.160)$$

$$E_{My} = \frac{y_n - y_{n+1}}{y_n^* - y_{n+1}} \quad (2.161)$$

These efficiencies relate to overall stage values i.e. x_{n-1} and y_{n+1} refer to concentrations of streams entering the stage and x_n and y_n refer to the concentrations leaving the same stage.

The volumetric efficiency, E_v is given by (Lo and Prochazka, 1983; Karr, 1980):

$$E_v = \frac{\text{total throughput}}{HETS} = \frac{U_c + U_d}{HETS} \quad (2.162)$$

The overall efficiency is defined as the ratio of the number of ideal to real stages required to achieve the same duty (i.e. the same concentration change with the given flows) and only applies for a linear equilibrium relationship (Pratt, 1983a):

$$E_o = \frac{N_{S,ideal}}{N_{S,real}} \quad (2.163)$$

The relationship between overall efficiency and Murphree efficiency is given by (Pratt, 1983a):

$$E_o = \frac{\log[1 + E_{Mx}(E - 1)]}{\log E} = \frac{\log[1 + E_{My}(S - 1)]}{\log S} \quad (2.132)$$

CHAPTER 3

EXPERIMENTAL

3.1 Choice of system

The toluene-acetone-water system is the standard system recommended by the European Federation of Chemical Engineering as a test system for liquid extraction (EFCE). This system was chosen for the experimental work done on the vibrating plate extraction column. Saïen et al, 2006 chose the toluene-acetone-water system for their investigation because of the high accuracy and repeatability when using gas chromatography for the analysis.

The experimental part of the research was split into two broad sections viz. hydrodynamics and mass transfer. During the hydrodynamics part of the research experiments were performed using water as the continuous phase flowing down the column while toluene was used as the dispersed phase flowing up the column (fig. 3.1) due to the density difference between toluene and water. As a result of this arrangement an interface between the two immiscible phases (water and toluene) was located at the top of the column in the upper settling tank. Toluene and water are considered to be completely immiscible in each other. Investigations were performed on dispersed phase holdup and dispersed phase droplet size and size distribution. During the mass transfer part of the research, experiments were performed using water as the continuous phase and an arbitrary mixture of 6 mass % acetone in toluene as the feed for the dispersed phase. Mass transfer took place from the dispersed to the continuous phase.

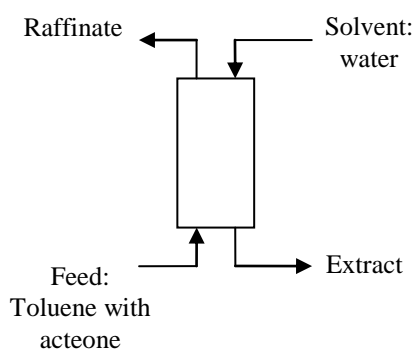


Fig. 3.1 Feed and solvent flow directions

3.2 Toluene-Acetone-Water Physical Properties

The equilibrium phase diagrams for the test system are given in fig. 3.2 and fig. 3.3.

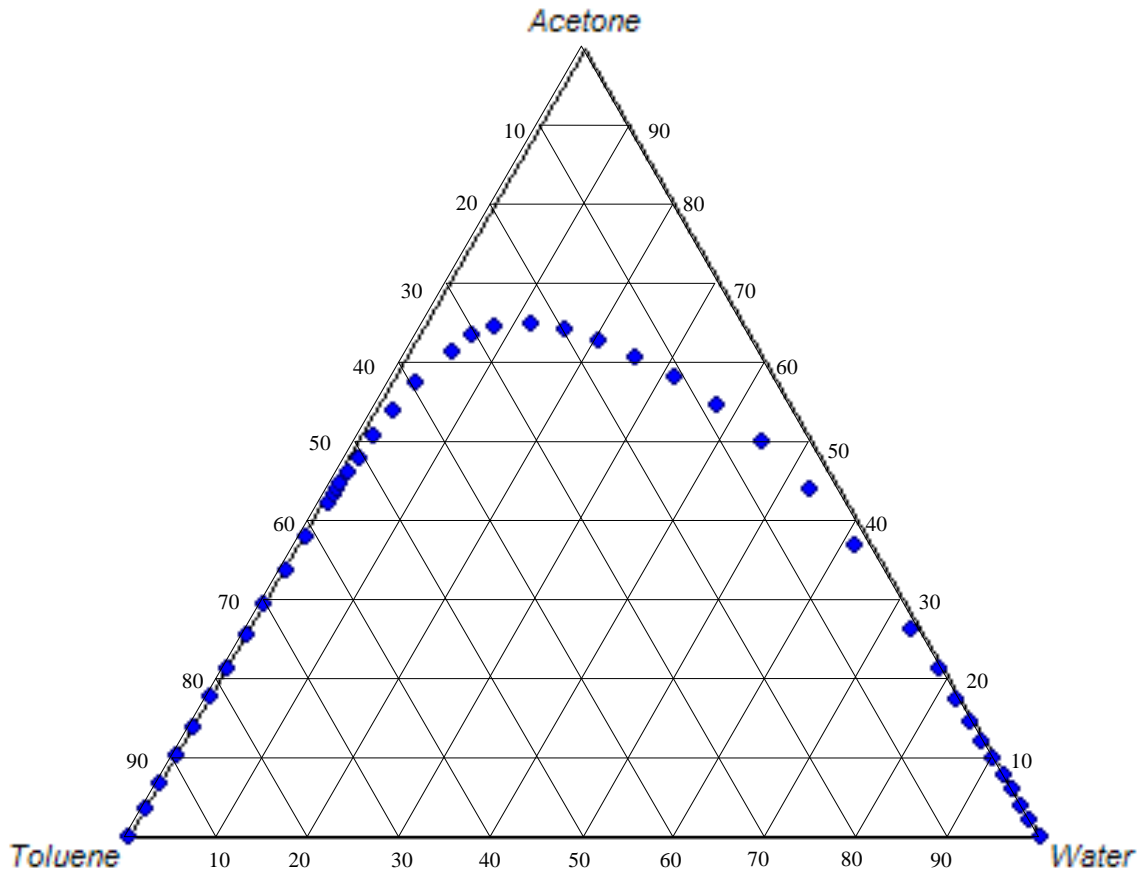


Fig. 3.2 Toluene-acetone-water phase diagram (CHEMCAD)

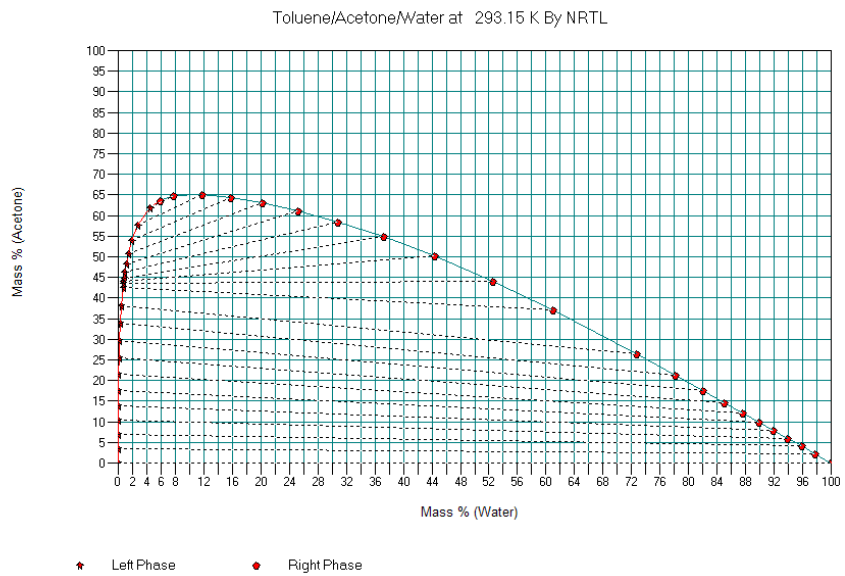


Fig. 3.3 Alternate phase diagram (CHEMCAD)

The partition coefficient for the toluene-acetone-water system is less than one (0.83) indicating that the equilibrium solute concentration is higher in the aqueous phase than the organic phase (Lisa et al., 2003). A diffusion coefficient of $0.923 \times 10^{-5} \text{ cm}^2/\text{s}$ for water and $2.88 \times 10^{-5} \text{ cm}^2/\text{s}$ for toluene was used.

Saien et al. (2006) report the equilibrium distribution of acetone between the water and toluene phases at 20°C (within the concentration $1 < C_c < 35 \text{ g/l}$) in terms of mass concentrations as follows - also confirmed by Lisa et al (2003):

$$C_d^* = 0.832C_c \quad (3.1)$$

Other physical properties of toluene, water and acetone are given in tables 3.1 and 3.2.

Values at 20°C	Toluene	Water	Acetone
Density (kg/m^3)	866.9	998	790.5
Viscosity (g/m s)	0.6712	1.0118	0.3976
Interfacial tension (mN/m)	36.1		
Diffusion coefficient in water (10^{-6} m/s)			$10.93 \pm 2.9\%$
Diffusion coefficient in toluene (10^{-6} m/s)			$25.51 \pm 2.3\%$

Table 3.1 Physical properties (Brodkorb et al., 2003)

Property at 20°C	Dispersed phase	Continuous phase
Density (kg/m^3)	866.7	998.2
Viscosity (kg/m s)	0.628×10^{-3}	
Diffusivity (m^2/s)	2.55×10^{-9}	1.09×10^{-9}

Table 3.2 Alternate physical properties (Saien et al., 2006; Bahmanyar et al., 2008)

The surface tension found experimentally for mixtures of acetone and water by Enders et al. (2007) was found to decrease exponentially as the concentration of acetone increased while for mixtures of acetone and water, the surface tension decreased linearly as the concentration increased. Surface tensions of pure samples are given in the table 3.3:

Component	Surface Tension (mN/m)
Acetone	23.02
Toluene	27.76
Water	71.98

Table: 3.3 Surface tension of pure components at 25 °C (Enders et al., 2007)

3.3 Experimental Objectives

Hydrodynamics:

Investigate the effects of:

- agitation level (af – product of amplitude and frequency of vibration) on drop size/distribution and holdup
- solvent to feed (S/F) ratio on drop size/distribution and holdup

Mass Transfer:

Investigate the effects of

- agitation level and S/F ratio on drop size/distribution and holdup
- agitation level and S/F ratio on extent of mass transfer
- agitation level and S/F ratio on NTU and efficiency
- mass transfer on drop size/distribution and holdup
- tray spacing on drop size/distribution and holdup
- tray spacing on extent of mass transfer
- tray spacing on NTU and efficiency.

Develop a mathematical model to predict the number of transfer units (NTU) and the mass transfer coefficient based on agitation level (af), solvent to feed ratio (S/F ratio) and tray spacing (h).

3.4 Experimental Equipment

Fig. 3.4 illustrates the process flow diagram together with the experimental equipment.

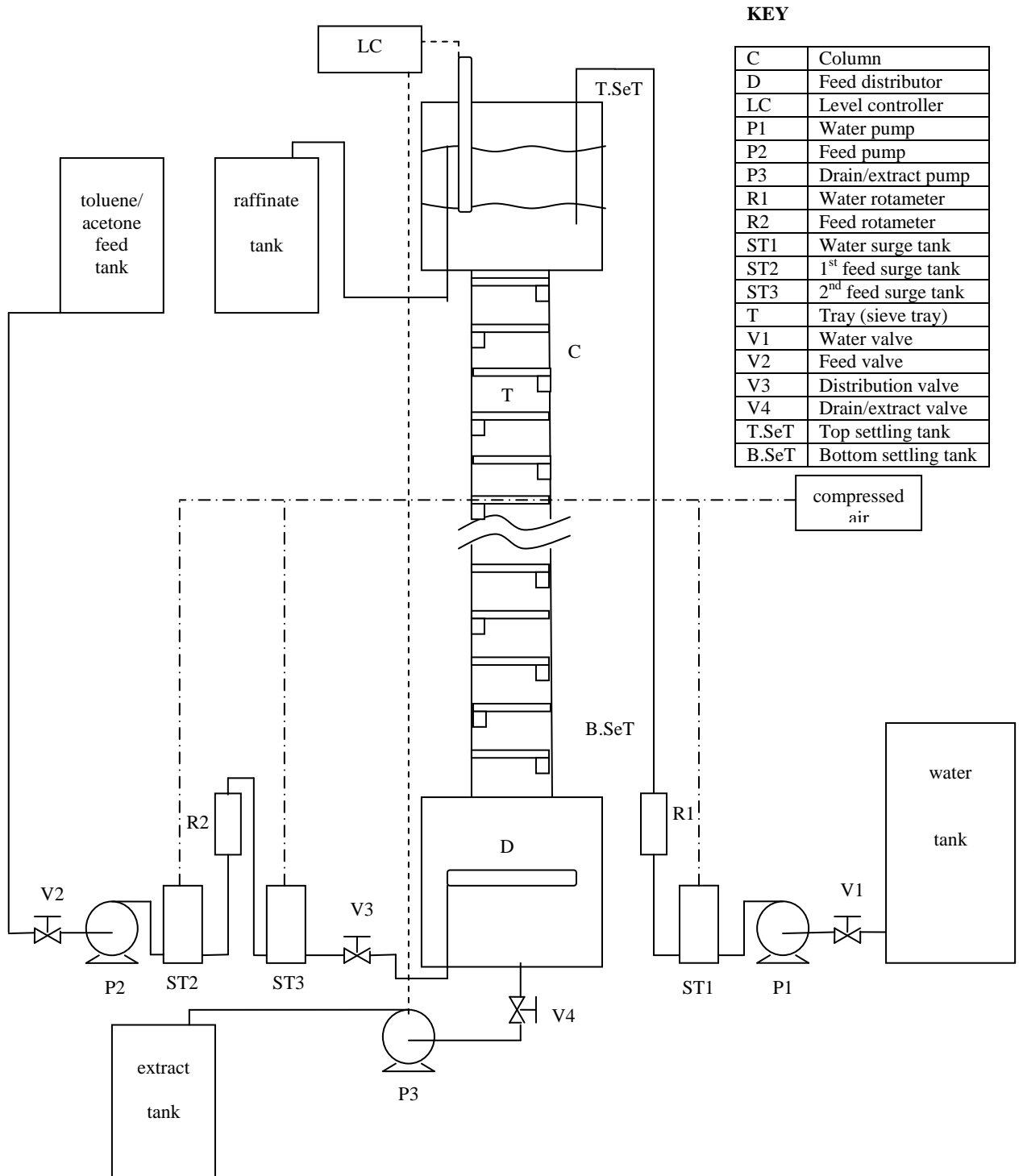


Fig. 3.4 Process flow diagram of experimental equipment

3.5 Equipment Description

3.5.1 Column

The active part of the column was made up of 8 glass tubes that were flanged together and had the following specifications:

Glass Tubes	ID	= 47.7 mm
	OD	= 58.7 mm
	Thickness	= 5.7 mm
	No.	= 8
	Length	= 550 mm

Cross sectional area of column = $1.787 \times 10^{-3} \text{ m}^2$

These flanged glass tubes formed the active part of the column giving it an effective height of 4.76 m and housed the plate stack for the column.

3.5.2 Trays

The trays in the column were sieve plates made of stainless steel and had small holes for the flow of the dispersed phase and downcomers for the flow of the continuous phase (fig. 3.5).

The plates had the following specifications:

Trays	Diameter	= 47.4 mm
	Thickness	= 2 mm
	Hole diameter	= 2.98 mm
	No. of holes	= 37
	Downcomer D	= 10.9 mm/tube (3 tubes per tray)

Downcomer L = 43.3 mm

No. of plates = 47

Cross sectional area of tray = $1.764 \times 10^{-3} \text{ m}^2$

Total area of holes = $0.258 \times 10^{-3} \text{ m}^2$

Free area for dispersed phase = 14.6 %

Total area of downcomers = $0.280 \times 10^{-3} \text{ m}^2$

Free area of continuous phase = 15.9%

The small holes on the plate allowed for the dispersed phase to flow and to be re-dispersed after each plate. The downcomers were arranged so that consecutive plates had the downcomers on opposite sides. This allowed for the continuous phase to flow across the plate.



Fig. 3.5 Sieve plates

The trays were made of stainless steel which is preferentially wetted by water (as opposed to toluene) and as a result allowed the water to be the continuous phase. If the material of the plate was Teflon or polyethylene (PE), the plate will be preferentially wetted by toluene which would force the toluene to be the continuous phase and water to be dispersed in the column.

3.5.3 Settling Tanks

The top and bottom settling tanks were identical and had the following specifications:

Settling tanks	OD	= 160 mm
	ID	= 150 mm
	Thickness	= 5 mm
	Length	= 250 mm

Cross sectional area of settling tank = $17.671 \times 10^{-3} \text{ m}^2$

The purpose of the settling tanks was to allow for the separation of phases. The bottom tank contained the distributor for the dispersed phase. The top tank helped to maintain the liquid-liquid interface between the two phases (aqueous and organic – fig. 3.6).

3.5.4 Level Controller

The level controller consists of a conductivity probe (fig. 3.6), a control box that houses the controller electronics and a variable speed pump which is the same pump used for the drain/extract. The electrical conductivity of water is very low compared to that of a hydrocarbon substance (toluene). The probe was able to detect the change in conductivity when it came into contact with either liquid. This information was then used to set the speed of the drain pump so that when the conductivity meter read the low conductivity of the water it would allow the drain pump to increase the flow of the extract leaving the column (reducing the interface in the top settling tank) and vice versa. This allowed the level of the interface to be kept fairly constant (the change in level was between 1 and 3 mm). The controller could be adjusted in order to keep the speed of the pump at specific values for the upper and lower limits of the conductivity. Since the flow rates that were used for the experiments discussed above were fairly low (overall throughput equal to 30 l/h), the drain pump lower limit speed was set to zero.

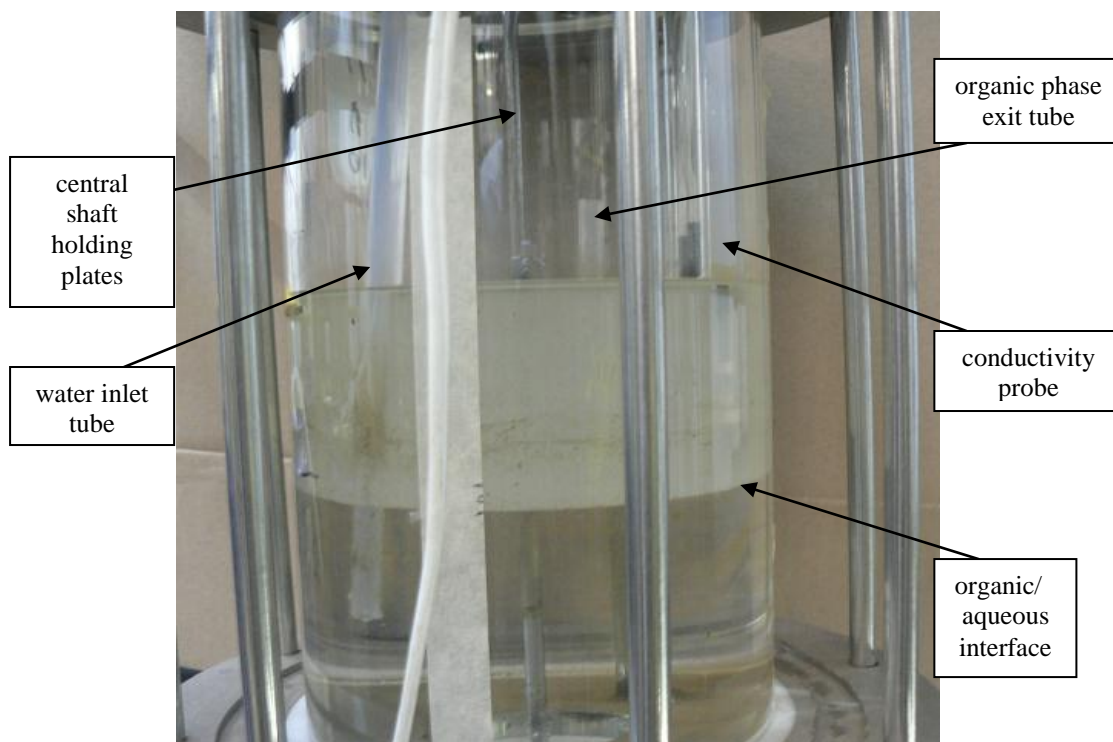


Fig. 3.6 Top settling tank (showing the interface level and conductivity probe)

3.5.5 Pumps

All three pumps (water feed, toluene feed and drain) had exactly the same specifications (Heidolph PD5106; speed: 24 – 600 rpm; max. flow = 160l/h). They were all positive displacement pumps that used a rotor to control the amount of liquid that passed through a silicon tubing. They were all variable speed pumps and the flow rates were adjusted by changing the speed of the pump. The pumps could be operated in either of two directions by changing the direction of the rotor motion (clockwise or anticlockwise). The flow rate range of the pumps was between 0 and 300 l/h.

3.5.6 Rotameters

The rotameters were designed specifically for the type of liquid it was used for. Each rotameter was calibrated using a bucket/stopwatch system in order to mark the 3 required flow rates that were used (10, 15 and 20 l/h).

3.5.7 Surge Tanks

The surge tanks (OD 115 mm; height 265 mm) were designed to hold a maximum of 2 litres of liquid and were made of stainless steel. They were equipped with side transparent tubing so that the level of liquid could be seen. The purpose of the surge tanks was to reduce the fluctuations caused by the peristaltic motion of the pumps and the vibration of the trays in the column so that the flow rate may be read easily on the rotameter. The tanks were pressurized from the top with compressed air.



Fig. 3.7 Feed surge tank

The tank situated on the water line was between the pump and the rotameter since the only cause of the fluctuating flow rate was the peristaltic motion of the pump. This reduced the fluctuations drastically and allowed for a stable flow rate reading to be taken from the rotameter.

The organic line proved to be more problematic since the fluctuations were caused by two independent factors i.e. the peristaltic motion of the pump and the vibration of the plates in the column which caused a variation in pressure at the bottom of the tank where the dispersed phase entered. One surge tank was placed between the pump and the rotameter

(fig. 3.7) to reduce the fluctuations caused by the pump while a second surge tank was placed between the rotameter and the distributor in the column which was used to reduce the fluctuations caused by the variation in pressure at the bottom of the column (as a result of the vibration of the plates). This allowed the operator to take a reading on the rotameter without a lot of fluctuations. The reading did however change when the drain pump changed its speed between its upper and lower limits; however, this change was minimal.

3.5.8 Water Storage Tank

The water tank was chosen to hold sufficient water for two complete runs at the maximum flow rate as well as for washing the column between runs. Tap water was used as the solvent.

3.5.9 Feed, Raffinate and Extract Tanks

These tanks were 25 liter drums and were sufficient to hold the liquids for the duration of the experiments.

3.5.10 Digital camera

The camera used was a Panasonic Lumix DMC-FZ5 camera with a 12x optical zoom. The picture size was chosen to be the maximum i.e. 2560 with the maximum quality also being chosen.

3.5.11 Gas Chromatograph

The GC unit was a Shimadzu unit equipped with a flame-ionization detector (FID) and a packed column with the following specifications:

Name:	Shimadzu GC-2014
Injector Temp.:	198 °C
Run time:	3 minutes
Column Name:	CBP1-525-050
Column Pressure:	0.4 kPa
Column flow:	35 ml/min
Column temp.:	65 °C
Column Length:	25 m
Column ID:	0.32 mm
Detector Temp.:	250 °C

Hydrogen and air were supplied to produce a flame in the unit. Nitrogen was used as a carrier gas for the sample. 1 μ l of the sample was injected through an injector into a packed column in the unit. The organic molecules were broken down into ions which was collected by an electrode that produced an electrical signal. This signal was unique to the hydrocarbon and the hydrocarbon was identified from this.

The GC had to be calibrated for the combinations of samples that were to be analysed (raffinate, extract and local samples). Standards were prepared using a mass balance (providing readings correct to 3 decimal places) for the 2 systems (acetone in water and acetone in toluene) in the range from 2 to 8 mass percent acetone. For the acetone/water system, one peak was visible indicating the amount of acetone present (water cannot be detected using FID). The area of the peak was plotted against the concentration of the standard to obtain the calibration chart (appendix B). This chart was used to analyse the extract samples.

For the acetone/toluene system, 2 peaks were identified; one for acetone and the other for toluene. The ratio of the area of the acetone peak to the toluene peak was plotted against the concentration of the standard to produce the calibration chart that was used to analyse the feed and dispersed phase samples. These calibration charts are shown in appendix B.

Although the FID could not identify water, it was used to calculate the amount of acetone in the extract since the extract was assumed to contain only two components viz. water and acetone (which is acceptable since water and toluene are virtually immiscible).

3.5.12 Perspex Box

The box (fig. 3.8) had dimensions 130 x 135 x 250 mm and was situated between plates 14 and 15 (when the plate spacing was 100 mm) and between plates 7 and 8 (when the plate spacing was 200 mm) from the bottom of the column. The box was open at the top to allow water to be filled and had a drain point at one of the bottom corners.

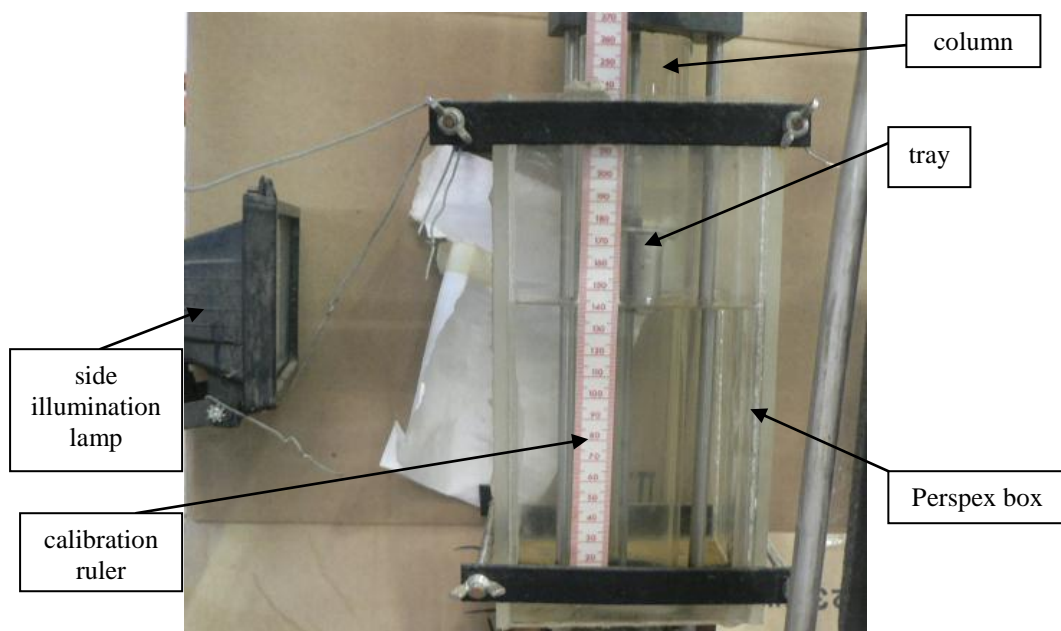


Fig. 3.8 Perspex box (used during photography of droplets)

The purpose of the Perspex box was to reduce the error on the droplets caused by the curvature of the column during the photography of the drops. The box was illuminated from the rear and the sides to allow a high contrast photo to be taken.

3.5.13 Vibration motor

The plate stack was mounted on a central shaft which was connected eccentrically to a motor at the top of the column. By adjusting the spacing between the connection point and the center of the motor through an adjustable yoke, the amplitude of the vibrations could be changed. By adjusting the speed of the motor, the frequency of the vibrations could be changed. The specifications of the motor were as follows:

(220Δ; 50 Hz; 0.75 kW, 1430 min⁻¹; 3.37 amp).

Refer to appendix B for the calibration chart of the motor.

3.5.14 Samplers

Four pairs of samplers were placed along the length of the column (at heights of 0.56, 1.76, 2.96 and 4.16 m from the bottom of the column) in order to extract each of the phases independently and evaluate the concentration at that particular position in the column (fig. 3.10). Table 3.4 below indicates the location of the samplers for the different tray spacings where the distance and stage number is from the bottom of the column.

Sample number	1	2	3	4
Distance (m)	0.56	1.76	2.96	4.16
Stage number ($h = 100$ mm)	6	18	30	42
Stage number ($h = 200$ mm)	3	9	15	21

Table 3.4 Location of samplers

The continuous (aqueous) phase sampler had a stainless-steel tip (fig. 3.9) and was positioned to face upwards (continuous phase flows down the column). The wetting preference of steel is the aqueous phase (as opposed to the organic phase) and it was possible to remove just the continuous phase from that sampler.

The dispersed (organic) phase sampler had a Teflon tip (fig. 3.9) and was faced downwards opposite to the flow direction of the dispersed phase. Teflon has a preferred wettability for the organic phase and as a result it was possible to remove only the organic phase from that sampler.

The samplers had screws at the ends that controlled the position of Teflon plugs in a glass tube. The adjustment of the screws controlled the flow of fluid in the sampler.

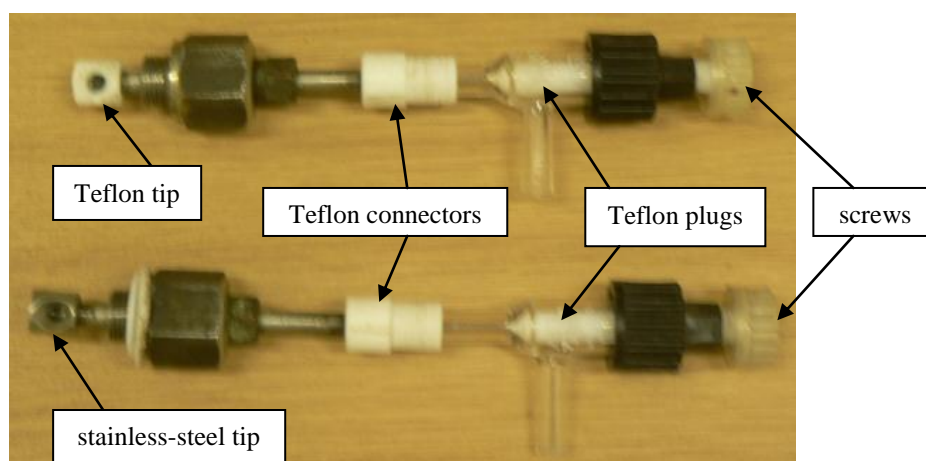


Fig. 3.9 Dispersed and continuous phase samplers



Fig. 3.10 Samplers attached to the Column

3.6 Hydrodynamics Experimental Procedure:

The toluene and water were allowed to circulate (one tank for feed and product) through the column.

1. The conductivity probe (measures interface level) was set at a fixed measured level below the raffinate overflow point.
2. The water was allowed to fill up to the level set by the probe.
3. The water flow rate was set by adjusting the speed of the water pump and the operation of the level controller was tested.
4. The agitation level was set to the required value (NB. The amplitude is fixed and only the frequency was changed).
5. The toluene pump was started, and the toluene valve was opened; the toluene flow rate was set by adjusting the speed of the pump.
6. Time was allowed for steady state to be obtained (preliminary experiments showed that 45 minutes was sufficient).
7. The lights around the Perspex box were switched on so that the droplets are illuminated and the droplets were photographed.
8. The interface level at the top of the column that was being maintained by the level controller was marked.
9. The toluene feed pump and the water feed pump were stopped.
10. The frequency of vibrations was set to around 1.5 Hz (corresponding to the minimum holdup) with the toluene droplets being allowed to coalesce and collect in the top settling take.
11. Sufficient amount of time was allowed for all of the toluene to collect in the top (20 minutes proved to be sufficient).
12. The amount of toluene collected below the marked interface level in the top settling tank was measured.
13. With the diameter of the settling tank being known, the volume of the toluene was calculated.

14. By dividing the volume of the toluene collected by the volume of the active part of the column (7.8 liters with $h = 100$ mm and 8 liters with $h = 200$ mm), the fraction holdup was obtained.
15. The photograph of the droplets was analysed using computer software to obtain the frequency distribution of the droplets and to calculate the Sauter mean diameter.

3.7 Mass Transfer Experimental Procedure:

The feed, solvent, raffinate and extract had to have separate tanks. None of the liquids were allowed to circulate.

1. Feed solutions of acetone in toluene was prepared (6 mass % acetone was chosen).
2. Steps 1 – 8 as stated in the hydrodynamics experimental procedure was performed.
3. Samples of the extract, raffinate and samples from each of the four pairs of samplers along the length of the column were taken.
4. Steps 9 – 15 as stated in the hydrodynamics experimental procedure was performed.
5. All the samples taken from the column were analysed using the GC to obtain the amount of acetone present.

3.8 Chemicals Used

- Tap water
- Commercial grade acetone
- Commercial grade toluene

Safety data sheets are included in appendix F.

3.9 Additional Equipment Used

- Mass balance
- Sample vials
- Glass beakers
- Measuring cylinders
- Measuring tape

3.10 Experimental Plan

Since the free area available for flow for the dispersed and continuous phases was approximately the same (14.6 and 15.9 %, respectively) the solvent to feed (S/F) flow ratios were chosen to be around 1:1. Experiments were performed for three ratios (1:1, 1:2 and 2:1) while keeping the total throughput (combined flow rates of dispersed and continuous phases) the same (at 30 l/h).

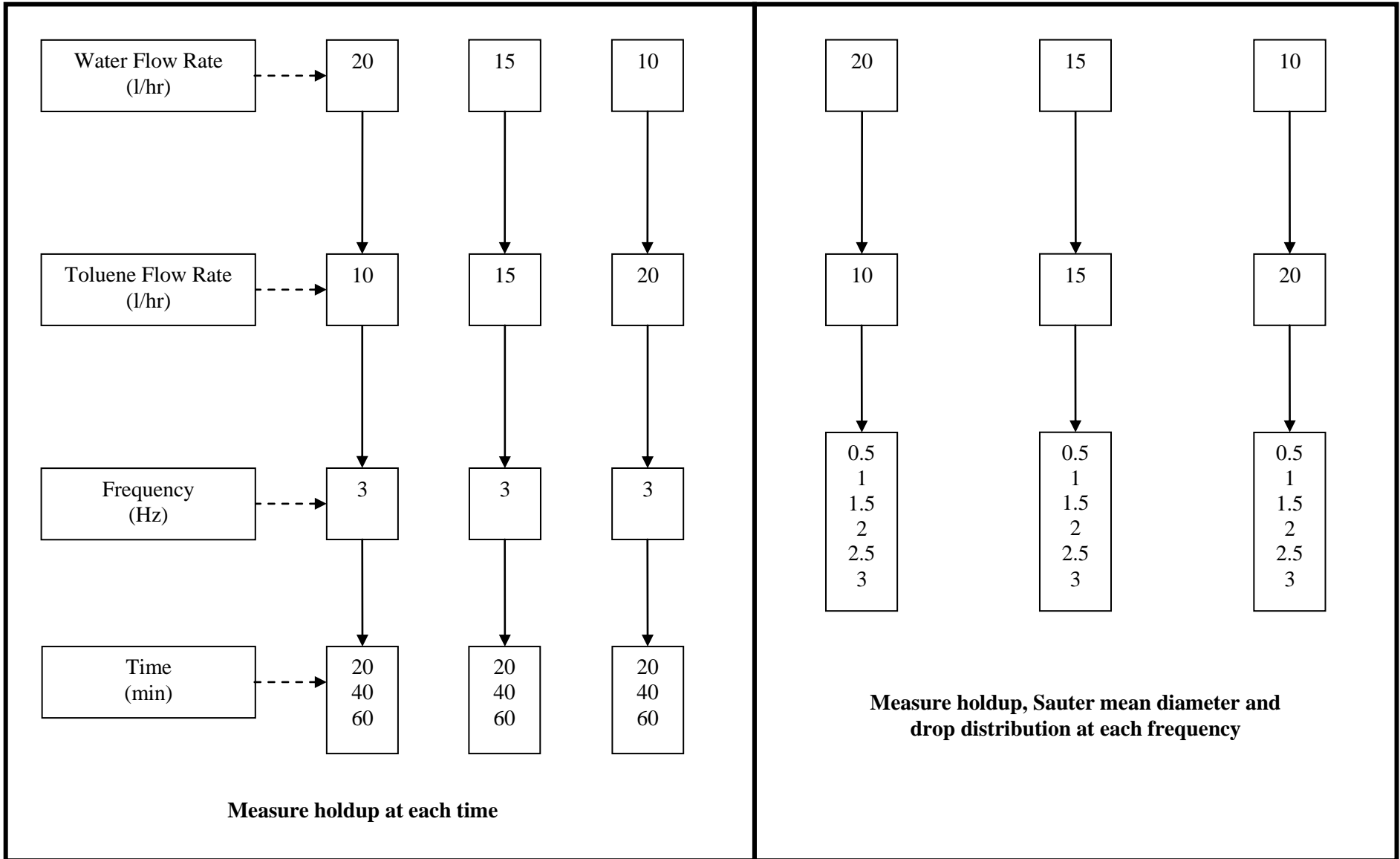
Initially it was required to investigate how long the column should be operated before steady state was reached so as to determine when measurements could be taken and when the experiment could be stopped.

The next step was to conduct the hydrodynamics investigations. Literature stated that the holdup, droplet size and efficiency of mass transfer were best correlated for a product of frequency and amplitude (af). As a result it was decided to keep the amplitude constant and vary the frequency only.

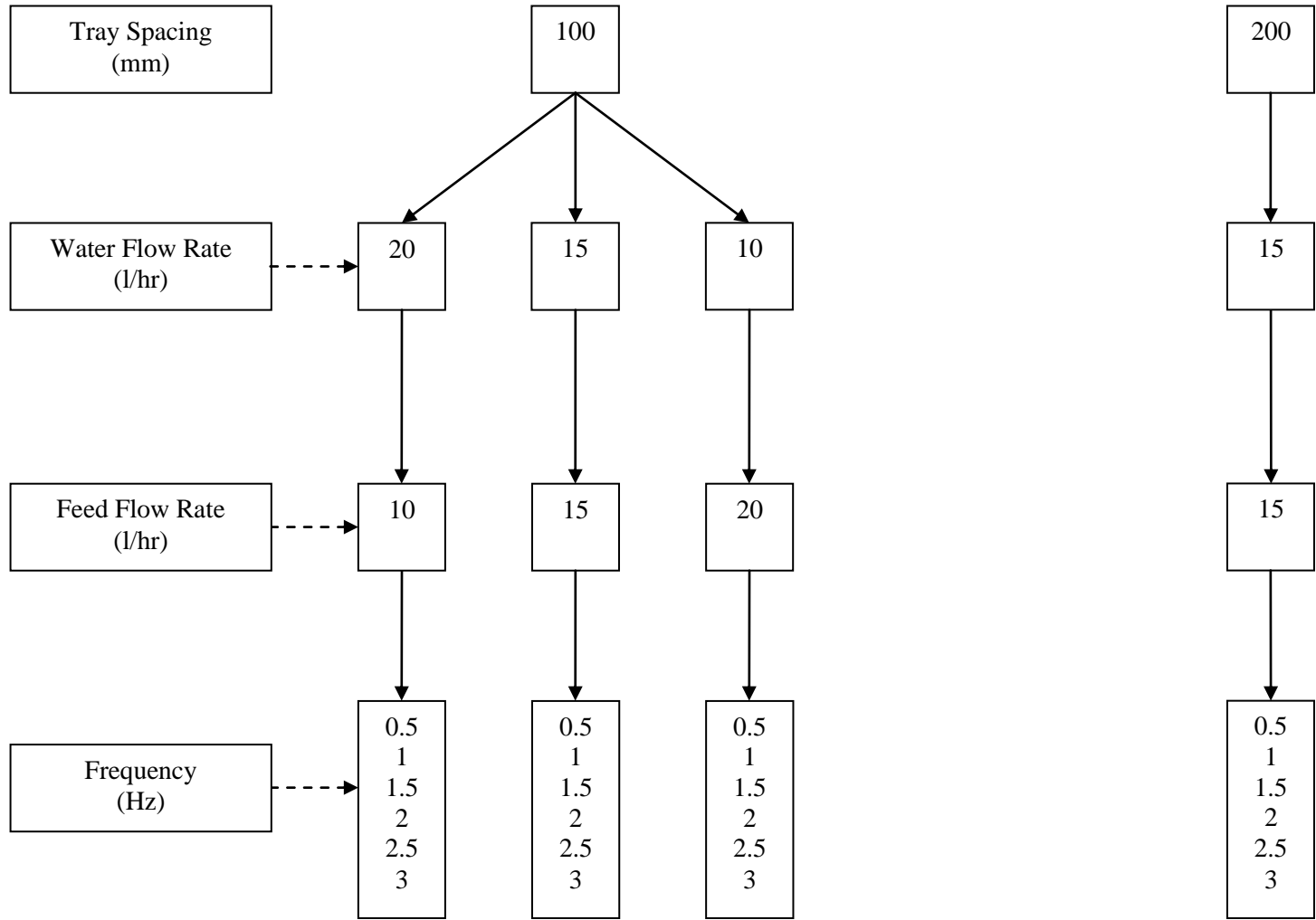
The last experimental step was to conduct the mass transfer investigations. During these experiments, the holdup, droplet size, extract, raffinate and local (along the length of the column) concentrations were measured for the three different ratios at varying agitation levels. The only other variable that could affect these properties was the tray spacing and for the mass transfer experiments, two different tray spacings were considered (100 mm and 200 mm).

The following experimental plan was developed:

Hydrodynamics Experiments (stroke = 2 x amplitude = 5 mm)



Mass Transfer Experiments
Stroke = 2 x amplitude = 5 mm; Feed = 6 mass % acetone in toluene



Measure extract, raffinate and local concentrations, holdup, Sauter mean diameter and drop distribution at each frequency

3.11 Experimental Procedure:

3.11.1 Holdup

The level controller at the top settling tank served the purpose of controlling the interface level between the organic the aqueous phases. When it was time to take measurements, the interface level was marked in the top settling tank. The water pump, feed pump and the distribution valve were all closed at the same time. It was not necessary to stop the raffinate flow as this stopped automatically since there was no input into the system. It was also not necessary to close the drain valve or stop the drain pump as this stopped automatically since the conductivity probe was reading the conductivity of water which was set to stop the drain pump.

The plates were vibrated at a frequency of around 1.5 Hz which corresponded to the lowest holdup frequency and the dispersed phase was allowed to accumulate in the top settling tank. When this process was complete the level of the toluene phase below the marked interface level was measured and the volume was calculated by multiplying this height by the area of the settling tank.

The volume of liquid (water) occupied in the active part of the column was measured by collecting the water during a draining process starting at the top of the plate stack and ending at the bottom of the plate stack. This volume was measured as 7.8 liters when h was 100 mm and 8 liters when h was 200 mm. This is the volume that was occupied by the continuous phase when no dispersed phase was present (dispersed phase holdup = 0).

The measured volume of toluene accumulated was divided by 7.8 or 8 (depending on the tray spacing) in order to calculate the volume fraction of the holdup. This value is represented as a percentage in the holdup graphs.

3.11.2 Size and Distribution of Droplets

The Perspex box was filled with water so as to reduce the effect of the curvature of the column on the size of the droplets seen. Although this reduces the effect, some error is expected. Ideally, the effect of the change in refractive index as light passes from air through the Perspex and into the water should be taken into account. The box was illuminated from the two sides by a flash light on each side (150 watts) and was illuminated from the rear through a sheet of white paper by two 60 watt spot lights. This helped to improve the image of the droplets obtained. A ruler was placed in the box in order to have a linear reference for the measurement of the size of the droplets. Three to five photographs were taken for each run.

The droplets were analysed using a software package called Image Tool 3. The photos were acquired by the software and were calibrated using the image of the ruler in the photo. The size of the droplets was measured by drawing lines across the diameter of the droplets. At least 250 droplets were measured using this technique and the results were copied onto an excel spreadsheet for further analysis. There were a few instances where fewer than 250 droplets were analysed. This could be due to the fact that under low agitation levels, fewer droplets were formed and at very high agitation levels, all of the droplets seemed clustered together and it was difficult to identify sufficient droplets.

The size distribution was calculated by expressing the number of droplets in 0.2 mm intervals as a percentage of the total number of droplets. This gave the percentage of droplets that occurred in a particular range.

The Sauter mean diameter was then calculated from the following equation:

$$d_{32} = \frac{\sum_{i=1}^N 6V_i}{\sum_{i=1}^N S_i} = \frac{\sum_{i=1}^N n_i d_i^3}{\sum_{i=1}^N n_i d_i^2}$$

3.11.3 Phase Samplers

The tubes leading into the raffinate and extract product tanks were removed briefly and samples of the raffinate and extract were taken from the tubes after the system had reached stability.

The procedure for taking the local samples along the length of the column was slightly more complicated. The screw at the end of the sampler was opened slightly and the fluid was allowed to flow into a waste flask. When it was seen that only the desired phase was being removed from the sampler, the fluid was collected in a sample bottle. These samples were used to calculate the concentration of both the phases along the length of the column.

3.11.4 GC analysis

Samples of the extract and raffinate were obtained after the system had reached stability. $1 \mu\text{l}$ of the sample was injected into the GC unit for analysis. Each sample was analysed 3 times with the average value being reported. From the calibration charts the mass concentrations of the raffinate and extract was obtained. Calibration charts are included in appendix B.

3.12 Repeatability Analysis

The repeatability of all the experiments was tested. During the hydrodynamics and mass transfer experiments, each experimental run was repeated at least once. Three to five photographs were taken of the droplets during each run in order to obtain acceptable results of distribution and Sauter mean diameters. During the GC analysis, each sample was analysed at least 3 times with average values being taken as the final result.

CHAPTER 4

RESULTS AND DISCUSSION

4.1 Time to reach stability

All readings for the experiments had to be taken when the system had reached a stable steady state (i.e. constant flow rates, constant holdup and droplet sizes and constant concentrations). In order to decide how long the experiments should run before stability was reached, preliminary runs were performed at the 3 different solvent to feed ratios of 1:1, 1:2 and 2:1 with no mass transfer while keeping the plate spacing at 100 mm. The holdup was measured after allowing the column to run for 20 minutes, then for 40 minutes, 60 minutes and finally for 80 minutes.

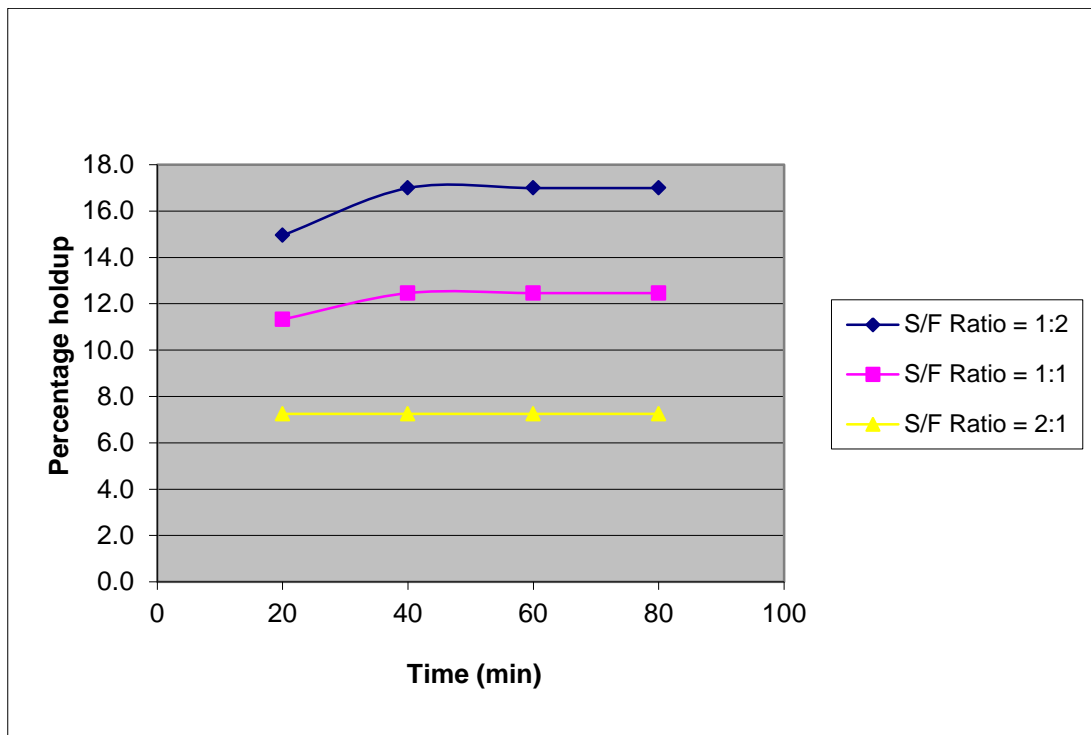


Fig. 4.1 Time to reach stability

From fig. 4.1, it can be seen that 45 minutes is a sufficient time to allow the experiment to run before stability is reached in terms of holdup for all three flow ratios. It is assumed that this time is also sufficient for complete stability to be obtained in terms of droplet sizes and concentration profiles and as a result all the experiments were conducted for a minimum of 45 minutes.

4.2 Hydrodynamics Results

Hydrodynamics experiments were conducted by circulating the aqueous and organic phases with no solute being present.

4.2.1 Holdup

Holdup was calculated for the 3 different solvent to feed flow ratios of 1:1, 1:2 and 2:1 for agitation levels (af) starting at 1.25 mm/s increasing by 1.25 mm/s up until flooding occurred in the column (NB. The amplitude of 2.5 mm was kept constant and the frequency was increased from 0.5 Hz at 0.5 Hz intervals up until flooding occurred). The total throughput was kept constant at 30 l/hr and the feed flow rate was fixed at 10, 15 and 20 l/hr for the three different flow ratios. The results are indicated in fig. 4.2.

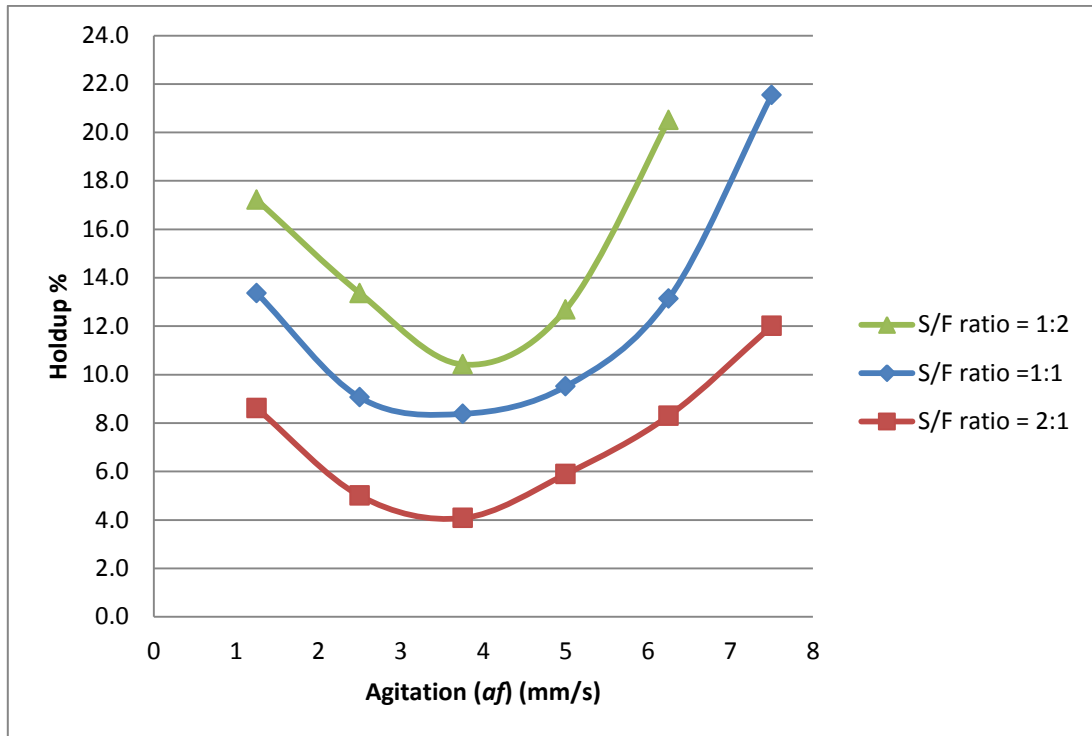


Fig. 4.2 Hydrodynamics holdup

The graph shows that for all three ratios the change in holdup followed similar trends. Initially the holdup is high due to the fact that the system is operating in the mixer-settler regime where most of the holdup is due to a layer of the dispersed phase (coalesced) being maintained under each tray. As the agitation level is increased, this layer is reduced and as a result the holdup is reduced. The holdup eventually reaches a minimum value which corresponds to the transition from mixer-settler to dispersion regime. As frequency is increased from this point, the holdup increases because the vibrating plates cause the droplet sizes to be decreased and more droplets are formed (discussed later). Some small droplets are seen to circulate in a particular stage instead of moving vertically upwards all of the time which increases the residence time of the droplets in the column and thus also increases the holdup for a given flow ratio. As the agitation is increased further the holdup is expected to increase exponentially as the system moves towards the emulsion regime and then becomes unstable as the column approaches the flooding condition.

The holdup trends are consistent with literature. Most of the literature, however, showed trends mostly for the Karr column (which does not operate in the mixer-settler regime) and as a result only the second half of the trend was shown where the holdup increased

exponentially from a minimum holdup (Aravamudan and Baird, 1999; Baird and Lane, 1973; Baird and Shen, 1984).

The transition from mixer-settler to dispersion regime (minimum holdup) is shown to be independent of flow rates as it occurs at the same agitation level of 3.75 mm/s for all of the flow ratios tested.

At any particular agitation level the holdup for the S/F ratio of 1:2 is always higher than that for the flow ratio of 1:1 which in turn is always higher than that for the ratio of 2:1 indicating that the holdup decreases as the S/F flow ratio increases. As the toluene flow is decreased there is less dispersed phase in the column and as such the holdup decreases. Graphs in appendix C indicate that there is a weak relationship between holdup and the continuous phase flow. Therefore holdup may be considered to be independent of continuous phase flow but decreases with a decrease in dispersed phase flow.

Experiments could not be carried out at an agitation level of 7.5 mm/s for the flow ratio 1:2 or for higher agitation levels for the other ratios as flooding was seen to occur in the column. Flooding was noticed visually in the column and started with the dispersed phase accumulating between the plates and eventually starting to accumulate at the top of the bottom settling tank. This accumulated layer does not even enter the active part of the column. This accumulation increases with time and the dispersed phase starts filling up the column from the top to bottom. Holdup is expected to increase unstably as flooding is approached and eventually when flooding occurs.

4.2.2 Droplet size distribution

At each agitation level for the different flow ratios photos were taken of the droplets and analysed to determine the size distribution of the droplets. Sample photos of the droplets are shown in fig. 4.3 for 2 agitation levels showing the size difference in the droplets.

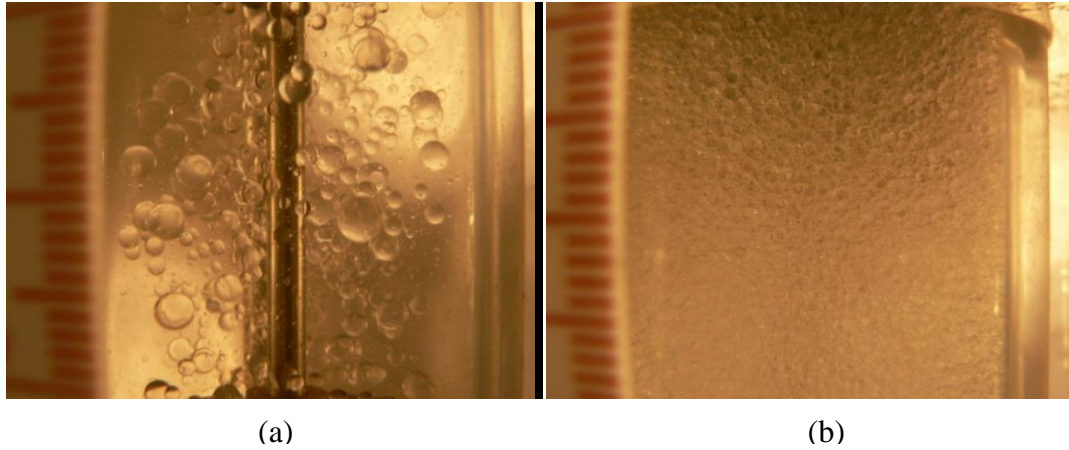
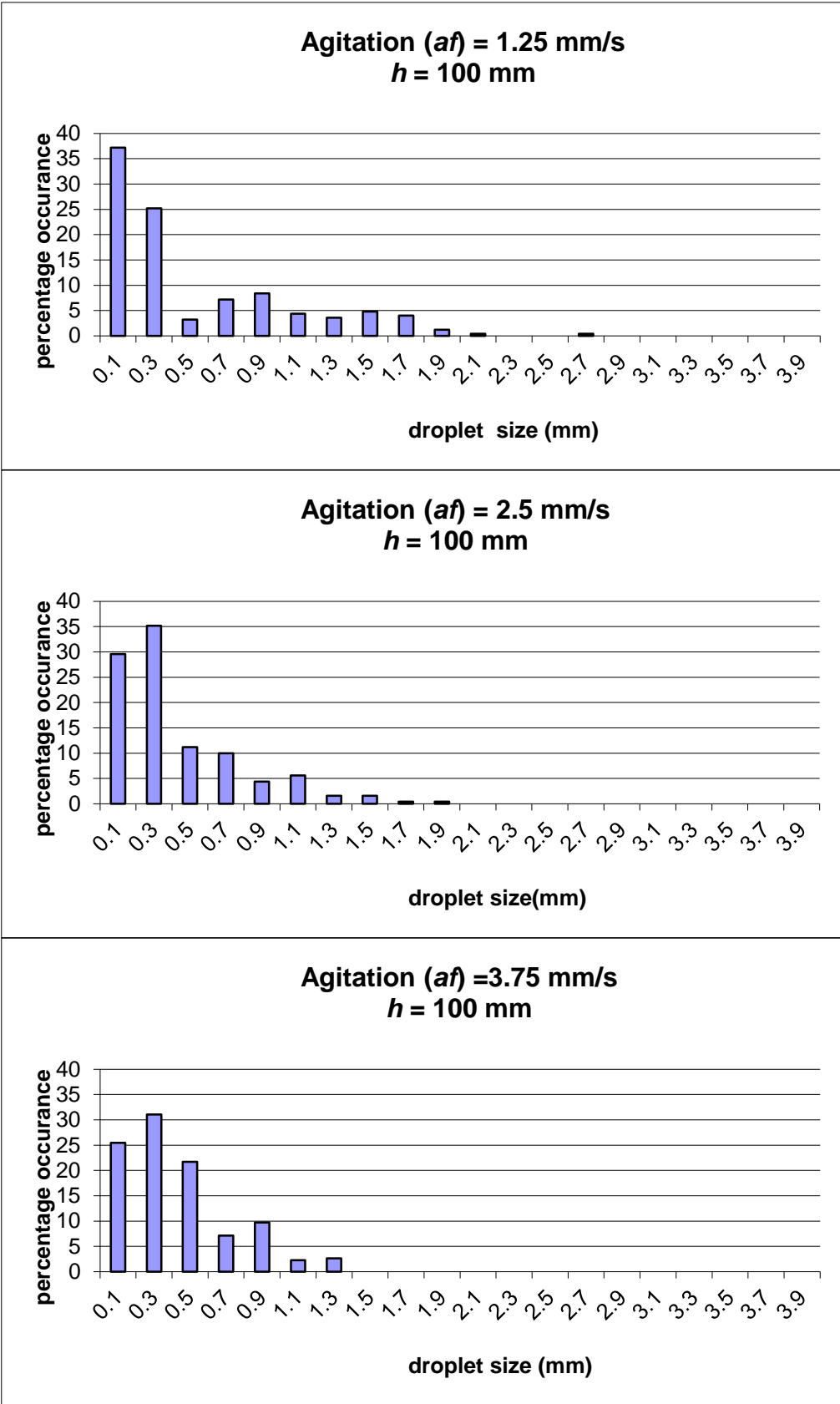


Fig. 4.3 Photos of droplets for S/F ratio = 1:1

(a) Agitation level = 1.25 mm/s; (b) Agitation level = 7.5mm/s

The size distribution is shown in fig. 4.4 for the S/F ratio of 1:1 with $h = 100$ mm. The distribution for the other ratios are shown in appendix D.



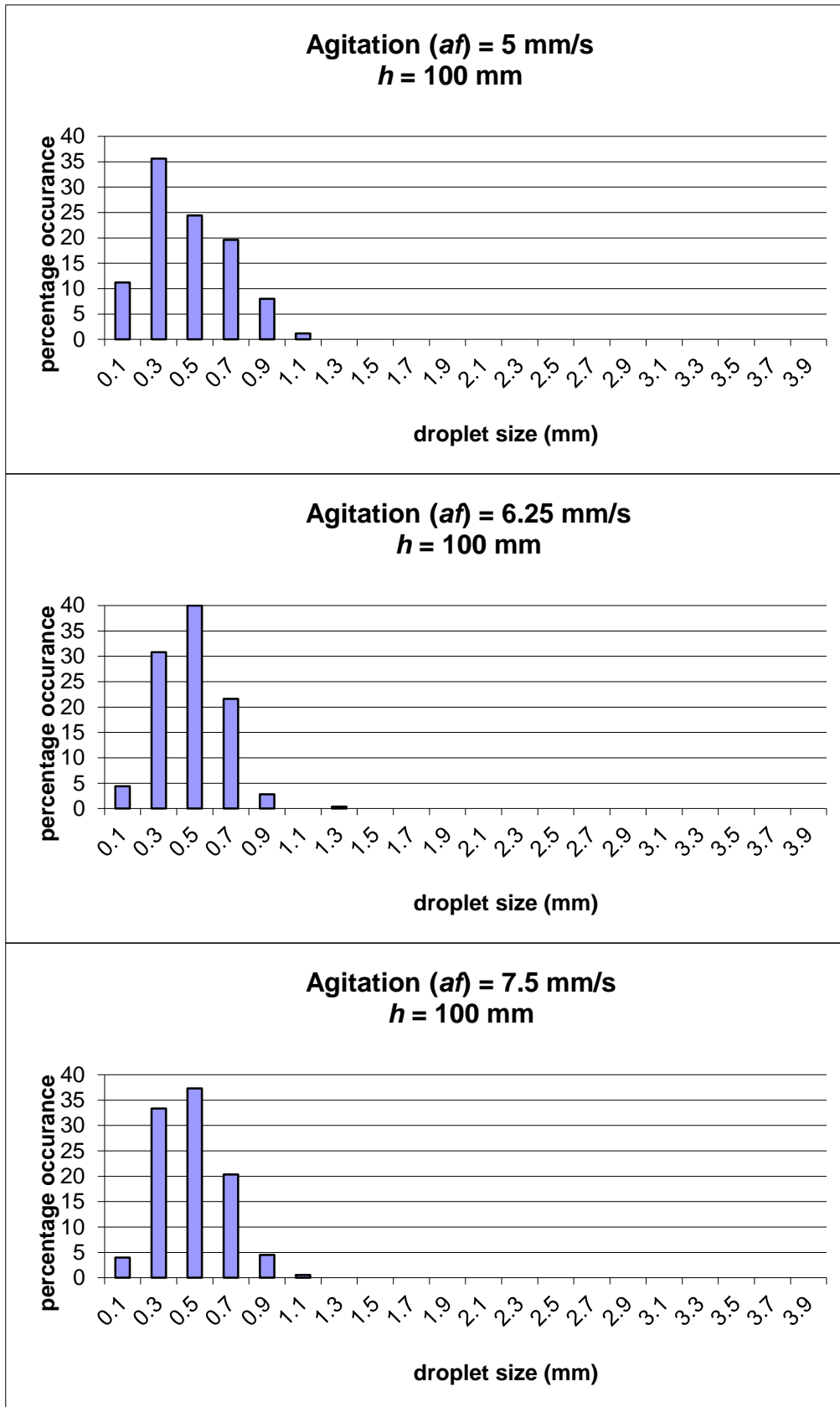


Fig. 4.4 Droplet size distribution for $S/F = 1:1$; $h = 100$ mm (without mass transfer)

It is clear from the graphs above and fig. 4.3 that there is a greater size distribution at lower agitation levels and much smaller distribution at higher agitation levels indicating that as agitation level is increased the droplets move from being of a wide variation of sizes to being more uniform (and smaller) in size. The same observation is observed with the other flow ratios as well as when the plate spacing was changed to 200 mm. It is this size distribution that is used to calculate the Sauter mean diameter. Also noticeable from the graphs is that at low agitation levels a multi-modal distribution is visible while at higher agitation levels a uni-modal distribution is seen. This confirms the observation by Josepha and Varma (1998) that under low agitation levels a dual mechanism of drop breakup exists (i.e. the flow through the perforations and the collision with the plates) while at higher agitation levels, the collision with the plates predominates, forming a uni-modal distribution.

4.2.3 Sauter Mean Diameter

The Sauter mean diameter was calculated from the size distribution using the following equation:

$$d_{32} = \frac{\sum_{i=1}^N n_i d_i^3}{\sum_{i=1}^N n_i d_i^2}$$

The results for the 3 different flow ratios at varying agitation levels with $h = 100$ mm are shown in fig. 4.5.

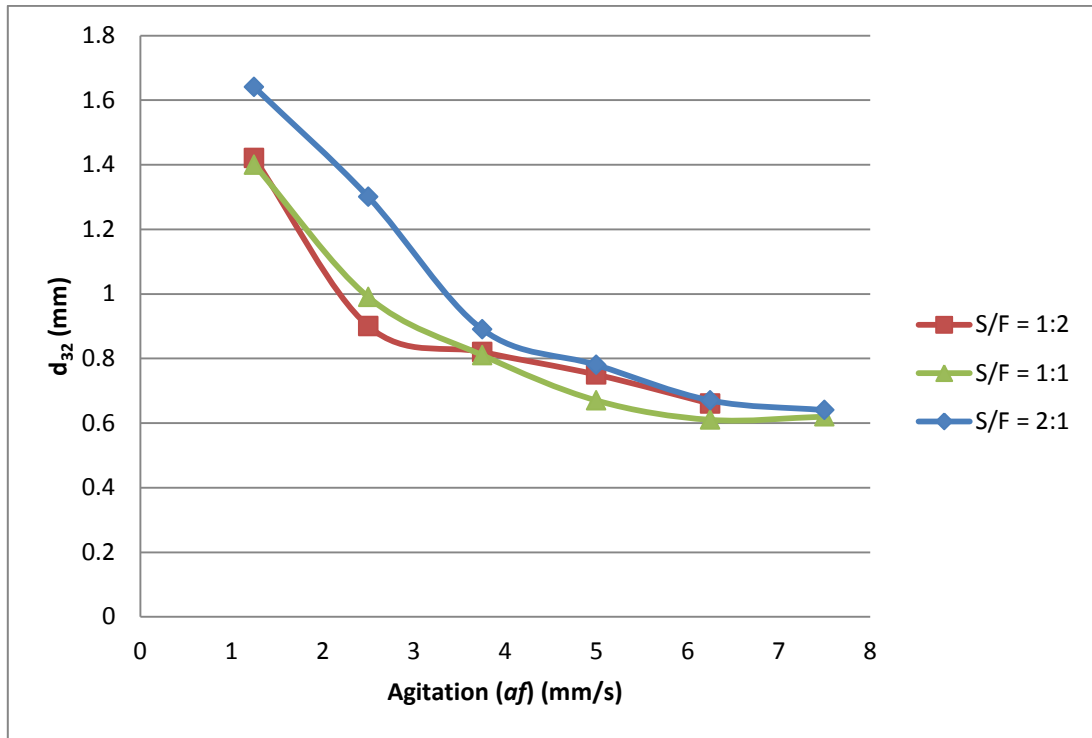


Fig. 4.5 Sauter mean diameter (hydrodynamics)

As can be seen from the chart, the Sauter mean diameter decreases as the agitation level is increased. As the plates move faster, they impart more energy to the fluids creating much smaller droplets and because the same amount of dispersed phase is being pumped into the column (for a given flow ratio), the number of droplets must increase. The size of the droplets (maximum 1.64 mm) is much smaller than the size of the perforations on the plate (3 mm). Although there is some difference between the sizes for the different flow ratios in the mixer-settler regime, the differences are minimal in the dispersion regime and it may be concluded that the Sauter mean diameter is independent of the flow ratios in the dispersion regime and is only affected by the agitation level. The droplet sizes level off as the agitation level is increased producing a minimum diameter of about 0.6 mm.

4.3 Mass Transfer Results

The mass transfer experiments were conducted with a feed of 6 mass % acetone in toluene and with water as the solvent.

4.3.1 Holdup

The calculated holdup for the different flow ratios at varying agitation levels during mass transfer (with 2 tray spacings) is given in fig. 4.6.

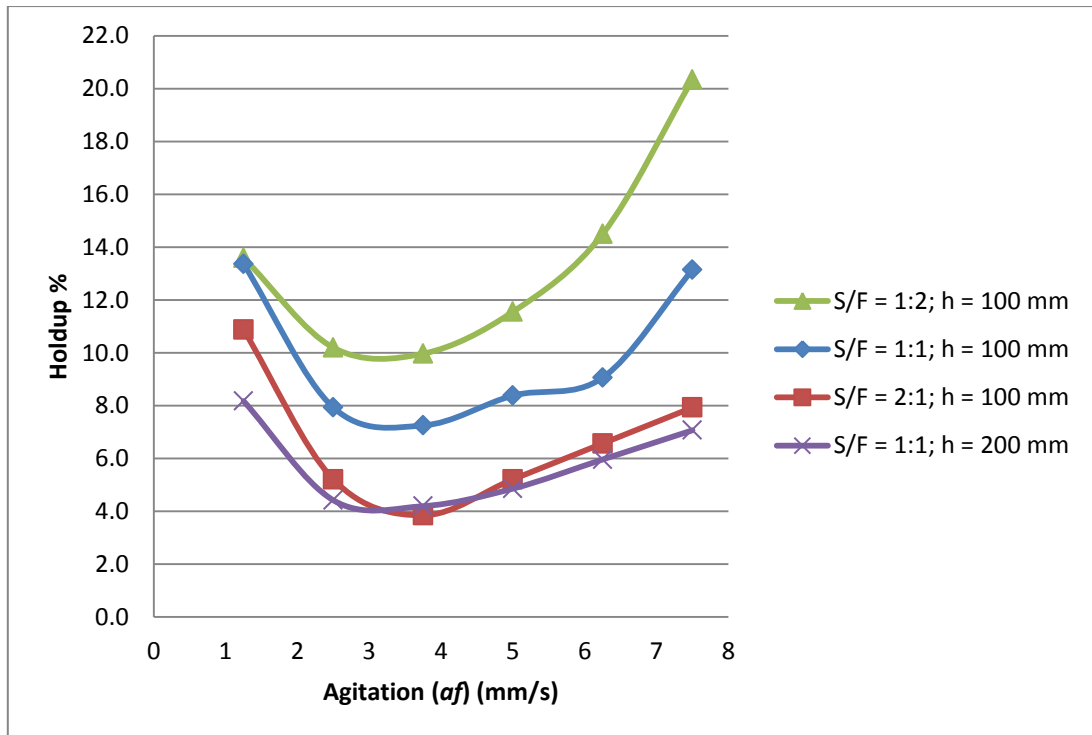


Fig. 4.6 Mass Transfer Holdup

The mass transfer holdup follows the same trend as the holdup calculated during the hydrodynamics experiments where the holdup decreases initially during the mixer-settler regime to a minimum at an agitation level of 3.75 mm/s (same as before) and then starts to increase in the dispersion regime. Initially the holdup is high due to the fact that the system is operating in the mixer-settler regime where most of the holdup is due to a layer of the

dispersed phase (coalesced) being maintained under each tray. As the agitation level is increased, this layer is reduced and as a result the holdup is reduced. The holdup eventually reaches a minimum value which corresponds to the transition from mixer-settler to dispersion regime. As frequency is increased from this point, the holdup increases because the vibrating plates cause the droplet sizes to be decreased and more droplets are formed. Some small droplets are seen to circulate in a particular stage instead of moving vertically upwards all of the time which increases the residence time of the droplets in the column and thus also increases the holdup for a given flow ratio. As the agitation is increased further the holdup is expected to increase exponentially as the system moves towards the emulsion regime and then becomes unstable as the column approaches the flooding condition.

It is also noted that the holdup when the plate spacing was changed to 200 mm is much lower than when the plate spacing was 100 mm. In the mixer-settler regime there is a large noticeable layer of dispersed phase under the plates while during the dispersion regime there is a very slight layer of dispersed phase under the plates. When the plate spacing was increased the dispersed phase did not have time to accumulate under the plates and as a result the layer that formed under the plates was minimal. This is the reason that the holdup is lower than when the tray spacing was 100 mm.

The biggest difference between the holdups is that the holdup without mass transfer is generally higher than that with mass transfer in both the mixer-settler and dispersion regimes although the minimum holdup with or without mass transfer seems to be the same. This is shown in fig. 4.7 for one of the flow ratios. Similar trends are observed for the other ratios.

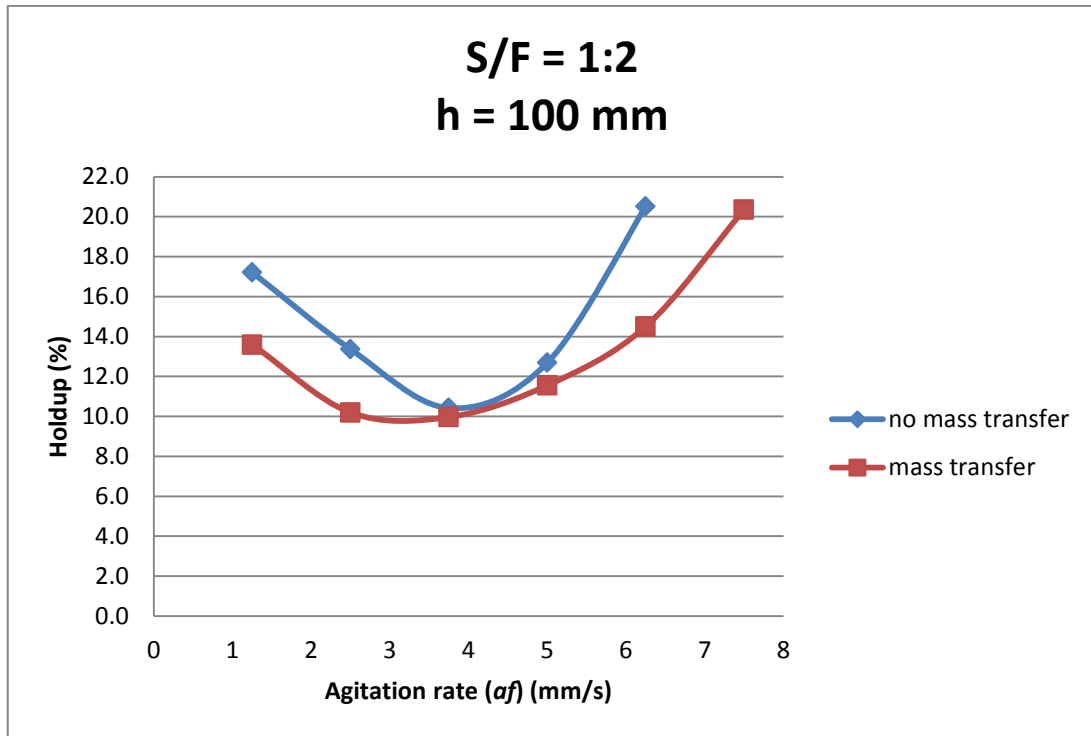
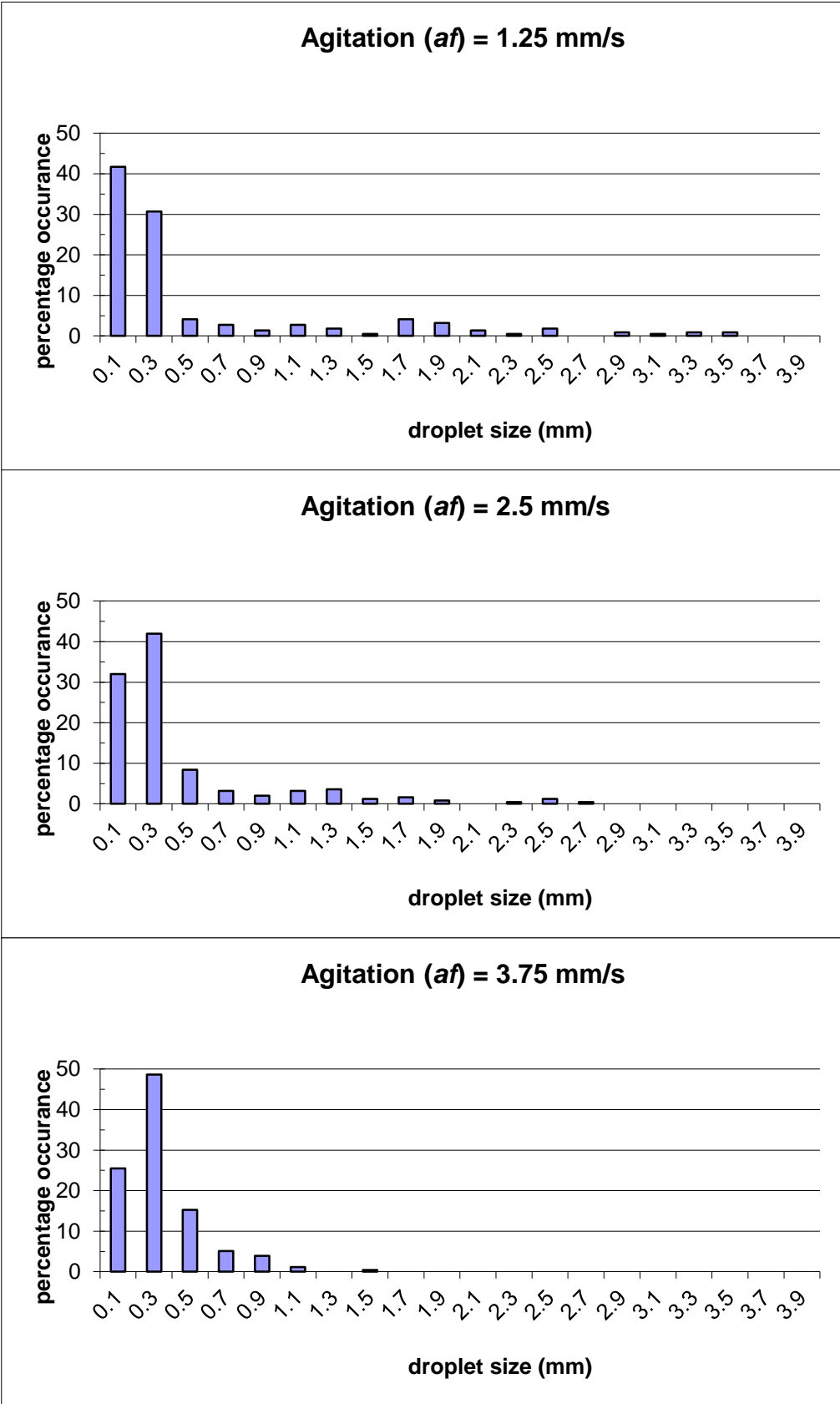


Fig. 4.7 Comparison of holdup during mass transfer and in the absence of mass transfer

This is due to the fact that the solute (acetone) is continuously being removed from the dispersed phase and as a result there is lesser dispersed phase during mass transfer than in the absence of mass transfer which results in the lower holdup. As a result, the column may be run at higher agitation levels with mass transfer than in the absence of mass transfer before flooding occurs confirming the observations made by Shen et al (1985). This also proves that predictions of mass transfer may not be done using measurements of holdup in the absence of mass transfer as the measurements are affected by mass transfer. As will be shown later, mass transfer also increases the Sauter mean diameter of the droplets which also contributes to the lower holdup.

4.3.2 Droplet size distribution

The size distribution was calculated in the same way as for the case in the absence of mass transfer. The results for the S/F ratio of 1:1 with $h = 100$ mm are shown in fig.4.8 with the distribution for the other ratios and plate spacing being given in appendix D.



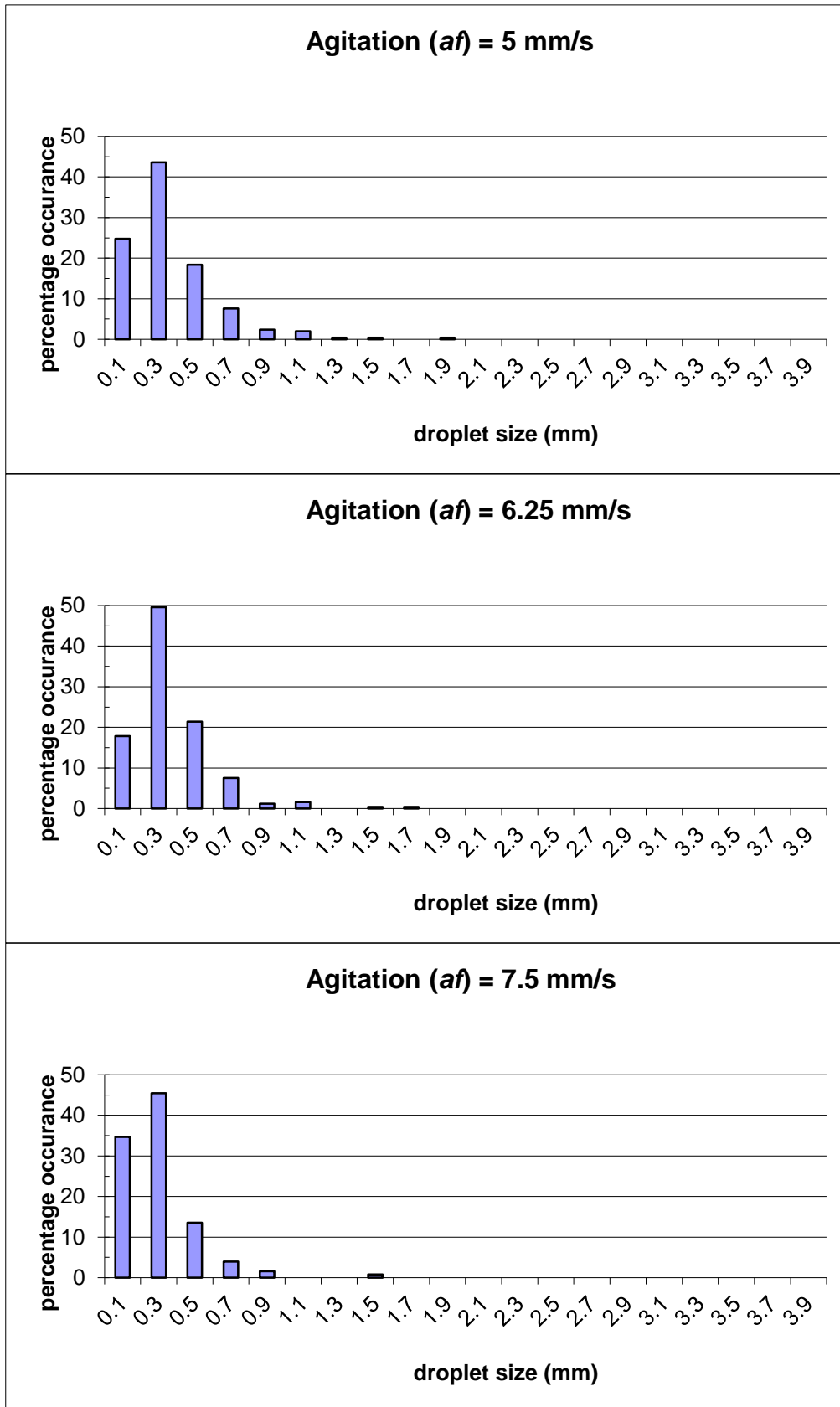


Fig. 4.8 Droplet size distribution for $S/F = 1:1$; $h = 100$ mm (with mass transfer)

Similar trends are seen with and without mass transfer. At low agitation levels there is a wide variety of droplet sizes with a multi-modal distribution while at high agitation levels the sizes are smaller and have a more uniform size producing a uni-modal distribution. However, during mass transfer, there is still some large drops present even at high agitation levels due to the enhanced coalescence effect (discussed later) during mass transfer. The size distributions for the increased tray spacing is also shown in appendix D. This size distribution seems wider and produces a larger droplet size. This is due to the fact the coalescence and breakup of droplets, which occur mostly in the vicinity of the plates, is reduced due to the lower number of plates.

4.3.3 Sauter mean diameter

The Sauter mean diameter is calculated exactly as before and the results for the three different flow ratios at varying agitation levels and tray spacing are shown in fig. 4.9.

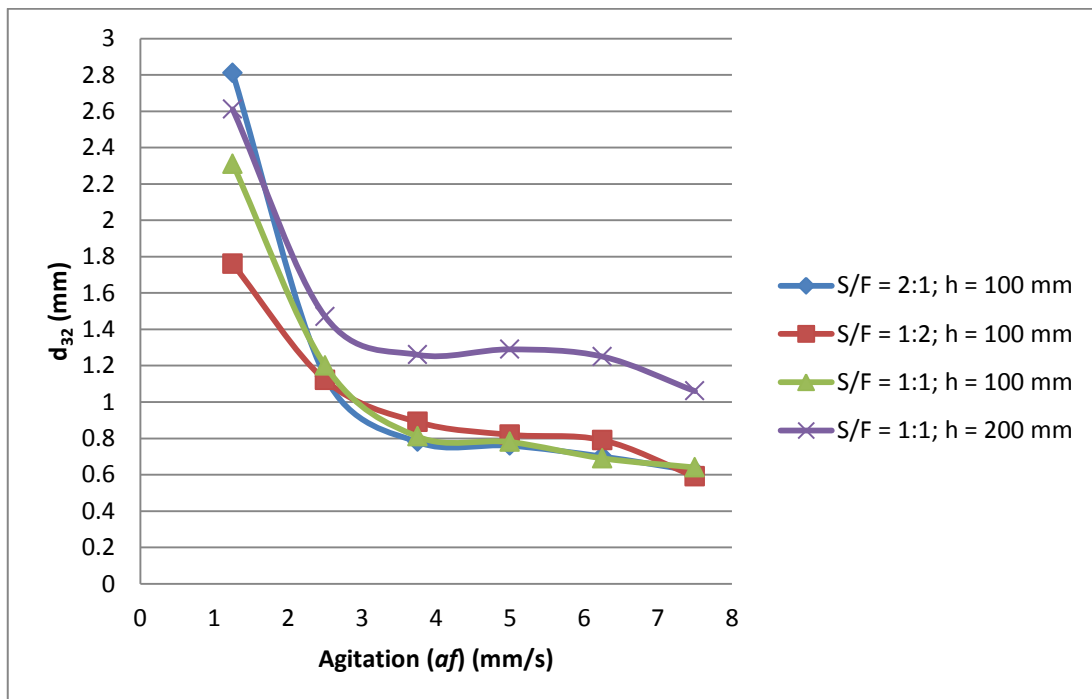


Fig. 4.9 Sauter Mean Diameter (mass transfer)

The Sauter mean diameter decreases as the agitation level is increased due to more, smaller droplets being formed. As with the case without mass transfer, there is a difference between the diameters for the different flow ratios in the mixer-settler regime, however the differences are minimal in the dispersion regime.

The Sauter mean diameter for the increased tray spacing case is shown to be much higher. Once again this is due to the reduced coalescence and breakup of the dispersed phase droplets because of the reduced number of plates since most of the coalescence and breakup occurs in the vicinity of the plates. The fewer number of plates in the column also reduces the amount of energy dissipated to the fluids which result in the drops not being as small as when there were more plates in the column dissipating more energy to the fluids.

The greatest difference is that the case with mass transfer has a greater Sauter mean diameter than the case without mass transfer especially in the mixer-settler regime shown in fig. 4.10 for one flow ratio. Similar trends are observed for the other flow ratios.

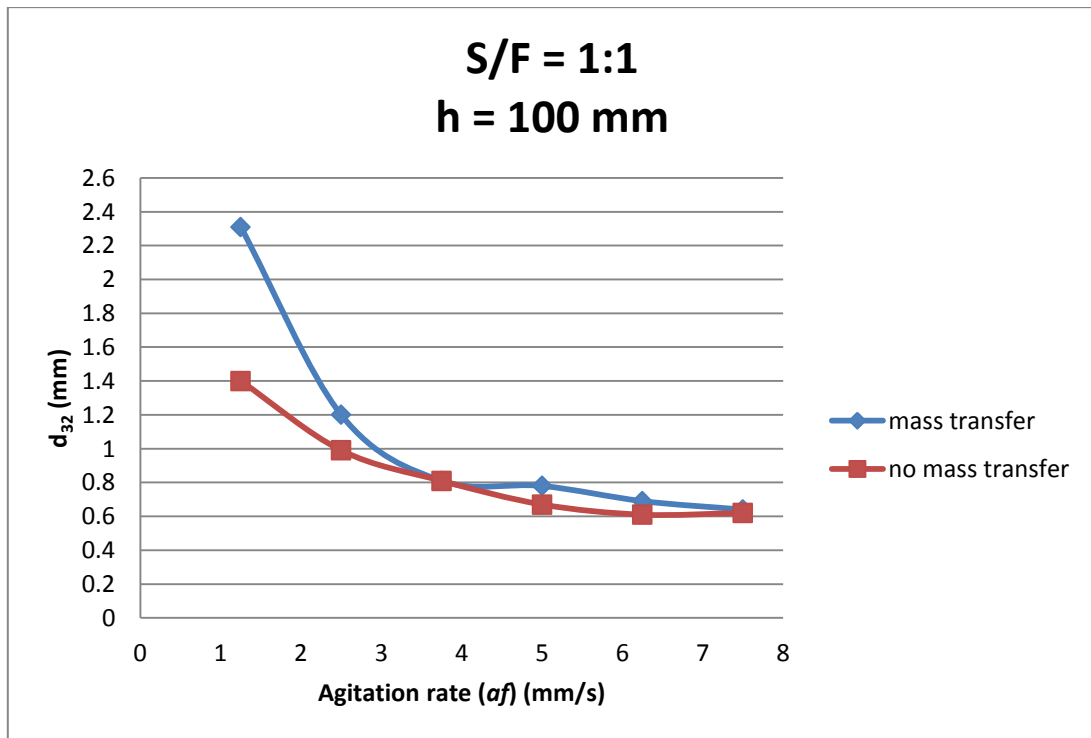


Fig. 4.10 Effect of mass transfer on Sauter mean diameter

This is due to the enhanced coalescence effects during mass transfer. As two drops approach each other, the surface tension is reduced due to the solute moving from the dispersed phase to the continuous phase. This causes the continuous phase between the drops to be drained and the drops coalesce forming bigger drops. This is consistent with literature (Shen et al, 1985; Aravamudan and Baird, 1999).

4.3.4 Extent of Mass Transfer

The extent of mass transfer was measured by analysing the extract and raffinate phases to determine their concentrations. The effect of agitation level on the extent of mass transfer for the three flow ratios and different plate spacings is illustrated in fig. 4.11.

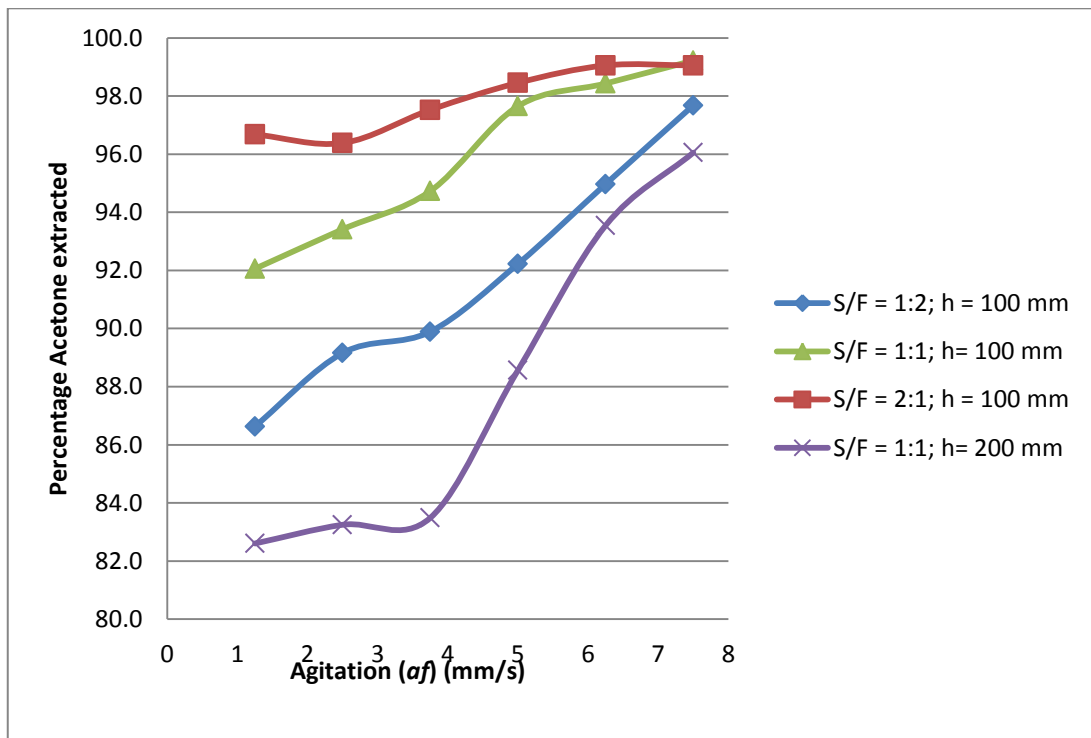


Fig. 4.11 Effect of agitation level and plate spacing on the extent of extraction

The percentage acetone extracted is calculated by subtracting the raffinate concentration from the feed concentration and expressing this difference as a percentage of the original feed concentration.

The effect of increasing agitation level is clearly indicated in the graph above showing that the amount of acetone extracted increases as the agitation level is increased with higher values being obtained when the S/F ratio is increased. From the holdup chart we have seen that an increase in agitation level increases the holdup and the d_{32} chart shows that this is accompanied by a larger number of droplets with smaller mean diameters. The total effect of this is that the interfacial area available for mass transfer is increased and therefore the effectiveness of the extraction should be improved. As shown in fig. 4.11, this corresponds to an increased amount of acetone extracted.

The reason that the effectiveness of extraction is higher for higher S/F ratios is because there is more solvent available to remove the acetone and the concentration gradient is increased. This in effect will improve the extraction effectiveness.

When the plate spacing is increased, the extraction effectiveness is drastically reduced due to the fewer number of transfer units being present for the mass transfer to take place. However, the column was not near its flooding condition at an agitation level of 7.5 mm/s like it was during the 100 mm tray spacing. As a result the agitation level may be increased beyond this limit before flooding occurred resulting in a greater extraction effectiveness being achieved.

4.4 Calculation of NTU

The true number of transfer units (N_{ox}) was obtained from the experimental equipment and was defined as the section between 2 consecutive plates. As a result for the tray spacing of 100 mm, there were 47 plates present corresponding to 46 true number of transfer units while for the tray spacing of 200 mm, 24 plates were present resulting in 23 true number of transfer units.

In order to find the ideal/theoretical number of transfer units, concentrations of both phases were evaluated from taking samples along the length of the column. This enabled the operating line to be obtained. The equilibrium line for the acetone-toluene-water system is linear with a slope of 0.832. Fig. 4.12 shows the graph for a solvent to feed ratio of 1:1, a

tray spacing of 100 mm and an agitation level of 1.25 mm/s. It can be seen from the operating line (fairly linear) that the fluids essentially move in a plug flow manner (indicated by a straight operating line) with minimal backmixing in the dispersed phase.

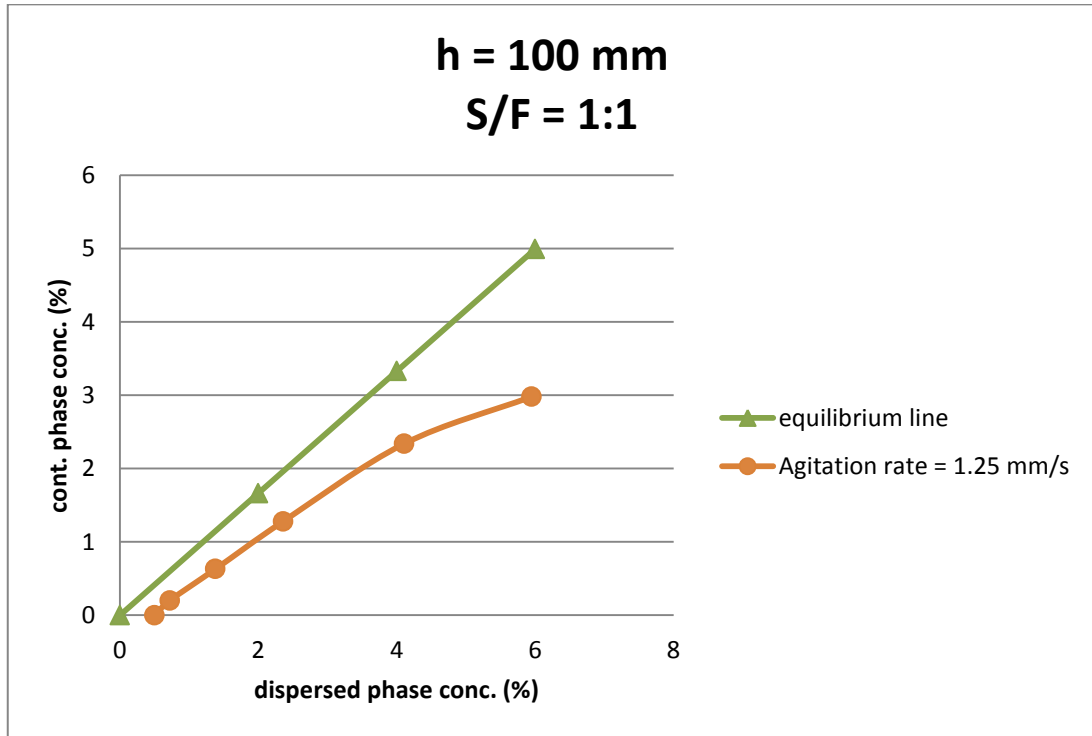


Fig. 4.12 Operating line construction (minimum agitation rate)

The ideal measured NTU (N_{oxm}) may be obtained by stepping off between the operating line and equilibrium line on a y versus x curve similar to the McCabe Thiele method in distillation. When the operating line is straight (indicating no backmixing), the ideal NTU (plug flow) may be calculated from the following equation:

$$N_{oxp} = \frac{1}{[(y_i - y_o)/m(x_o - x_i)] - 1} \ln \frac{(y_i - mx_o)}{(y_o - mx_i)} \quad (4.1)$$

where N_{oxp} is the plug flow overall NTU based on the x phase and the subscripts i and o refer to the inlet and outlet concentrations, respectively of the x and y phases.

Backmixing results in the operating line having a phase shift, as explained in section 2.18, towards the equilibrium line resulting in a higher value for NTU , therefore:

$$N_{oxp} \leq N_{oxm} \quad (4.2)$$

As agitation level is increased, the amount of backmixing in the dispersed phase also increases. This is shown in fig. 4.13 for a solvent to feed ratio of 1:1, a tray spacing of 100 mm and an agitation level of 7.5 mm/s.

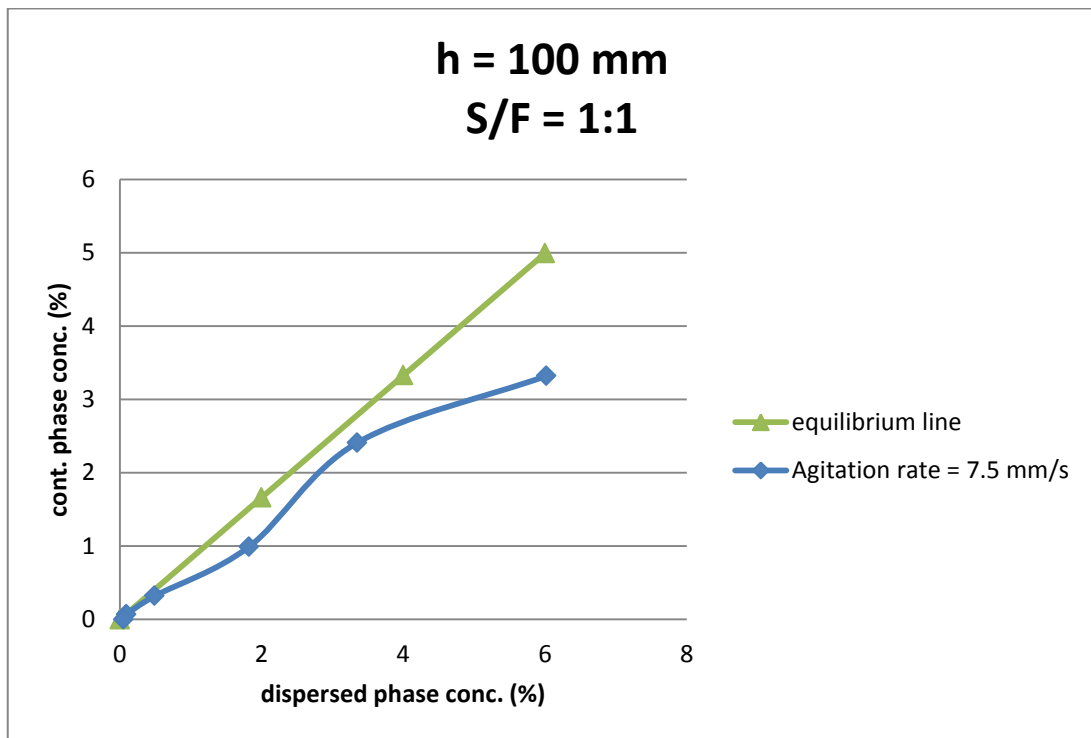


Fig. 4.13 Operating line construction (maximum agitation rate)

It is clear from this graph that $N_{oxm} > N_{oxp}$ due to the fact that at this agitation level there is evidence of backmixing in the dispersed phase. As agitation level is increased the layer of dispersed phase that exists under the plates is reduced. This layer, when present, prevents droplets of the dispersed phase from re-entering the previous stage and thus prevents backmixing in this phase. All the other profiles are shown in appendix E for all three flow ratios and the 2 tray spacings. For the S/F ratio = 1:2, there is significant backmixing for all agitation levels due to there being a large number of dispersed phase droplets being present

causing re-circulation in the stage and resulting in some of the dispersed phase re-entering the previous stage. For the S/F ratio = 2:1 case, there is essentially no backmixing because there is always a layer of dispersed phase under the plates that prevents droplets from re-entering the previous stage.

The graphical calculation of NTU is shown in appendix E. All the NTU values were rounded off upwards so that if a fraction of a transfer unit was found the NTU was increased to the next whole number. Table 4.1 summarises the calculations for N_{oxm} and includes the values for N_{exp} for comparison.

plate spacing	$h = 100 \text{ mm}$						$h = 200 \text{ mm}$	
solvent/feed ratio	S/F = 1:2		S/F = 1:1		S/F = 2:1		S/F = 1:1	
Agitation level (mm/s)	N_{oxm}	N_{exp}	N_{oxm}	N_{exp}	N_{oxm}	N_{exp}	N_{oxm}	N_{exp}
1.25	12	5	5	5	4	5	3	3
2.5	12	6	5	5	4	5	3	3
3.75	12	7	6	6	4	5	3	3
5	14	8	7	8	5	6	4	4
6.25	19	11	10	10	5	7	5	5
7.5	26	13	15	12	5	7	6	6

Table 4.1 Comparison of N_{oxm} and N_{exp}

As can be seen for most cases $N_{exp} \leq N_{oxm}$. There are some discrepancies especially for the S/F ratio of 2:1. This could be attributed to some experimental error in obtaining the samples along the length of the column. Another possible scenario is the case of forward mixing where some of the dispersed phase droplets move up the downspouts of the tray above and effectively skip a stage and mixes with the next consecutive stage. Very fine droplets may also experience forward mixing where they bypass a certain stage and effectively have a zero residence time in that stage.

4.5 Development of a Model for the Prediction of NTU

As can be seen from the discussion above, some of the dependent variables for NTU are the agitation level (product of amplitude and frequency of vibration), the solvent to feed flow ratio and the plate spacing. Fig. 4.14 shows this dependence for the flow ratio of 1:1 for both tray spacings.

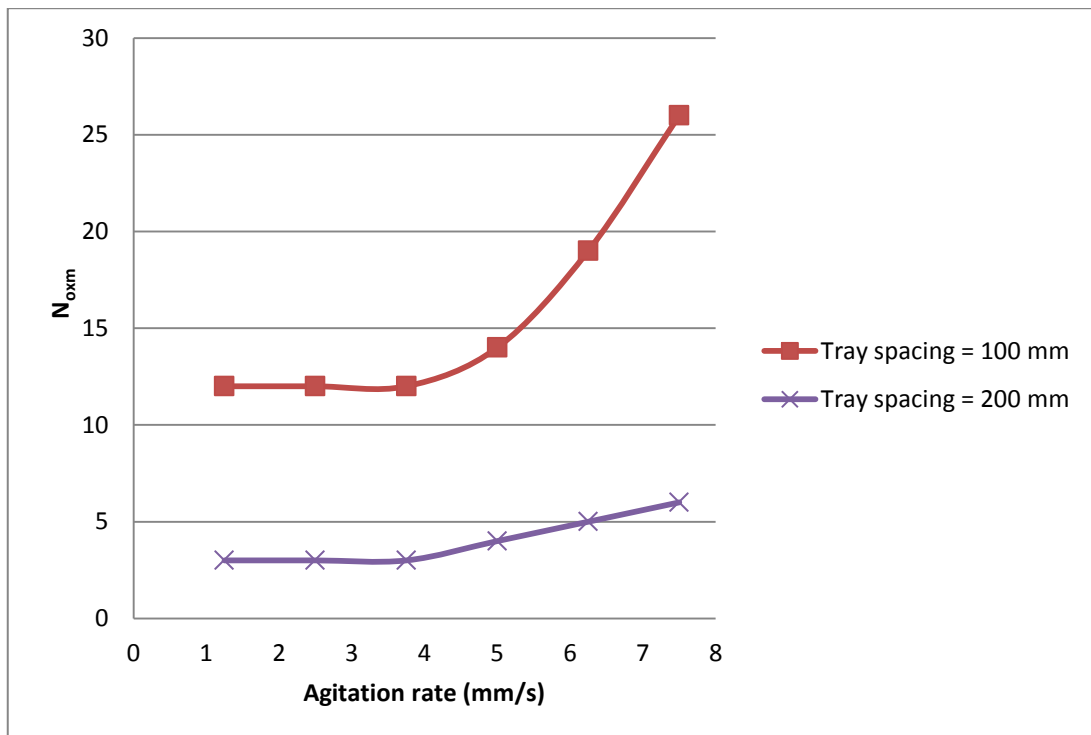


Fig. 4.14 NTU correlation

NTU remains constant until an agitation rate of 3.75 mm/s (which corresponds to the minimum holdup when the transition occurs from mixer-settler to dispersion regime) and then starts to increase exponentially.

The NTU correlation that the author has developed that best describes the data above is given as follows:

$$N_{oxm} = [5.5 + (1.8e^{0.28(af)} - 5.5)u]L\left(\frac{100}{h}\right) \quad (4.3)$$

where L is the feed to solvent ratio (reciprocal of S/F) and h the tray spacing (in mm).

u is a unit step function described as:

$$\begin{aligned} u &= 0 \text{ for } (af) < 3.75 && \text{(mixer-settler regime)} \\ &= 1 \text{ for } (af) \geq 3.75 && \text{(dispersion regime)} \end{aligned} \quad (4.4)$$

The above correlation was tested for the other 2 flow ratios using a tray spacing of 100 mm and the results are shown in fig. 4.15 (unfortunately insufficient data was obtained to test the correlation for the 200 mm tray spacing).

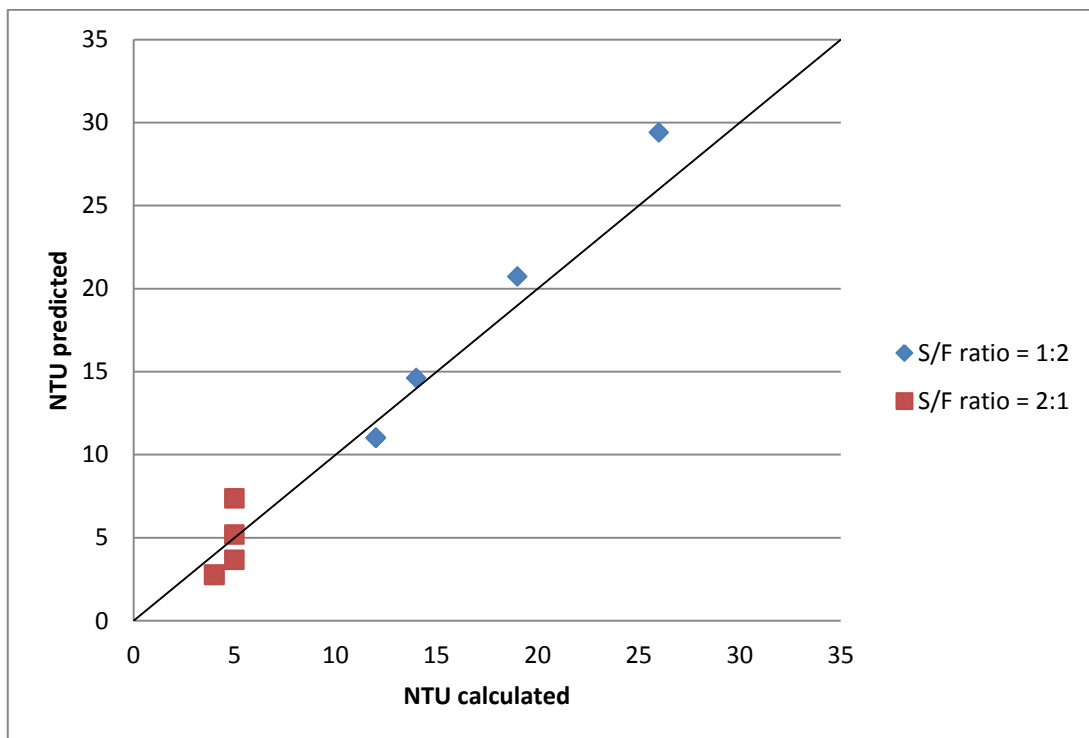


Fig. 4.15 *NTU* model verification

The 45° line above shows a perfect relation between the model prediction and the actual values. As can be seen, the correlation offers a close approximation of the actual values with a maximum error of 6%.

4.6 Calculation of HTU

The height of a transfer unit was simply calculated from the following equation:

$$HTU = H/NTU \quad (4.5)$$

with H , the height of the column being taken as 4.76 m. If we use the measured number of transfer units in the above equation, we will obtain the height equivalent to a theoretical stage (HETS) shown in fig. 4.16.

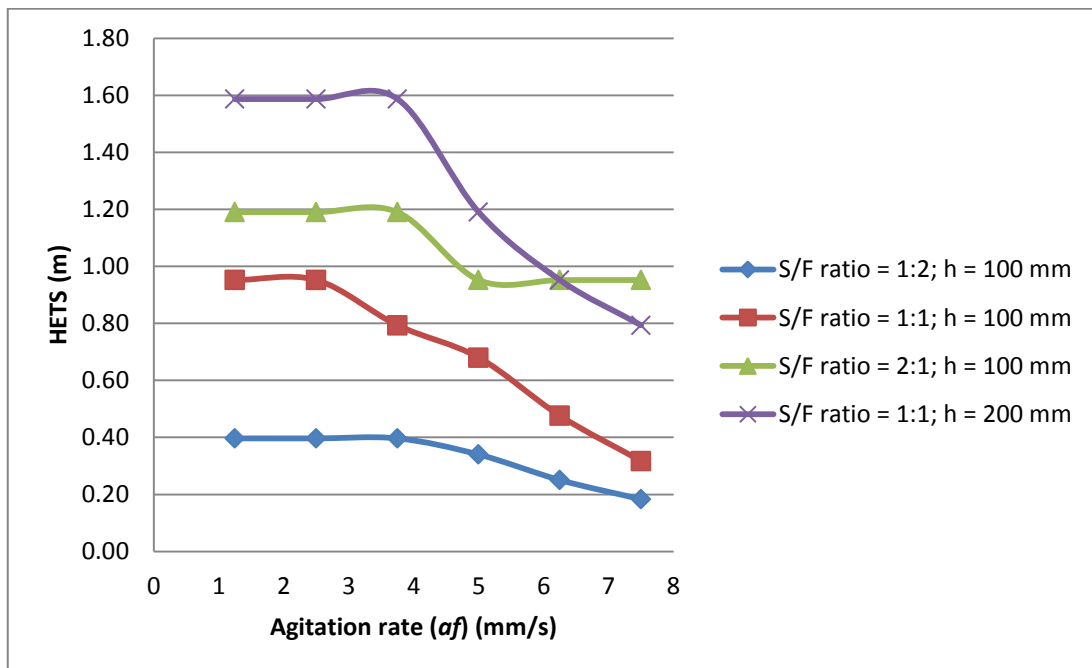


Fig. 4.16 Effect of agitation level on *HETS*

The correlation for the prediction of NTU may be used for the prediction of $HETS$ by replacing NTU by $H/HETS$.

$$\frac{H}{HETS} = [5.5 + (1.8e^{0.28(af)} - 5.5)u]L \left(\frac{100}{h} \right) \quad (4.6)$$

4.7 Mass Transfer Coefficient

The interfacial area of a drop distribution is related to holdup and d_{32} by:

$$a = \frac{6\phi}{d_{32}} \quad (4.7)$$

and that the true NTU is related to the interfacial area by:

$$N_{ox} = \frac{k_{ox}aH}{U_d} \quad (4.8)$$

As a result the true NTU and mass transfer coefficient may be related to holdup and Sauter mean diameter by:

$$k_{ox} = \frac{N_{ox}U_d}{aH} = \frac{N_{ox}U_d d_{32}}{6\phi H} \quad (4.9)$$

N_{ox} is fixed for a given tray spacing ($N_{ox} = 46$ for $h = 100$ mm; $N_{ox} = 23$ for $h = 200$ mm). U_d is also fixed for a given flow ratio and d_{32} and ϕ were calculated above for different agitation rates. As a result it is possible to develop a correlation for the prediction of mass transfer coefficient for varying agitation rates and plate spacing. Fig. 4.17 show the correlations for the 2 tray spacings for the 1:1 S/F flow ratio.

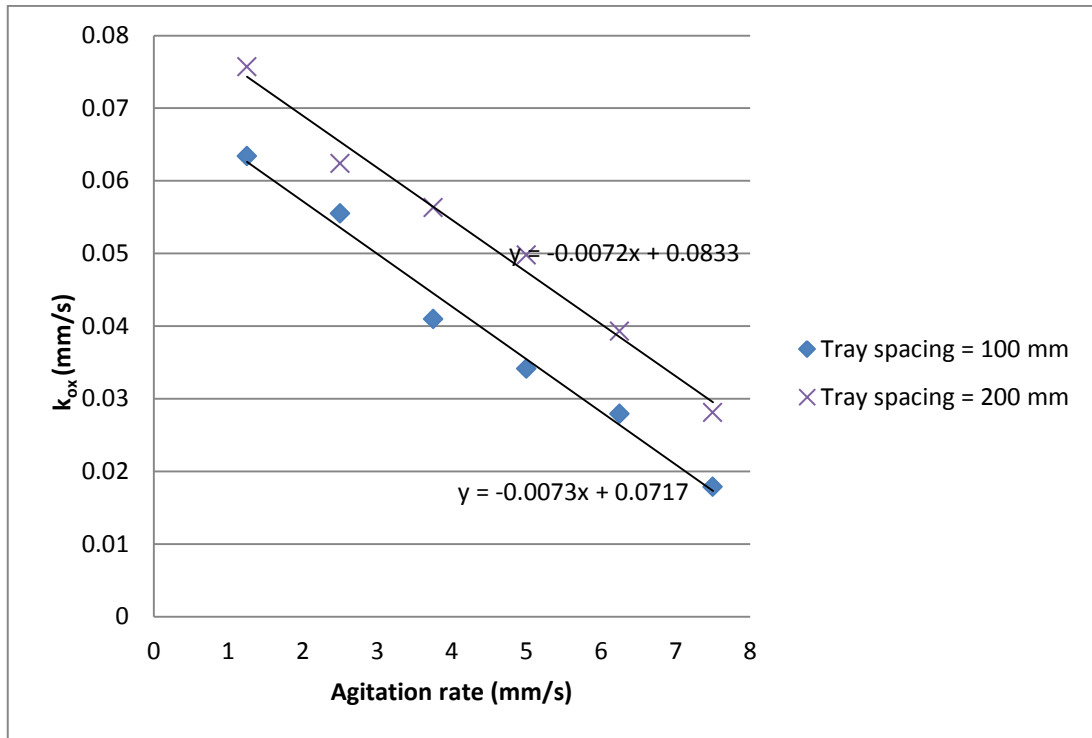


Fig. 4.17 Mass transfer coefficient correlation

A general correlation for the evaluation of mass transfer coefficient was developed by the author by combining the 2 equations above to give one correlation for the different tray spacings. This correlation is shown below where agitation rate and mass transfer coefficient are in mm/s and tray spacing is in mm:

$$k_{ox} = -0.007(af) + \left(0.06 + \frac{h}{10000}\right) \quad (4.10)$$

The correlation essentially only applies to the dispersion and emulsion regimes since the equation used to calculate the interface area involves the holdup of a drop dispersion. In the mixer-settler regime the holdup calculated includes the coalesced layer accumulated under the plates.

The above correlation was tested for the other 2 flow ratios using a tray spacing of 100 mm and the results are shown in fig. 4.18 (unfortunately insufficient data was obtained to test the correlation for the 200 mm tray spacing).

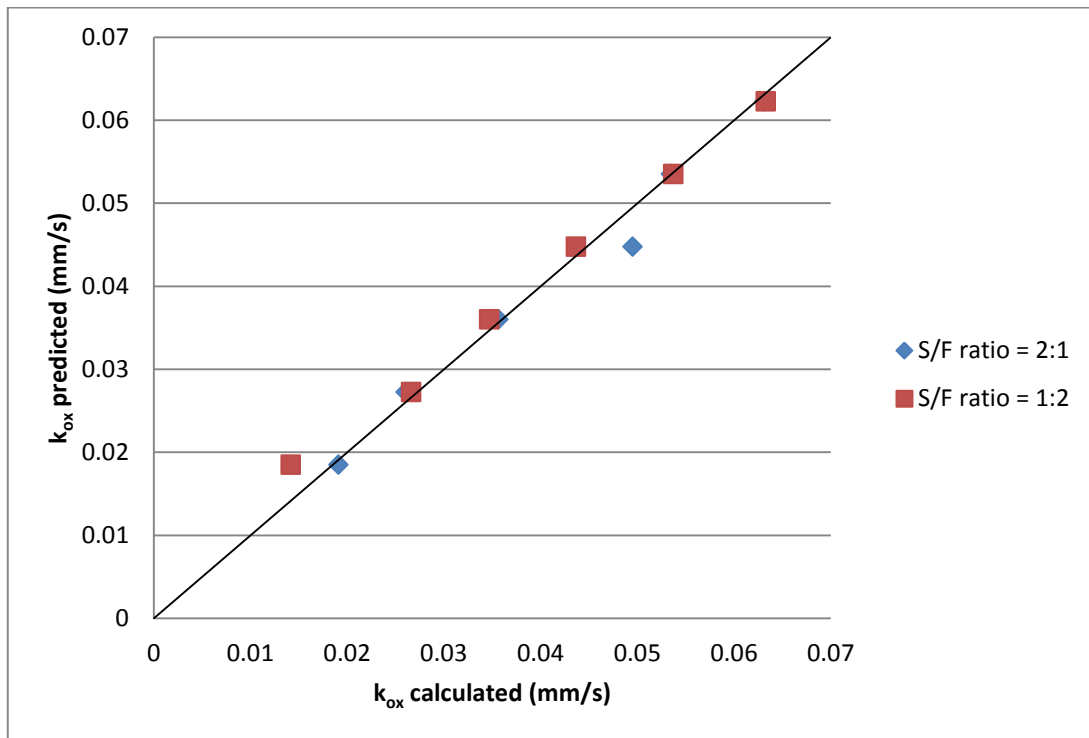


Fig. 4.18 Mass transfer coefficient model verification

Once again the 45° line shows a perfect relation between the model prediction and the actual values. As can be seen, the correlation offers a close approximation of the actual values with a maximum error of 13.4 %.

4.8 Efficiency Calculations

Volumetric efficiency may be calculated from:

$$E_v = \frac{\text{total throughput}}{HETS} = \frac{U_c + U_d}{HETS}$$

and is shown in fig. 4.19:

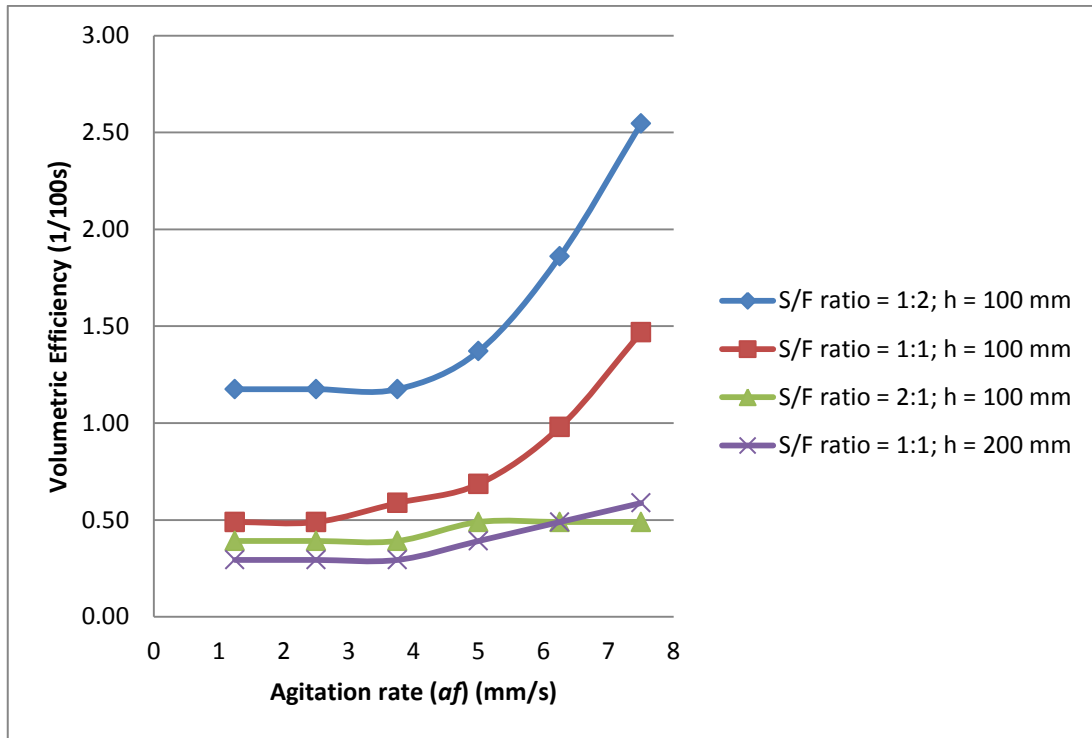


Fig. 4.19 Effect of agitation level on volumetric efficiency

The overall efficiency is defined as the ratio of the number of ideal to real stages required to achieve the same duty (i.e. the same concentration change with the given flows) and is given by the following equation:

$$E_o = \frac{N_{s,ideal}}{N_{s,real}}$$

The overall efficiency is illustrated fig. 4.20.

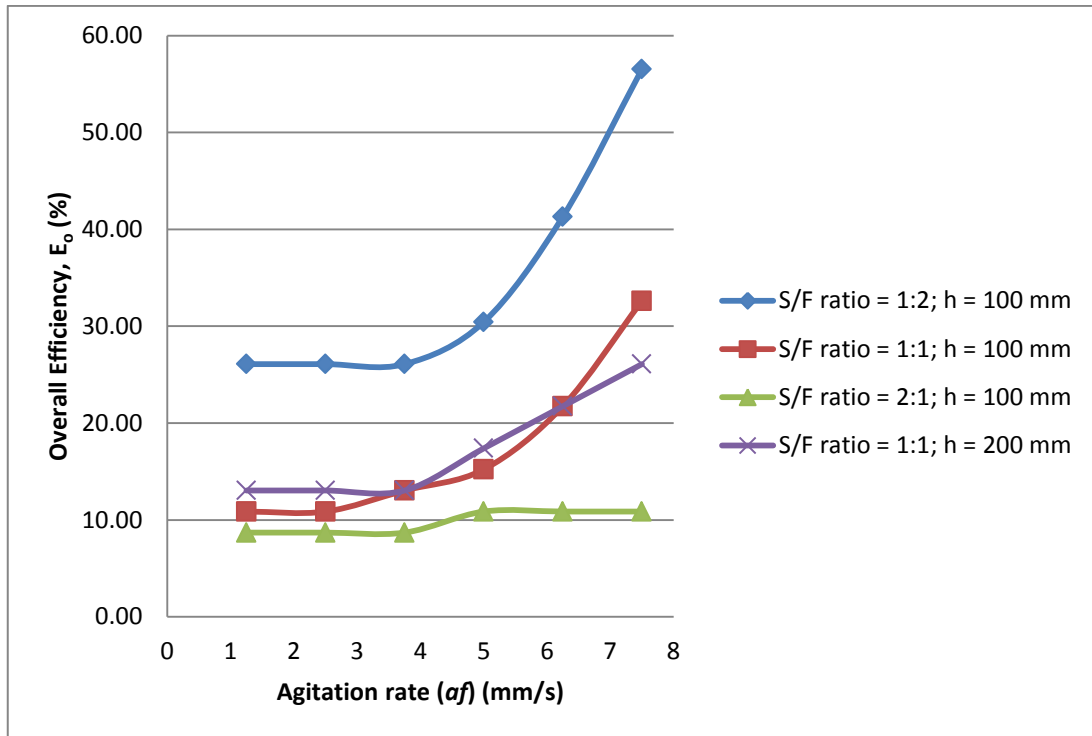


Fig. 4.20 Effect of agitation level on overall efficiency

The Murphree efficiency is defined as the ratio of the actual concentration change of a phase within a stage to that that would have occurred if equilibrium was achieved and may be calculated from the following equation:

$$E_{Mx} = \frac{N_{Ox}^1}{1 + N_{Ox}^1}$$

The Murphree efficiency is illustrated in fig. 4.21.

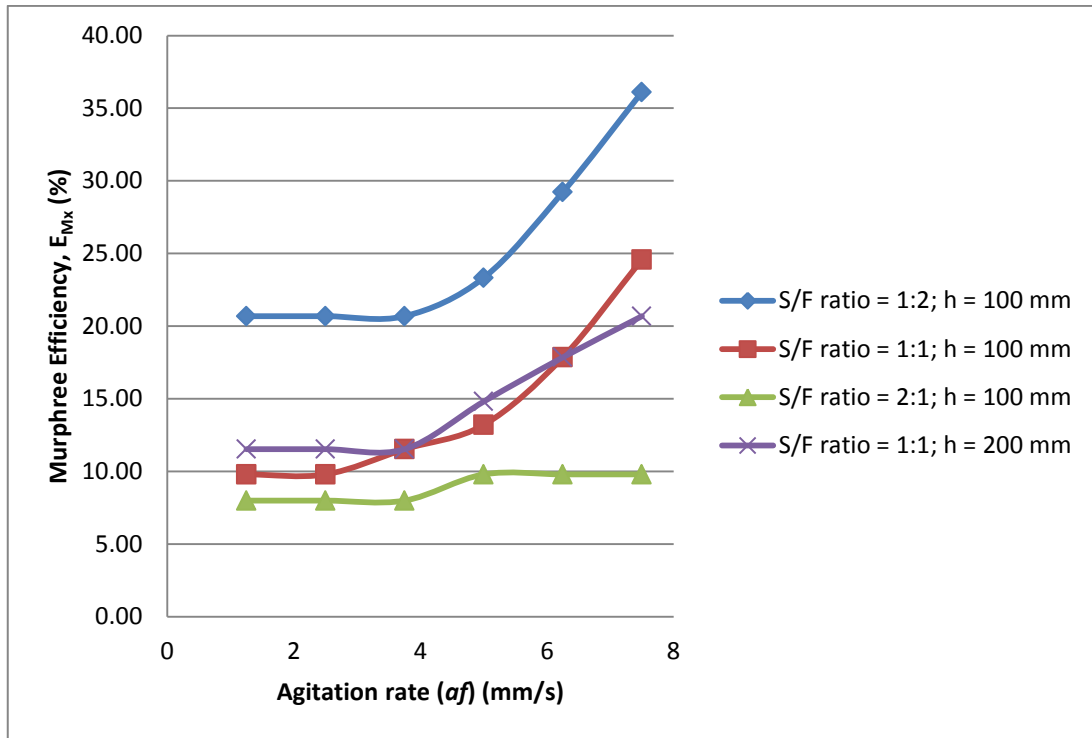


Fig. 4.21 Effect of agitation level on Murphree efficiency

All of the efficiencies above have similar trends and are seen to remain constant in the mixer-settler regime (corresponding to a constant NTU) and then increase exponentially as the agitation level is increased (corresponding to the increased NTU). Although the trends are the same, the efficiencies are defined differently and as a result have different absolute values.

4.9 Repeatability

As explained in section 3.12, each experimental run was repeated at least once. Three to five photographs were taken of the droplets during each run in order to obtain acceptable results of distribution and Sauter mean diameters. During the GC analysis, each sample was analysed at least 3 times with average values being taken as the final result. Appendix A has all the raw data of the experiments showing the multiple results obtained. It can be said that the results are highly repeatable.

CHAPTER 5

CONCLUSIONS AND RECOMMENDATIONS

This research aimed at developing a mathematical model for the prediction of *NTU/HETS* and the mass transfer coefficient for the VPE based on the agitation level of the plates (af – the product of frequency and amplitude of the plate reciprocation), the plate spacing, and the flow rates of the fluids, which will allow for the simplification in the design of this type of column.

The system chosen was the acetone-toluene-water system with the acetone in toluene forming the feed that is dispersed in the column and moves upward while the water moves as a continuous phase countercurrently down the column. This system is a standard test system for liquid extraction as stipulated by the European Federation of Chemical Engineering. The total throughput of the system was kept constant at 30 l/h while varying the individual flow rates to achieve the 1:2, 1:1 and 2:1 solvent to feed ratios.

The experimental part of the research was divided into two broad sections viz. hydrodynamics and mass transfer. In attempting to develop the mathematical models, the following experimental investigations were examined: effects of agitation level and S/F ratio on drop size/distribution and holdup with and without mass transfer; effects of agitation level, S/F ratio and tray spacing on the extent of mass transfer, *NTU* and the efficiency; effects of mass transfer on drop size/distribution and holdup.

In the operation of the equipment it was found that flow rates could not be measured accurately with rotameters because of fluctuations caused by the peristaltic pumps and the pressure changes at the bottom of the column caused by the vibration of the plates. Surge tanks were designed, built and installed in order to overcome this limitation. One surge tank was placed between the water inlet pump and rotameter which allowed for steady flows to be read off the rotameter. A second surge tank was installed between the feed inlet pump and rotameter in order to absorb the fluctuations of the pump while a third tank, placed between the rotameter and the feed sparger, reduced the effects of the pressure changes at the bottom of the column from affecting the rotameter reading.

Preliminary tests showed that a minimum of 45 minutes was required for an experimental run for the system to reach steady state before readings, photos or samples could be taken.

The holdup during mass transfer and in the absence of mass transfer decreased initially as the agitation level was increased (during the mixer-settler regime) until it reached a minimum at an agitation level of 3.75 mm/s (transition between mixer-settler and diffusion regimes) before having an increasing trend beyond this limit (for the diffusion and eventually emulsion regimes). The holdup decreased as the S/F ratio increased and since it was found that there was a weak relationship between continuous phase flow and holdup, it was concluded that the holdup decreased with a decrease in dispersed phase flow and was independent of continuous phase flow. The holdup during mass transfer was lower than that in the absence of mass transfer due to the solute being continuously removed from the dispersed phase resulting in there being lesser dispersed phase and a lower holdup during mass transfer.

Drop size analysis showed that there was a wide distribution of sizes at low agitation levels which became narrower as the agitation level was increased corresponding to a decrease in the Sauter mean diameter as the agitation level increased. During mass transfer there were a few large drops that were observed even at high agitation levels as a result of enhanced coalescence effects. When the tray spacing is increased, the distribution is wider resulting in a much higher Sauter mean diameter for all the agitation rates. This is due to the reduced coalescence and breakup of the drops which occur predominantly in the vicinity of the plates.

From the differences in the measurements during hydrodynamics and mass transfer (for the measurement of holdup and droplet size/distribution) it was concluded that the measurements during hydrodynamics cannot be used in correlations for the prediction of performance of the extractor since the process of mass transfer affects the hydrodynamics of the column (although the shape of the holdup and droplet size graphs were the same, the actual values were different).

The amount of acetone extracted during the mass transfer experiments gradually increased with increasing agitation level and S/F ratio. As the agitation level was increased more and

smaller droplets were formed which increased the interfacial area available for mass transfer which improved the extent of acetone removal. As the S/F ratio increased, the concentration difference (driving force for mass transfer) was increased which increased the amount of acetone removal. With the increased plate spacing the extraction effectiveness is drastically reduced due to a fewer number of transfer units being present for the mass transfer to take place. The amount of energy dissipated to the fluids from the vibrating plates is also reduced due to the fewer plates, resulting in larger drops and lower holdup. This contributes to the poorer performance.

The ideal number of transfer units taking into account the backmixing of the phases was calculated graphically using the McCabe Thiele method. By plotting the operating line for the various cases the extent of backmixing was noticed. For the 1:1 flow ratio, the backmixing was minimal for the low agitation levels with evidence of the start of backmixing in the dispersed phase at the maximum agitation while there was no notice of backmixing in the continuous phase. For the 2:1 flow ratio, no backmixing was seen to occur in either phase. During the 1:2 flow ratio, there was backmixing for all the agitation levels in the dispersed phase while the start of backmixing in the continuous phase was seen.

Using the information of NTU calculations an empirical correlation was developed for the prediction of the measured NTU taking into account axial dispersion (N_{oxm}). The data for the 1:1 flow ratio with both tray spacings was used to develop the correlation for the effects of agitation level, tray spacing and flow ratio. The correlation was tested with data for the other 2 flow ratios and showed reasonable accuracy with a maximum error of 6 %. The correlation was also adapted to calculate the $HETS$.

From the holdup and drop size data and the actual number of transfer units identified in the column, a correlation was developed for the prediction of mass transfer coefficient for the 1:1 flow ratio at both tray spacings as a function of agitation level and tray spacing. The correlation was tested for the other 2 flow ratios and showed reasonable accuracy with a maximum error of 13 %. The mass transfer coefficient was found to be independent of flow ratios.

The volumetric, overall and Murphree efficiency calculated was seen to remain constant in the mixer-settler regime and increase exponentially in the dispersion and emulsion regimes and decreased with an increase in flow ratio and tray spacing.

Recommendations and Future Work:

The flow rate through the feed pump was unstable and was dependent on the positioning and flexibility of the tube than ran through the pump and as a result it is highly recommended that a flow controller be installed in order to maintain a constant flow rate.

Additional experiments are required to test the models developed for tray spacing and amplitude changes.

More experiments are also required for agitation levels in the emulsion regime near the flooding point.

NOMENCLATURE

a	= amplitude (half-stroke), m
A	= stroke, m
A_c	= cross-sectional area of column, m ²
A_{in}	= interfacial area in stage, m ²
Ar	= Archimedes number
b	= constant defined by equation
B	= constant defined by equation = H/d_c
C_N	= orifice coefficient = 0.67 for circular holes
C_o	= orifice discharge coefficient through perforations
c_i	= concentration of the i^{th} phase (mass or volume basis)
c_i^*	= concentration at equilibrium (mass or volume basis)
d	= dispersed phase drop diameter, m
d_c	= characteristic dimension, m
d_e	= equivalent drop diameter, m
d_e^0	= value of d_e at a linear velocity of 3 cm/s in the perforation, m
d_0	= perforation diameter, m
d_{32}	= Sauter mean drop diameter, m
D	= diffusivity, m ² /s
D_c	= column diameter, m
e_i	= coefficient of back-mixing in the i^{th} phase
E_t	= tray efficiency
E	= extraction factor = mU_x/U_y
E_o	= overall sieve tray efficiency
E_c	= axial dispersion coefficient of continuous phase, m ² /s
E_B	= extraction factor of component B
E_{Mi}	= Murphree efficiency in terms of the i^{th} phase
E_n	= entrainment of dispersed phase, ppm (by volume)
E_v	= volumetric efficiency, 1/hr = solute-free extract flow, kg/h
f	= frequency, Hz
F_i/Q_i	= volumetric flow rate of the i^{th} phase, m ³ /s = solute-free feed flow, kg/h
g	= acceleration due to gravity, m/s ²

g_c	= gravitational conversion factor, $\text{kg.m/s}^2.\text{N}$
h	= centre to centre plate spacing, mm
h_t	= liquid head of static holdup, m
H	= height of the active part of the extractor, m
$HETS$	= height equivalent to a theoretical stage, m
H_{ox}	= true height of transfer unit, m
H_{exp}	= plug flow height of transfer unit, m
J	= interfacial flux, $\text{kmol/m}^2.\text{s}$
k_E	= extract mass transfer coefficient, m/s
k_R	= raffinate mass transfer coefficient, m/s
K_i	= dimensionless constant
K_A	= distribution coefficient of component A
K_C	= distribution coefficient of component C
K_{equ}	= equilibrium ratio
$K_E, K_R,$	= overall mass transfer coefficient, m/s
k_{ox}, k_{oy}	
k_m	= Marangoni mass transfer coefficient, m/s
L	= ratio U_d/U_c
L_I	= $1/L$ (same as S/F)
m	= slope of the equilibrium curve
m_I	= height of well mixed region, m
n	= number of perforations
n_s	= number of actual stages
n_{si}	= number of actual stages required at zero back-mixing
N	= number of plates
N_{ox}	= 'true' overall number of transfer units based on the x phase
N_{oxm}	= measured overall number of transfer units based on the x phase
N_{exp}	= apparent or piston number of transfer units assuming plug flow
N_{ox}^I	= number of transfer units per stage
N_R	= solute flux, m/s
p	= coefficient of short-cut flow (forward mixing)
P	= as defined in equation
\bar{P}	= time-average power dissipation, W
Pe_i	= turbulent Peclet number of the i^{th} phase = $U_i d_c / e_i$
Pe^*	= average droplet Peclet number = $u_t d_{32} / D_{AB}$

Δp	= pressure difference across a plate, kPa
P_{in}	= power input, W
q	= backmixing between adjacent stages
q_c	= effective coefficient of backmixing in the continuous phase
R	= as defined in equation = solute-free raffinate flow, kg/h
Re_T	= Reynolds number at terminal velocity
s	= cross sectional area of the column, m ²
S_I	= fractional open area of plate
S_i	= surface area of a drop, m ²
S_N	= area of all the holes in a plate, m ²
S_t	= area of the sieve plate, m ² = solute-free solvent flow, kg/h
S	= stripping factor = U_y/mU_x
Sh	= Sherwood number = $k_d d_{32}/D_{AB}$
t	= time, s
U_c	= superficial velocity of continuous phase, m/s
U_d	= superficial velocity of dispersed phase, m/s
U_T	= total throughput = $U_c + U_d$, m/s
U_o	= hole/perforation velocity, m/s
u_k	= characteristic slip velocity, m/s
u_N	= velocity at the nozzle or orifice, m/s
u_p	= velocity of plate, m/s
u_s	= slip velocity, m/s
u_{sF}	= slip velocity at flooding, m/s
u_T	= terminal velocity, m/s
v	= phase volume in stage, m ³
V	= stage volume, m ³
W_1, W_2	= adjustable velocity parameters defined by equation
X, Y	= as defined in equation
x	= mol fraction in raffinate phase
x^*	= raffinate mol fraction in equilibrium with extract phase
y	= mol fraction in extract phase
y^*	= extract mol fraction in equilibrium with raffinate phase

Greek Letters

- α_i = backmixing ratio of phase i = *backflow*/ F_i
- ϵ_d = specific energy dissipation rate of the dispersed phase, W/kg
- ϵ_m = specific energy dissipation rate relating to mechanical agitation, W/kg
- ϕ_l = defined by equation
- ϕ = dispersed phase holdup
- β = separation factor
- μ_c = continuous phase viscosity, Pa.s
- μ_d = dispersed phase viscosity, Pa.s
- μ_w = viscosity of water = 10^{-3} Pa.s
- ρ_c = continuous phase density, kg/m³
- ρ_d = dispersed phase density, kg/m³
- $\Delta\rho$ = density difference, ($\rho_c - \rho_d$), kg/m³
- $\bar{\rho}$ = mean density of dispersion = $\rho_c(1 - \phi) + \rho_d\phi$, kg/m³
- δ = standard deviation
- γ = interfacial tension, N/m
- γ_{ref} = interfacial tension of pure substance, N/m
- γ_{eq} = interfacial tension at equilibrium, N/m
- $\Delta\gamma$ = difference in surface tension, N/m
- γ_{AB} = activity coefficient of component A in B
- γ_{Be} = activity coefficient of component B in extract phase
- γ_{Br} = activity coefficient of component B in raffinate phase
- η = stage efficiency
- η_m = mechanical efficiency of vibration
- δ = plate thickness, m
- σ = fraction open area of plate
- Ψ = power dissipation per unit volume of dissipation, W/m³
- Ψ_m = power dissipation per unit mass, W/kg
- Ψ_1 = gravitational power dissipation per unit volume, W/m³

Subscripts

c, y = continuous phase

d, x = dispersed phase

F = flooding

A = component A

C = component C

i = interface

e = effective

E = extract phase

R = raffinate phase

n = nth stage

REFERENCES

- 1 **Al-Sugair, K.A., Abd El-Aleem, F., Ibrahim, A. & Al-Masry, W.A.**, 2006. Enhancement of mass transfer in bubble columns using vibrating plates. *Journal of Saudi Chemical Society*, 10 (2), pp. 295-302.
- 2 **Aravamudan, K. & Baird, M.H.I.**, 1996. Effect of unstable density gradients on back-mixing in a reciprocating plate column. *AIChE Journal*, 42 (8), pp. 2128-2140.
- 3 **Aravamudan, K. & Baird, M.H.I.**, 1999. Effects of mass transfer on the hydrodynamic behavior of a Karr reciprocating plate column. *Industrial & Engineering Chemistry Research*, 38 (4), pp. 1596-1604.
- 4 **Arendt, B. & Eggers, R.**, 2007. Interaction of Marangoni convection with transfer effects at droplets. *International Journal of Heat & Mass Transfer*, 50, pp. 2805-2815.
- 5 **Bahmanyar, H., Nazari, L. & Sadr A.**, 2008. Prediction of effective diffusivity and using of it in designing pulsed sieve plate extraction columns. *Chemical Engineering & Processing*, 47, pp. 57-65.
- 6 **Baird, M.H.I.**, 1974. Axial dispersion in a pulsed plate column. *The Canadian Journal of Chemical Engineering*, 52 (3), pp. 750-757.
- 7 **Baird, M.H.I. & Lane, S.J.**, 1973. Drop size and holdup in a reciprocating plate extraction column. *Chemical Engineering Science*, 28 (3), pp. 947-957.
- 8 **Baird, M.H.I. & Rama Rao, N.V.**, 1991. Axial mixing in a reciprocating plate column with very small density gradients. *AIChE Journal*, 37 (7), pp. 1019-1026.
- 9 **Baird, M.H.I. & Rama Rao, N.V.**, 1988. Characteristics of a countercurrent reciprocating plate bubble column. II: Axial mixing and mass transfer. *The Canadian Journal of Chemical Engineering*, 66, pp. 222-231.
- 10 **Baird, M.H.I. & Shen, Z.J.**, 1984. Holdup and flooding in reciprocating plate extraction columns. *The Canadian Journal of Chemical Engineering*, 62 (2), pp. 218-227.
- 11 **Ban, T., Kawaizumi, F., Nii, S. & Takahashi, K.**, 2000. Study of drop coalescence behavior for liquid-liquid extraction operation. *Chemical Engineering Science*, 55 (22), pp. 5385-5391.
- 12 **Bell, R.L. & Babb, A.L.**, 1969. Holdup and axial distribution of holdup in a pulsed sieve-plate solvent extraction column. *Industrial & Engineering Chemistry Process Design & Development*, 8 (3), pp. 392-400.

- 13 **Bensalem, A., Steiner, L. & Hartland, S.**, 1986. Effect of mass transfer on drop size in a Karr column. *Chemical Engineering & Processing: Process Intensification*, 20 (3), pp. 129 – 135.
- 14 **Boyadzhiev, L. & Spassov, M.**, 1982. On the size of drops in pulsed and vibrating plate extraction columns. *Chemical Engineering Science*, 37 (2), pp. 337-340.
- 15 **Brodkorb, M.J., Bosse, D., von Reden, C., Gorak, A. & Slater, M.J.**, 2003. Single drop mass transfer in ternary and quaternary liquid-liquid extraction systems. *Chemical Engineering & Processing*, 42 (11), pp. 825-840.
- 16 **Camurdan, M.C., Baird, M.H.I. & Taylor, P.A.**, 1989. Steady state hydrodynamics and mass transfer characteristics of a Karr extraction column. *The Canadian Journal of Chemical Engineering*, 67 (4), pp. 554-559.
- 17 **CHEMCAD**, 2005. *Chemstations software tools for chemical engineering productivity and accuracy*, v5.5.
- 18 **Din, G.U., Chughtai, I.R., Inayat, M.H. & Khan, I.H.**, 2008. Axial dispersion, holdup and slip velocity of dispersed phase in a pulsed sieve plate extraction column by radiotracer residence time distribution analysis. *Applied Radiation & Isotopes*, 66, pp. 1818-1824.
- 19 **Enders, S., Kahl, H. & Winkelmann, J.**, 2007. Surface tension of the ternary system water + acetone + toluene. *Journal of Chemical & Engineering Data*, 52, pp. 1072-1079.
- 20 **European Federation of Chemical Engineering**, 1985. Standard test system for liquid extraction. *E Publications Series*, 46, 2nd ed.
- 21 **Glatz, D. & Parker, W.**, 2004. Enriching liquid-liquid extraction – A step by step guide to evaluating and improving column efficiency. *Chemical Engineering*, www.che.com, November 2004, pp. 44-48.
- 22 **Hafez, M.M., Baird, M.H.I. & Nirdosh, I.**, 1979. Flooding and axial dispersion in reciprocating plate extraction columns. *The Canadian Journal of Chemical Engineering*, 57 (2), pp. 150-158.
- 23 **Heyberger, A., Kratky, M. & Prochazka, J.**, 1983a. Parameter evaluation of an extractor with back mixing. *Chemical Engineering Science*, 38 (8), pp. 1303-1307.
- 24 **Heyberger, A., Sovova, H. & Prochazka, J.**, 1983b. Hold-up and flooding in a vibrating plate extractor. *Collection of Czechoslovak Chemical Communications*, 48, pp. 989 – 1000.
- 25 **Holmes, T.L., Karr, A.E. & Baird, M.H.I.**, 1991. Effect of unfavourable continuous phase density gradient on axial mixing. *AIChE Journal*, 37 (3), pp. 360-366.

- 26 **Hubbard, D.W.**, 1980. Phase equilibria for liquid-liquid extraction. *AIChE Modular Instruction, Series B: Stagewise & Mass Transfer Operations*, 3: Extraction & Leaching, Module B3.1.
- 27 **Humphrey, J. L. & Keller II, G.E.**, 1997. Extraction. *Separation Process Technology*, McGraw-Hill, Chapter 3, pp. 113-151.
- 28 **Hussain, A.A., Liang, T.-B. & Slater, M.J.**, 1988. Characteristic velocity of drops in a liquid-liquid extraction pulsed sieve plate column. *Chemical Engineering Research & Design*, 66 (6), pp. 541-554.
- 29 **Ioannou, J., Hafez, M. & Hartland, S.**, 1976. Mass transfer and power consumption in reciprocating plate extractors. *Industrial & Engineering Chemistry Process Design & Development*, 15 (3), pp. 469-471.
- 30 **Jiricny, V., Kratky, M. & Prochazka, J.**, 1979a. Counter-current flow of dispersed and continuous phase – I. Discrete polydispersed model. *Chemical Engineering Science*, 34, pp. 1141-1149.
- 31 **Jiricny, V., Kratky, M., & Prochazka, J.**, 1979b. Counter-current flow of dispersed and continuous phase – II. Simulation of holdup and particle size distribution profiles. *Chemical Engineering Science*, 34, pp. 1151-1158.
- 32 **Jiricny, V. & Prochazka, J.**, 1980. Counter-current flow of dispersed and continuous phase – III. Measurement of hold-up profiles and particle size distributions in a vibrating plate contactor. *Chemical Engineering Science*, 35 (11), pp. 2237-2245.
- 33 **Joseph, S. & Varma, Y.B.G.**, 1998. A correlation for drop size and slip velocity in reciprocating plate columns. *Bioprocess Engineering*, 18, pp. 367-371.
- 34 **Ju, J.-D., Yu, Y.-H. & Kim, S.D.**, 1990. Axial dispersion and phase holdup characteristics in reciprocating plate extraction columns. *Separation Science & Technology*, 25 (7-8), pp. 921-940.
- 35 **Kannan, A., Harikrishnan, T.L. & Varma, Y.B.G.**, 1990. A numerical Technique for the estimation of the true mass transfer coefficient in extraction columns. *Chemical Engineering Journal & the Biochemical Engineering Journal*, 25 (2), pp. 133-135.
- 36 **Karr, A.E.**, 1980. Design, scale-up, and applications of the reciprocating plate extraction column. *Separation Science & Technology*, 15 (4), pp. 877-905.
- 37 **Karr, A.E., Ramanujam, S., Lo, T.C. & Baird, M.H.I.**, 1987. Axial mixing and scaleup of reciprocating plate columns. *The Canadian Journal of Chemical Engineering*, 65 (3), pp. 373-381.

- 38 **Kim, S.D. & Baird, M.H.I.**, 1976a. Axial dispersion in a reciprocating plate extraction column. *The Canadian Journal of Chemical Engineering*, 54, pp. 81-89.
- 39 **Kim, S.D. & Baird, M.H.I.**, 1976b. Effect of hole size on hydrodynamics of a reciprocating perforated plate extraction column. *The Canadian Journal of Chemical Engineering*, 54, pp. 235-237.
- 40 **Komasawa, I. & Ingham, J.**, 1978. Effect of system properties on the performance of liquid-liquid extraction columns – III Mass transfer characteristics: systems toluene-acetone-water, MIBK-acetic acid-water. *Chemical Engineering Science*, 33, pp. 541-546.
- 41 **Kostanyan, A.E., Pebalk, V.L. & Pelevina, T.K.**, 1980. Investigation of the operating characteristics of column extractors with vibrating plates. *Theoretical Foundations of Chemical Engineering*, 14 (2), pp. 115-118.
- 42 **Kumar, A. & Hartland, S.**, 1988. Prediction of dispersed-phase holdup and flooding velocities in Karr reciprocating-plate extraction columns. *Industrial & Engineering Chemistry Research*, 27 (1), pp. 131-138.
- 43 **Kumar, A. & Hartland, S.**, 1996. Unified correlations for the prediction of drop size in liquid-liquid extraction columns. *Industrial & Engineering Chemistry Research*, 35 (8), pp. 2682-2695.
- 44 **Kumar, A. & Hartland, S.**, 1995. Unified correlations for the prediction of dispersed-phase hold-up in liquid-liquid extraction columns. *Industrial & Engineering Chemistry Research*, 34 (11), pp. 3925-3940.
- 45 **Laddha, G.S. & Degaleesan, T.E.**, 1983. Dispersion and coalescence. In: T.C. Lo, M.H.I. Baird, C. Hanson, ed. 1983. *Handbook of Solvent Extraction*. John Wiley & Sons. Ch. 4.
- 46 **Lisa, G.A., Tudose, R.Z. & Kadi, H.**, 2003. Mass transfer resistance in liquid-liquid extraction with individual phase mixing. *Chemical Engineering & Processing*, 42 (11), pp. 909-916.
- 47 **Lo, T.C.**, 1996. Commercial liquid-liquid extraction equipment. In: P.A. Schweitzer, ed. 1996. *Handbook of Separation Techniques for Chemical Engineers*. McGraw-Hill, 3rd ed. Part 1, Section 1.10.
- 48 **Lo, T.C., Baird, M.H.I. & Rama Rao, N.V.**, 1992. The reciprocating plate column – development and applications. *Chemical Engineering Communications*, 116, pp. 67-88.
- 49 **Lo, T.C. & Karr, A.E.**, 1972. Development of a laboratory-scale reciprocating plate extraction column. *Industrial & Engineering Chemistry Process Design & Development*, 11 (4), pp. 495-501.

- 50 **Lo, T.C. & Prochazka, J.**, 1983. Reciprocating-plate extraction columns. In: T.C. Lo, M.H.I. Baird, C. Hanson, ed. 1983. *Handbook of Solvent Extraction*. John Wiley & Sons. Ch. 12.
- 51 **Logsdail, D.H. & Slater, M.J.**, 1983. Pulsed perforated-plate columns. In: T.C. Lo, M.H.I. Baird, C. Hanson, ed. 1983. *Handbook of Solvent Extraction*. John Wiley & Sons. Ch. 11.2.
- 52 **Mogensen, A.O.**, 1980. Choice of solvent in extraction. *AIChE Modular Instruction, Series B: Stagewise & Mass Transfer Operations*, 3: Extraction & Leaching, Module B3.5.
- 53 **Nemecek, M. & Prochazka, J.**, 1974. Longitudinal mixing in a vibrating-sieve-plate column two-phase flow. *The Canadian Journal of Chemical Engineering*, 52, pp. 739-749.
- 54 **Novotny, P., Prochazka, J. & Landau, J.**, 1970. Longitudinal mixing in reciprocating and pulsed sieve-plate column – single phase flow. *The Canadian Journal of Chemical Engineering*, 48, pp. 405-410.
- 55 **Othmer, D.F., White, R.E. & Trueger, E.**, 1941. Liquid-liquid extraction data. *Industrial & Engineering Chemistry*, 33 (10), Pages 1240-1248.
- 56 **Parthasarathy, P., Sriniketan, G., Srinivas, N.S. & Varma, Y.B.G.**, 1984. Axial mixing of continuous phase in reciprocating plate columns. *Chemical Engineering Science*, 39 (6), pp. 987-995.
- 57 **Pertler, M., Haberl, M., Rommel, W. & Blass, E.**, 1995. Mass transfer across liquid-phase boundaries. *Chemical Engineering & Processing*, 34, pp. 269-277.
- 58 **Pratt, H.R.C.**, 1983a. Computation of stagewise and differential contactors: Plug flow. In: T.C. Lo, M.H.I. Baird, C. Hanson, ed. 1983. *Handbook of Solvent Extraction*. John Wiley & Sons. Ch. 5.
- 59 **Pratt H.R.C.**, 1983b. Interface mass transfer. In: T.C. Lo, M.H.I. Baird, C. Hanson, ed. 1983. *Handbook of Solvent Extraction*. John Wiley & Sons. Ch. 3.
- 60 **Pratt H.R.C. & Baird M.H.I.**, 1983. Axial dispersion. In: T.C. Lo, M.H.I. Baird, C. Hanson, ed. 1983. *Handbook of Solvent Extraction*. John Wiley & Sons. Ch. 6.
- 61 **Prvcic, L.M., Pratt, H.R.C. & Stevens, G.W.**, 1989. Axial dispersion in pulsed-, perforated-plate extraction columns. *AIChE Journal*, 35 (11), pp. 1845-1855.
- 62 **Prochazka, J., Heyberger, A., Landau, J. & Souhrada, F.**, 1971. Reciprocating-plate extraction column. *British Chemical Engineering*, 16 (1), pp. 42-44.

- 63 **Rama Rao, N.V. & Baird, M.H.I.**, 1988. Back mixing in a reciprocating plate column with stable density gradients. *AIChE Journal*, 44 (4), pp. 859-863.
- 64 **Rama Rao, N.V., Vijayan, S. & Baird, M.H.I.**, 1991. Hydrodynamics of a vibrating perforated plate extraction column. *The Canadian Journal of Chemical Engineering*, 69 (1), pp. 212-221.
- 65 **Robbins, L.A.**, 1996. Liquid-liquid extraction. In: P.A. Schweitzer, ed. 1996. *Handbook of Separation Techniques for Chemical Engineers*. McGraw-Hill, 3rd ed. Part 1, Section 1.9.
- 66 **Saien, J., Riazikhah, M. & Ashrafizadeh, S.N.**, 2006. Comparative investigations on the effects of contamination and mass transfer direction in liquid-liquid extraction. *Industrial & Engineering Chemistry Research*, 45, pp. 1434-1440.
- 67 **ScienceLab.com**, 2008a. *Material safety data sheet acetone MSDS*. [Online] (Updated 11 June 2008)
Available at: <http://www.sciencelab.com/msds.php?msdsId=9927062>
[Accessed 8 Jan 2009].
- 68 **ScienceLab.com**, 2008b. *Material safety data sheet toluene MSDS*. [Online] (Updated 11 June 2008)
Available at: <http://www.sciencelab.com/msds.php?msdsId=9927301>
[Accessed 8 Jan 2009].
- 69 **Seader, J.D. & Henley, E.J.**, 2006. *Separation Process Principles*, 2nd ed. John Wiley & Sons. Ch. 4 & 8.
- 70 **Shen, Z.J., Rama Rao, N.V. & Baird, M.H.I.**, 1985. Mass transfer in a reciprocating plate extraction column – effects of mass transfer direction and plate material. *The Canadian Journal of Chemical Engineering*, 63 (1), pp. 29-36.
- 71 **Slater, M.J.**, 1985. Liquid-liquid extraction column design. *The Canadian Journal of Chemical Engineering*, 63 (6), pp. 1004-1005.
- 72 **Smith, K.H., Bowser, T. & Stevens, G.W.**, 2008. Performance and scale-up of Karr reciprocating plate extraction columns. *Industrial & Engineering Chemistry Research*, 47 (21), pp. 8368-8375.
- 73 **Sovova, H.**, 1983. A model for dispersion hydrodynamics in a vibrating plate extractor. *Chemical Engineering Science*, 38 (11), pp. 1863-1872.
- 74 **Sovova, H. & Havlicek, A.**, 1986. Transient behavior of holdup in a reciprocating plate extraction column. *Chemical Engineering Science*, 41 (10), pp. 2579-2583.

- 75 **Stella, A., Mensforth, K.H., Bowser, T., Stevens, G.W. & Pratt, H.R.C.,** 2008. Mass transfer performance in Karr reciprocating plate extraction columns. *Industrial & Engineering Chemistry Research*, 47 (11), pp. 3996-4007.
- 76 **Stella, A. & Pratt, H.R.C.,** 2006. Backmixing in Karr reciprocating-plate extraction columns. *Industrial & Engineering Chemistry Research*, 45 (19), pp. 6555-6562.
- 77 **Stevens, G.W. & Baird, M.H.I.,** 1990. A model for axial mixing in reciprocating plate columns. *Chemical Engineering Science*, 45 (2), pp. 457-465.
- 78 **Takacs, I., Beszedics, G., Fabry, G. & Rudolf, P.,** 1993. Apparatus to contact liquids of different density. *United States Patent*, patent number 5194152.
- 79 **Treybal, R.E.,** 1981. Liquid-liquid operations. *Mass-transfer operations*, 3rd ed. McGraw-Hill. Part 3.
- 80 **Usman, M.R., Hussain, S.N., Rehman, L., Bashir, M. & Butt, M.A.,** 2006. Mass transfer performance in a pulsed sieve-plate extraction column. *The Proceedings of the Pakistan Academy of Sciences*, 43 (3), pp. 173-179.
- 81 **Usman, M.R., Rehman, L. & Bashir, M.,** 2008. Drop size and drop size distribution in a pulsed sieve-plate extraction column. *The Proceedings of the Pakistan Academy of Sciences*, 45 (1), pp. 41-46.
- 82 **Vatanatham, T., Terasukaporn, P. & Lorpongpaiboon, P.,** 1999. HTU of acetone-toluene-water extraction in a pulsed column. *Proceedings of Regional Symposium on Chemical Engineering*, Prince of Songkhla University, Thailand.
- 83 **Wankat, P.C.,** 1980. Basic extraction calculations on ternary diagrams. *AIChE Modular Instruction, Series B: Stagewise & Mass Transfer Operations*, 3: Extraction & Leaching, Module B3.2.
- 84 **Wichterlova, J., Rod, V. & Hancil, V.,** 1991. Prediction of the performance of an extraction column from tracer experiments with a stationary continuous phase. *Chemical Engineering & Processing*, 29 (1), pp. 39-47.
- 85 **Yadav, R.L. & Patwardhan, A.W.,** 2008. Design aspects of pulsed sieve plate columns, *Chemical Engineering Journal*, 138, pp. 389-415.
- 86 **Yang, N.S., Shen, Z.-Q., Chen, B.H. & McMillan, A.F.,** 1986. Pressure drop, gas holdup, and interfacial area for gas-liquid contact in Karr columns. *Industrial & Engineering Chemistry Process Design & Development*, 25 (3), pp. 660-664.

APPENDIX A

Raw Data

Time to reach stability data:

Water Flow l/hr	Toluene Flow l/hr	S/F ratio	time min	holdup		
				mm	m ³	%
10	20	1:2	20	66	0.001166	15.0
10	20	1:2	40	75	0.001325	17.0
10	20	1:2	60	75	0.001325	17.0
10	20	1:2	80	75	0.001325	17.0
15	15	1:1	20	50	0.000884	11.3
15	15	1:1	40	55	0.000972	12.5
15	15	1:1	60	55	0.000972	12.5
15	15	1:1	80	55	0.000972	12.5
20	10	2:1	20	32	0.000565	7.2
20	10	2:1	40	32	0.000565	7.2
20	10	2:1	60	32	0.000565	7.2
20	10	2:1	80	32	0.000565	7.2

Table A1 Data for calculation of time to reach stability

Sample calculations:

The height of raffinate collected below the original interface level in the top settling tank after the system was stopped is reported in the above table under holdup in mm. This value is converted to volume by multiplying by the cross-sectional area of the top settling tank = 0.01767 m². The volume of liquid that is occupied in the active part of the column, when the tray spacing is 100 mm, is 7.8 l.

$$\begin{aligned}\text{Volume of raffinate} &= \left(\frac{66}{1000}\right) * 0.01767 \\ &= 0.001166 \text{ m}^3\end{aligned}$$

$$\begin{aligned}\text{Fractional holdup} &= \left(\frac{0.001166}{7.8/1000}\right) * 100 \\ &= 15\%\end{aligned}$$

First set of hydrodynamics experiments:

Water Flow l/hr	Toluene Flow l/hr	S/F ratio	Freq Hz	<i>af</i> mm/s	holdup		
					mm	m ³	%
15	15	1:1	0.5	1.25	56	0.00099	12.7
15	15	1:1	1	2.5	42	0.000742	9.5
15	15	1:1	1.5	3.75	38	0.000671	8.6
15	15	1:1	2	5	47	0.00083	10.6
15	15	1:1	2.5	6.25	66.5	0.001175	15.1
15	15	1;1	3	7.5	flooding		
20	10	2:1	0.5	1.25	41.5	0.000733	9.4
20	10	2:1	1	2.5	22	0.000389	5.0
20	10	2:1	1.5	3.75	20.5	0.000362	4.6
20	10	2:1	2	5	29.5	0.000521	6.7
20	10	2:1	2.5	6.25	36.5	0.000645	8.3
20	10	2:1	3	7.5	45	0.000795	10.2
10	20	1:2	0.5	1.25	76.5	0.001352	17.3
10	20	1:2	1	2.5	58	0.001025	13.1
10	20	1:2	1.5	3.75	46.5	0.000822	10.5
10	20	1:3	2	5	62	0.001096	14.0
10	20	1:4	2.5	6.25	83	0.001467	18.8
10	20	1:5	3	7.5	flooding		

Table A2 Results for the first set of hydrodynamics experiments

Sample calculations:

For all of the experiments the amplitude was kept constant at 2.5 mm while the frequency was changed in order to change the agitation level, *af*.

$$\begin{aligned} \text{Agitation level } (af) &= 2.5 \text{ mm} * 0.5 \text{ Hz} \\ &= 1.25 \text{ mm/s} \end{aligned}$$

The fractional holdup was calculated as before.

Second set of hydrodynamics experiments:

Water Flow	Toluene Flow	S/F ratio	Freq	af	holdup		
					mm	m ³	%
15	15	1:1	0.5	1.25	59	0.001043	13.4
15	15	1:1	1	2.5	40	0.000707	9.1
15	15	1:1	1.5	3.75	37	0.000654	8.4
15	15	1:1	2	5	42	0.000742	9.5
15	15	1:1	2.5	6.25	58	0.001025	13.1
15	15	1;1	3	7.5		0.00168	21.5
20	10	2:1	0.5	1.25	38	0.000671	8.6
20	10	2:1	1	2.5	18	0.000318	5.0
20	10	2:1	1.5	3.75	18	0.000318	4.1
20	10	2:1	2	5	26	0.000459	5.9
20	10	2:1	2.5	6.25	30	0.00053	8.3
20	10	2:1	3	7.5	53	0.000937	12.0
10	20	1:2	0.5	1.25	76	0.001343	17.2
10	20	1:2	1	2.5	59	0.001043	13.4
10	20	1:2	1.5	3.75	46	0.000813	10.4
10	20	1:2	2	5	56	0.00099	12.7
10	20	1:2	2.5	6.25		0.0016	20.5
10	20	1:2	3	7.5			

Table A3 Results for the second set of hydrodynamics experiments

In terms of repeatability, the holdup calculated for the 2 different sets of results above are very close with a maximum difference of 2% and it was concluded that the reproducibility of the results is very good.

First set of mass transfer experiments:

Water Flow	Toluene Flow	S/F ratio	Freq	af	holdup		
					mm	m ³	%
15	15	1:1	0.5	1.25	59	0.001043	13.4
15	15	1:1	1	2.5	35	0.000618	7.9
15	15	1:1	1.5	3.75	32	0.000565	7.2
15	15	1:1	2	5	37	0.000654	8.4
15	15	1:1	2.5	6.25	40	0.000707	9.1
15	15	1:1	3	7.5	58	0.001025	13.1
20	10	2:1	0.5	1.25	48	0.000848	10.9
20	10	2:1	1	2.5	23	0.000406	5.2
20	10	2:1	1.5	3.75	17	0.0003	3.9
20	10	2:1	2	5	23	0.000406	5.2
20	10	2:1	2.5	6.25	29	0.000512	6.6
20	10	2:1	3	7.5	35	0.000618	7.9
10	20	1:2	0.5	1.25	60	0.00106	13.6
10	20	1:2	1	2.5	45	0.000795	10.2
10	20	1:2	1.5	3.75	44	0.000777	10.0
10	20	1:2	2	5	51	0.000901	11.6
10	20	1:2	2.5	6.25	64	0.001131	14.5
10	20	1:2	3	7.5	67	0.001587	20.3

$h = 200$ mm

15	15	1:1	0.5	1.25	37	0.000654	8.2
15	15	1:1	1	2.5	20	0.000353	4.4
15	15	1:1	1.5	3.75	19	0.000336	4.2
15	15	1:1	2	5	22	0.000389	4.9
15	15	1:1	2.5	6.25	27	0.000477	6.0
15	15	1:1	3	7.5	32	0.000565	7.1

Table A4 Results for the first set of mass transfer experiments

In the above table, the first part of the results is for a tray spacing of 100 mm, while the second part is for a tray spacing of 200 mm. The volume of liquid that is occupied in the active part of the column, when the tray spacing is 200 mm, is 8 l.

$$\begin{aligned} \text{Fractional holdup} &= \left(\frac{0.000654}{8/1000} \right) * 100 \\ &= 8.2\% \end{aligned}$$

Second set of mass transfer experiments showing concentrations along the length of the column

water flow	toluene flow	S/F ratio	Freq	Agitation	holdup	x_f	d_1	d_2	d_3	d_4	x_r	x_e	c_1	c_2	c_3	c_4	solvent
l/h	l/h		Hz	mm/s	mm	%	%	%	%	%	%	%	%	%	%	%	%
15	15	1:1	3	7.5	60	6.02	3.35	1.82	0.49	0.15	0.05	3.32	2.41	0.99	0.32	0.07	0
15	15	1:1	2.5	6.25	47	6.00	4.28	2.15	0.79	0.26	0.10	3.25	2.52	1.21	0.46	0.10	0
15	15	1:1	2	5	38	6.01	4.39	2.58	1.15	0.43	0.15	3.18	2.45	1.32	0.57	0.15	0
15	15	1:1	1.5	3.75	30	6.08	4.36	2.62	1.37	0.75	0.34	3.09	2.40	1.35	0.65	0.21	0
15	15	1:1	1	2.5		6.02	4.24	2.49	1.38	0.74	0.42	3.04	2.37	1.32	0.64	0.21	0
15	15	1:1	0.5	1.25	61	5.95	4.11	2.36	1.38	0.72	0.50	2.98	2.34	1.28	0.63	0.20	0
10	20	1:2	3	7.5		6.08	4.96	3.07	1.33	0.35	0.15	4.2	3.81	2.35	0.9	0.23	0
10	20	1:2	2.5	6.25	57	6	4.96	3.64	2.21	1.17	0.32	4.23	3.9	2.78	1.65	0.63	0
10	20	1:2	2	5	45	6.07	5.08	3.78	2.23	1.27	0.5	4.22	3.9	2.69	1.69	0.64	0
10	20	1:2	1.5	3.75	36	6.08	5.06	3.65	2.44	1.39	0.65	4.1	3.94	2.69	1.63	0.63	0
10	20	1:2	1	2.5	45	5.94	4.57	3.23	2.12	1.02	0.68	3.91	3.6	2.27	1.36	0.49	0
10	20	1:2	0.5	1.25	67	5.96	4.68	3.27	2.05	1.28	0.84	3.64	3.49	2.46	1.45	0.55	0
20	10	2:1	3	7.5	38	5.96	3.22	0.91	0.19	0.08	0.06	1.74	0.97	0.2	0.04	0.04	0
20	10	2:1	2.5	6.25	29	5.96	3.22	1.13	0.23	0.08	0.06	1.59	1	0.3	0.1	0.05	0
20	10	2:1	2	5	21	6.08	3.36	1.3	0.43	0.16	0.1	1.54	1.06	0.4	0.15	0.06	0
20	10	2:1	1.5	3.75	20	6.08	3.62	1.88	0.77	0.32	0.16	1.65	1.05	0.46	0.19	0.09	0
20	10	2:1	1	2.5		6.02	3.485	1.56	0.715	0.29	0.185	1.64	1.08	0.46	0.175	0.085	0
20	10	2:1	0.5	1.25	49	5.96	3.35	1.24	0.66	0.26	0.21	1.63	1.11	0.46	0.16	0.08	0

h = 200 mm

15	15	1:1	3	7.5	32	6.08	4.52	2.62	1.32	0.75	0.25	2.65	2.31	1.46	0.62	0.21	0
15	15	1:1	2.5	6.25	27	5.95	4.36	2.37	1.75	0.98	0.4	2.64	2.28	1.46	0.76	0.22	0
15	15	1:1	2	5	22	6.13	3.99	2.97	1.95	1.21	0.73	2.58	2.24	1.45	0.74	0.29	0
15	15	1:1	1.5	3.75	19	5.93	3.93	3.09	2.22	1.41	1.02	2.54	2.19	1.39	0.75	0.31	0
15	15	1:1	1	2.5	20	5.96	4.18	3.03	1.83	1.32	1.04	2.42	1.99	1.25	0.61	0.26	0
15	15	1:1	0.5	1.25	37	5.96	4.28	3.12	1.95	1.33	1.08	2.56	2.02	1.25	0.66	0.26	0

Table A5 Results for the second set of mass transfer experiments

For the first set of mass transfer experiments, only the exit raffinate and extract concentrations together with the holdup was evaluated, while during the second set of experiments the concentrations of both phases at 4 different positions along the length of the column in addition to the exit concentrations were evaluated. These concentrations are labelled as c_i for the continuous phase and d_i for the dispersed phase. Once again, the first part of the table reflects results for a tray spacing of 100 mm, while the second part reflects results for the a tray spacing of 200 mm.

APPENDIX B

Equipment Calibration

GC Calibration

Acetone in water:

Standards were prepared with exact amounts of acetone in water and these samples were tested in the GC to achieve the standard areas listed in the following table. Using these standards, a calibration chart was constructed as indicated in fig. B1. Since the FID cannot detect water, only one peak was obtained on the GC (that of acetone). As a result the peak area indicated in the following table is the actual peak area of acetone. A calibration equation obtained from the chart was used to evaluate the concentrations of the unknown samples of the extract phase.

Sample no.	Water	Ace + Water	Ace	Mass %	Peak area
	(g)	(g)	(g)		*100000000
1	4.8994	5.0024	0.103	2.06	1.44
2	4.8222	5	0.1778	3.56	2.37
3	4.7237	4.9918	0.2681	5.37	3.48
4	4.6002	4.9968	0.3966	7.94	5.10
5	4.4942	4.9928	0.4986	9.99	6.31

Table B1 Data for extract phase calibration chart

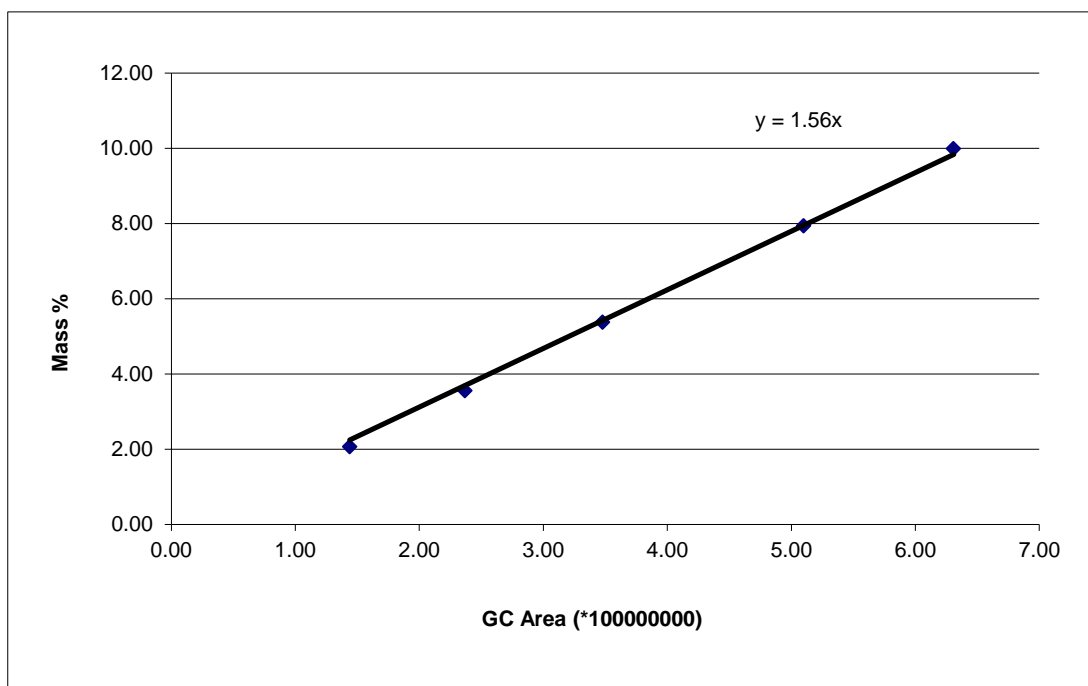


Fig. B1 Acetone in water calibration chart

Acetone in toluene:

In a similar procedure as for acetone in water, standards were prepared for acetone in toluene and after running the samples on the GC, the calibration chart was constructed which was used to evaluate the concentrations of the unknown samples of the raffinate phase. Here two peaks were observed on the GC, one for acetone and the other for toluene. The x axis of the calibration chart was the ratio of the peak areas of acetone to toluene expressed as a percentage.

Sample no.	Tol (g)	Acet + Tol (g)	Ace (g)	Mass %	Area % (A/T)
1	2.4	2.502	0.102	4.08	2.07
2	2.143	2.314	0.171	7.39	3.74
3	4.891	5.031	0.14	2.78	1.45
4	4.491	4.998	0.507	10.14	5.46

Table B2 Data for raffinate phase calibration chart

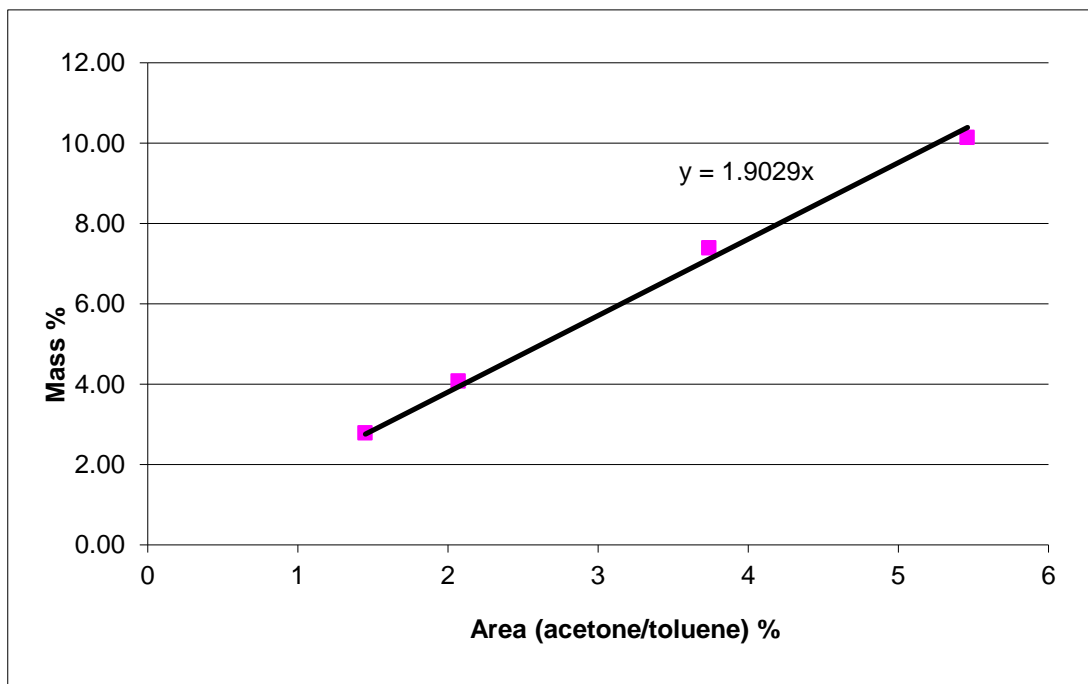


Fig. B2 Acetone in toluene calibration chart

Vibration motor calibration

The plate stack is mounted on a central shaft that is connected eccentrically via a yoke at the top of the column to a variable speed motor. The motor had to be calibrated so that the frequency could be obtained from the values on the controller. The following graphs show the value of the speed of the motor (rpm) and frequency for the different settings on the controller. As can be seen from the second graph, the actual frequency of vibration is half of the setting of the controller.

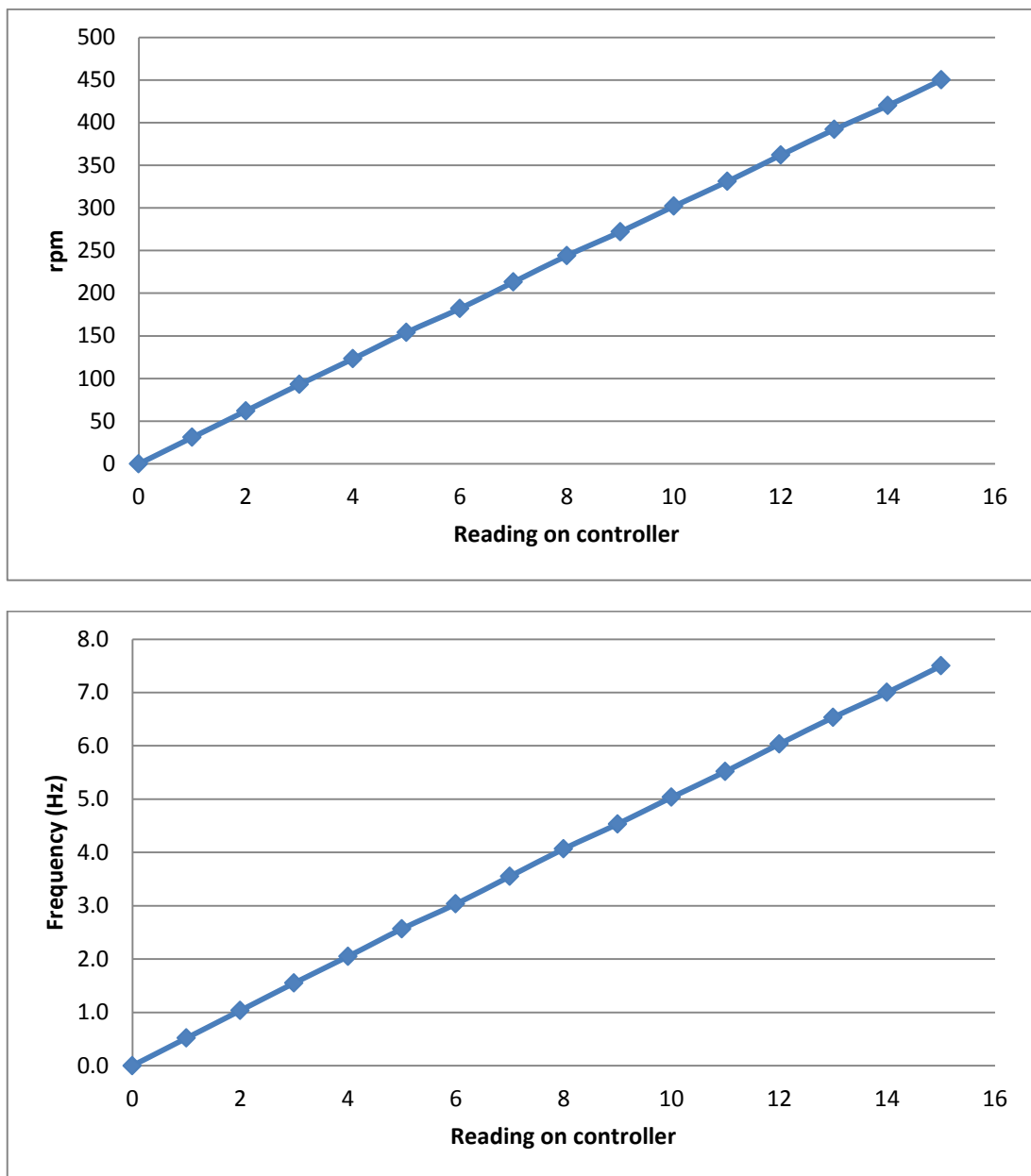


Fig. B3 Vibration motor calibration charts

Drain pump calibration

The conductivity probe that controls the level of the interface in the top settling tank is connected to a controller that controls the speed of the drain pump. The flow rate passing through the pump had to be calibrated for the readings on the controller, shown in the following graph. During operation the controller was set so that it changed between 0 and 3 corresponding to flow rates of 0 and 40 l/h. This setting was used for all three flow ratios and the interface was maintained at a fairly constant value.

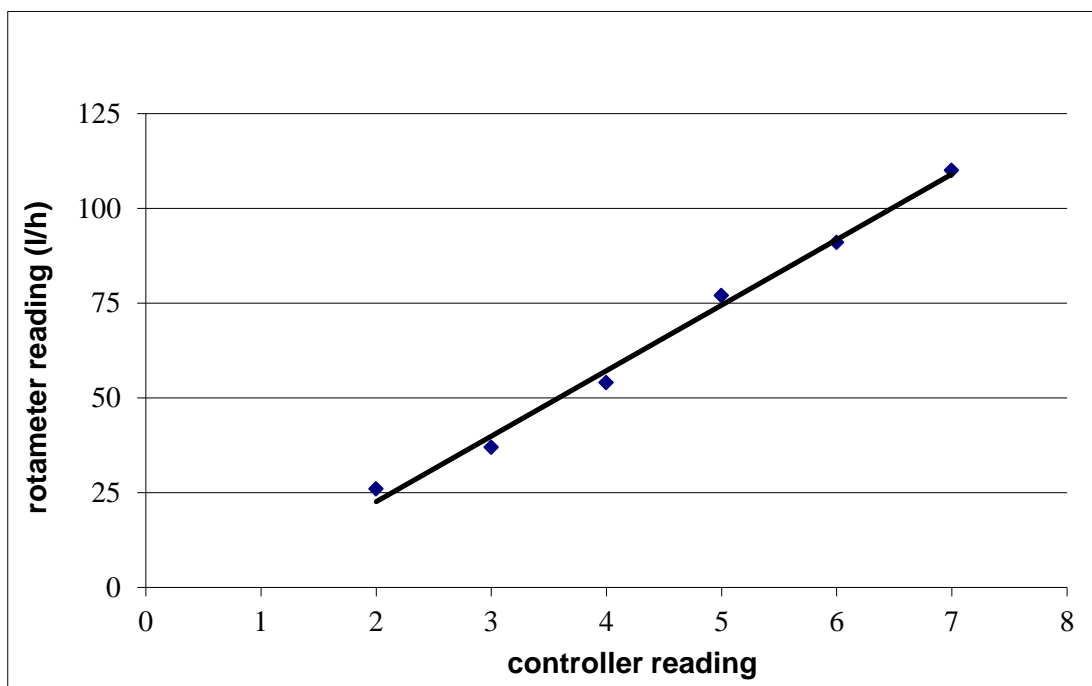
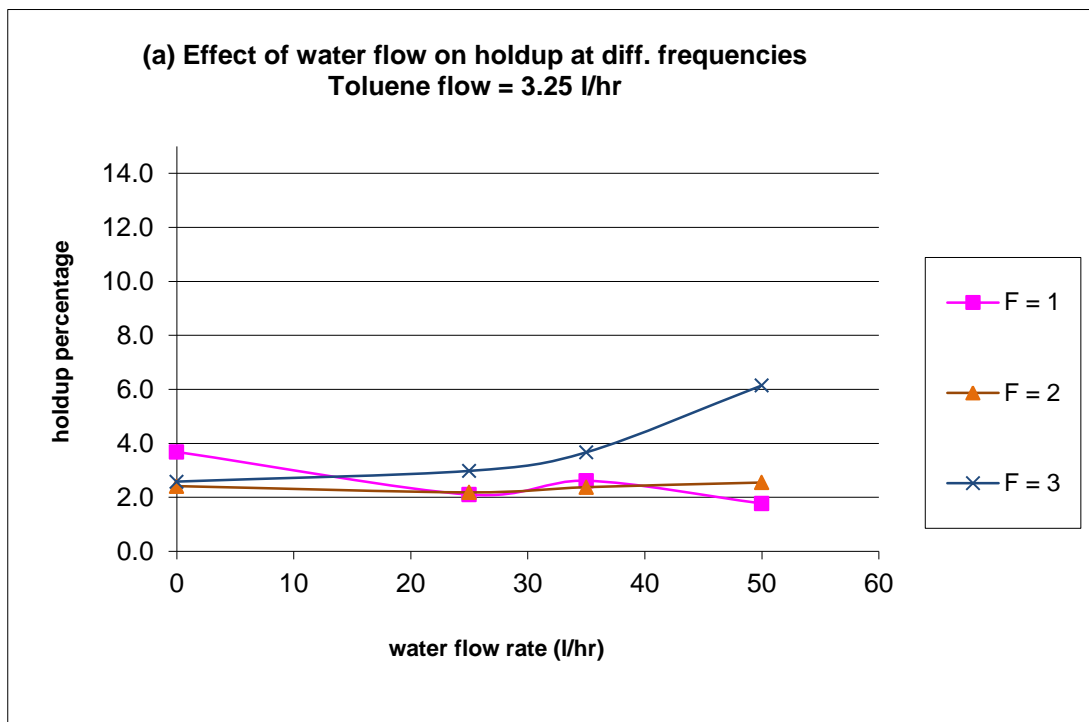


Fig. B4 Drain pump controller calibration

APPENDIX C

Effect of Flow Rates on Holdup

The effect of the individual phase flow rates on dispersed phase holdup in the absence of mass transfer was tested. In fig. C1 (a) the dispersed phase flow rate was kept constant and the continuous phase flow rate was changed from 0 to 50 l/h. The graph shows that the effect of continuous phase flow on holdup is minimal (especially in the range of 10 to 20 l/h) except at high frequency and high continuous phase flow rate where the holdup increases with flow rate. In fig. C1 (b) the continuous phase flow was kept constant while varying the dispersed phase flow. It can be seen that even at low dispersed phase flows, the holdup increases with increasing dispersed phase flow. Holdup also increases with the frequency of agitation.



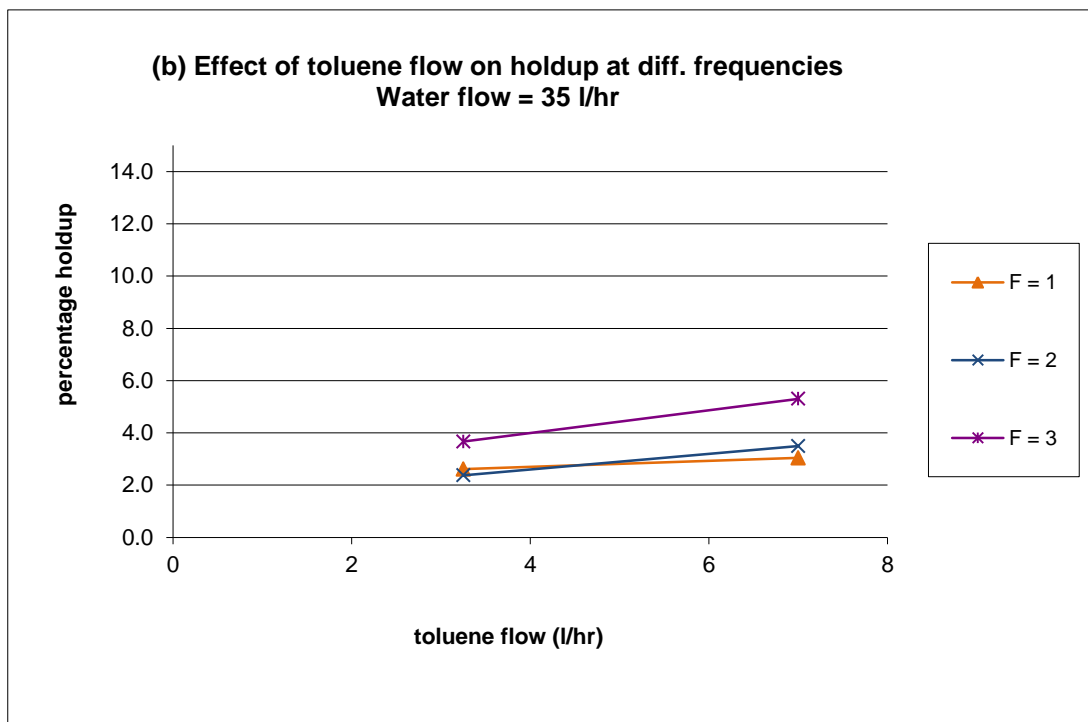


Fig. C1 Effect of individual flow rates on holdup

APPENDIX D

Drop Size Distribution (dsd)

In order to evaluate the drop size distribution (dsd), photographs were taken of the dispersed phase droplets and the number of droplets that fell into a certain size range (intervals of 0.2 mm) was plotted against the mean size to evaluate the distribution of the sizes. A sample distribution table is shown below.

Size range (mm)	No. of drops (n)	Fraction of drops %	Average size (d) (mm)	nd ³	nd ²
0 - 0.2	32.00	13	0.1	0.03	0.32
0.2 - 0.4	136.00	54	0.3	3.67	12.24
0.4 - 0.6	26.00	10	0.5	3.25	6.50
0.6 - 0.8	6.00	2	0.7	2.06	2.94
0.8 - 1.0	5.00	2	0.9	3.65	4.05
1.0 - 1.2	10.00	4	1.1	13.31	12.10
1.2 - 1.4	6.00	2	1.3	13.18	10.14
1.4 - 1.6	11.00	4	1.5	37.13	24.75
1.6 - 1.8	8.00	3	1.7	39.30	23.12
1.8 - 2.0	5.00	2	1.9	34.30	18.05
2.0 - 2.2	0.00	0	2.1	0.00	0.00
2.2 - 2.4	2.00	1	2.3	24.33	10.58
2.4 - 2.6	0.00	0	2.5	0.00	0.00
2.6 - 2.8	1.00	0	2.7	19.68	7.29
2.8 - 3.0		0	2.9	0.00	0.00
3.0 - 3.2		0	3.1	0.00	0.00
3.2 - 3.4	2.00	1	3.3	71.87	21.78
3.4 - 3.6		0	3.5	0.00	0.00
3.6 - 3.8		0	3.7	0.00	0.00
3.8 - 4.0		0	3.9	0.00	0.00
Total	250.00	100.00		265.76	153.86
		d ₃₂	1.73		

Table D1 Data for drop size distribution

The distribution was used to calculate the Sauter mean diameter from the following equation:

$$d_{32} = \frac{\sum_{i=1}^N n_i d_i^3}{\sum_{i=1}^N n_i d_i^2}$$

Sample Calculation:

$$nd^3 = (32)(0.1)^3$$

$$= 0.03 \text{ mm}^3$$

$$nd^2 = (32)(0.1)^2$$

$$= 0.32 \text{ mm}^2$$

$$\sum n_i d_i^3 = 265.76 \text{ mm}^3$$

$$\sum n_i d_i^2 = 153.86 \text{ mm}^2$$

$$d_{32} = \frac{\sum_{i=1}^N n_i d_i^3}{\sum_{i=1}^N n_i d_i^2}$$

$$= \frac{265.76}{153.86}$$

$$= 1.73 \text{ mm}$$

The distribution graphs for varying flow ratios, tray spacings, and agitation levels are shown below.

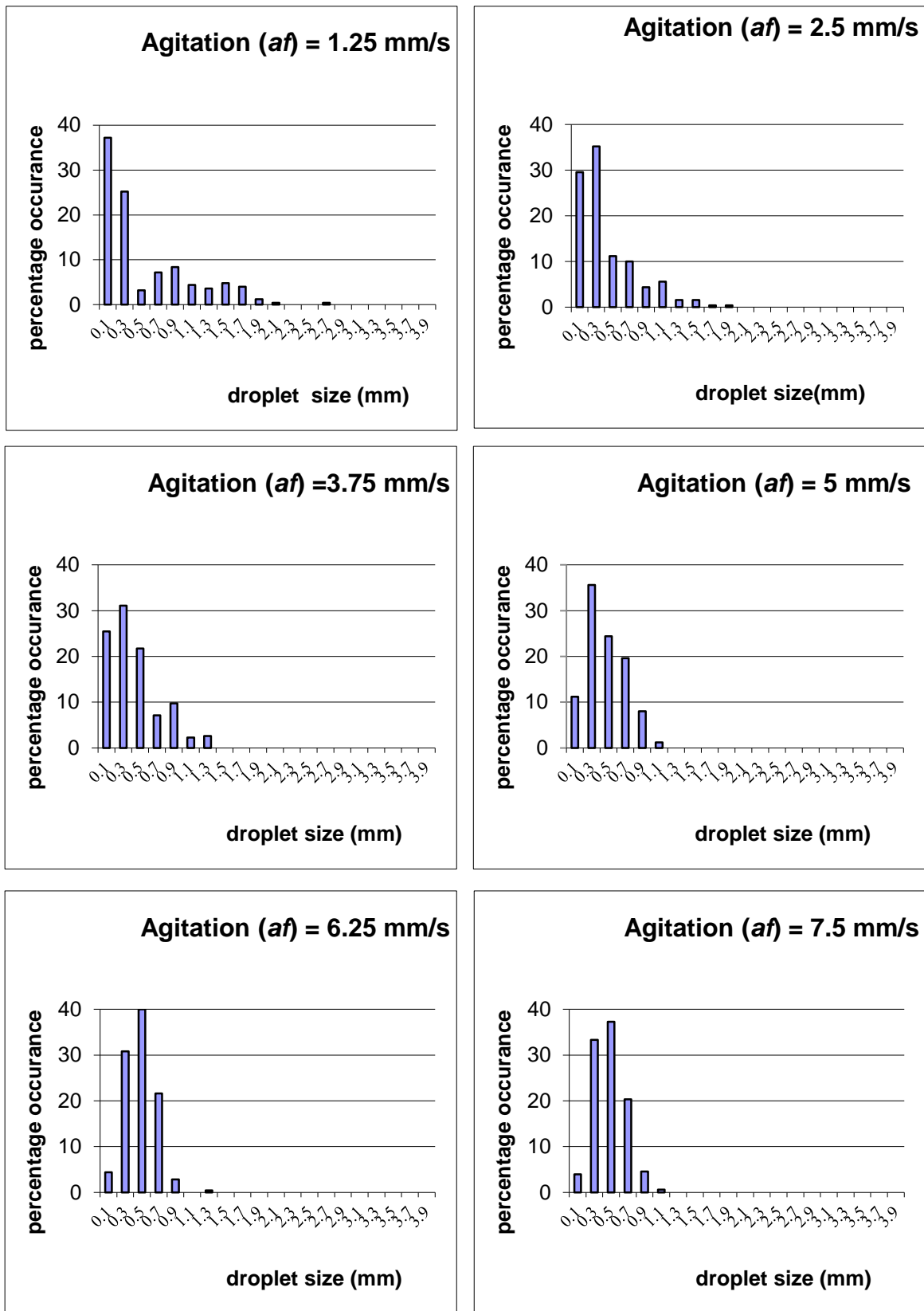


Fig D1 dsd – hydrodynamics (S/F = 1:1; h = 100mm)

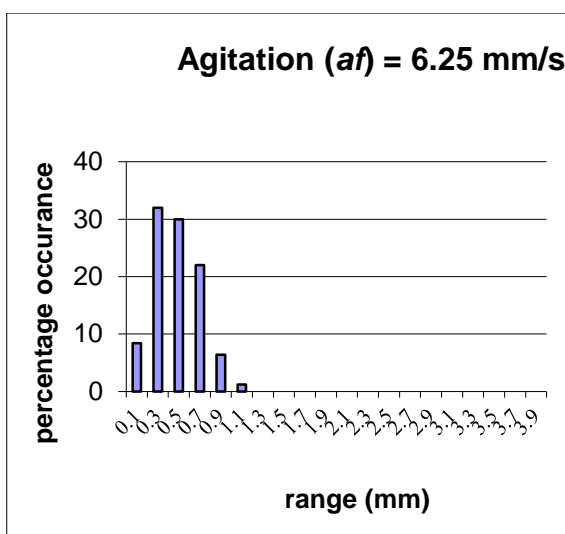
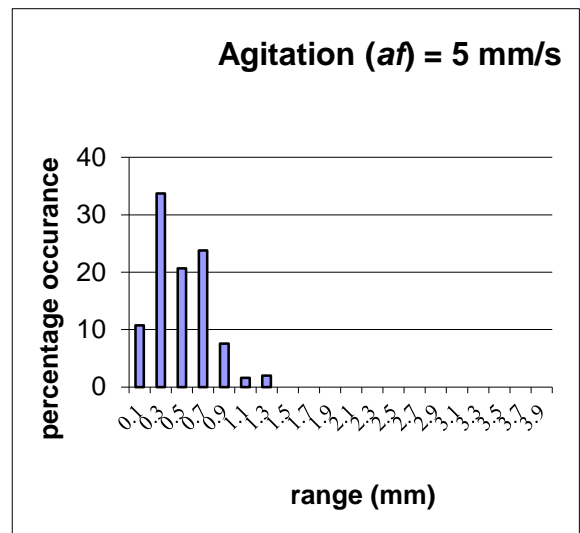
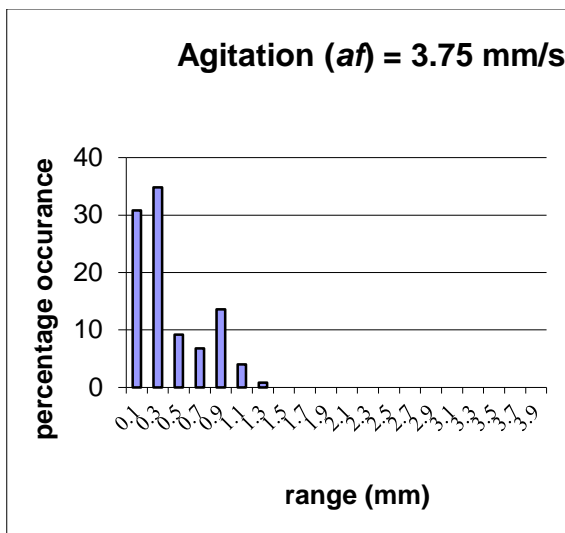
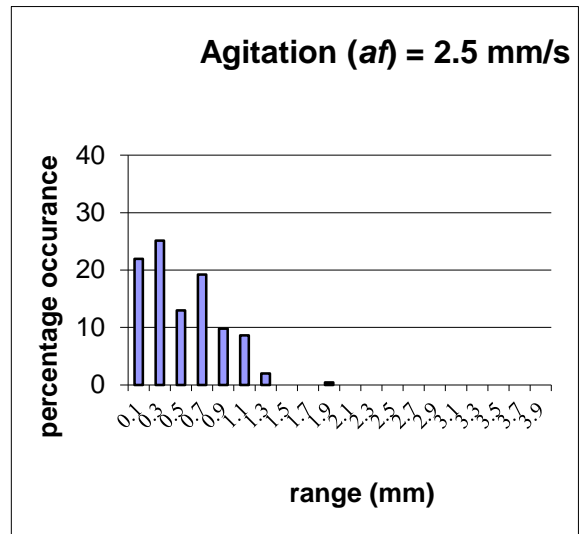
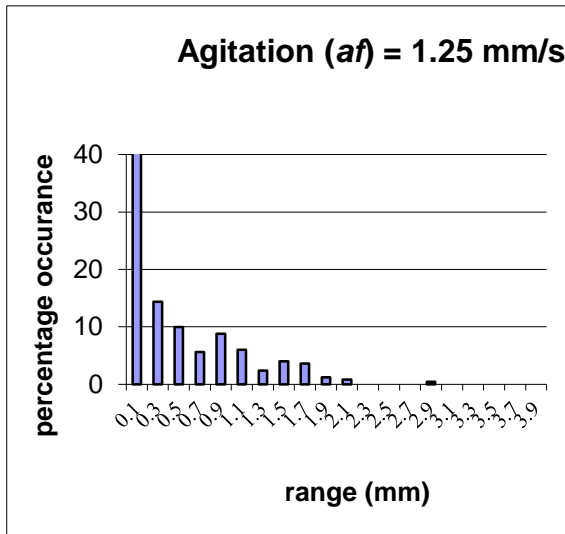


Fig D2 dsd – hydrodynamics ($S/F = 1:2$; $h = 100\text{mm}$)

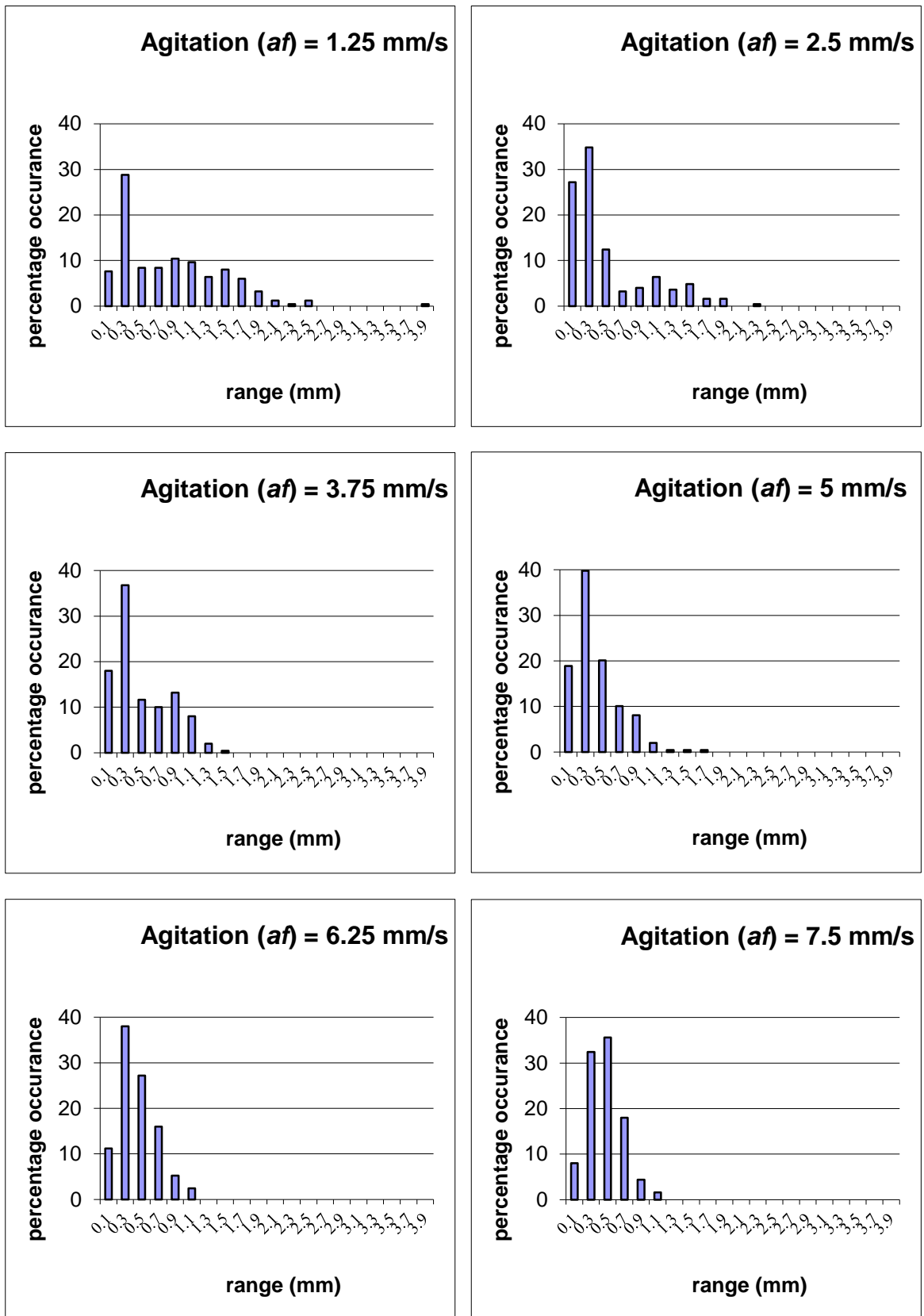


Fig D3 dsd – hydrodynamics ($S/F = 2:1$; $h = 100\text{mm}$)

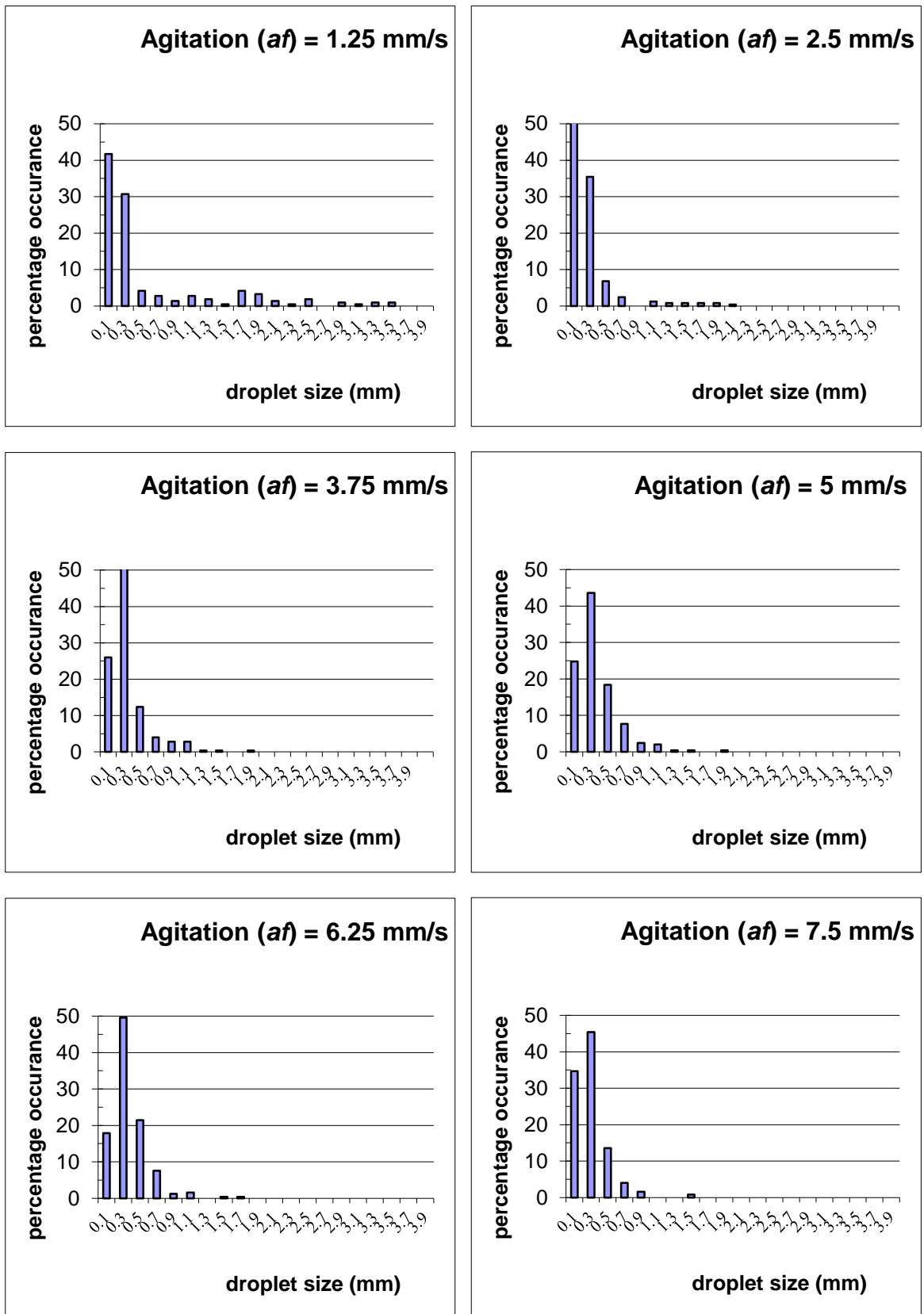


Fig D4 dsd – mass transfer (S/F = 1:1; h = 100mm)

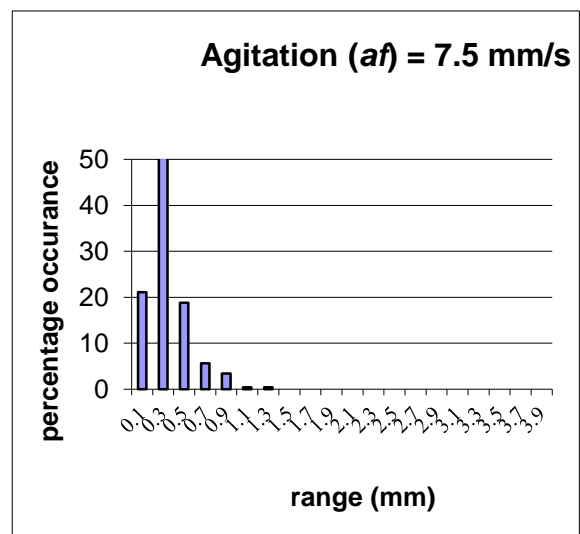
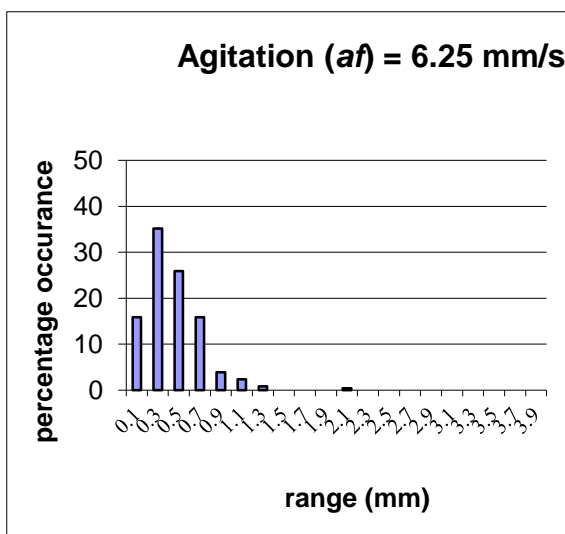
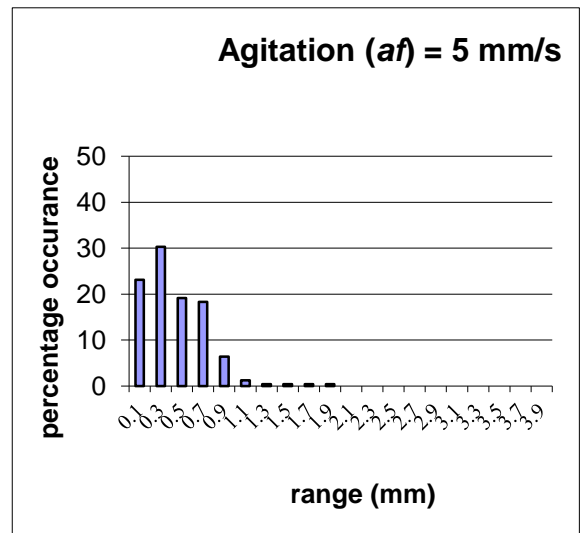
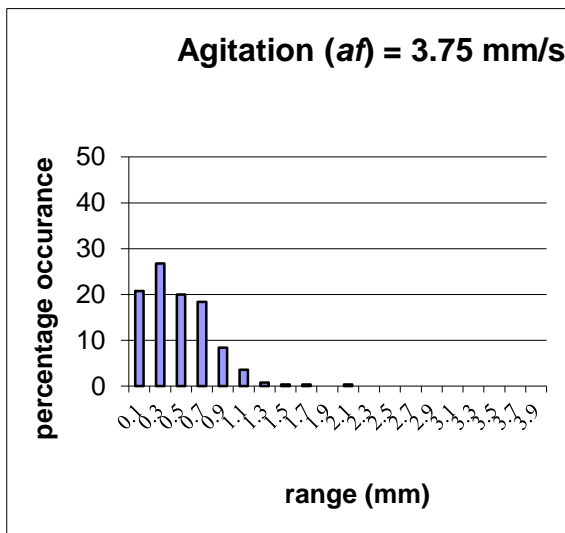
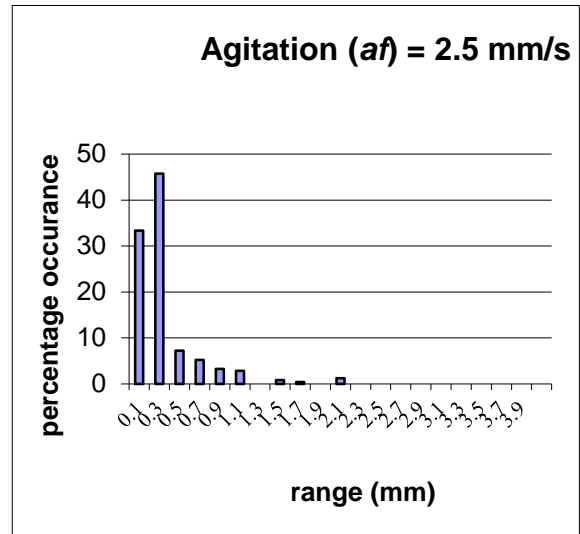
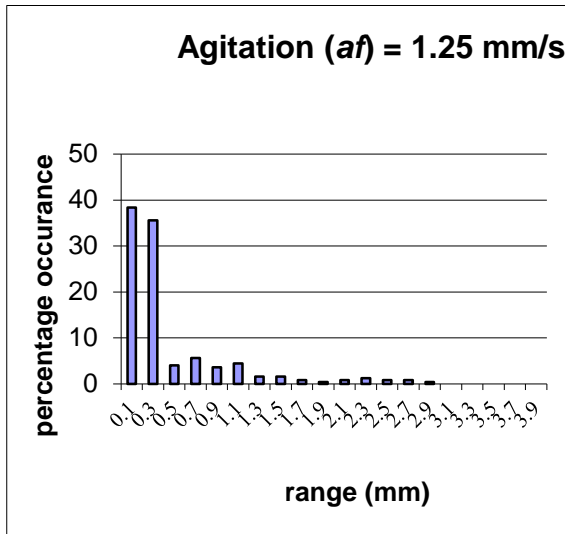


Fig D5 dsd – mass transfer (S/F = 1:2; h = 100mm)

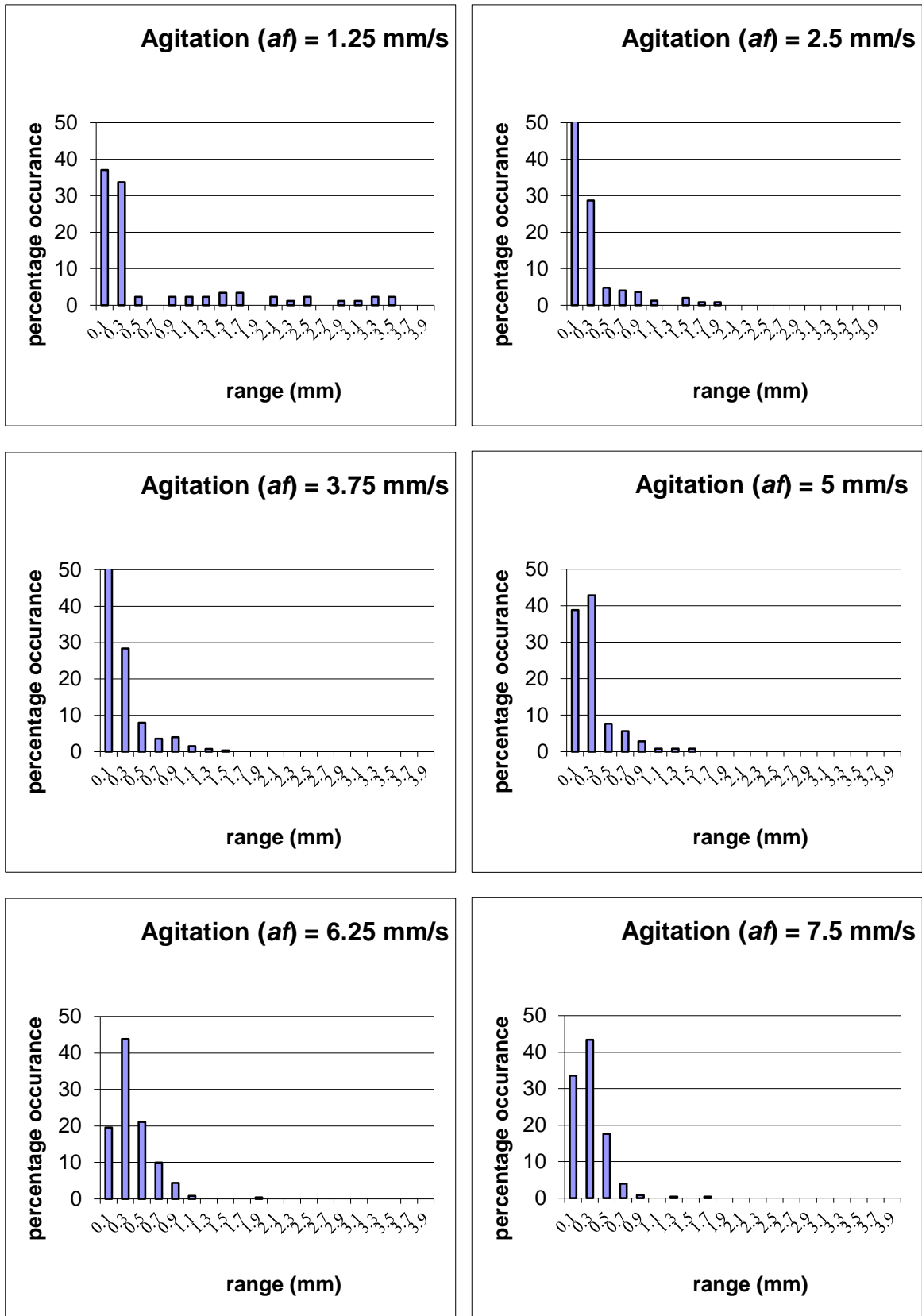


Fig D6 dsd – mass transfer ($S/F = 2:1$; $h = 100\text{mm}$)

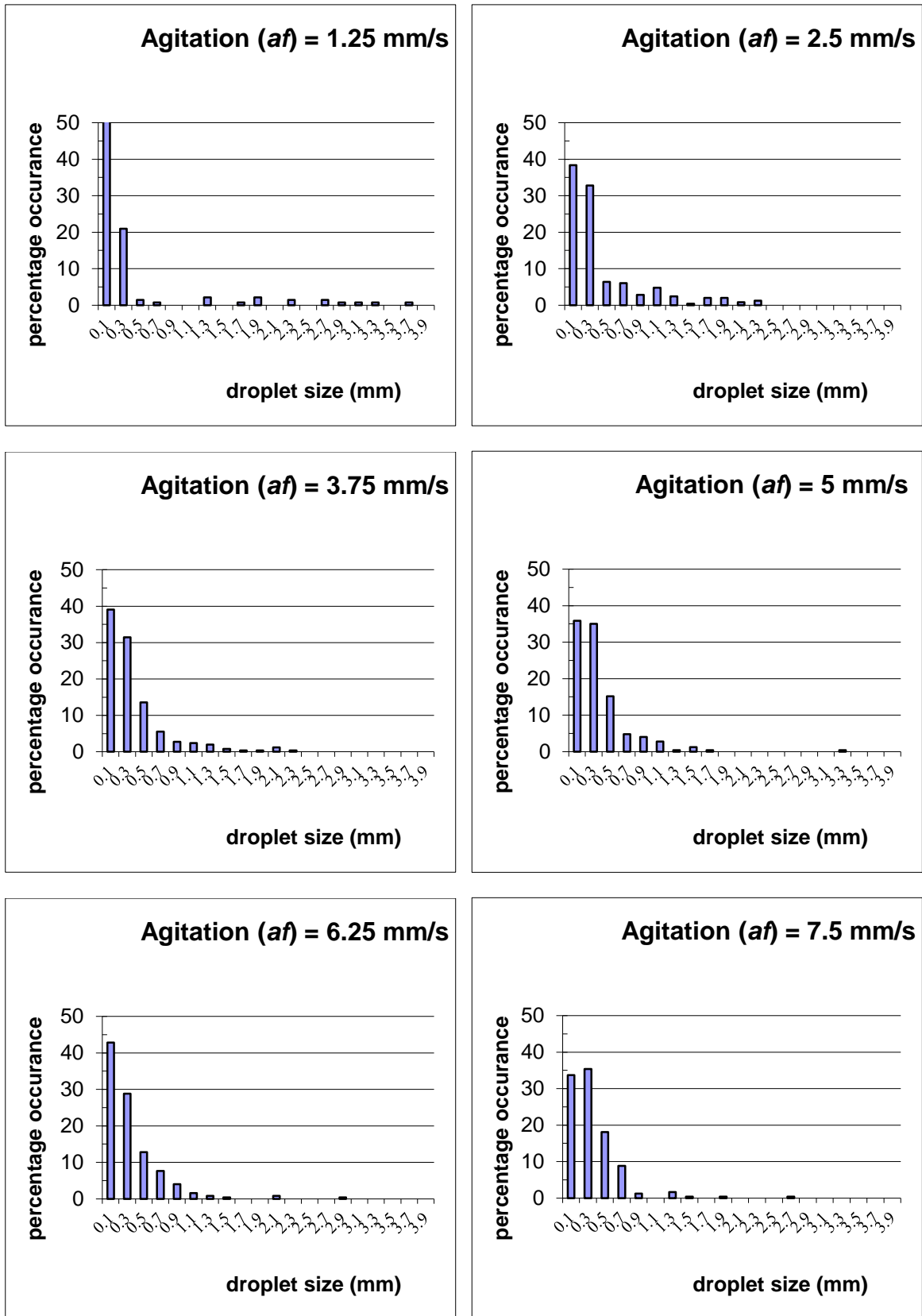


Fig D7 dsd – mass transfer (S/F = 1:1; h = 200mm)

APPENDIX E

Profile Charts

The profile charts are given below for the three S/F ratios and two tray spacings. In all of the charts the equilibrium line is shown together with profile charts for all agitation levels. The operating lines were evaluated by plotting the concentration of the continuous phase against the concentration of the dispersed phase at different points along the length of the column.

In addition to the profile chart, the change in concentration of the continuous and dispersed phases as a function of the length of the column is also shown for all S/F ratios and tray spacings.

It can be seen that for $h = 100$ mm and S/F = 1:1, most of the operating lines are straight (with the exception at an agitation level of 7.5 mm/s) indicating that there is no backmixing taking place and the profile is the same as the case for plug flow. At the agitation level of 7.5 mm/s, the start of backmixing in the dispersed phase is noticed.

For $h = 100$ mm and S/F = 1:2, there is substantial backmixing in the dispersed phase for all agitation levels indicated by the phase shift of the x axis. At high agitation levels there is a slight phase shift in the y axis as well indicating backmixing in the continuous phase.

The operating lines for $h = 100$ mm and S/F = 2:1 are all straight indicating no backmixing in either of the phases. Similar trends are seen for $h = 200$ mm with S/F = 1:1.

The graphs for the calculation of the NTU_m are given in figs. E5 to E8.

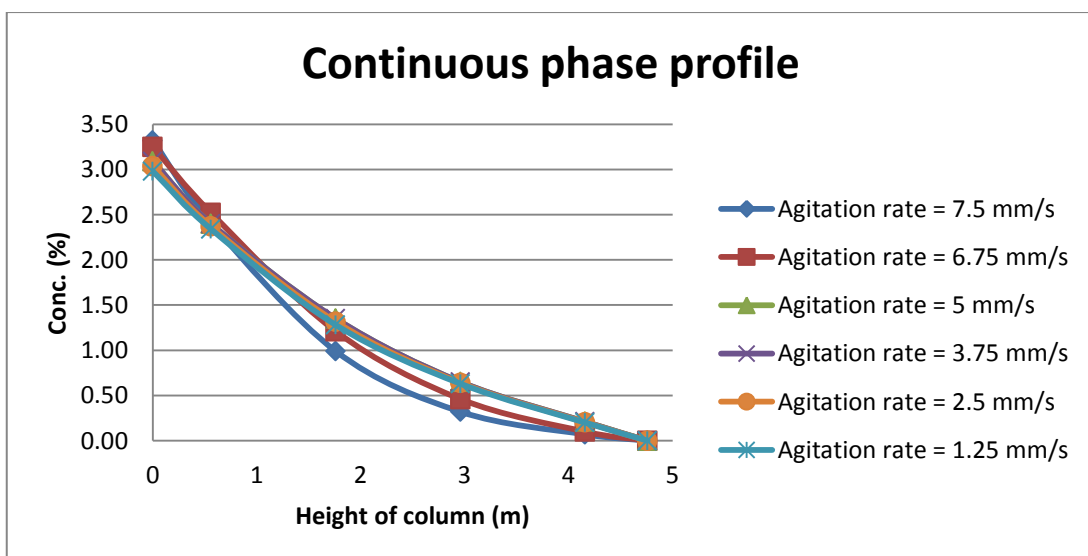
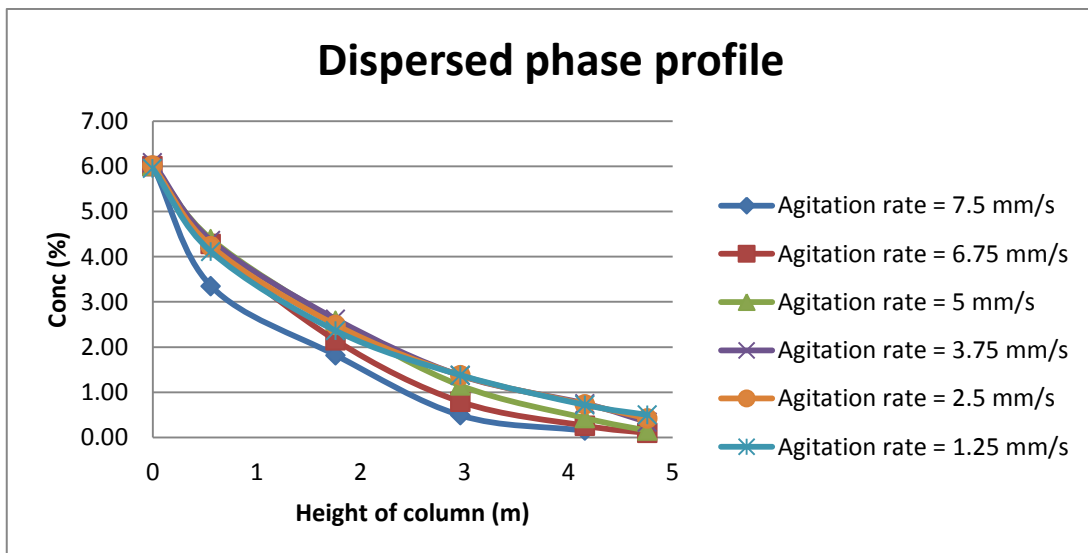
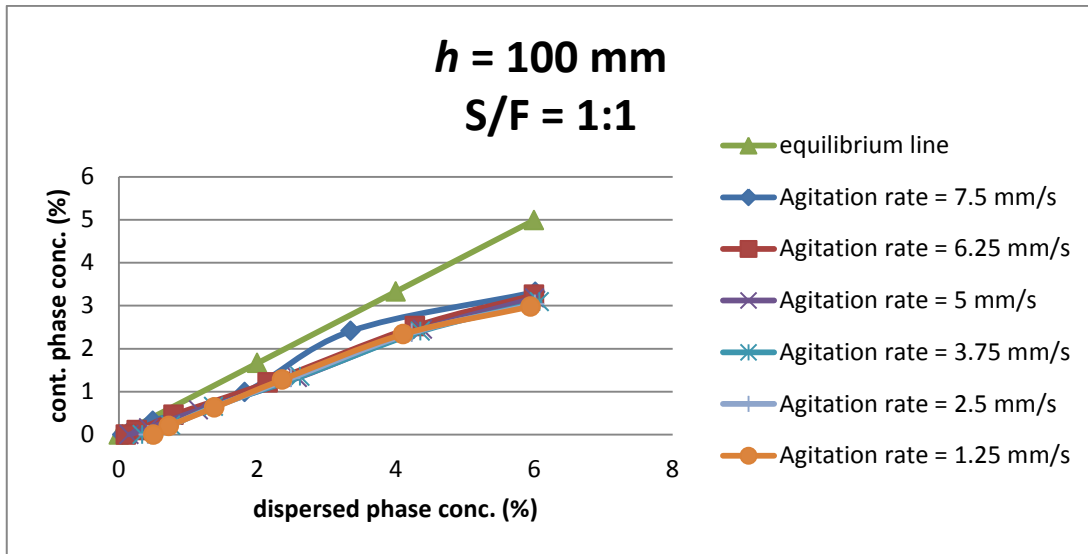


Fig. E1 Profile charts for $h = 100 \text{ mm}$; $S/F = 1:1$

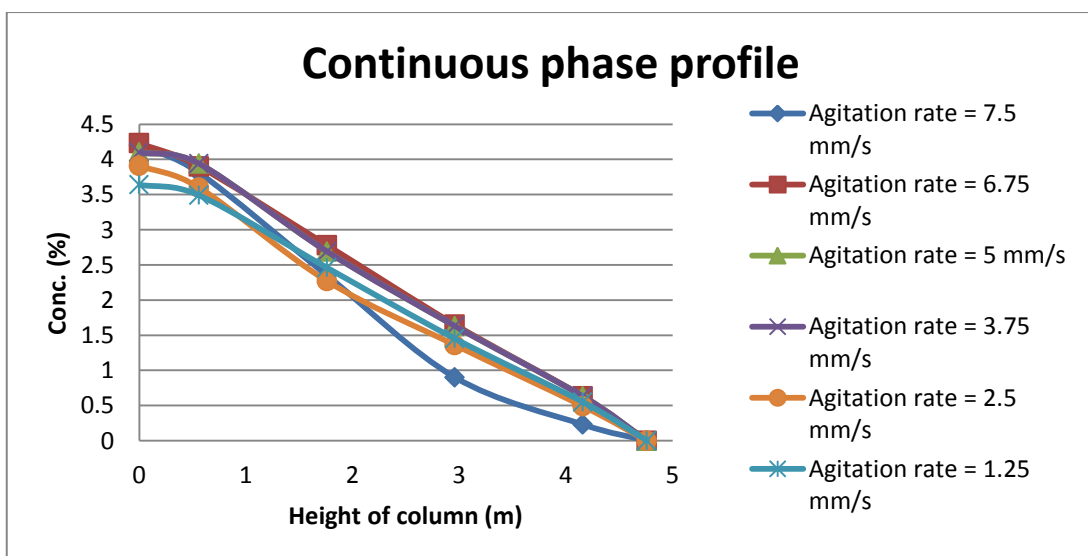
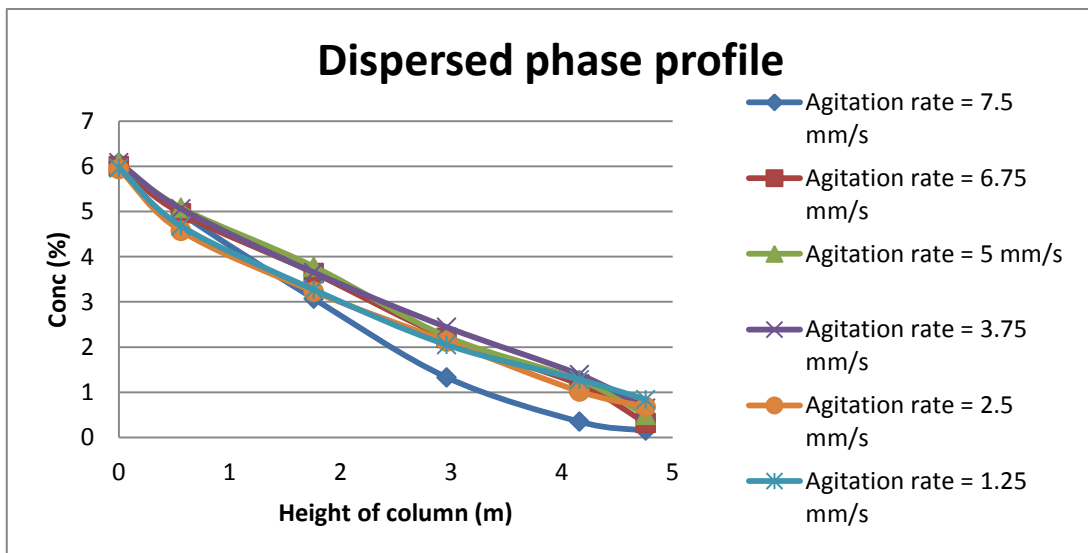
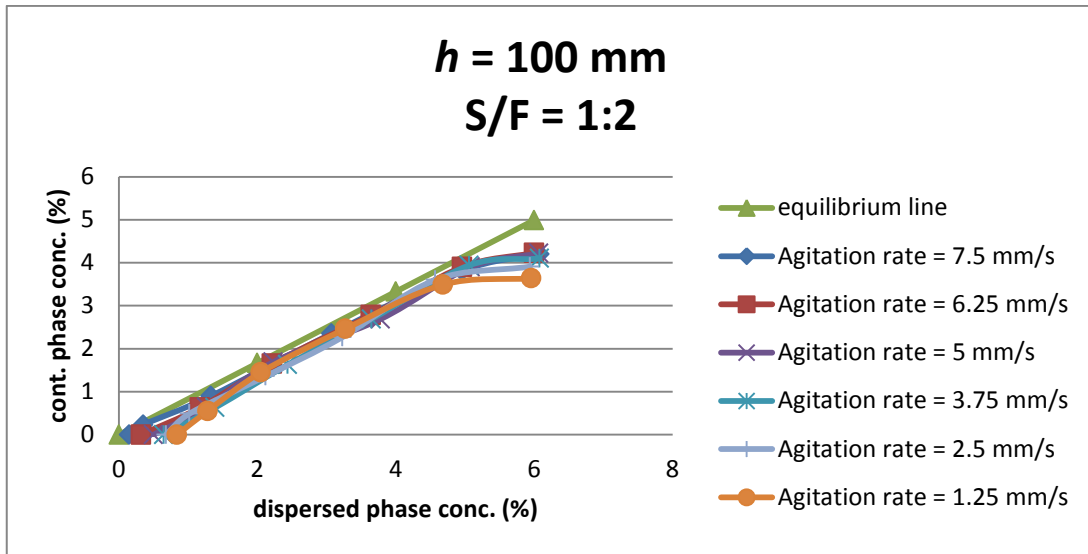


Fig. E2 Profile charts for $h = 100 \text{ mm}$; $S/F = 1:2$

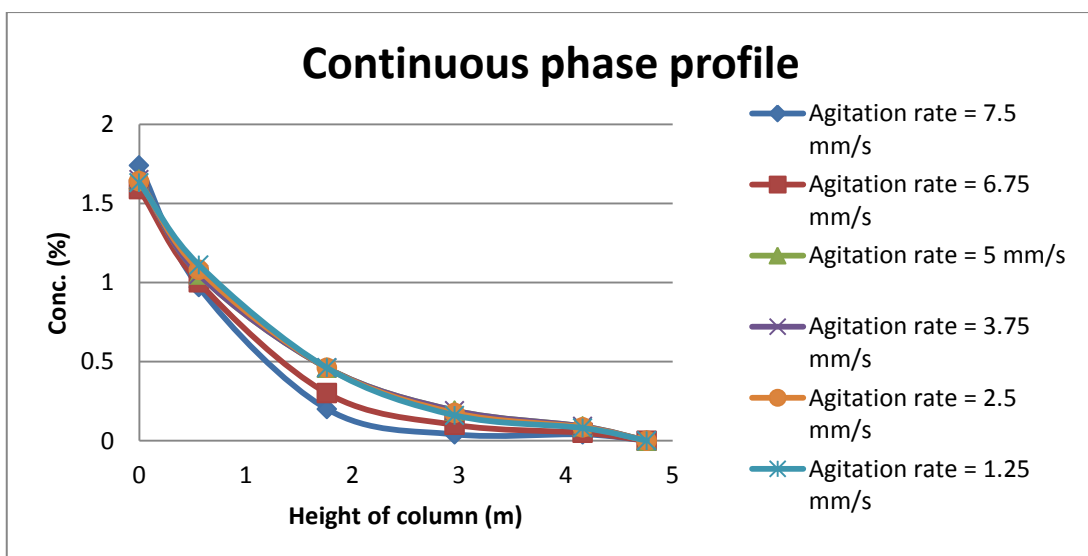
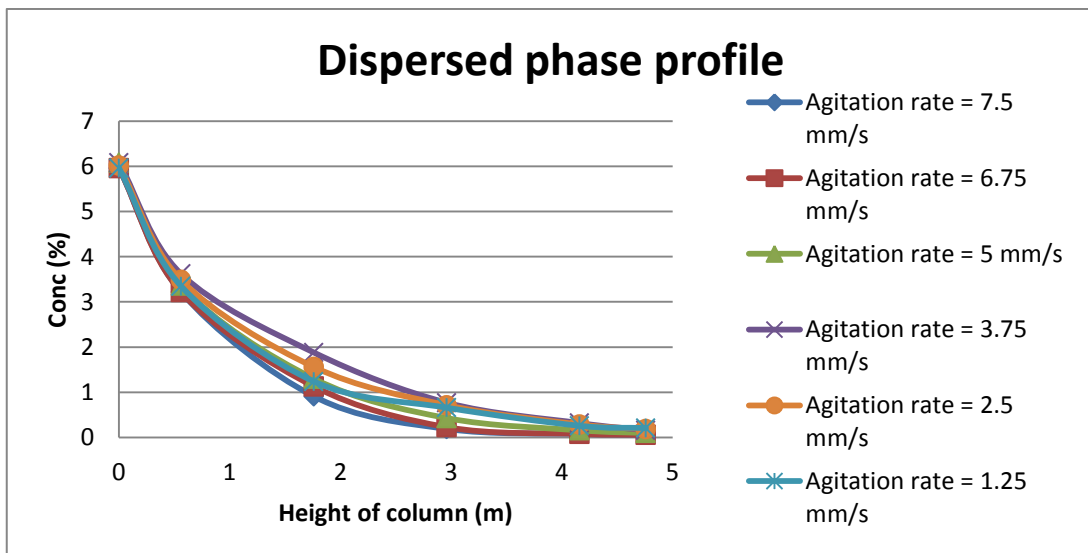
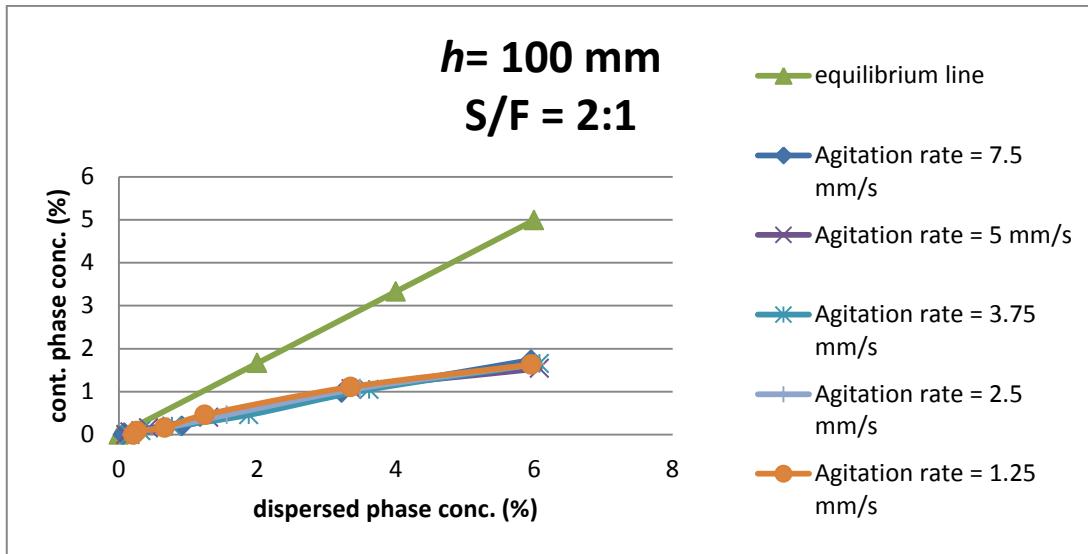


Fig. E3 Profile charts for $h = 100 \text{ mm}$; $S/F = 2:1$

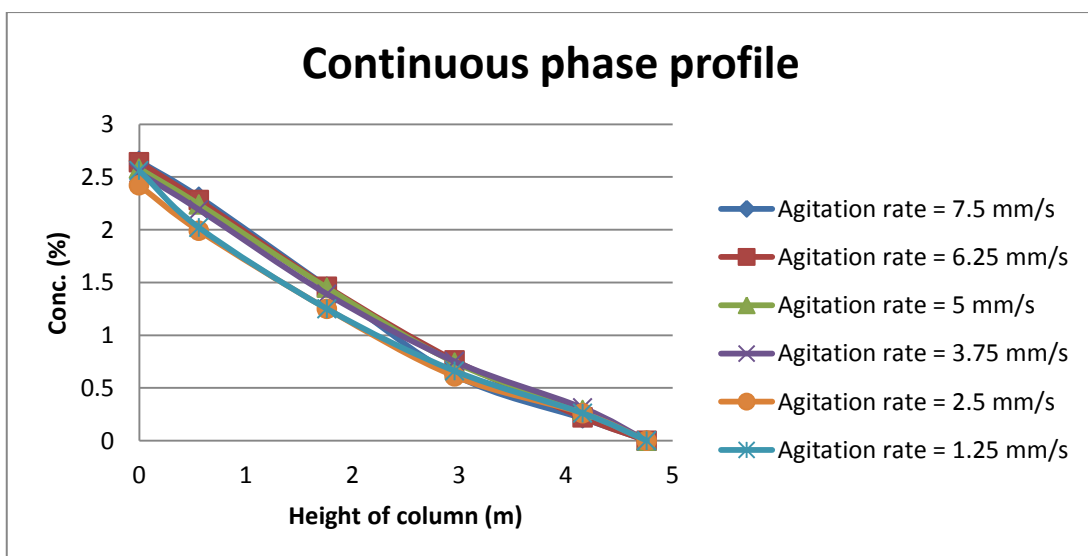
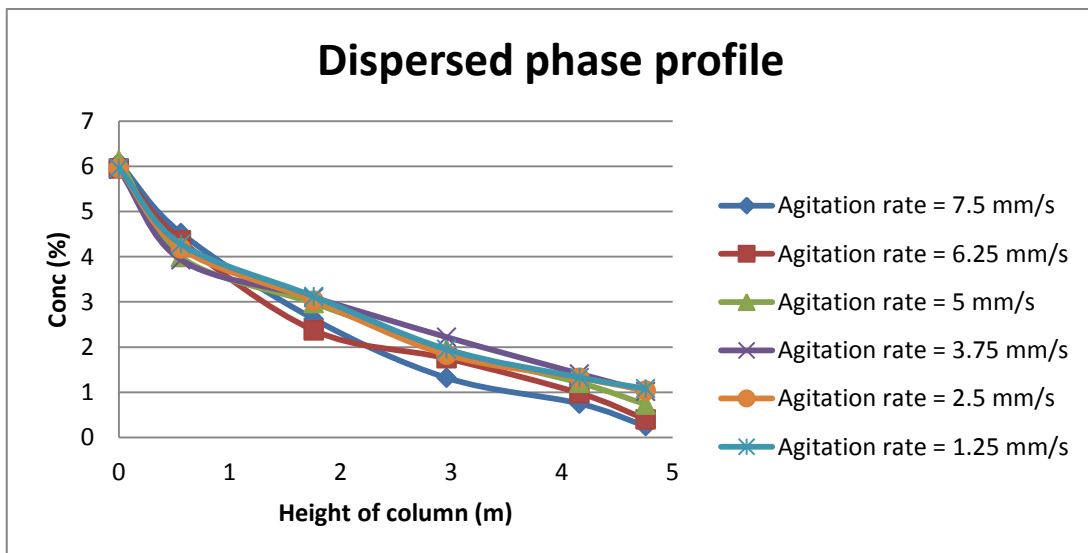
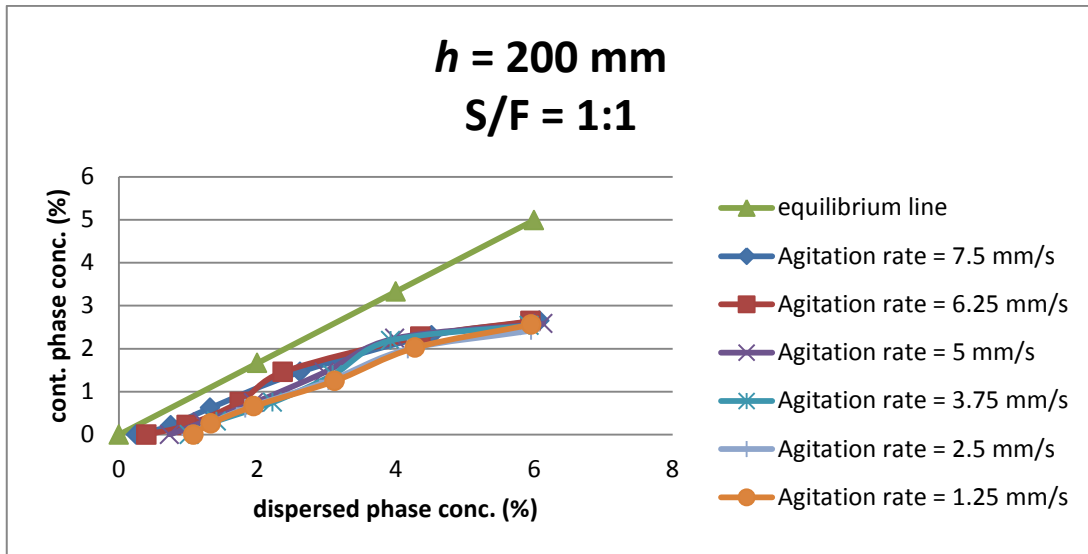
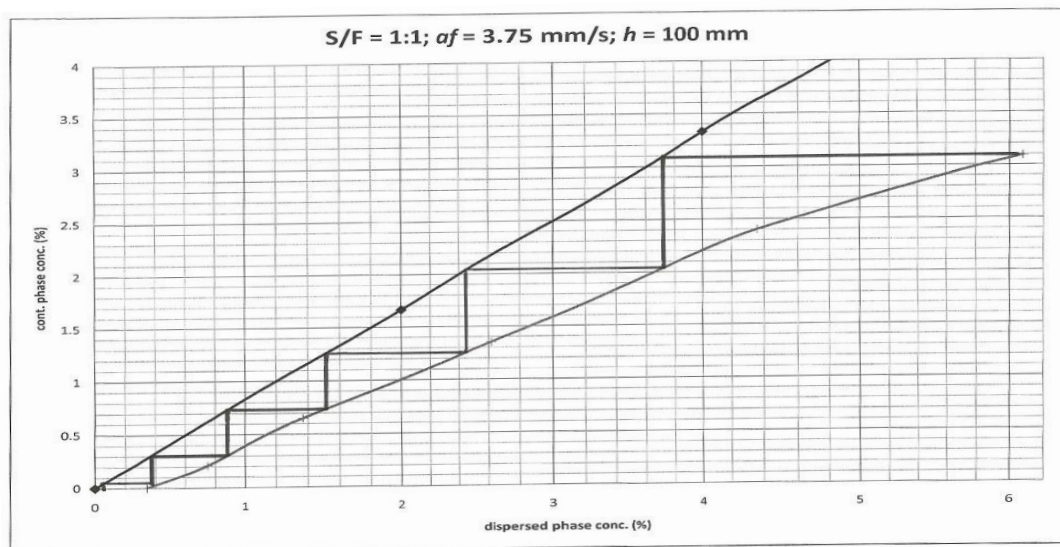
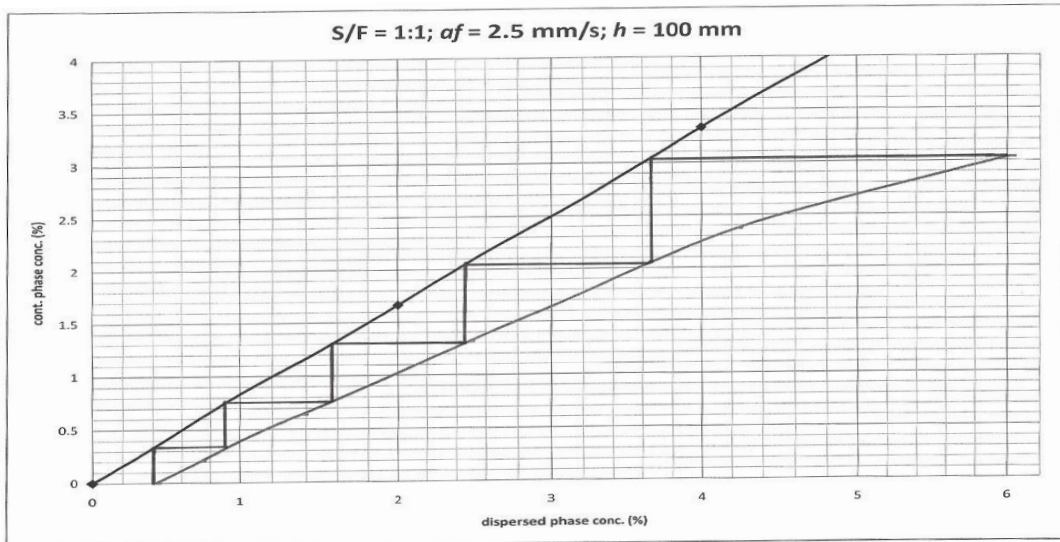
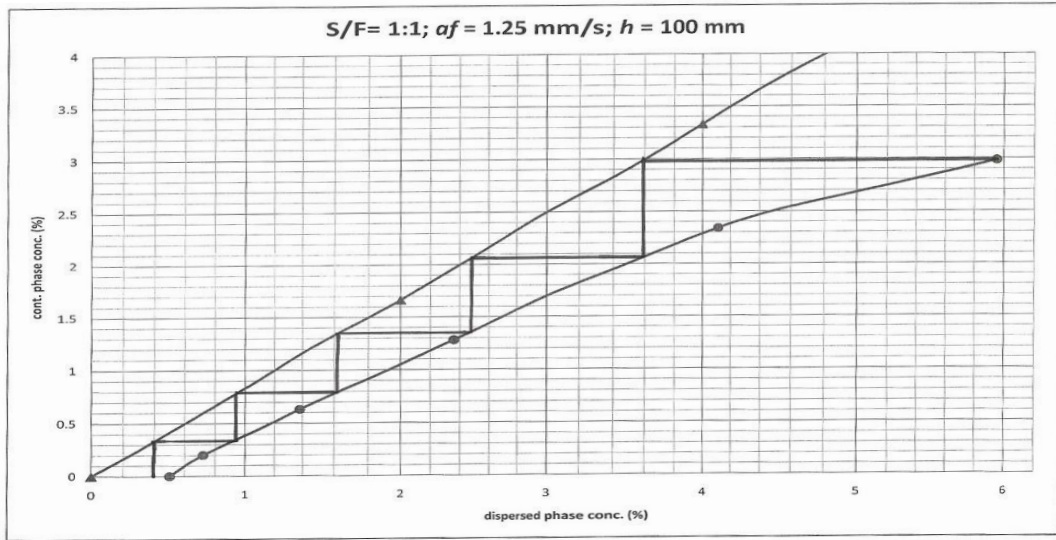


Fig. E4 Profile charts for $h = 200 \text{ mm}$; $S/F = 1:1$



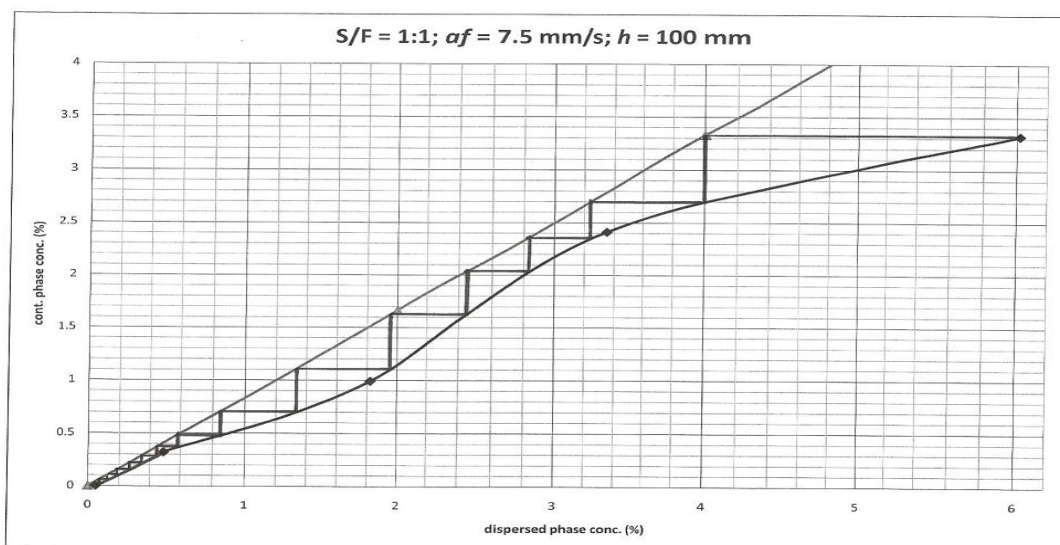
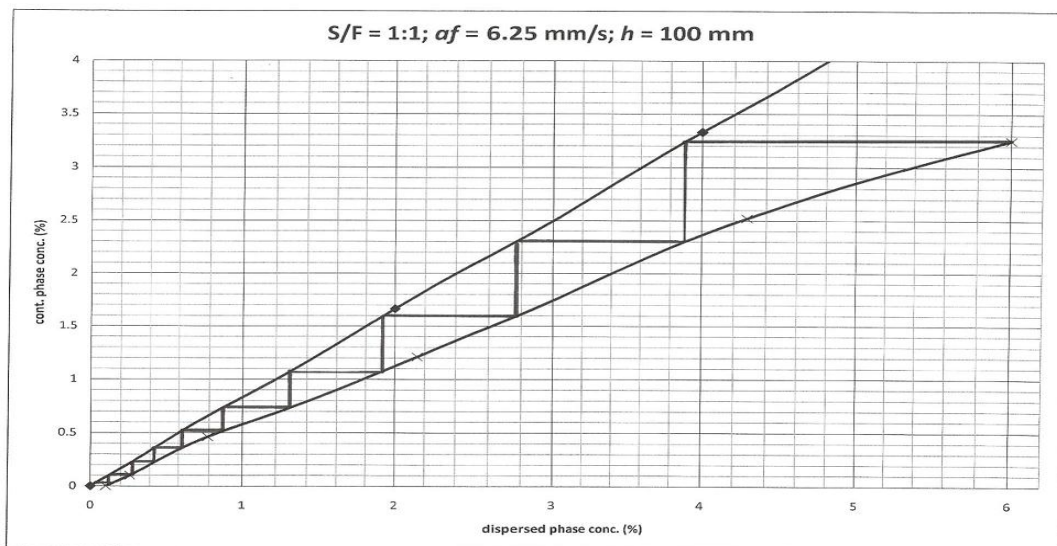
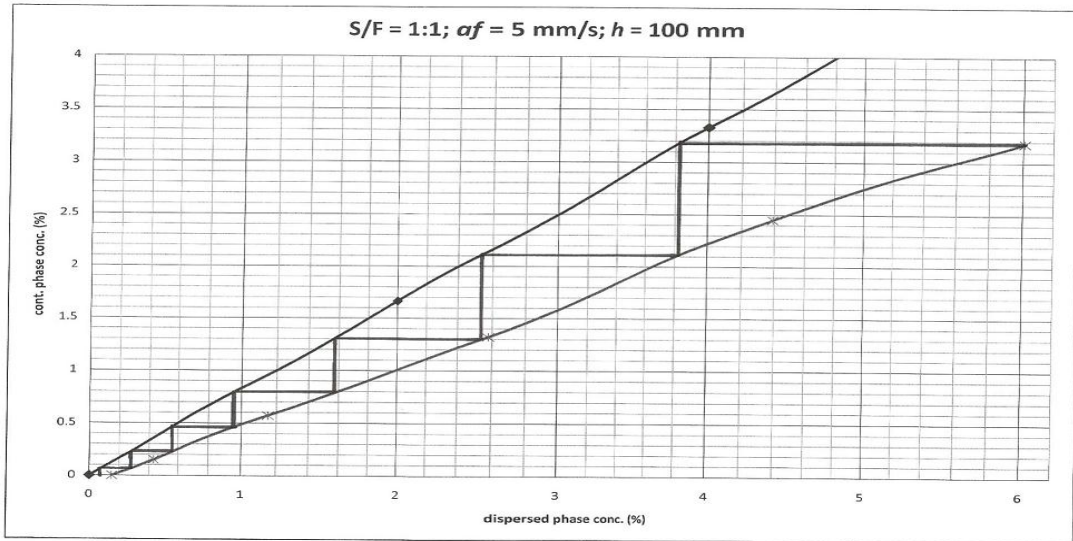
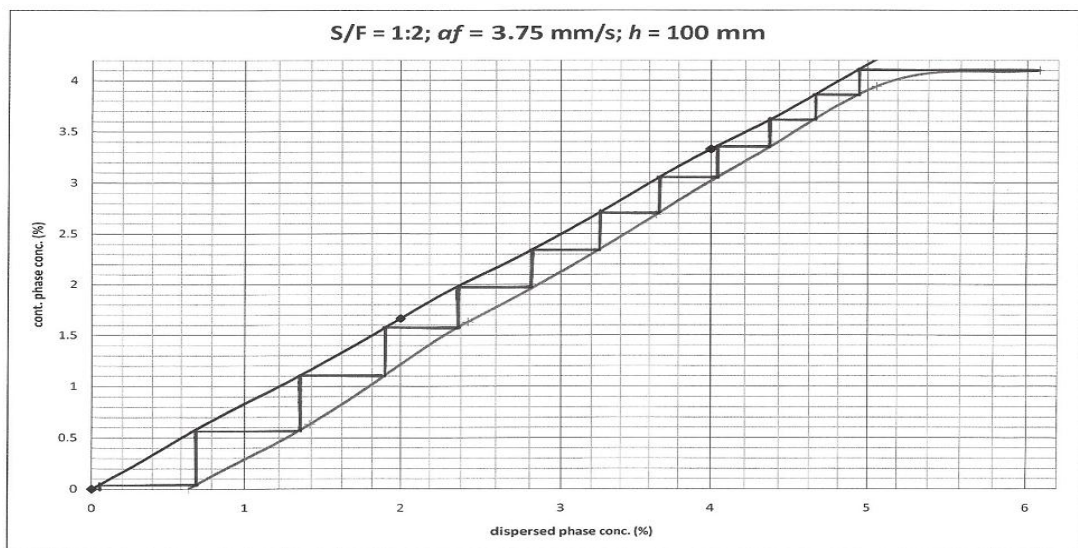
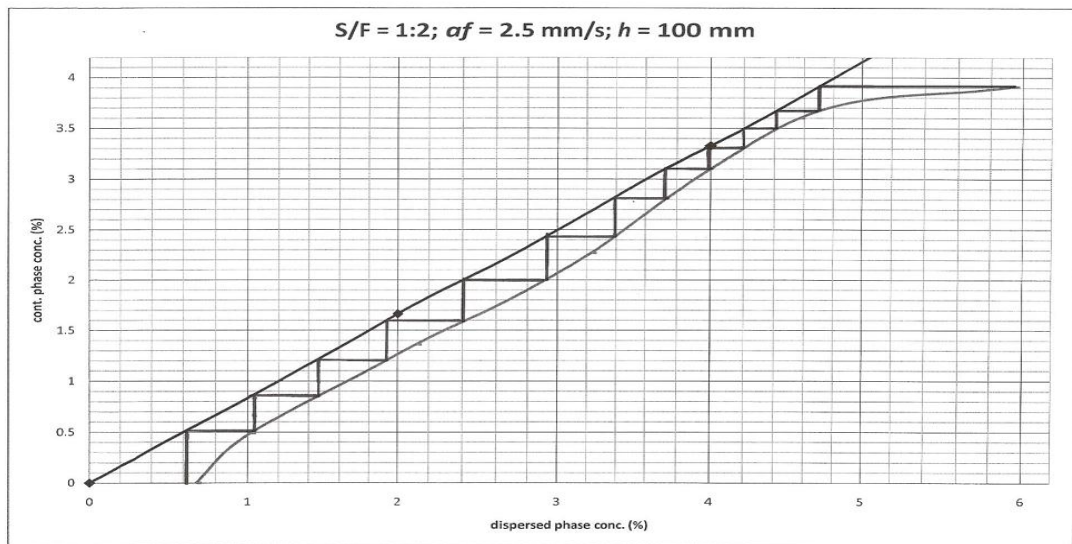
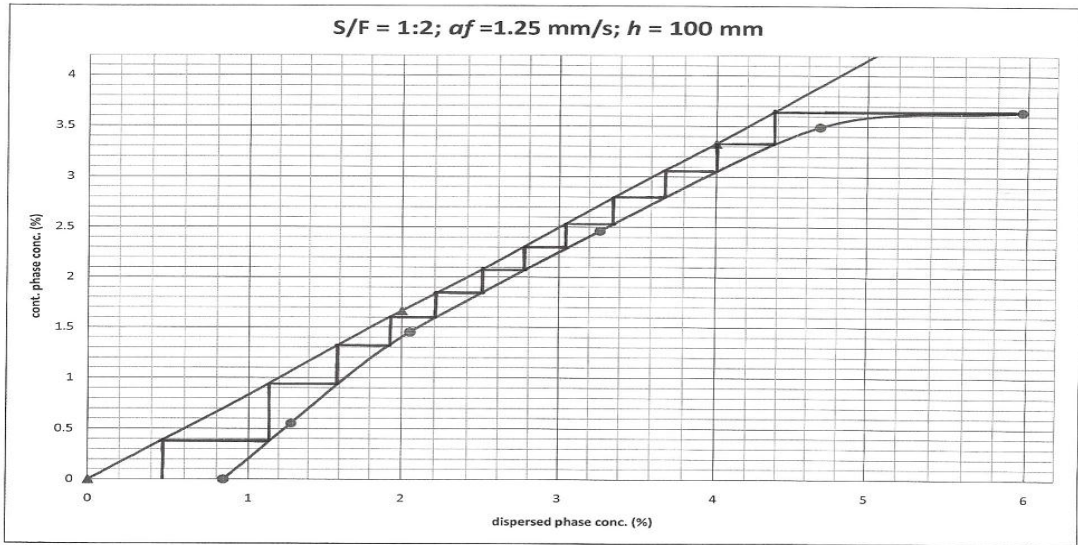


Fig E5 Calculations of NTU_m ($S/F = 1:1; h = 100 \text{ mm}$)



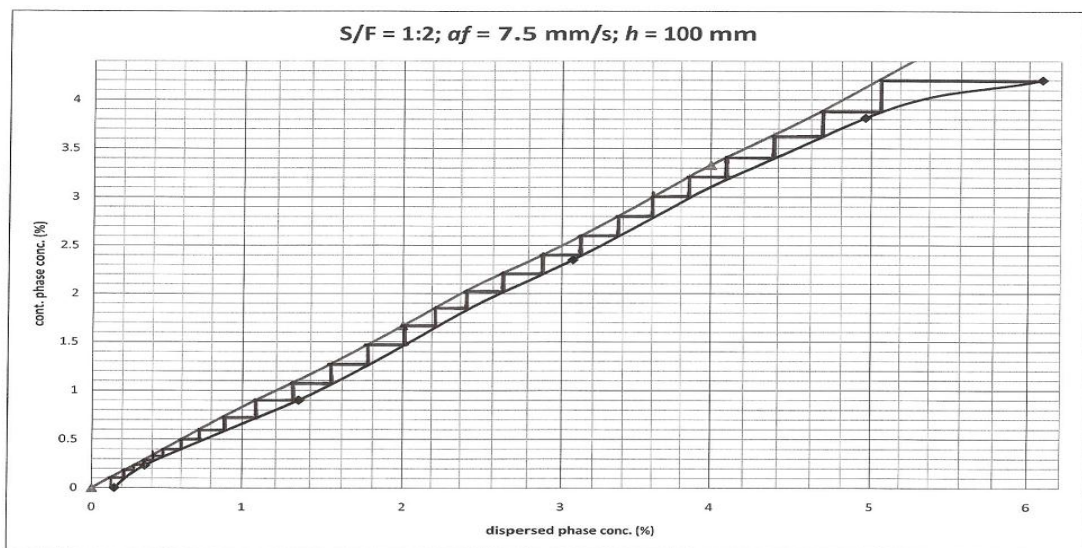
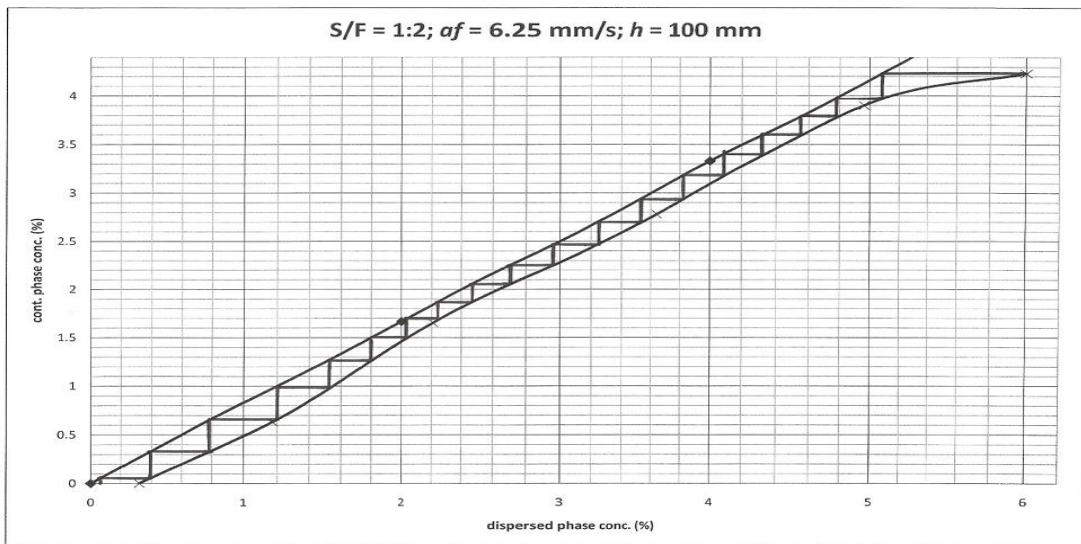
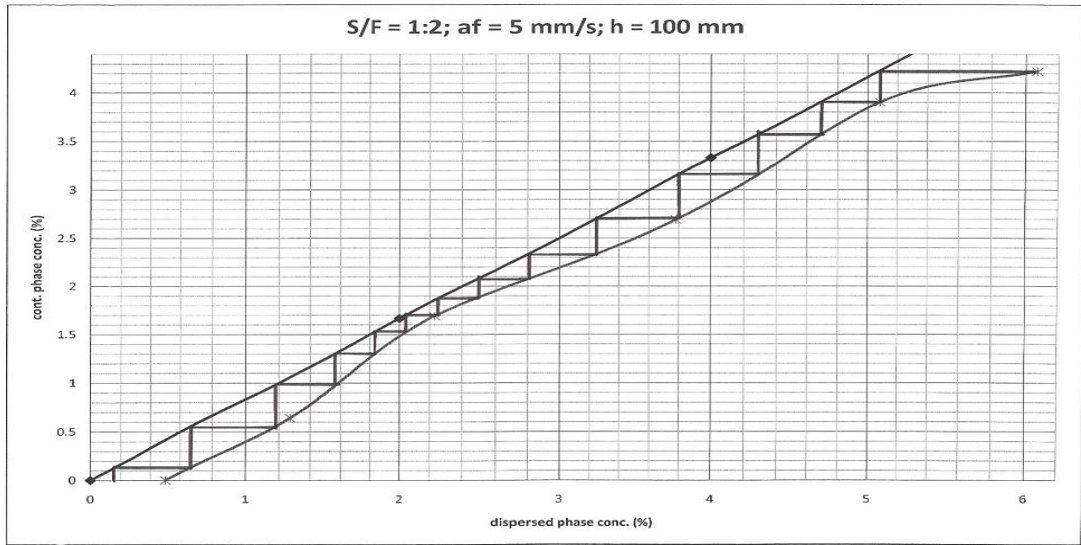
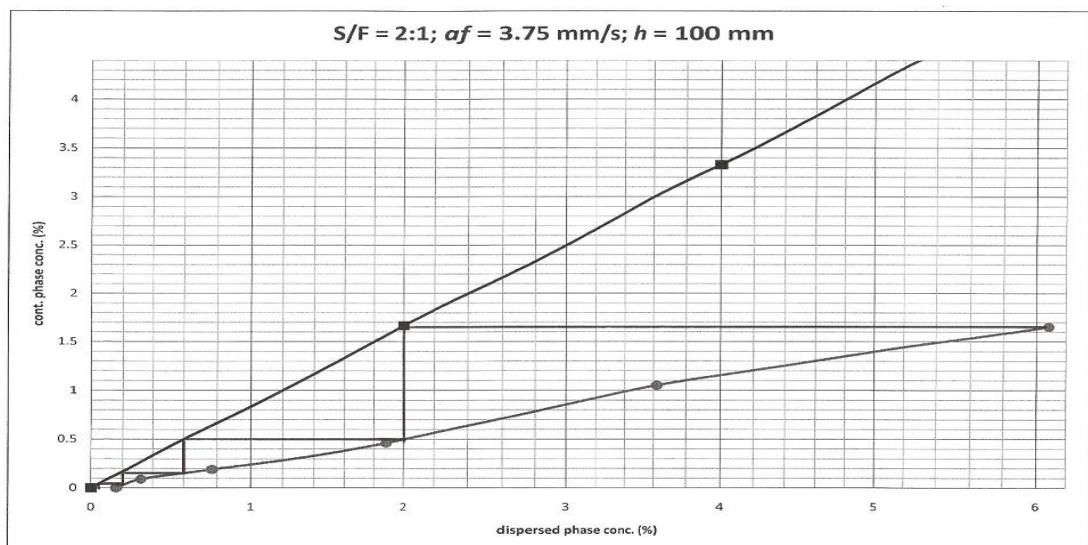
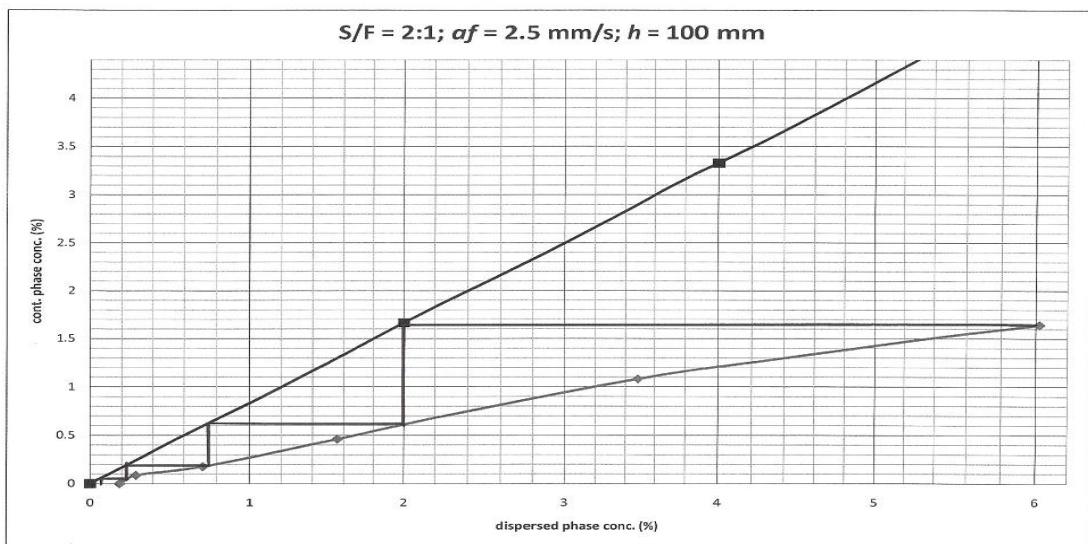
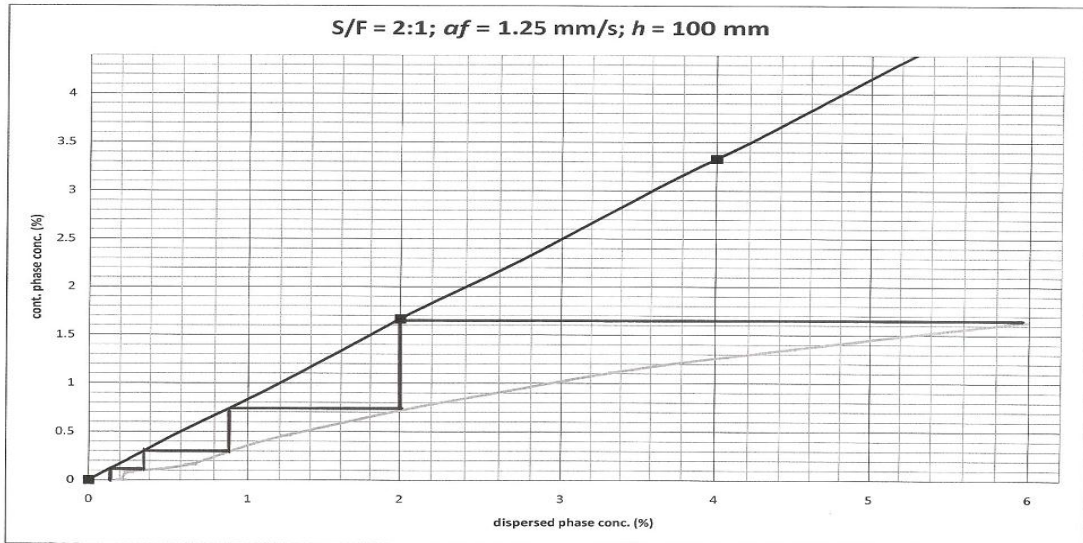


Fig E6 Calculations of NTU_m ($S/F=1:2$; $h = 100$ mm)



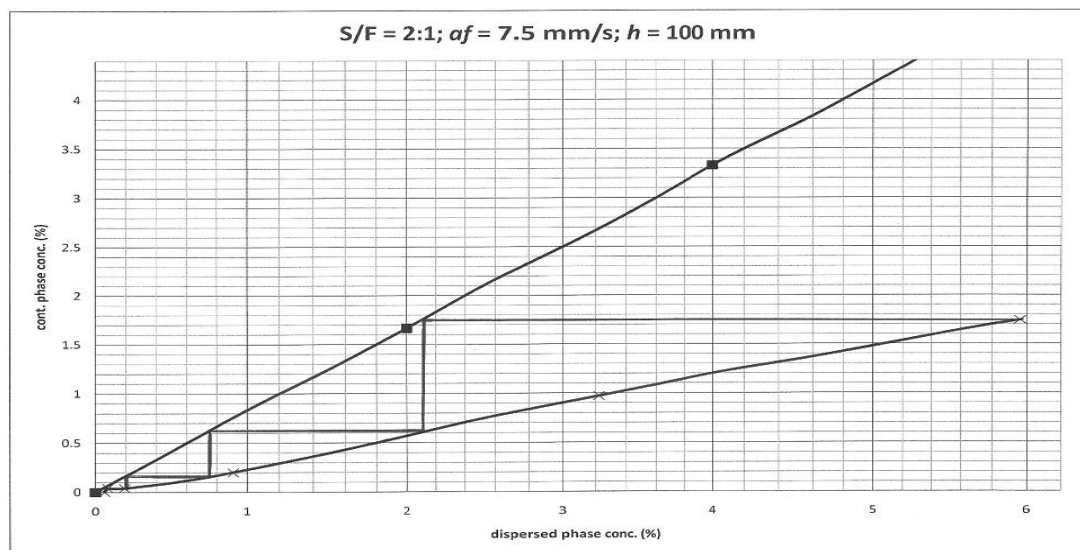
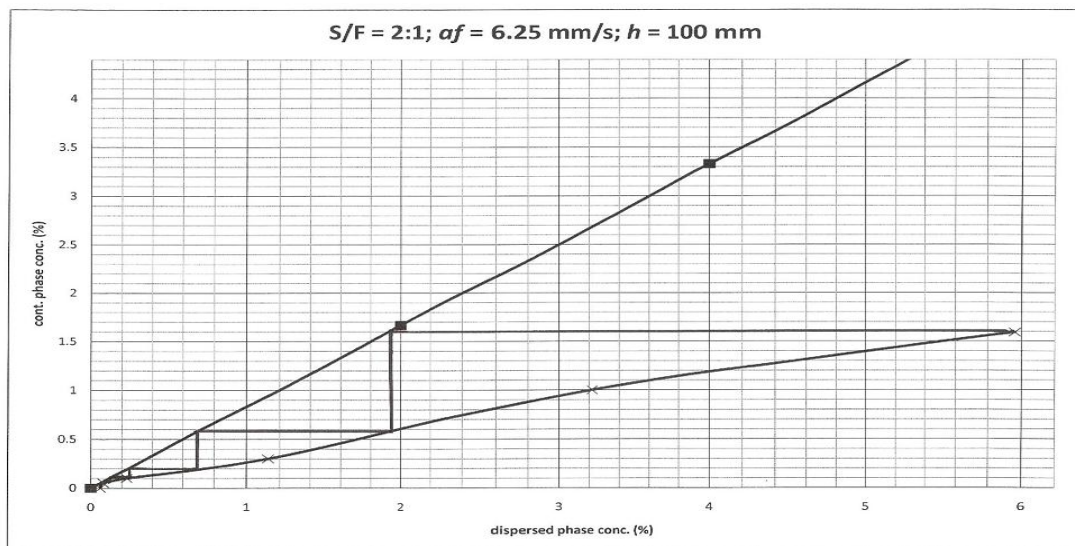
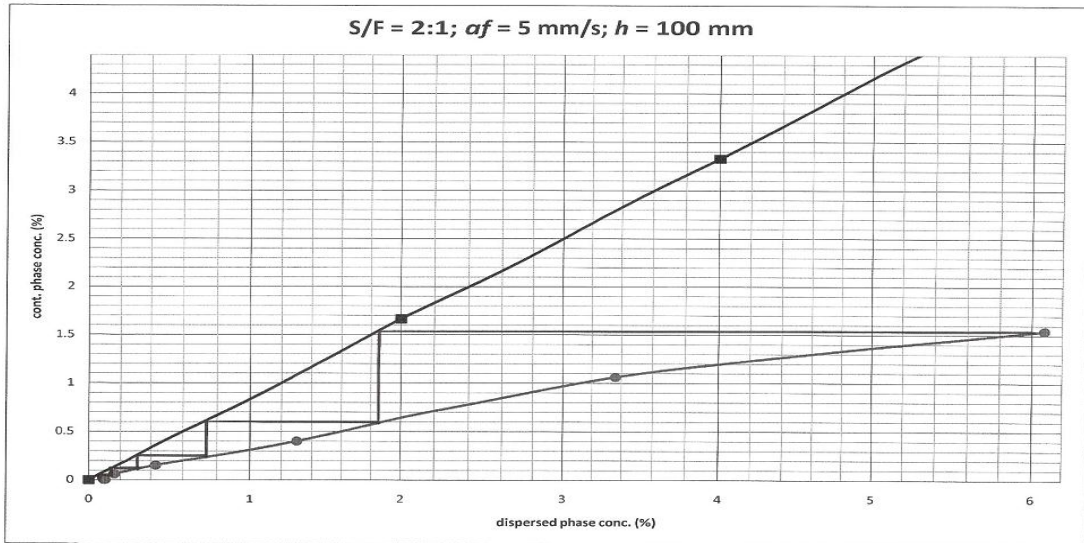
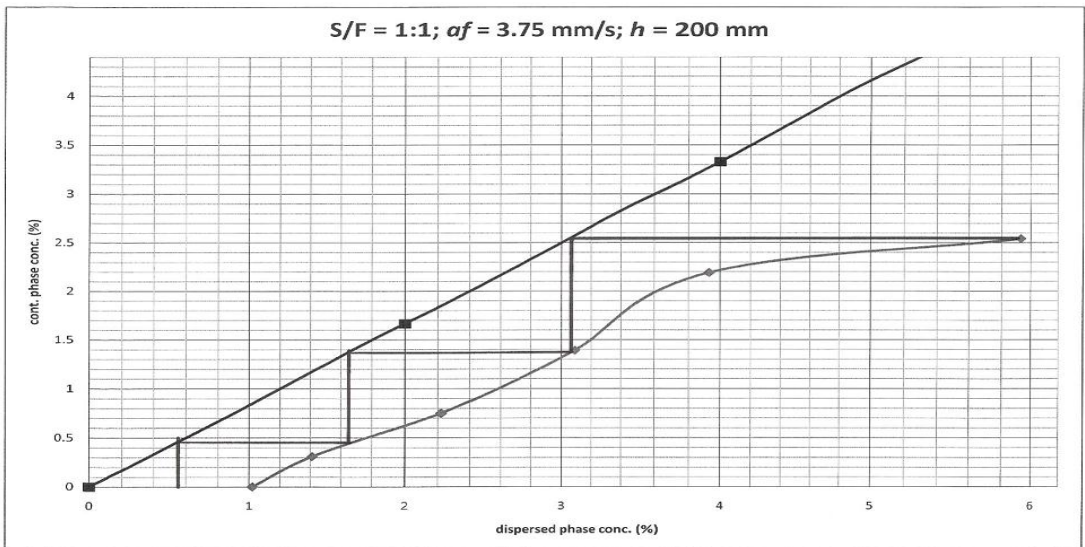
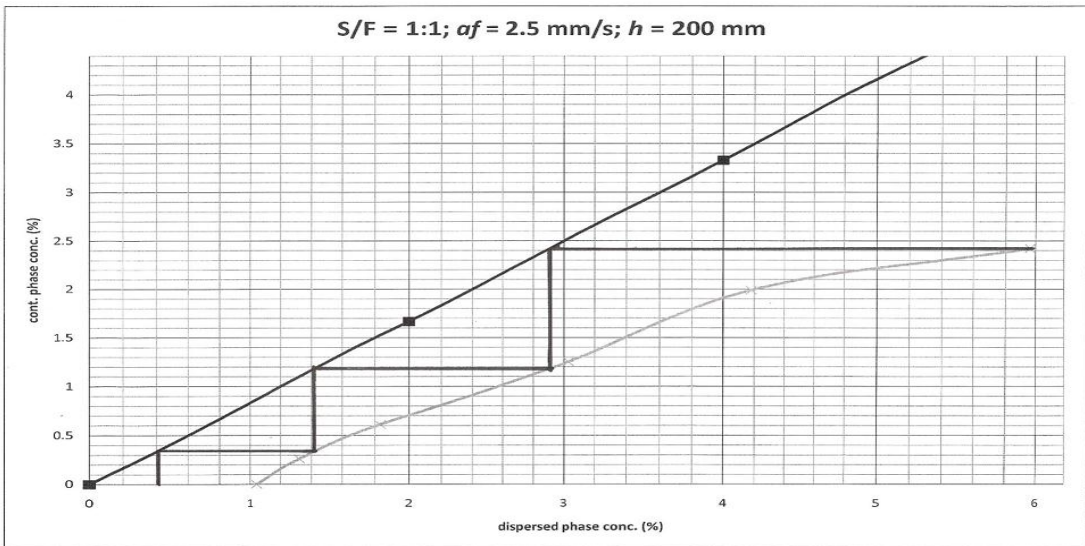
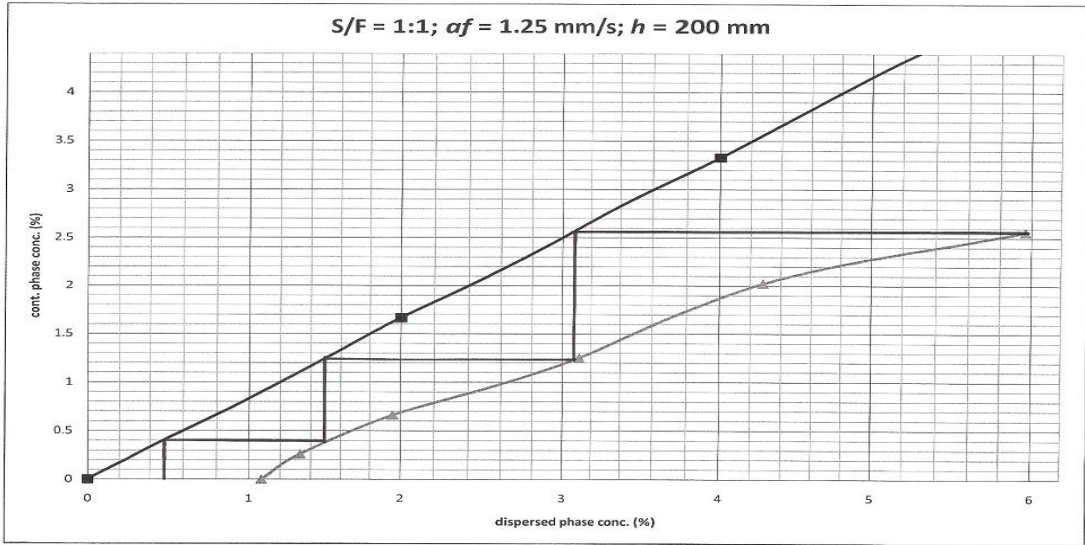


Fig E7 Calculations of NTU_m (S/F = 2:1; $h = 100$ mm)



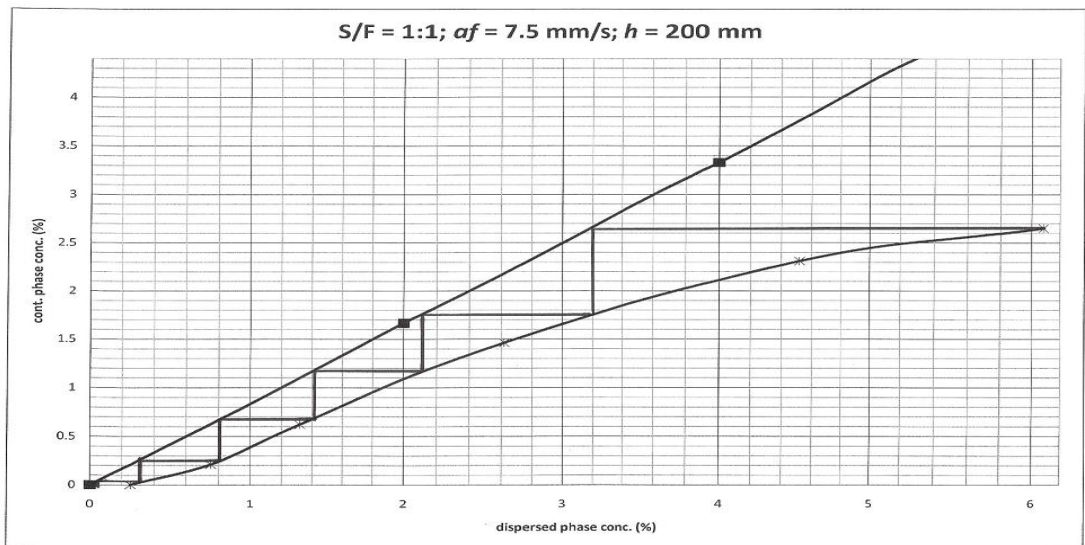
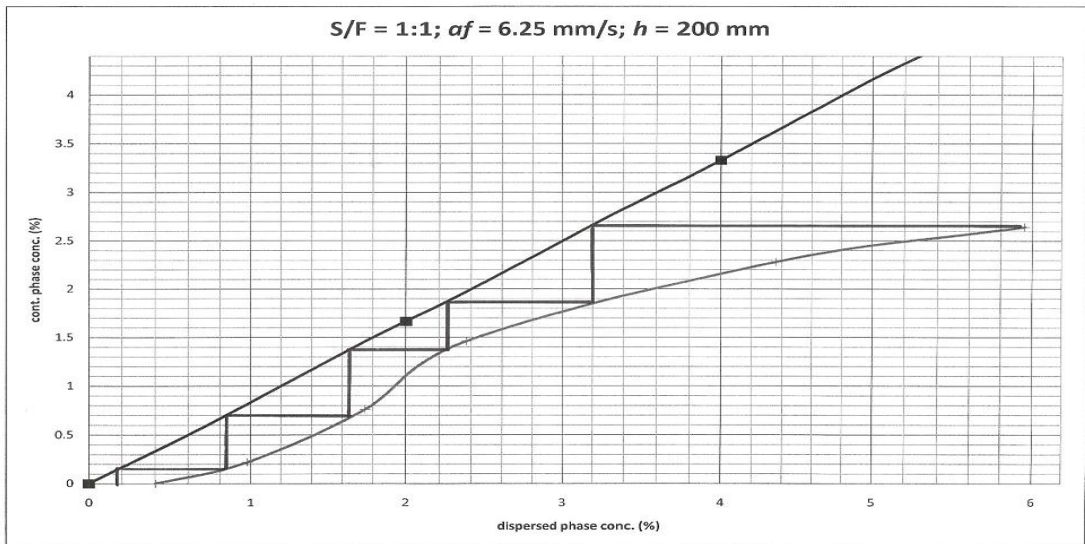
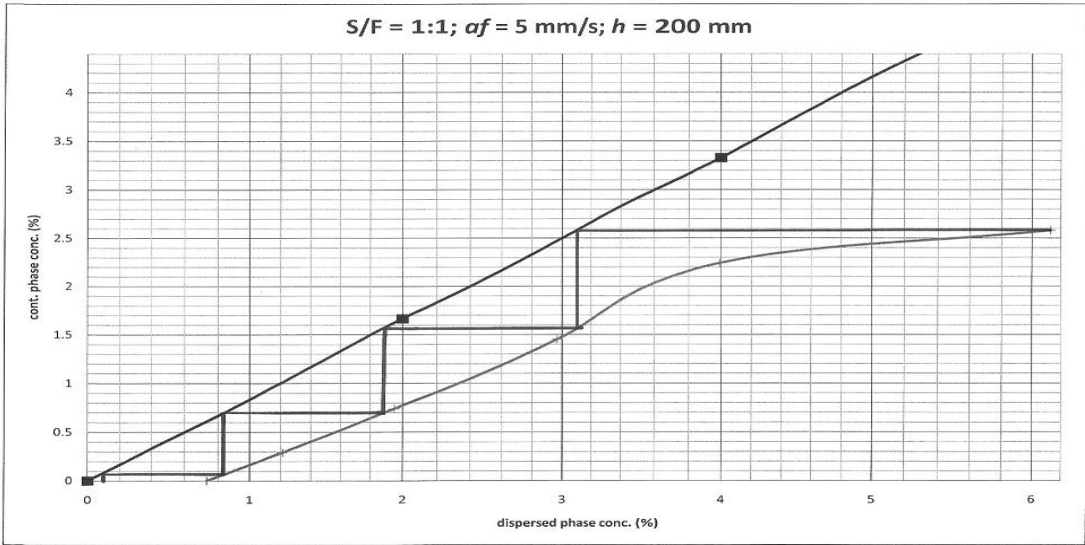


Fig E8 Calculations of NTU_m ($S/F = 1:1; h = 200 \text{ mm}$)

APPENDIX F

Material Safety Data Sheets

(ScienceLab.com, 2008a; ScienceLab.com. 2008b)



Health	2
Fire	3
Reactivity	0
Personal Protection	H

Material Safety Data Sheet Acetone MSDS

Section 1: Chemical Product and Company Identification	
Product Name: Acetone	Contact Information:
Catalog Codes: SLA3502, SLA1645, SLA3151, SLA3808	Sciencelab.com, Inc. 14025 Smith Rd. Houston, Texas 77396
CAS#: 67-64-1	US Sales: 1-800-901-7247 International Sales: 1-281-441-4400
RTECS: AL3150000	Order Online: ScienceLab.com
TSCA: TSCA 8(b) inventory: Acetone	CHEMTREC (24HR Emergency Telephone), call: 1-800-424-9300
CI#: Not applicable.	International CHEMTREC, call: 1-703-527-3887
Synonym: 2-propanone; Dimethyl Ketone; Dimethylformaldehyde; Pyroacetic Acid	For non-emergency assistance, call: 1-281-441-4400
Chemical Name: Acetone	
Chemical Formula: C ₃ H ₆ O	

Section 2: Composition and Information on Ingredients								
Composition:								
<table border="1"><thead><tr><th>Name</th><th>CAS #</th><th>% by Weight</th></tr></thead><tbody><tr><td>Acetone</td><td>67-64-1</td><td>100</td></tr></tbody></table>	Name	CAS #	% by Weight	Acetone	67-64-1	100		
Name	CAS #	% by Weight						
Acetone	67-64-1	100						
Toxicological Data on Ingredients: Acetone: ORAL (LD50): Acute: 5800 mg/kg [Rat]. 3000 mg/kg [Mouse]. 5340 mg/kg [Rabbit]. VAPOR (LC50): Acute: 50100 mg/m 8 hours [Rat]. 44000 mg/m 4 hours [Mouse].								

Section 3: Hazards Identification
Potential Acute Health Effects: Hazardous in case of skin contact (irritant), of eye contact (irritant), of ingestion, of inhalation. Slightly hazardous in case of skin contact (permeator).
Potential Chronic Health Effects: CARCINOGENIC EFFECTS: A4 (Not classifiable for human or animal.) by ACGIH. MUTAGENIC EFFECTS: Not available. TERATOGENIC EFFECTS: Not available. DEVELOPMENTAL TOXICITY: Classified Reproductive system/toxin/female, Reproductive system/toxin/male [SUSPECTED]. The substance is toxic to central nervous system (CNS). The substance may be toxic to kidneys, the reproductive system, liver, skin. Repeated or prolonged exposure to the substance can produce target organs damage.

Section 4: First Aid Measures

Eye Contact:

Check for and remove any contact lenses. Immediately flush eyes with running water for at least 15 minutes, keeping eyelids open. Cold water may be used. Get medical attention.

Skin Contact:

In case of contact, immediately flush skin with plenty of water. Cover the irritated skin with an emollient. Remove contaminated clothing and shoes. Cold water may be used. Wash clothing before reuse. Thoroughly clean shoes before reuse. Get medical attention.

Serious Skin Contact:

Wash with a disinfectant soap and cover the contaminated skin with an anti-bacterial cream. Seek medical attention.

Inhalation:

If inhaled, remove to fresh air. If not breathing, give artificial respiration. If breathing is difficult, give oxygen. Get medical attention if symptoms appear.

Serious Inhalation:

Evacuate the victim to a safe area as soon as possible. Loosen tight clothing such as a collar, tie, belt or waistband. If breathing is difficult, administer oxygen. If the victim is not breathing, perform mouth-to-mouth resuscitation. Seek medical attention.

Ingestion:

Do NOT induce vomiting unless directed to do so by medical personnel. Never give anything by mouth to an unconscious person. Loosen tight clothing such as a collar, tie, belt or waistband. Get medical attention if symptoms appear.

Serious Ingestion: Not available.

Section 5: Fire and Explosion Data

Flammability of the Product: Flammable.

Auto-Ignition Temperature: 465°C (869°F)

Flash Points: CLOSED CUP: -20°C (-4°F). OPEN CUP: -9°C (15.8°F) (Cleveland).

Flammable Limits: LOWER: 2.6% UPPER: 12.8%

Products of Combustion: These products are carbon oxides (CO, CO₂).

Fire Hazards in Presence of Various Substances: Highly flammable in presence of open flames and sparks, of heat.

Explosion Hazards in Presence of Various Substances:

Risks of explosion of the product in presence of mechanical impact: Not available.

Slightly explosive in presence of open flames and sparks, of oxidizing materials, of acids.

Fire Fighting Media and Instructions:

Flammable liquid, soluble or dispersed in water.

SMALL FIRE: Use DRY chemical powder.

LARGE FIRE: Use alcohol foam, water spray or fog.

Special Remarks on Fire Hazards: Vapor may travel considerable distance to source of ignition and flash back.

Special Remarks on Explosion Hazards:

Forms explosive mixtures with hydrogen peroxide, acetic acid, nitric acid, nitric acid + sulfuric acid, chromic anhydride, chromyl chloride, nitrosyl chloride, hexachloromelamine, nitrosyl perchlorate, nityl perchlorate, permonosulfuric acid, thiodiglycol + hydrogen peroxide, potassium ter-butoxide, sulfur dichloride, 1-methyl-1,3-butadiene, bromoform, carbon, air, chloroform, thitriazolperchlorate.

Section 6: Accidental Release Measures

Small Spill:

Dilute with water and mop up, or absorb with an inert dry material and place in an appropriate waste disposal container.

Large Spill:

Flammable liquid.

Keep away from heat. Keep away from sources of ignition. Stop leak if without risk. Absorb with DRY earth, sand or other non-combustible material. Do not touch spilled material. Prevent entry into sewers, basements or confined areas; dike if needed. Be careful that the product is not present at a concentration level above TLV. Check TLV on the MSDS and with local authorities.

Section 7: Handling and Storage

Precautions:

Keep locked up.. Keep away from heat. Keep away from sources of ignition. Ground all equipment containing material. Do not ingest. Do not breathe gas/fumes/ vapor/spray. Wear suitable protective clothing. In case of insufficient ventilation, wear suitable respiratory equipment. If ingested, seek medical advice immediately and show the container or the label. Avoid contact with skin and eyes. Keep away from incompatibles such as oxidizing agents, reducing agents, acids, alkalis.

Storage:

Store in a segregated and approved area (flammables area) . Keep container in a cool, well-ventilated area. Keep container tightly closed and sealed until ready for use. Keep away from direct sunlight and heat and avoid all possible sources of ignition (spark or flame).

Section 8: Exposure Controls/Personal Protection

Engineering Controls:

Provide exhaust ventilation or other engineering controls to keep the airborne concentrations of vapors below their respective threshold limit value. Ensure that eyewash stations and safety showers are proximal to the work-station location.

Personal Protection:

Splash goggles. Lab coat. Vapor respirator. Be sure to use an approved/certified respirator or equivalent. Gloves.

Personal Protection in Case of a Large Spill:

Splash goggles. Full suit. Vapor respirator. Boots. Gloves. A self contained breathing apparatus should be used to avoid inhalation of the product. Suggested protective clothing might not be sufficient; consult a specialist BEFORE handling this product.

Exposure Limits:

TWA: 500 STEL: 750 (ppm) from ACGIH (TLV) [United States]

TWA: 750 STEL: 1000 (ppm) from OSHA (PEL) [United States]

TWA: 500 STEL: 1000 [Australia]

TWA: 1185 STEL: 2375 (mg/m3) [Australia]

TWA: 750 STEL: 1500 (ppm) [United Kingdom (UK)]

TWA: 1810 STEL: 3620 (mg/m3) [United Kingdom (UK)]

TWA: 1800 STEL: 2400 from OSHA (PEL) [United States] Consult local authorities for acceptable exposure limits.

Section 9: Physical and Chemical Properties

Physical state and appearance: Liquid.

Odor: Fruity. Mint-like. Fragrant. Ethereal

Taste: Pungent, Sweetish

<p>Molecular Weight: 58.08 g/mole</p> <p>Color: Colorless. Clear</p> <p>pH (1% soln/water): Not available.</p> <p>Boiling Point: 56.2°C (133.2°F)</p> <p>Melting Point: -95.35 (-139.6°F)</p> <p>Critical Temperature: 235°C (455°F)</p> <p>Specific Gravity: 0.79 (Water = 1)</p> <p>Vapor Pressure: 24 kPa (@ 20°C)</p> <p>Vapor Density: 2 (Air = 1)</p> <p>Volatility: Not available.</p> <p>Odor Threshold: 62 ppm</p> <p>Water/Oil Dist. Coeff.: The product is more soluble in water; log(oil/water) = -0.2</p> <p>Ionicity (in Water): Not available.</p> <p>Dispersion Properties: See solubility in water.</p> <p>Solubility: Easily soluble in cold water, hot water.</p>

Section 10: Stability and Reactivity Data
<p>Stability: The product is stable.</p> <p>Instability Temperature: Not available.</p> <p>Conditions of Instability: Excess heat, ignition sources, exposure to moisture, air, or water, incompatible materials.</p> <p>Incompatibility with various substances: Reactive with oxidizing agents, reducing agents, acids, alkalis.</p> <p>Corrosivity: Non-corrosive in presence of glass.</p> <p>Special Remarks on Reactivity: Not available.</p> <p>Special Remarks on Corrosivity: Not available.</p> <p>Polymerization: Will not occur.</p>

Section 11: Toxicological Information
<p>Routes of Entry: Absorbed through skin. Dermal contact. Eye contact. Inhalation.</p> <p>Toxicity to Animals: WARNING: THE LC50 VALUES HEREUNDER ARE ESTIMATED ON THE BASIS OF A 4-HOUR EXPOSURE. Acute oral toxicity (LD50): 3000 mg/kg [Mouse]. Acute toxicity of the vapor (LC50): 44000 mg/m³ 4 hours [Mouse].</p> <p>Chronic Effects on Humans: CARCINOGENIC EFFECTS: A4 (Not classifiable for human or animal.) by ACGIH.</p>

DEVELOPMENTAL TOXICITY: Classified Reproductive system/toxin/female, Reproductive system/toxin/male [SUSPECTED].

Causes damage to the following organs: central nervous system (CNS).

May cause damage to the following organs: kidneys, the reproductive system, liver, skin.

Other Toxic Effects on Humans:

Hazardous in case of skin contact (irritant), of ingestion, of inhalation.

Slightly hazardous in case of skin contact (permeator).

Special Remarks on Toxicity to Animals: Not available.

Special Remarks on Chronic Effects on Humans:

May affect genetic material (mutagenicity) based on studies with yeast (*S. cerevisiae*), bacteria, and hamster fibroblast cells. May cause reproductive effects (fertility) based upon animal studies.

May contain trace amounts of benzene and formaldehyde which may cancer and birth defects. Human: passes the placental barrier.

Special Remarks on other Toxic Effects on Humans:

Acute Potential Health Effects:

Skin: May cause skin irritation. May be harmful if absorbed through the skin.

Eyes: Causes eye irritation, characterized by a burning sensation, redness, tearing, inflammation, and possible corneal injury.

Inhalation: Inhalation at high concentrations affects the sense organs, brain and causes respiratory tract irritation.

It also may affect the Central Nervous System (behavior) characterized by dizziness, drowsiness, confusion, headache, muscle weakness, and possibly motor incoordination, speech abnormalities, narcotic effects and coma. Inhalation may also affect the gastrointestinal tract (nausea, vomiting).

Ingestion: May cause irritation of the digestive (gastrointestinal) tract (nausea, vomiting). It may also affect the Central Nervous System (behavior), characterized by depression, fatigue, excitement, stupor, coma, headache, altered sleep time, ataxia, tremors as well as the blood, liver, and urinary system (kidney, bladder, ureter) and endocrine system. May also have musculoskeletal effects.

Chronic Potential Health Effects:

Skin: May cause dermatitis.

Eyes: Eye irritation.

Section 12: Ecological Information

Ecotoxicity:

Ecotoxicity in water (LC50): 5540 mg/l 96 hours [Trout]. 8300 mg/l 96 hours [Bluegill]. 7500 mg/l 96 hours [Fathead Minnow]. 0.1 ppm any hours [Water flea].

BOD5 and COD: Not available.

Products of Biodegradation:

Possibly hazardous short term degradation products are not likely. However, long term degradation products may arise.

Toxicity of the Products of Biodegradation: The product itself and its products of degradation are not toxic.

Special Remarks on the Products of Biodegradation: Not available.

Section 13: Disposal Considerations

Waste Disposal:

Waste must be disposed of in accordance with federal, state and local environmental control regulations.

Section 14: Transport Information

DOT Classification: CLASS 3: Flammable liquid.

Identification: : Acetone UNNA: 1090 PG: II

Special Provisions for Transport: Not available.

Section 15: Other Regulatory Information

Federal and State Regulations:

California prop. 65: This product contains the following ingredients for which the State of California has found to cause reproductive harm (male) which would require a warning under the statute: Benzene
California prop. 65: This product contains the following ingredients for which the State of California has found to cause birth defects which would require a warning under the statute: Benzene
California prop. 65: This product contains the following ingredients for which the State of California has found to cause cancer which would require a warning under the statute: Benzene, Formaldehyde
Connecticut hazardous material survey.: Acetone
Illinois toxic substances disclosure to employee act: Acetone
Illinois chemical safety act: Acetone
New York release reporting list: Acetone
Rhode Island RTK hazardous substances: Acetone
Pennsylvania RTK: Acetone
Florida: Acetone
Minnesota: Acetone
Massachusetts RTK: Acetone
Massachusetts spill list: Acetone
New Jersey: Acetone
New Jersey spill list: Acetone
Louisiana spill reporting: Acetone
California List of Hazardous Substances (8 CCR 339): Acetone
TSCA 8(b) inventory: Acetone
TSCA 4(a) final test rules: Acetone
TSCA 8(a) IUR: Acetone

Other Regulations:

OSHA: Hazardous by definition of Hazard Communication Standard (29 CFR 1910.1200).
EINECS: This product is on the European Inventory of Existing Commercial Chemical Substances.

Other Classifications:

WHMIS (Canada):

CLASS B-2: Flammable liquid with a flash point lower than 37.8°C (100°F).
CLASS D-2B: Material causing other toxic effects (TOXIC).

DSCL (EEC):

R11- Highly flammable.
R36- Irritating to eyes.
S9- Keep container in a well-ventilated place.
S16- Keep away from sources of ignition - No smoking.
S26- In case of contact with eyes, rinse immediately with plenty of water and seek medical advice.

HMIS (U.S.A.):

Health Hazard: 2

Fire Hazard: 3

Reactivity: 0

Personal Protection: h

National Fire Protection Association (U.S.A.):

Health: 1

Flammability: 3

Reactivity: 0

Specific hazard:

Protective Equipment:

Gloves.

Lab coat.

Vapor respirator. Be sure to use an approved/certified respirator or equivalent. Wear appropriate respirator when ventilation is inadequate.

Splash goggles.



Health	2
Fire	3
Reactivity	0
Personal Protection	H

Material Safety Data Sheet Toluene MSDS

Section 1: Chemical Product and Company Identification	
<p>Product Name: Toluene</p> <p>Catalog Codes: SLT2857, SLT3277</p> <p>CAS#: 108-88-3</p> <p>RTECS: XS5250000</p> <p>TSCA: TSCA 8(b) inventory: Toluene</p> <p>CI#: Not available.</p> <p>Synonym: Toluol, Tolu-Sol; Methylbenzene; Methacide; Phenylmethane; Methylbenzol</p> <p>Chemical Name: Toluene</p> <p>Chemical Formula: C6-H5-CH3 or C7-H8</p>	<p>Contact Information:</p> <p>Sciencelab.com, Inc. 14025 Smith Rd. Houston, Texas 77396</p> <p>US Sales: 1-800-901-7247 International Sales: 1-281-441-4400</p> <p>Order Online: ScienceLab.com</p> <p>CHEMTREC (24HR Emergency Telephone), call: 1-800-424-9300</p> <p>International CHEMTREC, call: 1-703-527-3887</p> <p>For non-emergency assistance, call: 1-281-441-4400</p>

Section 2: Composition and Information on Ingredients		
Composition:		
Name	CAS #	% by Weight
Toluene	108-88-3	100
<p>Toxicological Data on Ingredients: Toluene: ORAL (LD50): Acute: 636 mg/kg [Rat]. DERMAL (LD50): Acute: 14100 mg/kg [Rabbit]. VAPOR (LC50): Acute: 49000 mg/m 4 hours [Rat]. 440 ppm 24 hours [Mouse].</p>		

Section 3: Hazards Identification
<p>Potential Acute Health Effects: Hazardous in case of skin contact (irritant), of eye contact (irritant), of ingestion, of inhalation. Slightly hazardous in case of skin contact (permeator).</p> <p>Potential Chronic Health Effects: CARCINOGENIC EFFECTS: A4 (Not classifiable for human or animal.) by ACGIH, 3 (Not classifiable for human.) by IARC. MUTAGENIC EFFECTS: Not available. TERATOGENIC EFFECTS: Not available. DEVELOPMENTAL TOXICITY: Not available. The substance may be toxic to blood, kidneys, the nervous system, liver, brain, central nervous system (CNS). Repeated or prolonged exposure to the substance can produce target organs damage.</p>

Section 4: First Aid Measures

Eye Contact:

Check for and remove any contact lenses. In case of contact, immediately flush eyes with plenty of water for at least 15 minutes. Get medical attention.

Skin Contact:

In case of contact, immediately flush skin with plenty of water. Cover the irritated skin with an emollient. Remove contaminated clothing and shoes. Wash clothing before reuse. Thoroughly clean shoes before reuse. Get medical attention.

Serious Skin Contact:

Wash with a disinfectant soap and cover the contaminated skin with an anti-bacterial cream. Seek immediate medical attention.

Inhalation:

If inhaled, remove to fresh air. If not breathing, give artificial respiration. If breathing is difficult, give oxygen. Get medical attention.

Serious Inhalation:

Evacuate the victim to a safe area as soon as possible. Loosen tight clothing such as a collar, tie, belt or waistband. If breathing is difficult, administer oxygen. If the victim is not breathing, perform mouth-to-mouth resuscitation. **WARNING:** It may be hazardous to the person providing aid to give mouth-to-mouth resuscitation when the inhaled material is toxic, infectious or corrosive. Seek medical attention.

Ingestion:

Do NOT induce vomiting unless directed to do so by medical personnel. Never give anything by mouth to an unconscious person. If large quantities of this material are swallowed, call a physician immediately. Loosen tight clothing such as a collar, tie, belt or waistband.

Serious Ingestion: Not available.

Section 5: Fire and Explosion Data

Flammability of the Product: Flammable.

Auto-Ignition Temperature: 480°C (896°F)

Flash Points: CLOSED CUP: 4.4444°C (40°F). (Setaflash) OPEN CUP: 16°C (60.8°F).

Flammable Limits: LOWER: 1.1% UPPER: 7.1%

Products of Combustion: These products are carbon oxides (CO, CO₂).

Fire Hazards in Presence of Various Substances:

Flammable in presence of open flames and sparks, of heat.
Non-flammable in presence of shocks.

Explosion Hazards in Presence of Various Substances:

Risks of explosion of the product in presence of mechanical impact: Not available.
Risks of explosion of the product in presence of static discharge: Not available.

Fire Fighting Media and Instructions:

Flammable liquid, insoluble in water.
SMALL FIRE: Use DRY chemical powder.
LARGE FIRE: Use water spray or fog.

Special Remarks on Fire Hazards: Not available.

Special Remarks on Explosion Hazards:

Toluene forms explosive reaction with 1,3-dichloro-5,5-dimethyl-2,4-imidazolididione; dinitrogen tetraoxide;

concentrated nitric acid, sulfuric acid + nitric acid; N₂O₄; AgClO₄; BrF₃; Uranium hexafluoride; sulfur dichloride.
Also forms an explosive mixture with tetranitromethane.

Section 6: Accidental Release Measures

Small Spill: Absorb with an inert material and put the spilled material in an appropriate waste disposal.

Large Spill:

Toxic flammable liquid, insoluble or very slightly soluble in water.
Keep away from heat. Keep away from sources of ignition. Stop leak if without risk. Absorb with DRY earth, sand or other non-combustible material. Do not get water inside container. Do not touch spilled material. Prevent entry into sewers, basements or confined areas; dike if needed. Call for assistance on disposal. Be careful that the product is not present at a concentration level above TLV. Check TLV on the MSDS and with local authorities.

Section 7: Handling and Storage

Precautions:

Keep away from heat. Keep away from sources of ignition. Ground all equipment containing material. Do not ingest. Do not breathe gas/fumes/ vapor/spray. Wear suitable protective clothing. In case of insufficient ventilation, wear suitable respiratory equipment. If ingested, seek medical advice immediately and show the container or the label. Avoid contact with skin and eyes. Keep away from incompatibles such as oxidizing agents.

Storage:

Store in a segregated and approved area. Keep container in a cool, well-ventilated area. Keep container tightly closed and sealed until ready for use. Avoid all possible sources of ignition (spark or flame).

Section 8: Exposure Controls/Personal Protection

Engineering Controls:

Provide exhaust ventilation or other engineering controls to keep the airborne concentrations of vapors below their respective threshold limit value. Ensure that eyewash stations and safety showers are proximal to the work-station location.

Personal Protection:

Splash goggles. Lab coat. Vapor respirator. Be sure to use an approved/certified respirator or equivalent. Gloves.

Personal Protection in Case of a Large Spill:

Splash goggles. Full suit. Vapor respirator. Boots. Gloves. A self contained breathing apparatus should be used to avoid inhalation of the product. Suggested protective clothing might not be sufficient; consult a specialist BEFORE handling this product.

Exposure Limits:

TWA: 200 STEL: 500 CEIL: 300 (ppm) from OSHA (PEL) [United States]
TWA: 50 (ppm) from ACGIH (TLV) [United States] SKIN
TWA: 100 STEL: 150 from NIOSH [United States]
TWA: 375 STEL: 560 (mg/m³) from NIOSH [United States]
Consult local authorities for acceptable exposure limits.

Section 9: Physical and Chemical Properties

Physical state and appearance: Liquid.

Odor: Sweet, pungent, Benzene-like.

Taste: Not available.

Molecular Weight: 92.14 g/mole

Color: Colorless.

pH (1% soln/water): Not applicable.

Boiling Point: 110.6°C (231.1°F)

Melting Point: -95°C (-139°F)

Critical Temperature: 318.6°C (605.5°F)

Specific Gravity: 0.8636 (Water = 1)

Vapor Pressure: 3.8 kPa (@ 25°C)

Vapor Density: 3.1 (Air = 1)

Volatility: Not available.

Odor Threshold: 1.6 ppm

Water/Oil Dist. Coeff.: The product is more soluble in oil; log(oil/water) = 2.7

Ionicity (in Water): Not available.

Dispersion Properties: See solubility in water, diethyl ether, acetone.

Solubility:

Soluble in diethyl ether, acetone.

Practically insoluble in cold water.

Soluble in ethanol, benzene, chloroform, glacial acetic acid, carbon disulfide.

Solubility in water: 0.561 g/l @ 25 deg. C.

Section 10: Stability and Reactivity Data

Stability: The product is stable.

Instability Temperature: Not available.

Conditions of Instability: Heat, ignition sources (flames, sparks, static), incompatible materials

Incompatibility with various substances: Reactive with oxidizing agents.

Corrosivity: Non-corrosive in presence of glass.

Special Remarks on Reactivity:

Incompatible with strong oxidizers, silver perchlorate, sodium difluoride, Tetranitromethane, Uranium Hexafluoride.

Frozen Bromine Trifluoride reacts violently with Toluene at -80 deg. C.

Reacts chemically with nitrogen oxides, or halogens to form nitrotoluene, nitrobenzene, and nitrophenol and halogenated products, respectively.

Special Remarks on Corrosivity: Not available.

Polymerization: Will not occur.

Section 11: Toxicological Information

Routes of Entry: Absorbed through skin. Dermal contact. Eye contact. Inhalation. Ingestion.

Toxicity to Animals:

WARNING: THE LC50 VALUES HEREUNDER ARE ESTIMATED ON THE BASIS OF A 4-HOUR EXPOSURE.

Acute oral toxicity (LD50): 636 mg/kg [Rat].

Acute dermal toxicity (LD50): 14100 mg/kg [Rabbit].

Acute toxicity of the vapor (LC50): 440 24 hours [Mouse].

Chronic Effects on Humans:

CARCINOGENIC EFFECTS: A4 (Not classifiable for human or animal.) by ACGIH, 3 (Not classifiable for human.) by IARC.

May cause damage to the following organs: blood, kidneys, the nervous system, liver, brain, central nervous system (CNS).

Other Toxic Effects on Humans:

Hazardous in case of skin contact (irritant), of ingestion, of inhalation.

Slightly hazardous in case of skin contact (permeator).

Special Remarks on Toxicity to Animals:

Lowest Published Lethal Dose:

LDL [Human] - Route: Oral; Dose: 50 mg/kg

LCL [Rabbit] - Route: Inhalation; Dose: 55000 ppm/40min

Special Remarks on Chronic Effects on Humans:

Detected in maternal milk in human. Passes through the placental barrier in human. Embryotoxic and/or foetotoxic in animal. May cause adverse reproductive effects and birth defects (teratogenic). May affect genetic material (mutagenic)

Special Remarks on other Toxic Effects on Humans:

Acute Potential Health Effects:

Skin: Causes mild to moderate skin irritation. It can be absorbed to some extent through the skin.

Eyes: Causes mild to moderate eye irritation with a burning sensation. Splash contact with eyes also causes conjunctivitis, blepharospasm, corneal edema, corneal abrasions. This usually resolves in 2 days.

Inhalation: Inhalation of vapor may cause respiratory tract irritation causing coughing and wheezing, and nasal discharge. Inhalation of high concentrations may affect behavior and cause central nervous system effects characterized by nausea, headache, dizziness, tremors, restlessness, lightheadedness, exhilaration, memory loss, insomnia, impaired reaction time, drowsiness, ataxia, hallucinations, somnolence, muscle contraction or spasticity, unconsciousness and coma. Inhalation of high concentration of vapor may also affect the cardiovascular system (rapid heart beat, heart palpitations, increased or decreased blood pressure, dysrhythmia,), respiration (acute pulmonary edema, respiratory depression, apnea, asphyxia), cause vision disturbances and dilated pupils, and cause loss of appetite.

Ingestion: Aspiration hazard. Aspiration of Toluene into the lungs may cause chemical pneumonitis. May cause irritation of the digestive tract with nausea, vomiting, pain. May have effects similar to that of acute inhalation.

Chronic Potential Health Effects:

Inhalation and Ingestion: Prolonged or repeated exposure via inhalation may cause central nervous system and cardiovascular symptoms similar to that of acute inhalation and ingestion as well liver damage/failure, kidney damage/failure (with hematuria, proteinuria, oliguria, renal tubular acidosis), brain damage, weight loss, blood (pigmented or nucleated red blood cells, changes in white blood cell count), bone marrow changes, electrolyte imbalances (Hypokalemia, Hypophosphatemia), severe, muscle weakness and Rhabdomyolysis.

Skin: Repeated or prolonged skin contact may cause defatting dermatitis.

Section 12: Ecological Information**Ecotoxicity:**

Ecotoxicity in water (LC50): 313 mg/l 48 hours [Daphnia (daphnia)]. 17 mg/l 24 hours [Fish (Blue Gill)]. 13 mg/l 96 hours [Fish (Blue Gill)]. 56 mg/l 24 hours [Fish (Fathead minnow)]. 34 mg/l 96 hours [Fish (Fathead minnow)]. 56.8 ppm any hours [Fish (Goldfish)].

BOD5 and COD: Not available.

Products of Biodegradation:

Possibly hazardous short term degradation products are not likely. However, long term degradation products may

arise.

Toxicity of the Products of Biodegradation: The products of degradation are less toxic than the product itself.

Special Remarks on the Products of Biodegradation: Not available.

Section 13: Disposal Considerations

Waste Disposal:

Waste must be disposed of in accordance with federal, state and local environmental control regulations.

Section 14: Transport Information

DOT Classification: CLASS 3: Flammable liquid.

Identification: : Toluene UNNA: 1294 PG: II

Special Provisions for Transport: Not available.

Section 15: Other Regulatory Information

Federal and State Regulations:

California prop. 65: This product contains the following ingredients for which the State of California has found to cause cancer, birth defects or other reproductive harm, which would require a warning under the statute: Toluene

California prop. 65 (no significant risk level): Toluene: 7 mg/day (value)

California prop. 65 (acceptable daily intake level): Toluene: 7 mg/day (value)

California prop. 65: This product contains the following ingredients for which the State of California has found to cause birth defects which would require a warning under the statute: Toluene

Connecticut hazardous material survey.: Toluene

Illinois toxic substances disclosure to employee act: Toluene

Illinois chemical safety act: Toluene

New York release reporting list: Toluene

Rhode Island RTK hazardous substances: Toluene

Pennsylvania RTK: Toluene

Florida: Toluene

Minnesota: Toluene

Michigan critical material: Toluene

Massachusetts RTK: Toluene

Massachusetts spill list: Toluene

New Jersey: Toluene

New Jersey spill list: Toluene

Louisiana spill reporting: Toluene

California Director's List of Hazardous Substances.: Toluene

TSCA 8(b) inventory: Toluene

TSCA 8(d) H and S data reporting: Toluene: Effective date: 10/04/82; Sunset Date: 10/0/92

SARA 313 toxic chemical notification and release reporting: Toluene

CERCLA: Hazardous substances.: Toluene: 1000 lbs. (453.6 kg)

Other Regulations:

OSHA: Hazardous by definition of Hazard Communication Standard (29 CFR 1910.1200).

EINECS: This product is on the European Inventory of Existing Commercial Chemical Substances.

Other Classifications:

WHMIS (Canada):

CLASS B-2: Flammable liquid with a flash point lower than 37.8°C (100°F).

CLASS D-2A: Material causing other toxic effects (VERY TOXIC).

DSCL (EEC):

R11- Highly flammable.

R20- Harmful by inhalation.

S16- Keep away from sources of ignition - No smoking.

S25- Avoid contact with eyes.

S29- Do not empty into drains.

S33- Take precautionary measures against static discharges.

HMIS (U.S.A.):

Health Hazard: 2

Fire Hazard: 3

Reactivity: 0

Personal Protection: h

National Fire Protection Association (U.S.A.):

Health: 2

Flammability: 3

Reactivity: 0

Specific hazard:

Protective Equipment:

Gloves.

Lab coat.

Vapor respirator. Be sure to use an approved/certified respirator or equivalent. Wear appropriate respirator when ventilation is inadequate.

Splash goggles.